Data-Driven Analysis of Transportation Infrastructure Systems using Embedded Wireless Sensing and Cloud-Based Data Architectures

by

Kidus A. Admassu

A dissertation submitted in partial fulfillment
of the requirements for the degree of
Doctor of Philosophy
(Civil Engineering)
in the University of Michigan
2022

Doctoral Committee:

Professor Jerome P. Lynch, Co-Chair, Duke University
Associate Professor Neda Masoud, Co-Chair
Associate Professor Robert Goodspeed
Associate Professor Branko Kerkez
Assistant Professor Tierra Bills, University of California, Los Angeles

Kidus A. Admassu

kidusaam@umich.edu

ORCID iD: 0000-0002-0654-1946

To my mother Sira Dagnachew Wubetie, *for her unconditional love and care*

Acknowledgements

First and foremost, I would like to thank the Almighty God (i.e., the Father, the Son, and the Holy Spirit, One God) for He has been my life, my shield, my joy, and my savior. In addition, He has given me incredible strength and encouragement throughout all the challenging moments of completing this dissertation. I am truly grateful for His unconditional and endless love, mercy, protection, and grace.

I would like to express my deepest appreciation for my Ph.D. advisor Professor Jerome P. Lynch for his mentorship and valuable feedback. He has provided me with insightful comments on my research that have been substantially helpful in this accomplishment. Without his guidance and support, I would have never been able to complete my dissertation. Moreover, I have learned a great deal of personal and professional qualities from Professor Lynch during my stay at the University of Michigan that I believe are very helpful for my future endeavors. Further, I would like to extend my gratitude to my great graduate school course instructors that later became members of my dissertation committee. Therefore, thank you Dr. Robert Goodspeed, Dr. Neda Masoud, Dr. Branko Kerkez, and Dr. Tierra Bills for your willingness to serve on my committee. I have gained invaluable skills from your classes and rich inputs to this dissertation. Without your guidance, this dissertation would have not been possible.

I have had the pleasure of working in the Laboratory of Intelligent Systems Technology (LIST) at the University of Michigan alongside Dr. Patrick (Peng) Sun, Dr. Katherine Flanigan, Dr. Omid Bahrami, Dr. Hao Zhou, and Mr. Gabriel Draughon. I am

very grateful for their friendship, and I also consider myself lucky to have been able to collaborate with such a smart and hard-working group of scholars. Beside LIST, I would like to thank my friends Dr. Zerihun Bekele, Dr. Abdi Zeynu, Dr. Daniel Vignon, Mr. Jianzhong Chen, Mr. Leul Belayneh, Mr. Elvir Trujillo, Dr. Zelalem Aweke, Dr. Salessawi Yitbarek, Dr. Misiker Aga, and Mr. Hiruy Amare for all the good times we have had together. In addition, I greatly appreciate all of the kindhearted people I met while I attended St. Teklehaymanot Ethiopian Orthodox Tewahido Church service on Sundays, and other occasions: just to name a few, Ms. Mibrak Tewolde, Dr. Tewodros Dessalegn, Mrs. Masresha Gebre, Mr. Ephrem Zegeye, and Priest Solomon Bogale.

I am indebted to my family who have sacrificed a lot to lift me up to where I am at now, particularly my mother Mrs. Sira Dagnachew. She often says, “success is just a steppingstone, not a final point of destination!”, which I remembered a lot and so far held on to as her words have motivated me in whatever I do. Next, I would like to thank other beloved family members: Mr. Tesfaye Bekele, Mr. Abebaw Dagnew, Mr. Addis Admas, Mrs. Tiruwork Dagne, Mr. Bereket Tesfaye, and Mr. Tilahun Gizachew for their appreciation and emotional support in my trials and tribulations. Moreover, I have benefited a great deal from my former mentors, colleagues, and great friends such as Mr. Fitsum Gidey, Mr. Johnny Girma, Dr. Bikila Teklu, Mr. Asres Simeneh, Dr. Nasir Bedewi, Mr. Mesay Shemsu, Mr. Yonathan Bekele, and Mr. Kaleab Woldeyohannes. Thank you!

This research was sponsored and supported by the National Science Foundation (NSF) under grant number 1831347, the Michigan Department of Transportation (MDOT) via contract number 131529 OR15-114, and the Great Lakes Water Authority under grants 1900902 and 2102864. Thus, I appreciate their support that funded my graduate study.

Table of Contents

List of Tables

List of Figures

List of Appendices

Abstract

In 2021, America's infrastructure received an overall score of 'C-' from the American Society of Civil Engineers suggesting a national crisis may be looming due to aging infrastructure systems combined with chronic underinvestment in system renewal. Given the importance of transportation infrastructure systems in ensuring societal prosperity and quality of life, there is an urgent need to explore new approaches to managing these systems. While this is a universal problem, it is especially acute in cities and towns with extremely limited financial resources (i.e., under-resourced communities). While sensing technologies have been proposed to monitor such systems, current solutions have a number of challenges including: monitoring solutions (wired and wireless) remain expensive with proprietary architectures limiting versatility; there is a lack of data processing tools that extract information impacting decision making; solutions are not always tailored to the needs of the system end-user. This dissertation explores the creation of an end-to-end sensing and data management systems for the monitoring of transportation infrastructure systems. The work focuses on wireless telemetry as a primary approach to ease system installation in stationary assets and to support asset mobility for moving assets. Specifically, the work highlights efforts to develop wireless sensors that use cellular networks to seamlessly move their data to cloud-based data repositories. The second major contribution of the work is the development of automated data processing tools that can process raw sensor data to extract information specific to assessing, often in real-time, the performance of the system under study. The third is the mapping of information extracted

to drive stakeholder decision-making processes for each of the transportation systems studied. The first transportation system considered are retaining wall systems. Asset managers are reliant on visual inspection information to perform risk assessments; due to the nature of visual inspections these assessments are qualitatively done. This work explores the deployment of a cellular-based wireless monitoring solution that monitors the long-term behavior of reinforced concrete cantilevered retaining walls. The work focuses on automated algorithms that extract metrics associated with wall performance including lateral earth pressures and wall deflections before performing a quantitative risk assessment for asset manager decision-making. The same end-to-end data architecture is also shown to be versatile as a rapid-to-deploy monitoring system for under-resourced communities seeking affordable monitoring solutions to identify low-pressure zones in their drinking water distribution systems. This solution is demonstrated in Benton Harbor, Michigan with pressure measured sparsely across the city to identify locations where water pressure is low. The third transportation system considered in this study are highway assets (e.g., bridges) undergoing heavy truck loading. The thesis adopts the use of weigh-in-motion weight data from a state-wide network of weigh-in-motion stations to infer the travel trajectories of heavy trucks based on Bayesian inference methods. The last system explored by the work is the tracking of a transit system's fleet of buses with an end-to-end data architecture developed to visualize system performance, especially the on-time arrival of buses servicing fixed route service. The work engages community stakeholders to assess their data visualization needs in order to inform the design of a user dashboard that can empower stakeholder insight to the performance of the public transit system.

Chapter 1: Introduction

1.1. Background and Motivation

Civil infrastructure systems are physical and organizational structures that are essential for the overall operation of our modern society **[1]**. Specifically, civil infrastructure systems support a wide range of human activities such as providing safe shelter (i.e., buildings), freedom of movement (i.e., transportation systems), energy delivery (i.e., pipelines, electrical grids, etc.), and the ability to communicate (i.e., broadband networks) **[2]**. If one was to pick transportation infrastructure systems alone, this general class of civil infrastructure would include roads, railways, public transit systems, pipelines, and maritime ports, just to name a few **[3]**. Each of these transportation systems consists of a number of physical assets that are integral to their operations. For example, highway systems contain bridges, retaining walls, tunnels, signals, signage, and pavements **[4]**. Similarly, pipeline systems consist of pipes, valves, pumps, and reservoirs or tanks, and they are usually distinguished by the type of fluid (e.g., oil, gas, water, etc.) they transport **[5]**. Finally, public transportation systems contain buses and bus stops. The owners and managers of these public transit systems are required to maintain them and ensure that their performance safely meet the needs of system end-users.

1.1.1. Grand Challenges (Background)

While civil engineers have historically been responsible for the design and construction of new structural assets associated with transportation systems, their role is equally vital to the operational management of these critical infrastructure systems **[6], [7]**. This role has only expanded in recent years based on the rapidly growing need to better manage the health of aging transportation structures. In 2021, the American Society of Civil Engineers (ASCE) Report Card, which rates the overall condition of domestic infrastructure systems in the United States, provided a 'C-' grade to infrastructure systems due to their mediocre condition and lack of large-scale infrastructure investment. The ASCE report card evaluated 17 categories of infrastructure systems including multiple transportation-specific categories with grades ranging from a 'B' for rail infrastructure to a 'D-' for public transit systems **[8]**. U.S. roads received a grade of 'D' due to 1 in 5 miles of highways and major roads are rated as in poor condition. Similarly, bridges received a 'C' with 45,000 bridges (out of 617,000 bridges) that are structurally deficient and in poor condition **[9]**. Moreover, public transit received the lowest possible grade of 'D-' because 45% of Americans lack easy access to public transit **[8]**.

These low report card grades suggest a national crisis may be looming on the horizon due to chronic underinvestment in infrastructure renewal while large inventories of infrastructure systems continue to age. Another ASCE report indicates that $13 trillion of national investment is needed across 11 infrastructure system categories (highways, bridges, rail, transit, drinking water, stormwater, wastewater, electricity, airports, seaports, and inland waterways) between 2021 and 2039. While $7.3 trillion of infrastructure investment is expected over the next twenty years, there will still remain a $5.6 trillion

investment gap by the end of that period **[10]**. As time carries on, infrastructure inventories will continue to age requiring very strong political leadership to ensure the nation continues to prioritize infrastructure investment **[11]**. Some positive signs of national prioritization of infrastructure renewal are beginning to emerge including the passing of the $1 trillion Bipartisan Infrastructure Bill in November 2021 **[12]**. Although this bill helps to devote much-needed resources to infrastructure renewal, it will not alone close the aforementioned finance gaps; there still remains the need for additional investment and technological innovation. While financing remains a very much needed resource for most infrastructure operators, the lack of sufficient financial resources is an even more acute problem in developing nations **[13]**. Even in well-developed countries like the United States, under-resourced communities with low tax revenues are also vulnerable to finding ways to adequately finance their infrastructure operations and upkeep. For example, the Flint water crisis in Flint, Michigan (2014 to present) originated from a decision to reduce the cost of delivering drinking water to Flint residents due to severe financial constraints of the city **[14]**. Many more examples of deferred maintenance and upkeep of other infrastructure have been reported for under-resourced communities in the United States. In addition to financing challenges, political issues have also been cited as contributing to impeding successful long-term infrastructure development and management **[15]**.

Another challenge associated with the management of transportation infrastructure systems is the changing demands such systems are facing due to external factors including population shifts and the impact of climate change. For example, in the case of public transportation systems, system ridership changes due to growth (or shrinkage) of the community may necessitate the need to analyze if operations of the as-designed system are

meeting user demands; if they are not, then redesign may be necessary. The field of civil engineering also considers future demands on physical assets they design based on the assumption of stationarity in the statistical description of demand anticipated over the full life cycle of the asset. The assumed loads used in the system design are not later reviewed to ensure the system capacity can withstand the actual demands encountered. This is especially problematic in scenarios where the statistical profile of future loads is changing (i.e., nonstationary) as the field is encountering this with systems whose loads are influenced by climate change (e.g., stormwater systems). Needed are methods of continuously monitoring the load imposed on systems and ensuring system managers are evaluating these loads to ensure system capacities are sufficient (and when they are not, improving capacities by retrofitting their assets). The need to quantitatively assess the demands being placed on systems can be difficult to address by system owners and operators already struggling with the finance challenges previously described **[16]**.

In addition to assessing the demands placed on the system, there is a need to assess the performance (or response) of the system under those demands. The field is still highly reliant in qualitative observation methods to assess system responses to loads and overall system conditions. Specifically, the field relies on visual inspection of systems including the visual inspection of structural assets like retaining walls, bridges, etc., and the visual observation of buses (e.g., visual confirmation of arrival time at stops) and riders (e.g., counting riders getting on and off a bus) in public transportation systems. While such methods have worked well, they do offer limited insight to performance due to issues such as subjectivity associated with human interpretation of visual observations and the infrequency of deploying a visual inspector to collect those observations **[17]**. Heavy

reliance on visual inspection and qualitative observation methods is based on both historical inertia and reluctance to pay for sensing technologies that could potentially add quantitative data to the evaluation of system performances **[18]**.

The final challenge relevant to this dissertation is the large quantity of physical assets an owner and/or operator must oversee. The sheer volume of assets in an inventory can stretch the scarce resources (i.e., staff time, budgets, schedule) available. For example, a state department of transportation must manage vast inventories of bridges or extensive miles of retaining walls and pavements. This demands assessment methods that can scale with the size of these vast inventories. For example, the inspections of most highway structures are done on an every-other-year basis which ensures a limited team of trained inspectors can be used to inspect all bridges before they must be inspected again. Technology and innovation hold great promise to automate portions if not all of the visual inspection processes associated with the assessment of the performance and health of transportation infrastructure systems.

1.1.2. Grand Opportunities (Motivation)

The challenges previously presented are complex issues facing most transportation system owners and operators. While these challenges are indeed major, there are opportunities to tackle them to ensure systems have high levels of performance, issues with performance degradation are identified earlier, and resources devoted to system management are efficiently deployed. Technology and innovation offer the opportunity to address the challenges and to ensure transportation systems maximize their performance at minimal operational cost. Specifically, there now exist numerous sensing technologies that can monitor systems and analytical methods (including physics- and data-driven methods) that

use data to assess and predict system performance now available that can quantitatively objectify measures of system performance within existing management methods.

Performance assessment of transportation infrastructure systems can be considered within two quantification paradigms. The first paradigm aims to assess outlier events (and rare phenomena) that can jeopardize the performance and function of the system **[19]**. For example, structural health monitoring (SHM) which includes the development of algorithms to identify damage in structures and deterioration in systems would be considered integral to this paradigm **[20]**. The second paradigm aims to benchmark the performance of operational transportation systems so that current performance can be compared to desired performance to ensure systems meet user needs **[21]**. For example, sensors could be deployed to assess the behavior of structures to acquire quantitative and unambiguous data from which a rigorous assessment of structural performance can be assessed. This would present a major paradigm shift away from qualitative visual inspection methods that dominate current approaches **[22]**.

The research area of incorporating sensors to acquire data related to the performance of infrastructure systems is referred to by the research community under a number of different names including “intelligent systems”, “smart structures”, and more recently, “smart cities.” Regardless of the name used to describe this new area of research, the research itself deals with the integration of technologies such as sensing, actuation, and multifunctional materials that are embedded in the physical infrastructure system in order to observe and control the system with the aim of enhancing system performance, resiliency and sustainability **[23]**. Advances in wireless communications and digital electronics over the past three decades have paved the way for the wider use of sensor

networks in a variety of applications [24]. Since the late 1990's, sensor technology (including wireless telemetry) has rapidly evolved to be low-cost, miniaturized, and functionally rich [25], opening up its use in monitoring several transportation systems (and their functional assets) including structural health monitoring of bridges [26], [27], asset mapping of retaining walls [28], weigh-in-motion load measurement of trucks on roads [29], unmanned aerial vehicles (UAV) based imagery to map geotechnical engineering systems [30], global position system (GPS) tracking of mobile vehicles [31], LiDAR imaging for bridge defects [32], and leak detection using water pressure sensors [33].

While many of these reported studies have successfully prototyped the use of sensing to acquire useful data on the performance of systems, widespread adoption by those managing transportation systems has not yet occurred. There remains work to advance how sensors and the data their produce can be utilized to make better decisions about the performance of transportation systems and their associated functional assets. Specifically, there is a need to research how to integrate such sensing technologies with decision processes that tie to how systems are managed and financial investments in system upgrades are made. On the other hand, for under-resourced municipalities, data and sensing might be the easiest and cheapest ways to drive efficiencies and cost-savings allowing these communities to become "smart" with less operating budget. Sensor- and data-driven smart cities have usually been actualized with in "affluent" cities, but yet it is inequitable for under resourced municipalities due to resource constraints [34]. Nonetheless, devising low-cost decision support system (DSS) tools are invaluable for these communities [35].

Quantitative decision-making for assessing system performance and measuring service quality of existing transportation infrastructure systems requires extensive data

analytics. Data acquisition is the initial part of a broader analytical pipeline whose design aims to convert data into valuable information upon which decisions can be made. After data is collected, data must be stored in databases where analytical modules can reliably access the data. While relational database architectures have been widely used, innovation is occurring in distributed **[36]** and cloud-based **[37]** databases that offer reliable approaches to making data available to real-time data management systems **[38]**. Particularly when wireless sensors automate the flow of sensed data to cloud-based database systems that can scalable analyze the data (e.g., using data-driven methods), such systems are often referred to as a cyber-physical system (CPS). CPS examples in transportation infrastructure systems can today be found widely ranging from self-driving cars **[39]** to automated detection of landslides in geotechnical systems **[40]**.

Once data is safely stored in a database system, algorithms are needed to process the data to extract information that empower the decision processes of owners and operators of transportation infrastructure systems. Specifically, algorithms aim to provide a quantitative means of assessing system performance on varying time- and spatial-scales. Information should provide owners and managers the ability to make better decisions on how to ensure system performance meets current and future end-user needs. A variety of generalizable analytical methods have been explored including physical modeling **[41]**, statistical analysis **[42]**, machine learning **[43]**, cloud computing **[44]**, mathematical modeling **[45]**, and social science methods **[46]**. Within the infrastructure field, there have been tremendous efforts over the past few decades into using monitoring data from transportation systems to track the health of physical assets like bridges. Such systems are considered structural health monitoring (SHM) systems. The algorithms used in these

systems automate the processing of monitoring data to gain insights into system behaviors **[47], [48]**, identify damage and deterioration for operation and maintenance (O&M) decisions, and estimate the remaining safe, useful life of the system **[49]**. Elsewhere in the transportation field, data has grown to be an integral component of assessing the performance of roads and highways to improve their operations. For example, data collected from roadways such as vehicle detectors and traffic imagery is now used to inform the decision process of roadway managers to reduce traffic accidents, decrease congestion, and improve transportation safety **[50]**. Another transportation system where data is used to drive decisions is in public transit systems. Data from buses and other system vehicles are today processed to extract information about the transit system performance including on-time profile of buses **[51]**. While significant progress has been made over the past few decades in using data to attain better decisions, there remains a significant opportunity to continue to explore the advancement of existing data processing methods as well as to introduce new ones to ensure the value of data collected from transportation infrastructure systems is maximized.

Beyond transportation systems, sensors, data architectures, and data-driven decision processes are being deployed in a wide variety of infrastructure services. With wireless communications easing the deployment of sensors, there has been a proliferation of wireless sensing devices across the entire built environment. This "Internet of Things (IoT)" revolution is empowering the notion of the "smart city" **[52]**. Smart cities are beginning to emerge globally and challenging how planners, policy makers, engineers and community members conceptually think about the design of their cities **[53]**. In the United States, momentum has grown in the deployment of smart city services in a number of well-

resourced cities including Chicago **[54]**, New York City **[55]**, and San Francisco **[56]**, among many more **[57]**. Even though the adoption of the underlying IoT technologies of smart cities represents a major investment, smart city solutions uniquely offer an exciting opportunity for under-resourced cities. Under-resourced cities with declining populations due to the relocation of job opportunities struggle with ensuring standard infrastructure services given their weak tax base needed to finance city services **[58]**. IoT and smart city services may allow such cities to not only be more efficient in the delivery of city services but would allow for complete re-conceptualization of how city services are delivered. This is a completely unexplored area but one with the potential to dramatically improve the quality of life of community members in such cities.

1.2. Transportation Infrastructure Systems of Interest

Although there exists a very wide range of civil infrastructure systems that would motivate innovation in quantitative decision-making tools based on monitoring data, this dissertation focuses on four transportation infrastructure systems: *retaining wall systems*, *highway network systems*, *water distribution systems*, and *public transit systems*. The motivation for selecting these targeted systems is that they have some of the lowest national scores reported in the 2021 ASCE Infrastructure Report Card **[8]**. Hence, data-driven performance assessment would dramatically impact their operations (which in turn would impact communities reliant on these systems to ensure their quality of life). Particularly, this dissertation intends to explore end-to-end quantitative decision-making tools working in partnership with the owners of highway assets, water distribution systems and public transit systems in the State of Michigan using their operational systems as research platforms. Sensors will be embedded in these systems with data architectures supporting the

aggregation and processing of data to extract information desired by these system owners. While different transportation systems will be explored herein, the dissertation will advance a common but highly versatile CPS architecture based on wireless sensing and cloud computing to address the needs of different transportation system end-users.

Highway systems consist of many structures requiring vigilant inspection and maintenance. In the United States alone, 11.9 billion tons of freight is carried on highways that comprise approximately 615,000 bridges **[59]**, more than 2.5 million miles of paved roads **[60]**, and extensive inventories of retaining wall systems that grow by 160 million square feet each year **[61]**. While bridges and pavements have enjoyed advances in methods used to improve their long-term management, retaining walls have comparatively enjoyed less attention. Retaining walls are highly complex structures used to support geotechnical systems adjacent to highway roads. These systems are structurally loaded by the geotechnical systems they support often imposing massive soil and hydrostatic pressures with high variability based on seasonal changes. Visual inspectors can only see the performance of retaining walls from one side so there is a major need to be able to better understand the role of the geotechnical system behind the wall plays in the global wall response. Furthermore, there is a need to nondestructively assess the condition of the wall so that a risk assessment can be made. This thesis aims to explore long-term wireless monitoring of retaining walls to describe the behavior of a single retaining wall segment and assess wall reliability for risk-based decision processes.

Other highway structural assets besides retaining walls experience heavy traffic loads, especially the loading profiles associated with commercial trucks; these massive loads can accelerate the deterioration of these critical road surfaces **[62]**. Monitoring every

foot of pavement and every bridge in a state's inventory is simply not feasible. The dissertation explores data processing tools that can take spatially sparse measurement of highway loads from weigh-in-motion stations (WIMS) to estimate loads across the entire road network (i.e., at locations where loads are not observed). The work aims to offer owners with insight to the loading profile of all road-based structural assets in their networks leading to improved risk assessment of their systems.

Drinking water distribution systems require efficient operations to ensure high-quality drinking water is delivered to customers. Drinking water quality is based largely on the water treatment processes performance at the drinking plant; however, quality is also dependent on the operational profile of the distribution pipe network. Municipalities often adopt methods to analyze the operational profile of their pipeline systems to ensure they are meeting performance objectives. For example, pressure and flow sensors are commonly deployed but such sensors are spatially sparse in the distribution system with deployments often near system pump stations. However, in aging water distribution systems and in ones that have been modified over time (with large-scale expansion or major disconnections), there is a need to ensure water is delivered with adequate pressure to all customers given the importance of pressure in ensuring water quality. Especially in under-resourced communities, there is a need for water departments to have a means of rapidly collecting measurements that densely map pressures across the drinking water system, especially in locations far from pump stations.

Another system critical to the well-being of communities is their public transit system. Automated long-term observation of bus transit systems can help target system design and operational changes by identifying probable causes of low performance and

system inefficiency. Location data of bus fleets can be used to quantitatively assess the performance of existing transit services. Especially in under-resourced communities where car ownership may be comparatively low, the transit system is a vital resource for helping community members access essential services such as employment, healthcare, and education. Hence, assessing the performance of the public transit solution can offer an opportunity to improve community access to these essential services. Location information can be collected from GPS trackers installed on buses to continuously monitor their spatiotemporal behaviors. Converting these data sources into insightful and actionable information is a key challenge but has the potential to be a highly transformative approach

Table 1-1. Current needs or limitations associated with target transportation systems.

Transportation Systems	Current Needs or Limitations
Retaining wall systems	Observation of aged retaining wall assets is needed to complement visual inspection methods. Post-placement of sensors, there is the need to develop quantitative risk-based asset management tools using data collected.
Highway network systems	Road surfaces such as pavements and bridges experience massive traffic loads such as truck loads. There are few methods to measure loads aside from highly sparse WIMS measurements. Needed are data processing tools to extrapolate discrete WIMS measurements to estimate loads across the entire road network.
Water distribution systems	Pressure in water distribution systems is an important operational parameter to ensure quality drinking water and firefighting. There is a need to rapidly measure pressure across the system when there are community concerns, especially in systems affected by changes in community demand and distribution system design.
Public transit systems	Under-resourced communities are often highly dependent on public transit systems to access essential services. Operators in these communities need a cost-effective means of quantitatively assessing system performance to ensure essential needs of the community are met.

to helping transit agencies operate efficiently with lean operating budgets. In summary, **Table 1-1** summarizes current needs and limitations attributed to the selected target transportation systems identified for this dissertation.

Three owners will be associated with the testbeds developed in this dissertation. First, highway structural assets in the State of Michigan are managed by the Michigan Department of Transportation (MDOT). MDOT is interested in developing objective decision support systems to help them implement a risk-based asset management strategy for long-term management of their retaining wall systems. MDOT is also interested in understanding the loads imposed on their riding surface structures including pavement systems and bridges to advance existing risk-based management methods in place for these assets. The second partner of the work in this dissertation is the City of Benton Harbor which is an under-resourced community in southwest Michigan. The dissertation will explore IoT solutions based on the solutions developed for MDOT to help the city manage the city water distribution system including understanding its pressure profile. The third partner is the Twin Cities Area Transportation Authority (TCATA) which administers the public transit system for Benton Harbor and surrounding communities. The dissertation will explore the development of a data-driven support tool for TCATA to gain insight to the performance of their public transit system to ensure modification of the system can be objectively explored. While TCATA staff will be the primary partner in this effort, a broad set of community stakeholders are simultaneously engaged to ensure the decision support tools offered to TCATA ensure the agency is highly responsive to community needs.

1.3. Research Gaps

Even though there have been extensive research efforts focused on deploying sensing solutions into a variety of transportation systems, there remains a gap in making these monitoring solutions easy to deploy (i.e., through the different stages ranging from design, development, and implementation), while also ensuring the data they generate empower quantitative decision-making associated with ensuring systems perform as desired and are resilient. This dissertation aims to focus on the following gaps associated with data-driven decision support systems for transportation systems:

- Commercially available wireless sensing solutions that are based on wireless sensor networks (WSN) remain expensive and challenging to deploy because of the dependence of the WSN architecture on a base station (i.e., the required function to collect data from nodes before it transmits data to remote database systems).
- The value of data collected from some category of transportation systems largely remains untapped because there is a lack of scalable and versatile data architectures that can collect and process data to empower end-user decision-making.
- Retaining walls direly need monitoring solutions that are tailored to the soil loads they are exposed to. Analytics are needed to process response data collected from monitored retaining walls to quantitatively estimate their risk profiles for improved long-term asset management.
- Asset management of roadway assets (e.g., pavements, bridges) in highway systems is based on visual inspection with no knowledge of the loads responsible for deterioration. While WIMS measurements are sparsely available, such weight measurements only

provide a measure of trucks load at one spot in the network. There is a need to extrapolate and spatially map weight measurements to all assets in the network.

- Under-resourced communities lack access to versatile and easy-to-use sensing solutions that they can use to gain insight into the performance of infrastructure systems. Such a capability could provide communities a means of attaining a higher level of system performance while minimizing the need for resources. This need is most acute in the management of public transportation systems where there is a need for a data-driven approach to quantitatively tracking system performance in real-time.

1.4. Research Goals and Objectives

In light of the defined gaps, this dissertation has three major goals: (1) to design a scalable cloud-based data architecture for sensors deployed on stationary (i.e., retaining walls) and mobile (i.e., transit buses) assets with the architecture optimized to process data for informing the decision-making processes of transportation infrastructure systems; (2) to develop new approaches to analyze sparse and discrete sensor measurements of load on transportation networks to infer loads applied to portions of the network not monitored to use load in the asset management of all structural assets in the network; and (3) to demonstrate end-to-end decision-making tools for transportation system managers serving both under-resourced communities and as well as administering large-scale spatially distributed infrastructure systems. In order to meet these goals, a number of key research objectives are associated with the target transportation infrastructure system that will be focused on as part of this dissertation as summarized in **Table 1-2**.

As **Table 1-2** reveals, each target transportation infrastructure system example (see **Table 1-1**) has specific goals and objectives that translate into research tasks to be

Table 1-2. Key objectives corresponding to target transportation systems.

Thesis Goals	Retaining Wall Systems	Highway Systems	Drinking Water Systems	Public Transit Systems
Design of a scalable cloud-based data architecture for sensors	Design and deploy cell-based wireless tilt, strain, and temperature sensors for long-term monitoring of wall responses	Collect weigh-in-motion system (WIMS) data from State of Michigan highway system	Design and deploy water pressure sensors with a GPS receiver for rapid deployment	Design a GPS tracker data management system for a fleet of buses serving on-demand and fixed route service
Advancement of data-driven analytic frameworks to assess system performance	Use mechanical models to inversely estimate backfill lateral pressures	Develop a Bayesian probability-based truck identification algorithm to match freight trucks on a highway network level	Integrate a hydraulic model of the water distribution system to estimate pressure across the entire system	Extract on-time performance of fixed route buses using GPS data
	Quantify reliability index (β) values using demand and capacity for risk assessment	Map truck loads to the entire network based on estimated truck trajectories		Develop spatial analytics to identify areas of high origin and destination demand
Study data-driven decision making of resourced and under-resourced asset managers	Develop framework that uses reliability to assess retaining wall risk			Assess end-user needs for empowering decisions with data
				Create data dashboard for bus service provider needs

completed. These tasks will ultimately build for each application a transportation system cyber-physical system (CPS) architecture that begins with sensing and ends with decision making as shown in **Figure 1-1.** The CPS data pipeline created begins with data acquisition in each application. The data for analyzing *retaining wall systems* (e.g., tilt, strain, temperature) and *highway network systems* (e.g., truck weights) are from stationary sensors embedded into the physical systems monitoring. The data for assessing *water distribution systems* (e.g., pressure) and *public transit systems* (e.g., GPS coordinates) are from mobile

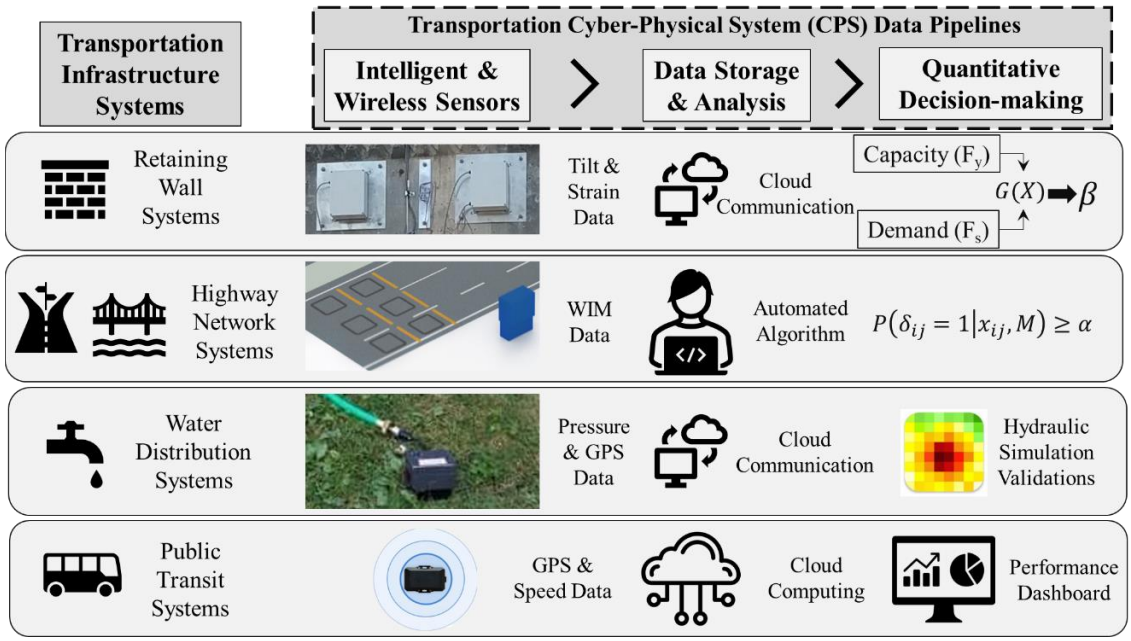

Figure 1-1. Highlights of key Transportation CPS data pipeline components.

wireless sensor units designed to move from location to location. These sensors rely on the use of GPS to track the location of the sensor and in the case of monitoring water distribution systems synchronize pressure readings at tracked locations.

For each respective CPS data pipeline shown in **Figure 1-1**, automated and cloud-based data storage and analytical frameworks are devised to store the data and expose it to processing tools that extract features from the data relevant to system performance. Specifically, the information extracted from measurement data is intended to drive the decision-making of the system manager. For *retaining wall systems*, the dissertation focuses on the quantification of the reliability index (β) of the wall for a user-defined limit state. When combined with the consequences of failure, a quantitative risk assessment can be made. The reliability index (β) will be extracted from wall measurement data by using wall tilt measurements to estimate the lateral pressures on the wall over the monitoring period with the lateral pressures used to assess the limit state relative to reinforcement bar yield stress. For this study, there are two main goals: (1) to demonstrate an instrumentation

strategy for monitoring highway retaining wall systems by emphasizing a strategy suitable for rapid installation after wall construction to provide data on wall behavior, and (2) to utilize long-term observation of retaining wall system behavior to quantitatively inform reliability analysis and risk assessment that may inform how asset managers assess which walls in their vast inventories need upkeep and repair.

Pavements and bridges in a *highway network system* are repeatedly loaded by truck loads that accelerate their deterioration. While loads are measured by WIM stations at discrete locations, there is a need to assess the load at every asset of the network. This dissertation will aim to aggregate the WIM station data from the State of Michigan to infer the location of truck loads in a network by performing truck re-identification between adjacent WIM station pairs. The goals of this work will be: (1) to explore a probabilistic automated truck re-identification system for an alternative and precise way of counting Commercial Annual Average Daily Traffic (C-AADT) on the state-level highway network; (2) to inform the distribution of freight truck loading profiles on pavements and bridges across the network for asset managers. The network-level distribution of truck loads is valuable for a number of applications including quantitatively informing the reliability-based pavement performance management of highway asset managers. As shown in **Figure 1-1**, a Bayesian framework is used to infer truck locations based on comparing WIM records from adjacent stations. The dissertation will explore the robustness of the method based on a controlled study using visual validation of truck re-identification.

For the study of *water distribution systems*, two goals are set: (1) design of a waterproof, standalone, and low-cost water pressure sensor that can easily be deployed on-demand across a city to measure locations and steady-state water pressure at each location;

(2) use distributed steady-state pressure measurements to assess water pressure across a city distribution system. This work is performed in the City of Benton Harbor, Michigan. With respect to the operations of the wireless pressure sensors, they are designed to move freely from consumer to consumer to allow for dense pressure mapping in a water distribution system with sensor locations tracked by a GPS smart antenna receiver synchronized in the sensor design. As a result, the operator of the water distribution system will be able to have a means of identifying low, medium, and high-pressure zones in their water distribution systems which is critical to assessing low-pressure zones where water pressures may jeopardize the water safety and the ability for the city to fight fires.

For *public transit systems*, the main goal of the study is to provide the transit agency, and the transit-dependent communities in Benton Harbor, with a trustworthy, transparent, adaptive, and quantitative view of the public transit system. A primary goal of the work will be to take data from GPS receivers installed in the system buses to automate the calculation of the performance of the existing transit system design including the on-time performance of fixed-route services. In addition, a database of dispatch logs associated with on-demand service will be integrated to observe the performance of an important transit solution for disabled and elderly community members. Dispatch data offers information about trip purposes, age of riders, disability status, number of companions, and the origin-destination pair of individual trips. A secondary goal of the effort is to design a real-time performance website dashboard (as highlighted in **Figure 1-1**) with the aim of ensuring trustworthiness and transparency between transit riders and the transit agency (Twin Cities Area Transportation Authority (TCATA)) is improved. The end utility of this website dashboard will be: 1) to help TCATA managers make continuous

and iterative improvements when quantitatively viewing the performance of their system; 2) enable reporting to state and federal officials easier; 3) improve the trust between TCATA and the community being served by sharing data openly; 4) raise the ridership of the system by showing a high level of system performance; and, 5) manage available human and material resources for more efficient operations.

1.5. Key Contributions and Intellectual Merits

This dissertation would illustrate the potential application of embedded wireless sensing and cloud-based data architectures for data-driven analysis of transportation infrastructure systems. The work focuses on making contributions to the transportation CPS data pipeline in seven parts (**Figure 1-2**): 1) development of wireless sensors for transportation systems; 2) innovative approaches to sensor deployment; 3) creation of an automated data acquisition process including wireless and cellular communications; 4) creation of scalable data storage solutions; 5) use of data science and traditional computational methods to extract information from raw sensor data; 6) quantified performance parameters specific to

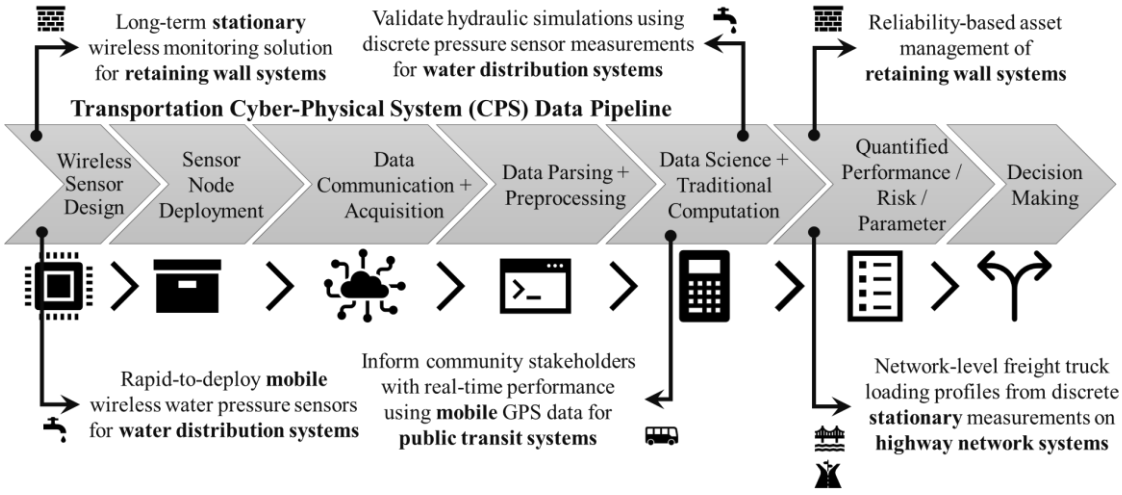

Figure 1-2. Key research contributions in the framework of Transportation Cyber-Physical System (CPS) data pipeline.

the application; and 7) decision making tools contextualized in the application. The key contributions this dissertation make are also delineated in **Figure 1-3** within these seven parts of the CPS framework. With respect to each application area considered in this thesis, the major contributions are summarized as follows:

- For retaining wall systems, existing asset management methods are largely based on qualitative visual inspection methods. Moreover, for aged retaining wall assets, the backfill soil would have to be excavated to inspect the condition of the wall on the backside. Therefore, this dissertation will illustrate that, with long-term wireless monitoring data collected from the retaining wall front façade, a quantitative Risk-based Asset Management (RBAM) is possible. This work will be one of the first to showcase how asset managers can quantitatively assess retaining wall risks using long-term monitoring data.
- For highway network systems, discrete weigh-in-motion (WIM) freight truck measurements have not been used previously aside for network-level assessments; they have historically been used to count trucks in the state for allocation of federal funding. This dissertation presents a Bayesian approach to re-identification of trucks between pairs of adjacent WIM stations to spatiotemporally map distribution of freight truck loading profiles. The work is validated using reliable ground truth data collected from two adjacent WIM stations in southeast Michigan. The spatial mapping of the loading profile in a highway network could inform highway asset managers on which aged bridges in the network are susceptible to service condition deterioration with fatigue sooner than other bridges in their inventory.

- The modular wireless sensors developed for retaining wall application has potential uses in other smart city applications. This thesis makes contribution of showing how the same cellular-enabled wireless sensors, when equipped with a GPS receiver and pressure sensors, can be used by a water system to spot check pressures. A major contribution of this work is in how the data is used to update a hydraulic model that can be used to assess pressures across the network and to identify leaking pipe segments. This is especially valuable for under-resourced communities that might lack pressure measurements from their networks yet are contending with aging water systems suspected of not meeting community needs.
- For public transit systems, most metropolitan transit agencies in the United States have public transit system performance dashboard embedded in their agency website, but their dashboards are usually updated every month. This dissertation intends to propose a low-cost and cloud-based automated data analytics architecture for real-time transit system performance assessment using mobile GPS data of tracked fleet consisting of 27 buses. The end utility of this work would be to inform community stakeholders for their iterative decisions. The major contribution made in this dashboard development work is how end-users of the dashboard are engaged in the dashboard design process, that is for a goal to contribute knowledge on how to make smart city technologies work in resource-restrained environments.

1.6. Dissertation Outline

This dissertation is organized as portrayed in **Figure 1-4**. As previously described, the thesis focuses on universal concepts in sensing empowering data analytics within a transportation CPS architecture. Two major information end-user types are considered: (1)

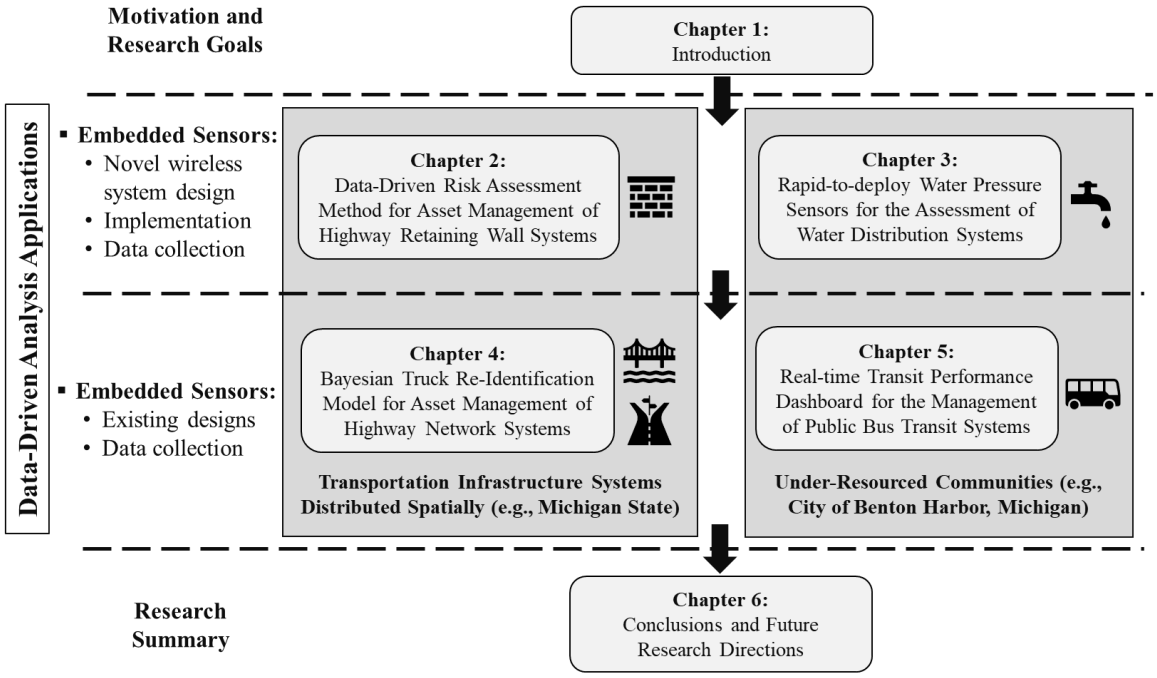

Figure 1-4. Layout of dissertation chapters.

state-level transportation agencies responsible for managing large inventories of structural assets like retaining walls, pavements, and bridges; (2) local city officials responsible for reliable delivery of local infrastructure services like water delivery and public transportation. In this thesis, the second end-user group is from an under-resourced city that must find ways to deliver services more efficiently given the limited resources available. The first group in this thesis are managers with the Michigan Department of Transportation (MDOT) while the second are city officials with the City of Benton Harbor (Michigan). The description of each chapter would be as highlighted in the following:

- The first chapter, Chapter 1, focuses on presenting the background, motivation, research goals, and key contributions of the dissertation. It starts with a broader view of the state-of-the-art for motivation of the research described herein before proposing a transportation CPS data pipeline architecture for selected targeted transportation infrastructure systems. The chapter also frames the analytical work performed to use

data from each transportation system application to quantitatively inform the decision-making process of each end-user.

- Chapter 2 demonstrates the collection of long-term time series wall response data from stationary wireless sensors installed on aged retaining wall assets followed by an illustrative example of Risk-based Asset Management (RBAM). Before presenting the illustrative example, the wall response measurements will be studied for dependency on environmental conditions, particularly seasonal variations of weather such as precipitation and temperature. The chapter showcases a reliability analysis performed to assess the probability of failure of the wall before describing a risk framework for asset managers using the reliability index estimated from the wall data.
- Chapters 3 presents the demonstration of wireless sensors design to rapidly measure pressure in a drinking water distribution system. It focuses on the mobile rapid-to-deploy wireless water pressure sensors designed for short-term pressure assessments. The chapter also presents the use of the pressure data to update a hydraulic model of the city distribution system which can lead to improved estimation of pressure across the entire system (e.g., to identify zones of low pressure that surface concerns on water quality and public safety).
- Chapter 4 presents a highway network-level truck re-identification tool comprised of a two-stage truck matching algorithm. It will be based on a heuristic procedure to inform a Bayesian probabilistic framework. Furthermore, the demonstration also includes validation using video data records collected at a hot spot corridor in southeast Michigan. Towards the end of the chapter, a framework for freeway asset management

is proposed that shows the fusion of freight truck loading profile information from this research with other relevant information for assessing service life of freeway assets.

- In Chapter 5, a real-time transit performance dashboard is demonstrated by analyzing the data coming from GPS tracking of a bus fleet and the logs from a shuttle dispatch system. The analyses include on-time performance, daily ridership by trip purpose, age group, and disability, and real-time transit information, among others. In addition, questionnaire surveys are performed to qualitatively assess the perspectives of the transit provider staff, key stakeholders, and community members about trustworthiness, transit performance, and how dashboard information may be used to inform the design of the dashboard developed.
- Chapter 6 summarizes this dissertation work by highlighting the key intellectual contributions made. The chapter also offers some future research directions that can be pursued based on the work presented by the thesis.

Chapter 2: Data-Driven Risk Assessment Method for Asset Management of Highway Retaining Wall Systems

2.1. Introduction

The construction of highways in dense urban areas and in challenging terrains often requires retaining wall systems to stabilize the geotechnical setting of roads. In the United States alone, more than 160 million square feet of new wall area constructed every year within the national highway and road network **[61]**. This results in massive inventories of retaining wall structures that must be managed by state and local transportation departments. Over the past 50 years, transportation departments have developed highly effective asset management methods that ensure the safe and cost-efficient operation of their structural assets, especially highway bridges and pavements. These methods include extensive use of visual inspection and in some cases structural monitoring and analytical modeling **[63]**, **[64]**. In the U.S., the Moving Ahead for Progress in the 21st Century Act (MAP-21) passed by Congress requires transportation agencies to adopt risk management strategies for all of their transportation assets **[65]**. MAP-21 has transformed how bridges are managed including the use of risk matrices to assign bridges to low-, medium-, and high-risk categories based on failure consequences **[66]**. Given the success of risk management methods for bridges and pavements and the recent mandates of MAP-21, have

shifted their attention toward developing risk assessment methods for geotechnical systems such as earth retaining structures (including retaining walls). For example, a recently completed report by the National Cooperative Highway Research Program (NCHRP) presents field consensus on the need for geotechnical asset management methods including the development of qualitative frameworks for asset management **[67]**. The first step of geotechnical asset management is the development of inventory and inspection methods that database the inventory of earth retaining structures and provide inspection methods that visually assess system conditions on a frequent time basis.

Today, many transportation agencies across the globe have developed an inventory and inspection program for retaining wall systems **[68]**. The majority of these programs adopt visual inspection methods to assess the physical condition of the retaining wall including the detection of movement and deformation of wall structures and the geotechnical system they support. Inspectors trained in visual inspection methods carry out inspections with primary and secondary wall elements (e.g., structural form, surface coating, backfill material, drainage system, foundation) assigned a condition rating similar to that done to rate bridge elements. The United States National Parks Service guides inspectors to offer condition narratives for each wall element with a translational framework to map narrative statements to a condition rating between 0 to 10 **[69]**. Some state agencies like the Nebraska Department of Roads (NDOR) and Colorado Department of Transportation (CDOT) use a rating system identical to what is used for bridges assigning a 0 to 9 rating **[70]**, **[71]** while others like the Oregon Department of Transportation (ODOT) simplify their ratings into “good”, “fair”, and “poor” ratings **[72]**. Visual inspection intervals range from every two years as in the case of VicRoads in

Australia **[73]** to every ten years as is the case with the National Park Service **[69]** with five years the most common (e.g., Alaska, New York City, Oregon, Pennsylvania). While inventory and inspection programs are an essential step toward the development of risk assessment methods for retaining wall structures, alone they are not sufficient due to the lack of quantitative data required to accurately assess the risk inherent to a retaining wall system using information specific to its *in-situ* performance.

Structural monitoring can augment visual inspection methods by offering quantitative evidence of retaining wall performance, including wall responses to varying lateral earth pressures and thermal loads. With structural monitoring evolving into a cost-effective tool for monitoring the performance and condition of bridges **[74]**, **[75]**, **[76]**, asset managers responsible for retaining walls have more recently explored monitoring methods to assist them in their work. The majority of data collection methods focus on assessing the movement of walls; manually applied surveying methods such as the use of total stations and global positioning system (GPS) receivers are widely used to measure wall movements over time. More recently, vehicle-mounted sensors including GPS, laser scanners, and cameras have also been explored to offer a more efficient approach to spatially mapping retaining wall geometries; repeated surveys are then used to track long-term wall deformations **[77]**, **[78]**. Specifically, LiDAR and photogrammetry offer three-dimensional point cloud data sets with sub-centimeter resolutions **[79]**, **[80]**. Mobile mapping methods based on LiDAR have been validated to accurately map 150 linear miles of wall surface profiles a day **[77]**. However, a limitation of these methods is that they only provide information at one point in time (*i.e.*, at the time of the scan) and fail to show continual behavior under diurnal and seasonal environmental variations. To provide

measurements continuously over time, permanent sensors installed on a retaining wall (or in the backfill behind the wall) are necessary **[81]**. Sensors installed onto retaining walls for long-term monitoring are typically tiltmeters (also termed inclinometers) that provide a measure of the rotation of the wall away from the system backfill **[82]**. Strain gages including discrete gages and distributed gages have also been explored to measure the strain response of retaining walls **[83]**, **[84]**. The availability of cost-effective instrumentation for monitoring retaining walls opens opportunities to more objectively assess the behavior and health of monitored wall systems.

In this study, a comprehensive risk assessment framework is proposed for the asset management of retaining walls based on long-term structural monitoring. The work builds from similar concepts applied to bridges including the work by **[85]**, **[86]**, **[76]**, among others. An RC cantilever retaining wall is selected as the primary wall type in the study given it is one of the most ubiquitous types of retaining wall designs. With structural monitoring technology rapidly evolving with increased function and reduced cost, retaining walls of interest (e.g., flagged after initial visual inspection) can be cost-effectively monitored over extended periods of time. The study proposes the use of modular wireless sensor networks to serve as a rapid-to-deploy structural monitoring solution that can monitor the response of the retaining wall structure over any measurement period (including indefinitely). Specifically, tilt and strain are measured to observe the strain and angle of the wall surface while surface temperature is also measured to associate strain responses to thermal loads. The study prioritizes sensor installation locations on the retaining wall face and does not explore sensors in the backfill soil system (which can be invasive and costly to place) to ensure the monitoring method is cost-effective and easy to

deploy thereby making it more likely to be used in practice. An analytical framework is proposed to first process the raw measurement data to disaggregate strain responses associated with thermal loads from those based on lateral earth pressures before using the flexural wall response to estimate the profile of lateral earth pressures on the back of the wall. Long-term monitoring data is then processed by the framework to estimate the lateral earth pressures on the backside of the wall at each data sample leading to a lateral load demand model with diurnal and seasonal variations included. The framework then utilizes the estimated lateral earth pressures to estimate the probability of failure of the monitored wall using Monte Carlo simulation based on assumed distributions of structural and soil properties that define the structural capacity of the retaining wall system. The probability of failure (and corresponding reliability index) is calculated for assumed levels of deterioration (e.g., corrosion of steel reinforcement) that are informed by the age of the wall and from visual inspection. The probability of failure can then be combined with the consequences of failure to quantitatively assess the risk of the retaining wall system. The study applies the proposed risk assessment framework to assess the reliability of a 30-year-old RC cantilever retaining wall along the submerged I-696 highway corridor in southeast Michigan. The study is organized as follows: first, the monitoring system and the retaining wall design is presented followed by description of the analytical framework used to assess the system reliability; next, results of the monitoring campaign are presented followed by an assessment of the monitored wall reliability; finally, the study concludes with a summary of the work contributions (including key results) and description of future extensions of the proposed risk assessment framework.

2.2. Methodology: Long-term Monitoring of Retaining Wall Systems

2.2.1. I-696 Reinforced Concrete Cantilever Retaining Wall System

A single panel of a reinforced concrete cantilever retaining wall system along the I-696 freeway in the metropolitan region of Detroit, Michigan is selected for this study. I-696 is a 28-mile east-west highway that connects I-96 and Farmington Hills, Michigan with I-94 and St. Clair Shores, Michigan in the northern suburbs of Detroit. Constructed in three stages from 1961 to 1979, the highway is submerged below street level in many sections with extensive use of retaining walls to support West Eleven Mile Road that exists on both sides of the highway. The Michigan Department of Transportation (MDOT) is the asset

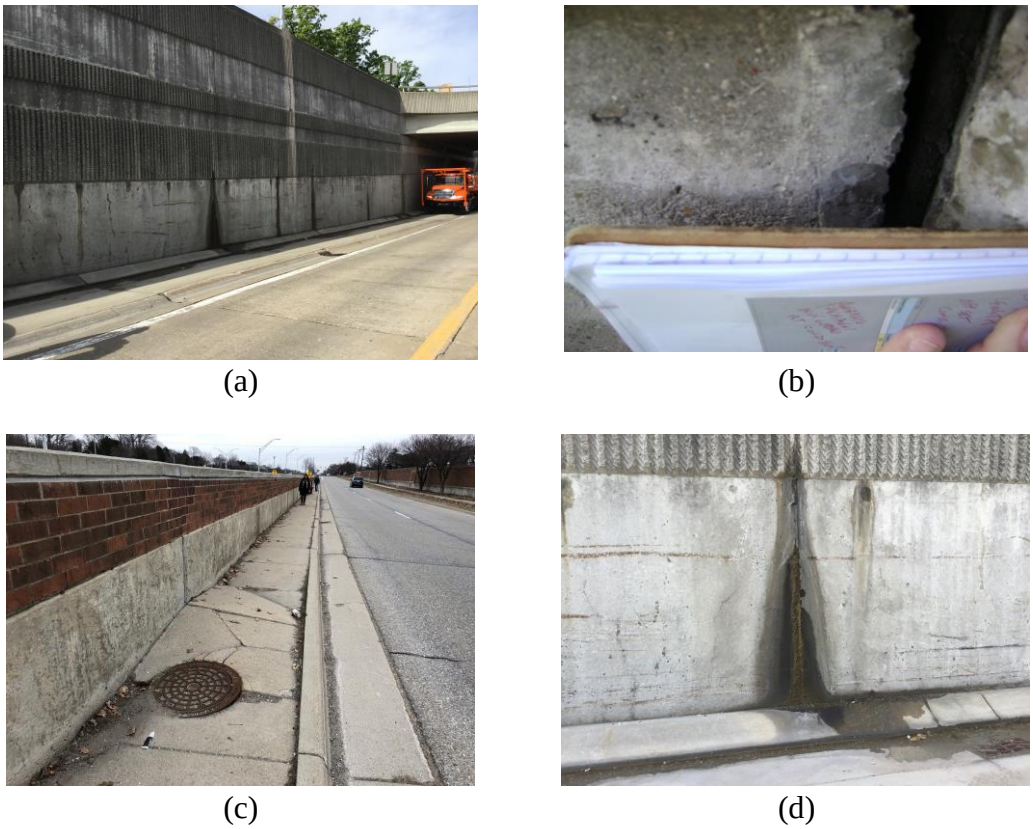

(a) (b)

(c) (d)

Figure 2-1. (a) I-696 RC cantilever retaining wall system; (b) relative displacement between wall panels; (c) road surface deformations on Eleven Mile Road; (d) drainage at the wall base.

owner of the highway including all of its structural assets including retaining walls. MDOT identified a segment of the reinforced concrete (RC) retaining wall system (**Figure 2-1a**) along eastbound I-696 in the vicinity of Central Park Boulevard; this segment was selected due to visual inspections identifying high levels of relative displacement between adjacent wall panels (**Figure 2-1b**), high deflections at the top of the wall as is evident with deformation of the Eleven Mile roadway (**Figure 2-1c**), and high amounts of persistent drainage emanating from the lower portions of the wall surface (**Figure 2-1d**) **[87]**. This segment of the retaining wall system was designed in 1986 and now over 30 years old.

The cantilever RC retaining wall system consists of 20 ft (6.1 m) wide panels with varying panel heights due to an exit ramp servicing vehicles exiting eastbound I-696 to reach Eleven Mile Road that is supported at the top of the wall. The wall segment selected for this study has a wall height of 28.5 ft (8.7 m) and is supported by a 3 ft (0.91 m) thick footing (**Figure 2-2**). On the far side (F.S.) of the wall, there exists a two layer backfill soil system that consists of a 13 ft (4.0 m) deep medium compacted sandy soil at the top of the soil column resting upon a 12.6 ft (3.8 m) deep medium compacted silty-sand soil stratum. The soil conditions of the lower silty-sand soil stratum of the backfill soil is less pervious than the top sandy soil layer. On the wall near side (N.S.), the sloped I-696 road surface ranges from 3 ft (0.91 m) to 4 ft (1.2 m) above the top of the footing. It is also noted that the wall N.S. has three horizontal strips of 3 in (7.62 cm) wide corrugated indentations of varying heights; these indentations are only of aesthetic value and play no role in the structural behavior of the wall **[88]**.

The construction of the wall panel occurred in multiple stages with the footing cast first. Next, the primary retaining wall was cast as two sections with a cold joint between

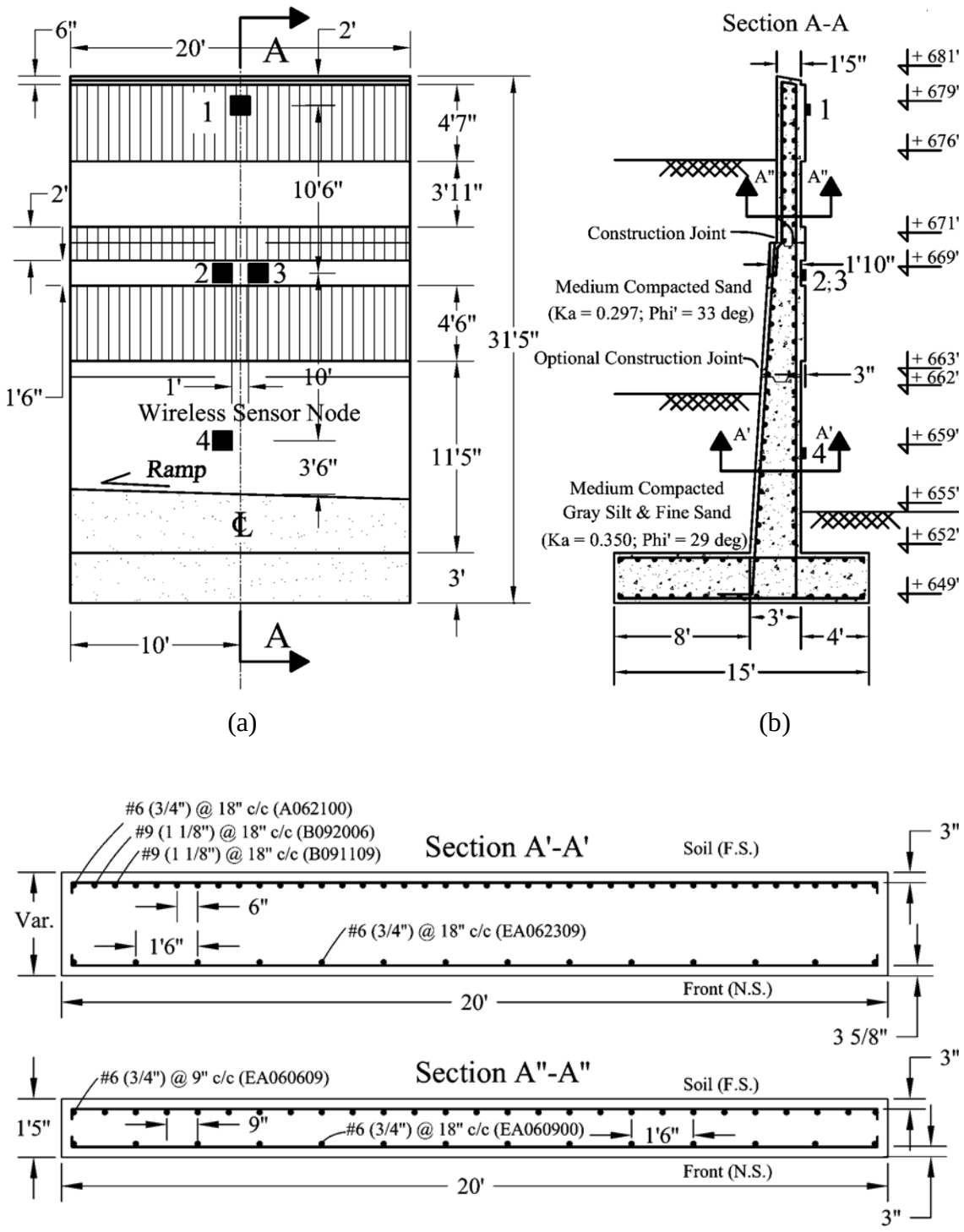

Figure 2-2. Dimensions and structural details of the wall panel at the I-696 retaining wall site: (a) front elevation view showing sensor locations (corresponding to Figure 2-4); (b) vertical cross-section; (c) horizontal cross-section.

the sections. The primary wall has a total height of 18.6 ft (5.7 m) with a tapered section with a 3 ft (0.91 m) bottom thickness to 1.8 ft (0.55 m) top thickness. The last stage of construction was the placement of a 9.9 ft (3.0 m) tall parapet wall with a constant thickness of 1.5 ft (0.46 m). At the street level, the far side (F.S.) surface of the parapet wall is bricked to enhance the wall aesthetic along Eleven Mile Road. Both horizontal and vertical steel reinforcement bars were used in the wall construction as shown in **Figure 2-2c**. To accommodate the high tensile response of the wall, the vertical steel rebar is denser on the F.S. of the wall to accommodate the high levels of tensile flexural strain. The F.S. reinforcement is also continuous through the height of the wall ensuring full compatibility of the wall segments. Due to the thicker section and denser steel reinforcement, the lower portion of the wall has a much higher flexural rigidity to accommodate the higher flexural moments induced by the lateral earth pressures on the F.S. side of the wall. In contrast, the top parapet wall is thinner and more lightly reinforced due to low flexural demands placed on this portion of the wall. The concrete cover over the wall reinforcement is 3 in (7.6 cm) in most locations of the F.S. and N.S. of the wall; however, the reinforcement bar cover is 3.625 in (9.2 cm) on the N.S. face of the lower wall portion. The steel reinforcement used is summarized in **Table 2-1**.

Table 2-1. Vertical steel reinforcement bars properties of I-696 wall.

Wall Section	Rebar Name	Size (Diameter)	Length	Bar Spacing	Rebar Shape
Bottom	A062100	#6 (0.75”)	21’-0”	18” (F.S.)	Straight
Bottom	B092006	#9 (1.125”)	20’-6”	18” (F.S.)	L-shaped
Bottom	B091109	#9 (1.125”)	11’-9”	18” (F.S.)	L-shaped
Middle	EA062309	#6 (0.75”)	23’-9”	18” (N.S.)	Straight, Epoxy Coated
Top	EA060609	#6 (0.75”)	6’-9”	9” (F.S.)	Straight, Epoxy Coated
Top	EA060900	#6 (0.75”)	9’-0”	18” (N.S.)	Straight, Epoxy Coated

2.2.2. I-696 Wireless Monitoring System

A wireless structural monitoring system is selected for long-term monitoring of the I-696 retaining wall segment **[89]**. Since their inception in the mid-1990's **[90]**, wireless structural monitoring systems have matured and today are a proven cost-effective solution for long-term monitoring of civil engineering structures including bridges **[91]**, buildings **[92]**, and wind turbines **[93]**. The wireless monitoring system is designed using the *Urbano* wireless sensor node **[94]** which is architecturally based on the *Narada* wireless node **[95]** that has been widely used for long-term monitoring of bridges **[76]**, **[96]**, **[97]**, **[98]**. *Urbano* was designed to operate on less battery energy than *Narada* and relies on the use of 4G cellular modem (Nimbelink Skywire) to transmit its data to the Internet. Cellular communications are attractive because they eliminate the need for on-site base stations while offering precise time synchronization of the node based on the GPS clock maintained by the cellular provide at the cell tower. The cellular modem consumes 616 mA (referenced at 3.3V) when transmitting, 48 mA when idle, and 8.6 mA when in low-power mode. The seemingly high-current associated with transmitting is offset by the high data rates supported by the radio including a 5 Mbps upload rate. When the radio is needed, *Urbano* is designed to turn the radio on for bursting out data and then placing it back into sleep mode to minimize battery energy consumption when not transmitting **[99]**. At the core of *Urbano* is an 8-bit microcontroller (Atmel Atmega2561V) clocked at 8 MHz and powered by a 3.3V power supply. The microcontroller has 256 kB of flash memory for program storage and 8 kB of SRAM for data storage. Volatile memory is further expanded with an additional 512 kB of SRAM (Cypress CY62148EV30) included in the node design. The 8-bit microcontroller includes a multi-channel 10-bit analog-to-digital converter (ADC)

capable of a maximum sample rate of 200 kHz. The Atmega2561V alone draws 7.3 mA when active, but 4.5 µA when in power-save mode.

To monitor the behavior of the I-696 wall segment, three sensing transducer types are selected and integrated with *Urbano*: tiltmeter to measure wall tilt, long-gage strain gage to measure thermal and flexural strain, and thermistor to measure wall temperatures. These three transducers are selected to offer insight to different aspects of the wall behavior in its loading environment. To measure tilt, a tri-axial accelerometer (Bosch BNO055) well suited for static tilt measurements is adopted to measure the pitch, roll and yaw of the wall. The BNO055 accelerometer has an acceleration measurement range of 2g with a resolution of 1 mg **[100]**. The three static accelerations measured by the BNO055 accelerometer are used to estimate the tilt of the sensor with a resolution of 0.01 degrees. The BNO055 accelerometer is interfaced to the wireless node using a serial interface with the *Urbano* microcontroller. The microcontroller is programmed to query the three static acceleration measurements of the sensor: A_x, A_y, A_z with *x*, *y*, and *z* directions corresponding to vertical along the wall face (in the direction of gravity), orthogonal to the wall plane, and horizontal along the wall face, respectively (as shown in **Figure 2-4a**). The tilt of the wall along the *z*-direction can be estimated in radians using the *x*- and *y*-directions of acceleration:

$$\theta_z = \tan^{-1}\left(\frac{A_x}{A_y}\right) \tag{2-1}$$

An additional feature of the BNO055 is that it includes temperature compensation providing thermally stable measurements between -40 ºC (-40 ºF) and 125 ºC (257 ºF). To improve the accuracy of the tilt measurement, *Urbano* is programmed to read 100 consecutive acceleration measurements at 100 Hz with the collected measurements averaged before tilt, θ_z, is autonomously calculated by the node using **Equation 2-1**.

To create a strain sensor to measure the thermal and flexural strain response of the wall, four 350 Ω metal foil strain gages (Omega KFH-6-350-C1-11L1M2R) are bonded to a long 1 ft (0.30 m) long, 2 in wide (5.1 cm) and 0.25 in (0.64 cm) thick aluminum plate in a cross configuration (as shown in **Figure 2-3a**). Two strain gages aligned with the main axis of the aluminum plate (with resistances denoted as R_{F1} and R_{F4}) are interfaced to opposite sides of a Wheatstone bridge while the other two gages are oriented orthogonal to the main axis (with resistances denoted as R_{F2} and R_{F3}) are interfaced to the other two opposite sides of the Wheatstone bridge (**Figure 2-3b**). This configuration enhances the sensitivity of the strain response along the length of the plate while using the two gages orthogonal to the plate longitudinal axis to thermally compensate the bridge circuit. The gages in the Wheatstone bridge are powered using a 3.3V source (V_{in}) with the bridge output voltage (V_{out}) fed into a standard instrumentation amplifier (Analog Devices AD623) whose internal gain is set to 1000 resulting in V_{strain} (= $1000V_{out}$). The amplified output of the amplifier, V_{strain}, is connected to the *Urbano* 10-bit ADC for data collection. This full bridge set-up allowed longitudinal strain, ε in the plate, to be calculated as:

$$\varepsilon = \frac{-2\left(\frac{V_{out}}{V_{in}}\right)}{GF\left((1+\nu)+\left(\frac{V_{out}}{V_{in}}\right)(1-\nu)\right)}, \tag{2-2}$$

where *GF* is the gage factor of the metal foil gages (*GF* = 2.05) and ν is the Poisson ratio of the aluminum plate (ν = 0.33). Prior to deployment of the aluminum plate, a conformal polymeric coating is applied to the gages and their lead wires to fully seal them from the harsh operational environment anticipated. The last sensor used to monitor the I-696 retaining wall panel is a standard, waterproof thermistor (TDK Group B57020M2). The thermistor is interfaced to a voltage divider circuit to convert resistance to a voltage that is

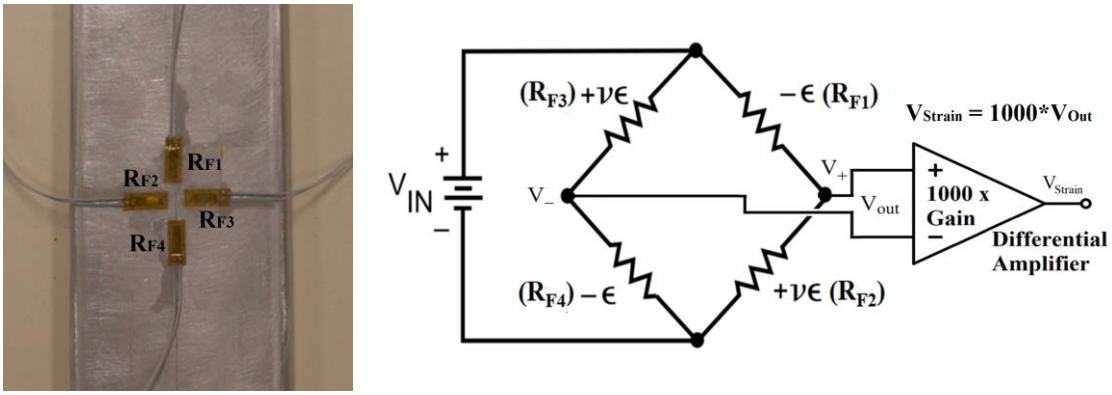

(a) (b)

Figure 2-3. Long-gage strain sensor: (a) long-gage aluminum plate with four active metal foil strain gages attached; (c) full-bridge circuit interfaced to *Urbano*.

read by the *Urbano* 10-bit ADC. The *Urbano* node is programmed to estimate the strain and wall temperature based on the voltages read from the signal conditioning circuits used for the aluminum plate strain sensors and thermistor.

The *Urbano* node is packaged in a water-tight NEMA-rated enclosure prior to deployment on the I-696 retaining wall systems. As shown in **Figure 2-4a**, inside each enclosure is an *Urbano* node, signal conditioning circuits, solar charge controller, and a 12V (2.9 A-hr) sealed rechargeable lead acid battery (Powersonic PS-1229). The enclosures also included the Bosch BNO055 bonded to the enclosure's bottom surface. The node enclosure is attached to the wall surface using four threaded bolts anchored into the wall as shown in **Figure 2-4b**. The aluminum plate strain sensors and thermistors are attached to the wall with wires from these sensors fed into the enclosures through watertight glands and attached to the *Urbano* node. The thermistor is epoxied to the wall surface while the aluminum plate strain sensor is attached using two threaded bolts anchored into the wall. Each node is powered by a 12V (10W) solar panel (Acopower HY010-12M) attached to a light pole that exists above the retaining wall (**Figure 2-4c**).

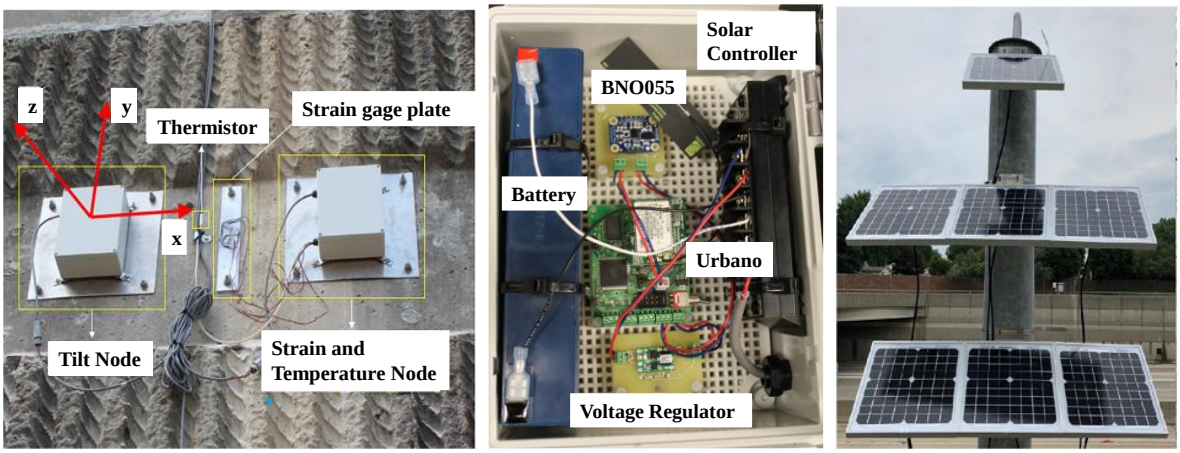

(a) (b) (c)

Figure 2-4. (a) *Urbano* wireless sensor enclosures (units 2 and 3 in Figure 2-2a) and an aluminum plate strain sensor; (b) interior view of wireless sensor NEMA enclosure showing *Urbano node*, solar charge controller, Bosch BNO055 tri-axial accelerometer, and lead acid rechargeable battery; (c) solar panels used to power nodes.

A total of four *Urbano* wireless sensor nodes are deployed along the center line of the I-696 retaining wall segment on August 25, 2018, during a warm and dry day; the locations of the four nodes are denoted in **Figure 2-2a**. To measure wall tilt at the top (θ_{top}) and mid-height (θ_{mid}), Node 1 is at installed 24 ft (7.3 m) above grade and Node 2 at 13.5 ft (4.1 m) above grade, respectively. To measure wall strain at mid-height (ε_{mid}) and bottom (ε_{bot}), Node 3 is installed 13.5 ft (4.1 m) above grade while Node 4 is installed at 3.5 ft (1.1 m) above grade, respectively. A thermistor is interfaced to both Nodes 3 and 4 to measure wall temperatures (T_{mid} and T_{bot}, respectively) in addition to strain. The *Urbano* wireless nodes are designed to operate on a schedule with each node programmed to collect data every hour; when not sensing, the nodes remain in a low-power state to preserve battery energy. After data is sampled by each *Urbano wireless* node, the nodes are programmed to communicate data to a cloud server using the cellular modem integrated with each node. The retaining wall monitoring system uses Exosite, a commercial cloud data portal, for

management of the measurement data **[101]**. In this study, the I-696 wall is monitored from August 2018 to February 2020.

2.3. Methodology: Analytical Framework for Reliability Assessment

2.3.1. Model of Wall Behavior to Extract Lateral Loads

The primary objective of the analytical framework is to process the measured response of the instrumented retaining wall to estimate the system reliability using user-defined limit states. A challenge to this task is the complex nature of the wall behavior. Specifically, the observed wall behavior will primarily be in response to both thermal variations and lateral earth pressures. The monitoring system is designed to produce response data that would allow the wall strain response to thermal and lateral earth pressure loads to be disaggregated as separate response components. Specifically, the thermal and flexural strain components will be denoted as ε_{temp} and ε_{flex}, respectively, with total strain, ε, the sum of the two components: $\varepsilon = \varepsilon_{temp} + \varepsilon_{flex}$. Absolute strain cannot be measured using the instrumentation described previously because there are residual strains inherent in the wall system at the time of the installation of the strain sensors. Hence, measured changes in strain, $\Delta\varepsilon$, as referenced from the start of the monitoring campaign and are associated with changes in wall temperature, ΔT, in addition to changes in the passive lateral earth pressures on the far side of the wall over the period of monitoring:

$$\Delta\varepsilon = \Delta\varepsilon_{temp} + \Delta\varepsilon_{flex} \quad (2\text{-}3)$$

Thermal strain changes, $\Delta\varepsilon_{temp}$, are a result of the change in the wall temperature, ΔT, as measured by the thermistors and they are assumed to be uniform across the cross-section of the wall. In theory, the relationship between thermal strain change and temperature is defined as:

$$\Delta\varepsilon_{temp} = \alpha_{eff}\Delta T \quad (2\text{-}4)$$

where α_{eff} is effective thermal expansion coefficient of the wall. Given the composite nature of the RC wall, α_{eff}, is not known *a priori* so **Equation 2-4** cannot be used to define $\Delta\varepsilon_{temp}$. An alternative approach is to determine $\Delta\varepsilon_{flex}$ using the tilt measurements allowing the flexural component to be subtracted from measured changes in strain, $\Delta\varepsilon$.

Wall tilt measurements, $\theta_{meas} = [\theta_{top} \quad \theta_{mid}]^T$, are primarily in response to the lateral earth pressures that exist behind the wall (**Figure 2-5**). Changes in lateral earth pressures will result from changes in the surcharge load, q, at the top of the wall and the level of hydraulic pressure applied to the wall based on the height of the groundwater table, h_{sat}. Soil properties such as soil friction angle, ϕ, bulk density, γ_b, and submerged density, γ', are assumed to remain unchanged during the monitoring period. A mechanical model of the flexural response of the wall is proposed to use the two absolute tilt measurements, θ_{top} and θ_{mid}, to estimate the height of the water table, h_{sat}, and surcharge load, q. Such a model

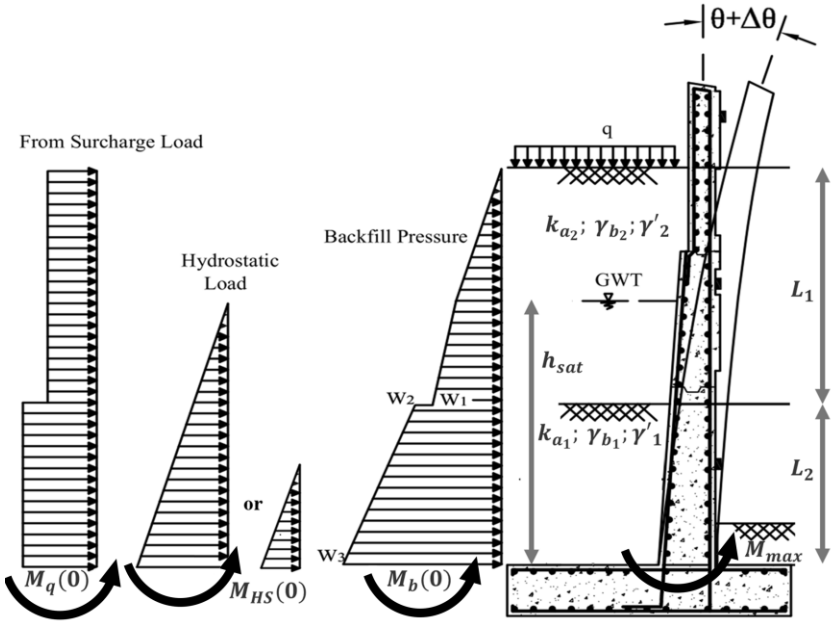

Figure 2-5. Active lateral earth pressures behind the monitored wall due to surface surcharge loading, hydrostatic pressure, and backfill pressure.

would allow each tilt measurement vector, θ_{meas}, to be converted to an estimated loading profile defined by q and h_{sat}. In using a mechanical model of the wall in this manner, an estimation of the lateral earth pressures is obtained from which the same model can be used to define ε_{flex} at any wall location. In reference to **Equation 2-3**, changes in flexural strain, $\Delta\varepsilon_{flex}$, over the monitoring period can then be used to estimate changes in thermal strain based on changes in the measured strain, $\Delta\varepsilon$: $\Delta\varepsilon_{temp} = \Delta\varepsilon - \Delta\varepsilon_{flex}$.

To develop a simple mechanical model of the retaining wall, it is modeled as a Euler–Bernoulli beam model (**Figure 2-6**) with the interaction between adjacent wall panels ignored to ensure model simplicity. The beam is assumed to be in static equilibrium governed by the moment balance:

$$E_e(x)I_{cr}(x)\left(\frac{d^2y(x)}{dx^2}\right) = E_e(x)I_{cr}(x)\left(\frac{d\theta(x)}{dx}\right) = M(x), \qquad (2\text{-}5)$$

where $M(x)$ is the flexural moment induced by the backfill, $y(x)$ is the displacement of the wall, and $\theta(x)$ is the wall tilt, as defined at the wall height, x. The effective modulus of the composite RC cross-section is defined as E_e and the moment of inertia of the section is defined based on the assumption a cracked section, I_{cr} (which assumes the concrete carries no tensile load on the far side (F.S.) of the wall). The cracked section assumption is a valid given the age of the wall, the large flexural loads present, and visual evidence of flexural cracking in previously excavated retaining walls of the same vintage in southeast Michigan **[102]**. To accommodate the tapered vertical profile of the wall and varying reinforcement detailing through the wall height, the beam model is discretized into k segments of uniform thickness δh = 1 in (2.54 cm). For a given loading profile, q and h_{sat}, the vertical profile of lateral earth pressures is established and the moment distribution, $M(x)$, calculated by standard equilibrium principles. The wall rotations, $\theta(x)$, and deflections, $y(x)$, are then

calculated for each element starting from the base element with index is *i*=1 to the top of the wall (whose index is *i*=*k*) using a discretized approach to analysis:

$$\theta(k+1) = \sum_{i=1}^{k} \frac{M(i)}{E_e I_{cr}(i)} = \theta(k) + \delta h \frac{M(k)}{E_e I_{cr}(k)}, \quad (2\text{-}6)$$

$$y(k+1) = \sum_{i=1}^{k} \theta(i)\delta h = y(k) + \theta(k)\delta h. \quad (2\text{-}7)$$

Given the age of the retaining wall system, the material properties of the concrete need to account for age, especially in the selection of the concrete modulus of elasticity. The effective modulus of the concrete is determined based on the 28-day compressive strength of the concrete (f_c' = 4,000 psi (27.6 MPa)) at the time of construction with creep and shrinkage considered. The effective modulus, E_e, is based on the initial modulus, $E_{ci} = 57{,}000\sqrt{f_c'}$ (in psi) and the creep coefficient, ϑ_t, with *t* specified in days **[103]**:

$$E_e = \frac{E_{ci}}{1+\vartheta_t}, \quad (2\text{-}8)$$

$$\vartheta_t = 2.35 * \frac{t^{0.6}}{1+t^{0.6}}. \quad (2\text{-}9)$$

Given the age of the wall (33 years), the effective modulus, E_e, was determined to be 1.1x10^6 psi (7.6 GPa) based on **Equations 2-8 and 2-9**.

To determine the moment of inertia of the cracked section, I_{cr}, the location of the neutral axis, $\bar{y}$, is calculated for the tapered section as a function of the wall height, x. Using the structural drawings to identify the wall geometries including reinforcement details, the cracked section is transformed based on the ratio of elastic modulus, *n*, between the steel ($E_s = 29.0$ x 10^6 psi (210 GPa)) and concrete ($E_e =$ 1.1 x 10^6 psi (7.6 GPa)). The neutral axis, $\bar{y}(x)$, is parameterized as a second-order polynomial given the wall tapering (which affects the depth to the tensile, $d(x)$, and compression, $d'(x)$,

reinforcement) and the effective cross-sectional area of steel in the tension zone, A_s, and the compression zone, A'_s:

$$\frac{1}{2}b\bar{y}^2 + (n-1)A'_s(\bar{y} - d') - nA_s(d(x) - \bar{y}) = 0 \tag{2-10}$$

The real positive root to **Equation 2-10** is found to identify the neutral axis, $\bar{y}(x)$, for each discrete element of the wall. The cracked moment of inertia, I_{cr}, about the neutral axis, $\bar{y}$, is found to be:,

$$I_{cr}(x) = (n-1)A'_{s,\,eff}(\bar{y}(x) - d')^2 + nA_{s,\,eff}\left(d - \bar{y}(x)\right)^2 + b\bar{y}(x)\left(\frac{\bar{y}(x)}{2}\right)^2 + \frac{b\bar{y}(x)^3}{12} \tag{2-11}$$

With respect to the geotechnical backfill, the soil boring elevation drawings document the backfill as a two-layer system with a 13.9 ft (4.2 m) thick layer of medium

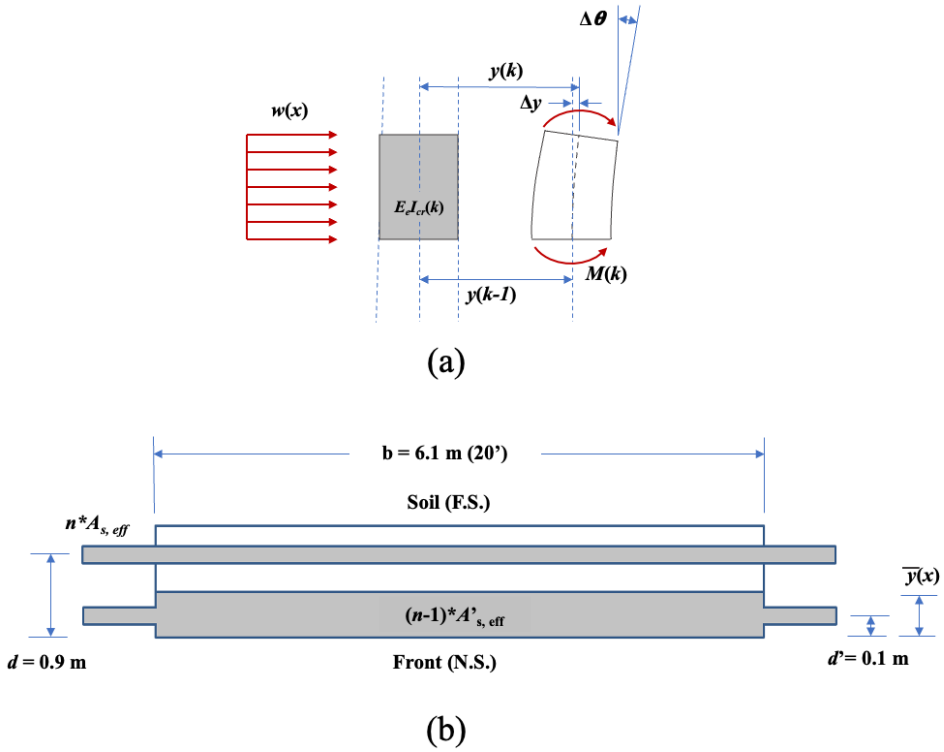

Figure 2-6. Beam model of cantilever retaining wall: (a) k[th] element of Euler–Bernoulli beam model; (b) assumed cracked cross-section of wall panel at the wall base.

compacted sand on top of a 9.6 ft (2.9 m) thick layer of medium compacted gray silt and fine sand. Based on **[104]** and **[105]**, the medium compacted sand is assumed to have a bulk density of γ_{b2} = 0.069 lb/in^3 (1909.9 kg/m^3) and submerged density of γ_2' = 0.038 lb/in^3 (1051.8 kg/m^3) while the medium compacted gray silt and fine sand layer is assumed to have a bulk density of γ_{b1} = 0.073 lb/in^3 (2020.6 kg/m^3) and submerged density of γ_1' = 0.042 lb/in^3 (1162.6 kg/m^3). Due to the unknown frictional properties of the soil on the wall surface, Rankine's theory is used to determine the pressures on the far side of the wall, and it is also favored by state transportation agencies including AASHTO and FHWA. The Rankine's earth pressure coefficient, k_a, for each layer is:

$$k_a = \frac{\cos(\beta - \theta)\sqrt{1 + \sin^2\emptyset - 2\sin\emptyset\cos\psi}}{\cos^2\theta\,(\cos\beta + \sqrt{\sin^2\emptyset - \sin^2\beta})} \quad (2\text{-}12)$$

$$\psi = \sin^{-1}\left(\frac{\sin\beta}{\sin\emptyset}\right) - \beta + 2\theta \quad (2\text{-}13)$$

where β is the slope of the top surface of the backfill relative to the horizon (in this case β = 0°), ϕ is the internal soil friction angle, and θ is the slope of the wall F.S. surface (relative to vertical). Typical angles of internal soil friction were acquired from **[106]**: sand with medium compaction, ϕ = 33°, and sandy silt with medium compaction, ϕ = 29°. The angle of the back surface of the instrumented wall, θ, is computed as 3.6° based on the structural drawings. Using **Equations 2-12 and 2-13**, the active earth pressure coefficients are computed as k_{a2} = 0.30 and k_{a1} = 0.35 for the upper and lower soil layers, respectively.

To simplify the analysis, permutations of q and h_{sat} are varied with the model used to estimate the top and mid-height wall rotations: θ_{model}. A total of 17 increments of surcharge pressure were considered between 0 and 1.74 psi (12.0 kPa); similarly, 282 increments of water saturation levels were considered between 0 and 282 in (7.16 m). A

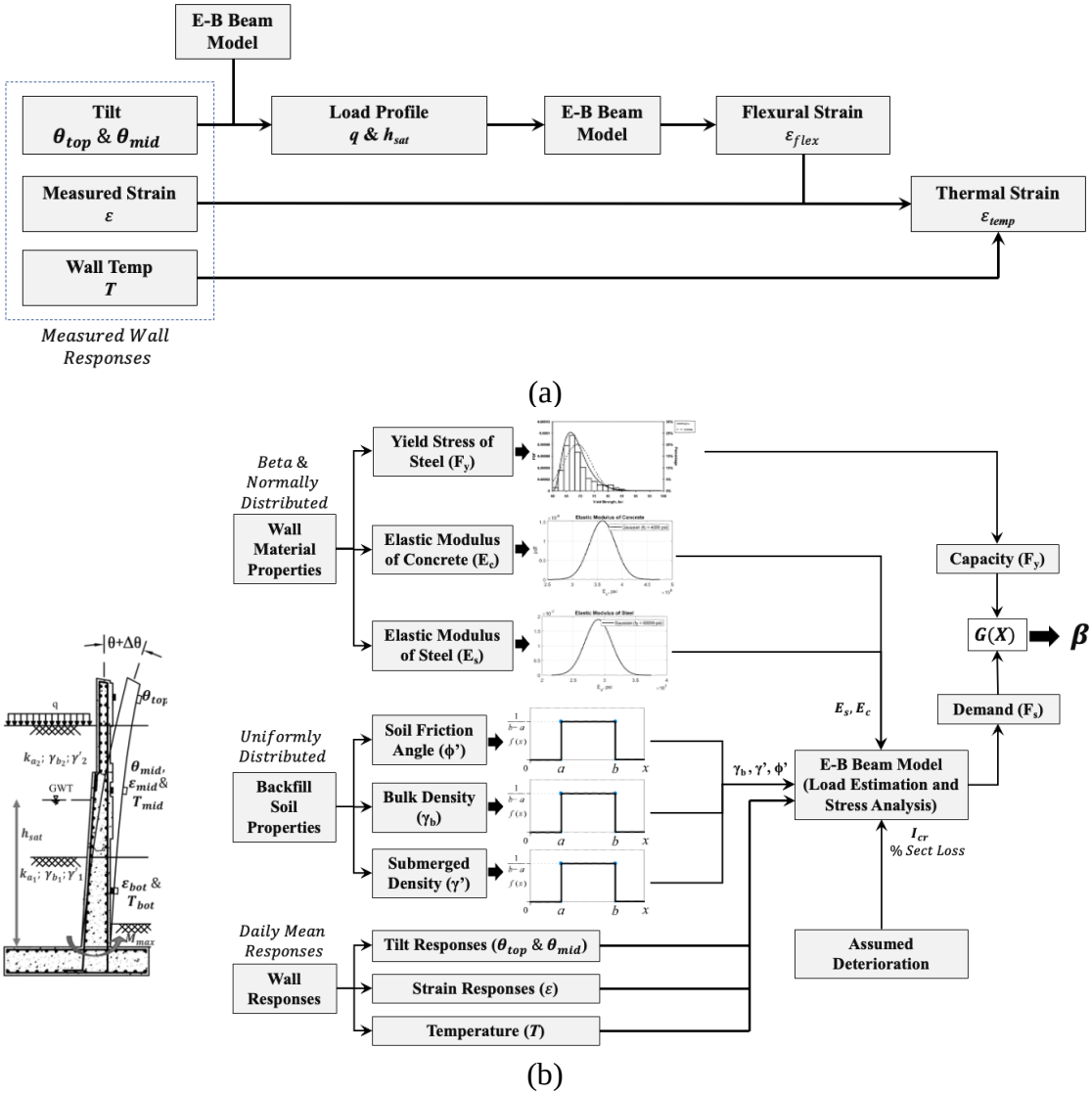

Figure 2-7. Analytical framework: (a) load estimation and thermal strain extraction from measurement; (b) reliability analysis using probabilistic models for system properties.

look-up table is created for every permutation of q and h_{sat}. For given measurement of wall tilt, θ_{meas}, the optimal load profile can be found by finding the table element that minimizes the difference between the measured and the model tilt,

$$\underset{q,h_{sat}}{argmin}\|\theta_{meas} - \theta_{model}\| \tag{2-14}$$

With the optimal load profile estimated, the flexural strain response, ε_{flex}, can be modeled anywhere in the wall cross-section. Using the initial flexural strain measurement

at the start of the monitoring campaign, changes in flexural strain, $\Delta\varepsilon_{flex}$, at the points of strain measurement can be calculated so that change in thermal strain, $\Delta\varepsilon_{temp}$, can be extracted from changes in the measured strain, $\Delta\varepsilon$, by **Equation 2-3**. It should be noted that this modeling approach is fully deterministic and assumes accurate estimation of the properties of the structural and backfill material properties. Measured changes in thermal strain, $\Delta\varepsilon_{temp}$, and wall temperature, ΔT, can then be used to empirically estimate the effective thermal expansion coefficient, α_{eff}, by linear regression analysis. A summary of the algorithmic framework for load estimations and thermal strain extractions is as illustrated in **Figure 2-7a**.

2.3.2. Reliability Methods for Retaining Wall Performance Assessment

At the core of quantitative risk assessment is a structural reliability assessment using monitoring data. Reliability assessments calculate the probability of exceeding a defined scalar limit state function, $G(\boldsymbol{X})$ where $\boldsymbol{X}$ is a vector of random variables, $\boldsymbol{X} = [X_1, X_2, \dots, X_n]^T$. The limit state function reflects the margin that exists between the system capacity, C, and demand, D: $G(\boldsymbol{X}) = C - D$. Various limit states can be formulated based on strength or serviceability considerations. The probability of failure, P_f, is defined as the probability of $\boldsymbol{X}$ existing in the failure domain, Ω:

$$P_f = \int_{\Omega} f_{\boldsymbol{X}}(\boldsymbol{X}) d\boldsymbol{X} \text{ where } \Omega \equiv G(\boldsymbol{X}) \leq 0 \quad (2\text{-}15)$$

When working within independent standard normal space, the reliability index, β, is defined as the minimum distance from the origin to where $G(\boldsymbol{X}) = 0$. As a result, P_f and β are related by $P_f = \Phi(-\beta)$ where $\Phi(\cdot)$ is the standard normal cumulative distribution function. The probability of failure can be multiplied by the consequence of failure, $C_\$$, to

estimate the system risk: $R = P_f \times C_\$$. The consequences can be described in the form of monetary costs such as the cost of system repair, cost of damage to other physical assets, opportunity cost (i.e., cost of road closure), and cost of human life lost. In this study, the analytical framework focuses on reliability assessment using monitoring data and leaves the complete risk assessment to end users who have defined the consequences of failure.

Reliability methods are integral to the design of earth retaining structures including retaining walls that are designed using load and resistance factor design (LRFD) codes such as those associated with AASHTO. Researchers have explored reliability methods to advance the design of retaining walls. For example, **[107]** explored the use of the Hasofer–Lind reliability index and the first-order reliability method (FORM) to design retaining walls to target reliability index values. **[108]** developed a reliability framework to optimize the design of reinforcing ties used in the design of reinforced earth retaining walls. A study on the use of neural networks to define nonlinear limit state functions define unacceptable excessive ground deformations associated with braced retaining walls used in excavation projects **[109]**. More recently, there has been research devoted to expanding the role of reliability from the design phase of a structure to that of asset management, especially of bridges. For example, **[85]** proposed a decision support system for bridge managers based on reliability methods using visual inspection ratings and associated data. The seminal study by **[86]** explored the inclusion of long-term strain data in estimating the reliability of bridge components based on the use of FORM to estimate the reliability index of an instrumented truss element. Similarly, **[76]** also proposed the use of strain data to assess the reliability of fatigue-critical structural elements in a railroad truss bridge. This study

builds upon the work of **[85]**, **[86]**, and **[76]** to develop a framework for assessing the reliability of retaining walls using long-term monitoring data.

At the core of the reliability assessment method proposed herein (**Figure 2-7b**) is the use of the Euler–Bernoulli beam model previously developed to determine the demand response, *D*, of the retaining wall to the observed lateral earth pressures and thermal loads estimated from the monitoring data. A Monte Carlo approach is taken to perform the reliability assessment given the computational simplicity of the Euler–Bernoulli beam model. First, for a given state of measurement $\boldsymbol{M} = [\theta_{top} \quad \theta_{mid} \quad \varepsilon_{mid} \quad \varepsilon_{bot} \quad T]^T$, a reliability assessment is performed to estimate the reliability index, β_M, to a user-defined limit state function, $G(\boldsymbol{X})$. In each iteration of the Monte Carlo implementation, the material properties for the wall and soil are treated as random variables, $\boldsymbol{X}= [E_{ci} \quad E_s \quad \phi \quad \gamma_b \quad \gamma']^T$ sampled from assumed distributions. For a sampling of $\boldsymbol{X}$, the measurements, $\boldsymbol{M}$, are used to extract the loads q and h_{sat} using the same beam model method as proposed before. Using the load parameters, are then applied to the beam model to determine the demand response of the wall, *D*. A statistical model of the system capacity, *C*, is sampled to determine if $G(\boldsymbol{X}) < 0$. For *N* iterations of the method, the number of times the limit state function is negative is counted, *n*, to determine the probability of failure: $P_f = n/N$. Finally, reliability index (β_M) is calculated as:

$$\beta_M = \Phi^{-1}(P_f). \tag{2-16}$$

A primary failure mechanism of cantilever retaining walls is the corrosion of the steel reinforcement at the base of the wall with lateral earth pressures producing an overturning moment, $M_b(0)$ that exceeds the flexural capacity of the base cross-section. In the case of the retaining wall studied in this work, evidence of continuous water drainage at the base

of the wall suggests corrosion of the steel reinforcement is a concern. Hence, this study considers the limit state function as the difference in the demand response, ε_s, in the tensile steel reinforcement at the base of the wall and its capacity as defined by its yield stress, F_y:

$$G(\boldsymbol{X}) = F_y - \varepsilon_s \cdot E_s. \quad (2\text{-}17)$$

For each iteration of the Monte Carlo analysis, the strain in the steel reinforcement is calculated based on the, $\varepsilon_{s,flex}$, using the lateral earth pressures estimated using the wall tilt measurements and changes in the thermal strain extracted from the strain data at the bottom of the wall $\Delta\varepsilon_{bot,temp}$ using **Equation 2-4**.

The elastic moduli of structural materials are well established to follow normal distributions. For concrete, the distribution of concrete elastic modulus is presented as Gaussian for different compressive strength grades in **[110]**, while it is presented likewise for structural steel **[111]** and reinforcement bars **[112]**. Hence, the elastic modulus of concrete, $E_{ci,}$ is assumed to be normally distributed with mean 3.6×10^6 psi (24.8 GPa) and standard deviation 0.25×10^6 psi (1.74 GPa) with **Equation 2-8** used to determine the effective elastic modulus, E_e. The elastic modulus of steel, E_s, is also treated as normally distributed with mean 29.0×10^6 psi (210 GPa) and standard deviation 1×10^6 psi (7.6 GPa). The probabilistic models used to define soil properties vary but are conservatively assumed to be uniformly distributed. The uniformly distributed bulk and submerged densities of the two soil types in this study are based on **[105]**. The medium compacted sand is assumed to have a bulk density that varies from γ_{b2} = 0.049 lb/in^3 (1462.3 kg/m^3) to 0.079 lb/in^3 (2357.5 kg/m^3) and submerged density that varies from γ_2' = 0.030 lb/in^3 (876.5 kg/m^3) to 0.042 lb/in^3 (1227.1 kg/m^3). The medium compacted gray silt and fine sand layer is assumed to have a bulk density that varies uniformly from γ_{b1} =

0.051 lb/in^3 (1411.7 kg/m^3) to 0.082 lb/in^3 (2269.7 kg/m^3) and submerged density that varies from γ_1' = 0.031 lb/in^3 (858.1 kg/m^3) to 0.046 lb/in^3 (1273.3 kg/m^3). Typical angles of internal soil friction were acquired from **[106]**: sand with medium compaction uniformly distributed from ϕ = 30^o to 35^o while sandy silt with medium compaction uniformly varied from ϕ = 20^o to 30^o. The internal soil friction angles were used to estimate the Rankine's earth pressure coefficient, k_a, by **Equation 2-12**. For the limit state function used in this study, a statistical distribution of F_y is assumed based on the comprehensive statistical modeling of steel reinforcement properties by **[113]**. For the ASTM A615 Grade 60 steel reinforcement used at the base of the wall, a normal distribution is assumed. Based on **[113]**, the mean yield strength of Grade 60 steel is 69 ksi (475 MPa) with a standard deviation between 4.3 ksi (29.6 kPa) and 5.0 ksi (34.5 kPa); this study selected 5.0 ksi (34.5 kPa) for the standard deviation.

2.4. Results

2.4.1. Long-Term Behavior of Retaining Wall

The cantilever retaining wall panel is monitored continuously from August 2018 to February 2020. **Figure 2-8** provides a continuous plot of the measured wall tilts (θ_{top} and θ_{mid}), strain (ε_{mid} and ε_{bot}), and wall temperature (T) for each day averaged over a 24-hour period from 12:00 am to 11:59 pm. It should be noted that the strain measurements are the raw change in strain with each strain sensor zeroed at the first reading in August 2018. Overall, the wireless sensors that collect data from the retaining wall sensors work well during the entire measurement campaign with only the *Urbano* node measuring strain and temperature at the bottom of the wall failing in late July 2019. Intermittently, some of the sensors do not report all its data resulting in some gaps in the measurement time

histories shown in **Figure 2-8**. Also included in **Figure 2-8** is a history of precipitation recorded by a weather station (i.e., KMISOUTH67 in Southfield, MI) in proximity (i.e., only 2 miles (3.2 km) away) to the retaining wall **[114]**. The precipitation is an important environmental parameter to track as it will directly influence h_{sat}.

The tilt history of the top portion of the wall system demonstrates a greater variation in daily mean tilt as compared to the mid-height tilt. Specifically, the top tilt varies from 0.5 to 3.5° while the mid-height tilt has a much smaller variation between 1.0 to 1.45°. The top-level tilt sensor was installed upon the thin parapet wall just 2 ft (0.6 m) below the wall top (**Figure 2-2a**). The wide variation in tilt of the parapet wall was attributed to the fact that maximum rotations of the wall due to lateral earth pressures will be at the top of the wall. Also contributing is the lower flexural rigidity of the parapet wall due to a lower thickness and lighter steel reinforcement. During certain periods, repeated days of precipitation seem to influence the top wall tilt possibly due to the build-up of hydraulic pressure in the top stratum of soil. For example, continuous days of rain in late September 2018 into early October 2018 induce a noticeable upper tilt of the top portion of the wall (going from 1.0 to 2.5°); after the rain ceases, the wall returns to 1.0°. Comparatively, the daily mean tilt of the lower portion of the wall is less sensitive to precipitation with little variations in daily mean wall tilts during periods of rain. This may be attributed to the high flexural rigidity of the wall; it may also be explained by the lack of variation in the hydrostatic pressures in the lower soil stratum behind the wall.

From late November 2018 to January 2019, the top tilt has a high level of day-to-day variation as the trend-line mean of the tilt time history increases slowly. The wall daily mean top tilt also dramatically varies from mid-January 2019 to mid-February 2019 when

the wall temperature is near or below freezing (32 °F (0 °C)). In the last few days of January 2019, the wall achieves a temperature of 0 °F after which a few days later the temperature was 42 °F; during this period, the daily mean top wall tilt varies from 0.5 to 3.5° suggesting freezing of the backfill soil may be adding additional lateral earth pressures. By May 2019, the wall reaches a maximum daily mean top tilt of 3.5°. After May 2019, the tilt at the top of the wall has less day-to-day variation and the mean trend-line decreases to about 1.5°

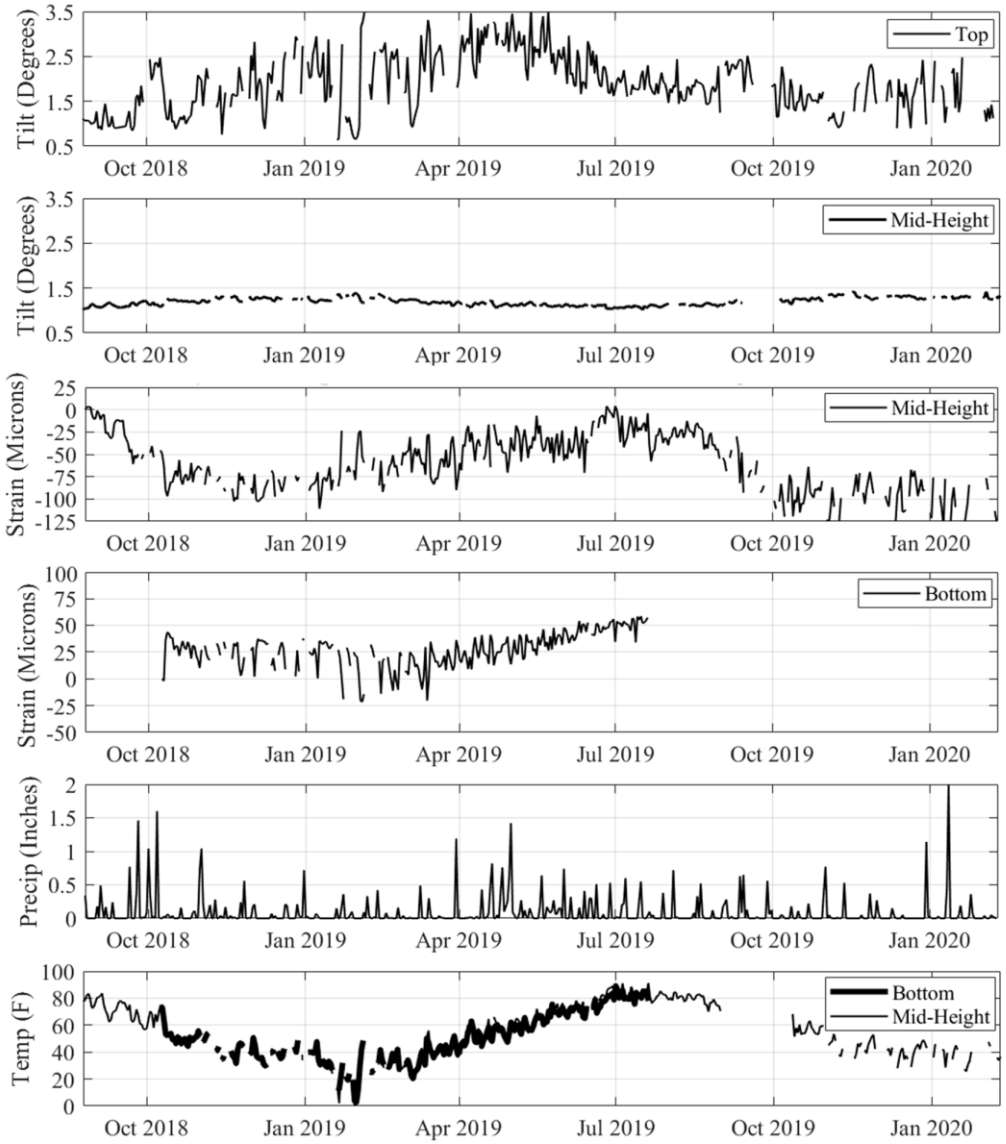

Figure 2-8. Daily mean responses of the I-696 retaining wall panel with daily mean precipitation added (August 2018 - February 2020).

by July 2019. It is hypothesized that the daily mean top wall tilt trend-line slowly increases from November to May due to lowering ambient temperatures and their effects on the backfill soil resulting in greater lateral earth pressures. Comparing the daily mean top tilt trendline with the wall temperature time history, the two appear to be correlated with a 30 to 45 day lag; this may be attributed to thermal inertia of the backfill.

The daily mean strain responses at the wall mid-height and bottom capture changes in strain of the wall near side; as previously mentioned, the absolute state of strain is unknown with strain relative to the start of monitoring in August 2018. Taking compressive strain to be of negative magnitude and tensile strain to be of positive magnitude, the daily mean wall strain histories exhibited a trend correlated to the wall temperature. The mid-height strain varied over the 15-month period of 125 με while the bottom strain varied only 75 με. Maximum compressive flexural strain (which would correspond to maximum tensile strain on the wall far side is during the winter).

The causality between environmental parameters and the wall behavior are studied using response scatter plots with linear regressed behavioral models fit. Plotted in **Figure 2-9** are scatter plots of lower wall responses (i.e., bottom strain, $\Delta\varepsilon_{bot}$, mid-height strain, $\Delta\varepsilon_{mid}$, and mid-height tilt, θ_{mid}) as a function of measured wall temperature, T. As shown, a strong linear relationship exists between these two measurands. Using linear regression to model the relationship, it is evident that the mid-height tilt of the lower portion of the wall varies roughly 0.004° per degree F of wall temperature. The greatest mid-height tilt is experienced during the colder months with a maximum tilt of 1.4° when the wall temperature is 0 °F. Similarly, the wall strain at the bottom and mid-height is dependent on

temperature. Based on linear regeression, the mid-height and bottom strain varies 0.92 με and 0.45 με per degree F, respectively.

While the top tilt exhibits sensitivity to precipitation, the lower portion of the retaining wall is relatively insensitive to precipitation supporting the hypothesis that the lower portions of the wall backfill are saturated. Recall, this hypothesis was supported by visual observation of steady weeping in the wall panels in their lower sections. Shown in **Figure 2-10**, the mid-height tilt and bottom strain of the wall panel are plotted as a function

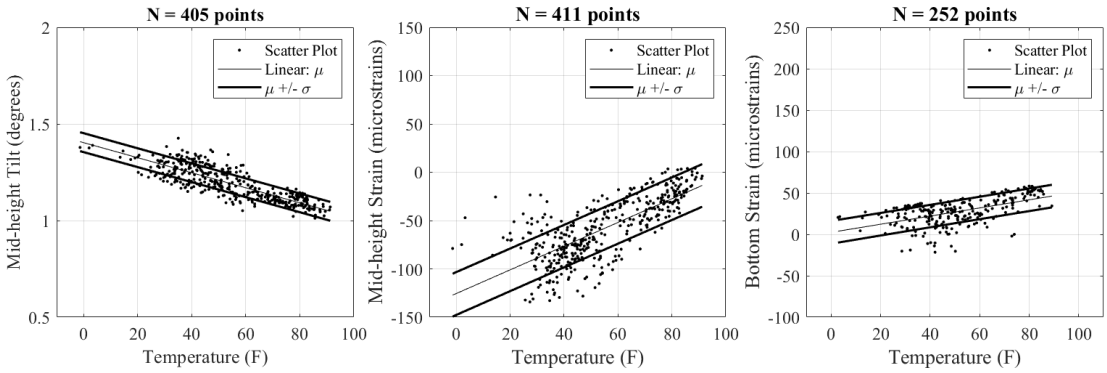

(a) (b) (c)

Figure 2.9. Thermal behavior of the monitored retaining wall: (a) mid-height tilt, (b) mid-height strain, and (c) bottom strain (August 2018 – February 2020).

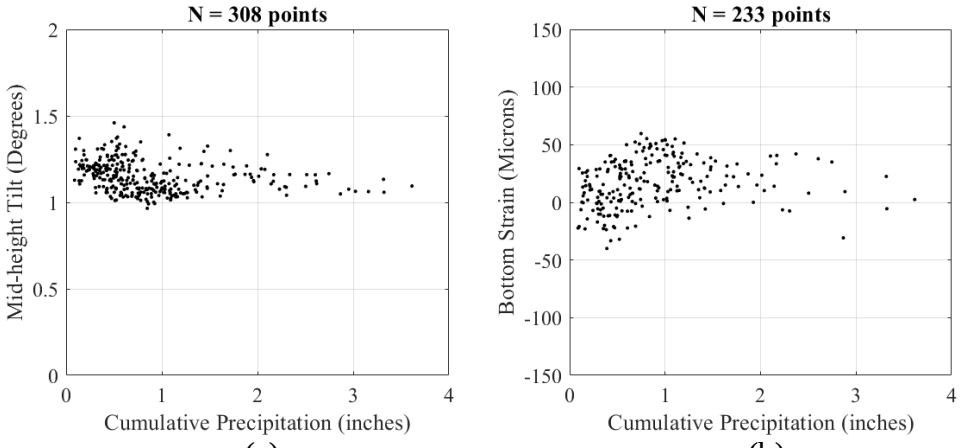

(a) (b)

Figure 2.10. Precipitation induced response of the I-696 retaining wall: (a) mid-height tilt and (b) bottom strain (August 2018 – February 2020).

of cumulative precipitation. Cumulative precipitation is intended to model the time it takes for rain water to permeate the soil and develop sustained hydrostatic pressure in the wall backfill. After periods of no precipitation, the cumulative precipitation model also assumes drying of the soil resulting in the alleviation of hydrostatic pressure. In this study, it is assumed the cumulative rain, *CR*, is:

$$CR = \sum_{j=0}^{i-1} \frac{j}{i} DR(j) + \sum_{j=i}^{t} e^{\alpha(i-j)} DR\,(j) \tag{2-18}$$

where *DR* is a daily time series of precipitation (in inches) with *j* serving as an index that begins at 0 and marches backward (*e.g.* 3 days prior is $j = 3$), *I* is a constant that reflects the tracking horizon (in days), *t* is a constant that reflects the time it takes (in days) for the soil to dry after being saturated, and α is a time constant on the tail portion of the weighted sum. Using the wall top tilt and precipitation measurements collected during a period of heavy precipitation (*e.g.,* late September 2018 into early October 2018), the cumulative rain function is empirically fit to find $i = 3$ days, $t = 18$ days and $\alpha = 0.1$. As shown in **Figure 2-10**, the mid-height tilt and bottom strain of the wall panel are insensitive to cumulative rain, reinforcing the hypothesis of a saturated back fill.

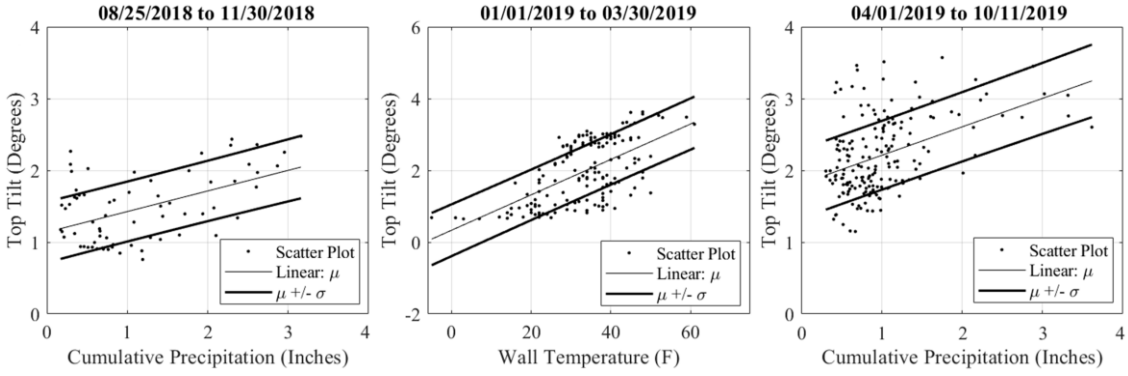

(a) (b) (c)

Figure 2-11. Tilt of wall top as a function of: (a) cumulative precipitation (August 25 to November 30, 2018), (b) temperature (January 1 to March 30, 2019), (c) cumulative precipitation (April 1 to October 11, 2019).

The behavior of the top portion of the wall panel, especially the parapet portion of the wall system, is observed to be sensitive to cumulative precipitation in the non-winter months while sensitive to temperature in the winter when there is less precipitation in the form of rain. **Figure 2-11** plots the wall top tilt as a function of precipitation from August 25 to November 30, 2018 and April 1 to October 11, 2019 revealing a linear relationship between top tilt and cumulative precipitation during the non-winter observation period. The figure also plots the top wall tilt as a function of wall temperature in the winter (January 1 to March 30, 2019) revealing a fairly strong linear relationship of 0.05° per °F due to thermal expansion of the soil applying backfill lateral pressure.

2.4.2. Modeling Loading of the Retaining Wall

Three lateral pressure profiles are explored on the I-696 wall panel: backfill lateral earth pressure, hydrostatic pressure, and surface surcharge pressure. The maximum lateral load on the wall is when all the three lateral pressures act on the wall, simultaneously. The dry backfill pressures remain constant while the hydrostatic and surcharge pressures correlate to h_{sat} and q, respectively. The maximum hydrostatic pressure occurs when h_{sat} is at the surface of the backfill (h_{sat} = 23.5 ft (7.2 m)). Similarly, a maximum surcharge pressure of q = 1.7 psi (11.7 kPa) is considered on the top surface of the backfill resulting in a uniformly distributed lateral earth pressure on the wall ($w = k_a q$). This surface surcharge is conservatively obtained from the load assumptions used to design retaining walls **[115]**. Using the Euler-Bernoulli beam model (**Equations 2-6 and 2-7**), the wall deflection, y, is modeled for the best case (no surcharge or hydrostatic pressure) and worse case (q = 1.7 psi (11.7 kPa) and h_{sat} = 23.5 ft (7.2 m)) scenarios as shown in **Figure 2-12**. The model is used in a deterministic fashion with structural and soil material mean properties used.

The Euler-Bernoulli beam model is also used to estimate the surcharge pressure, q, and level of groundwater table, h_{sat} from the top and mid-height tilts (θ_{top} and θ_{mid}) based on the algorithmic framework presented in **Figure 2-7a**. The estimated load parameters are shown in **Figure 2-13** over the monitoring period. The estimated loading parameters can then be used in the model to calculate the deflected shape of the wall. Considering all measurements from the 18 months of monitoring, the least and greatest deflected shapes of the wall are found. On January 21, 2019, the measured tilts result in the least deflection based on a surcharge of q = 0.87 psi (6 kPa) and groundwater table height of h_{sat} = 0 ft (0 m). The maximum deflection occurs on April 10, 2019, with an optimal surcharge of q = 1.7 psi (11.7 kPa) and groundwater table height of h_{sat} = 22.5 ft (6.9 m). Both deflected wall profiles are presented in **Figure 2-12**. Estimating the deflected shapes of the wall can aid in understanding the seasonal variations observed in the data, especially the wall responses to hydrostatic pressures associated with precipitation.

With load parameters extracted for each daily wall response, the flexural strain, ε_{flex}, is found for each load case at the bottom strain sensor location. Given the estimate of ε_{flex} at the point of the bottom wall strain measurement, the change in strain due to flexure, $\Delta\varepsilon_{flex}$, relative to the start of the measurement of strain is calculated. Using **Equation 2-3**, the change in thermal strain, $\Delta\varepsilon_{temp}$, is found by subtracting $\Delta\varepsilon_{flex}$ from $\Delta\varepsilon_{bot}$. Changes in $\Delta\varepsilon_{temp}$ between sequential days is calculated and plotted based on the change in daily temperatures, ΔT, as shown in **Figure 2-14**. The thermal expansion coefficient, α_{eff}, obtained was 1.89 με/°F which is close to those documented in the literature (i.e., 3 to 6 με/°F) for reinforced concrete **[116]**.

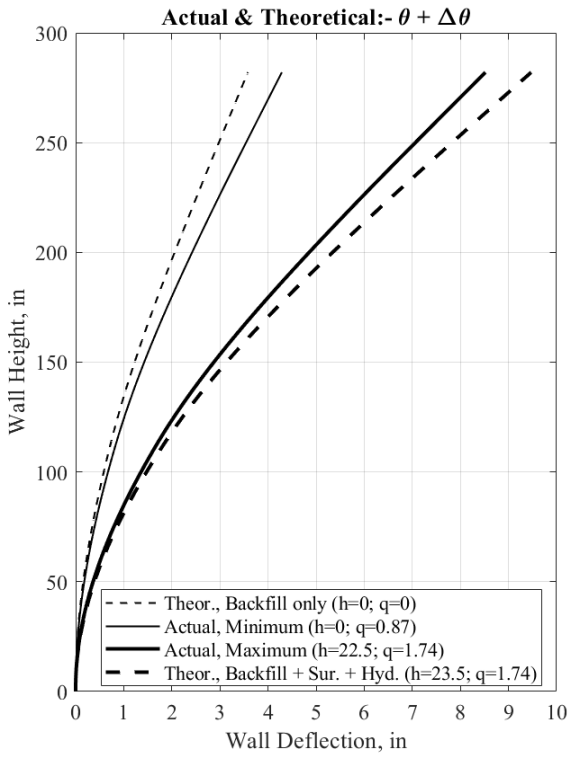

Figure 2-12. Deflected shapes of the monitored cantilever wall under theoretical and actual conditions.

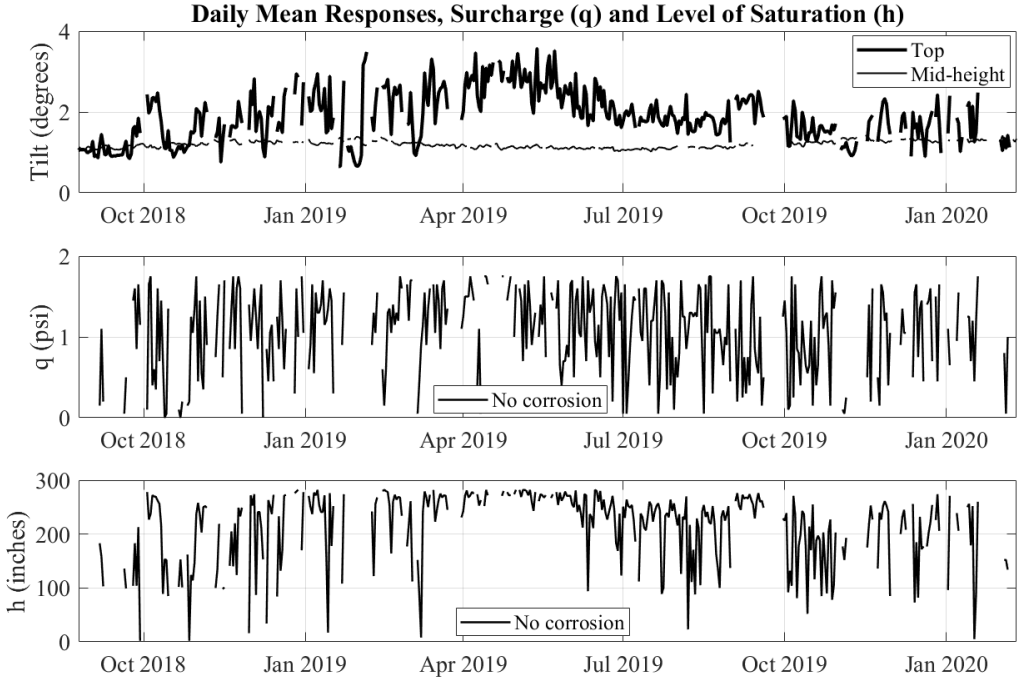

Figure 2-13. Daily mean response of tilt and estimation of surcharge load, q, and water saturation level, hsat, based on I-696 retaining wall tilt measurements over one year of monitoring period. Three states of steel section loss of the tensile reinforcement considered: 0, 10 and 20 %.

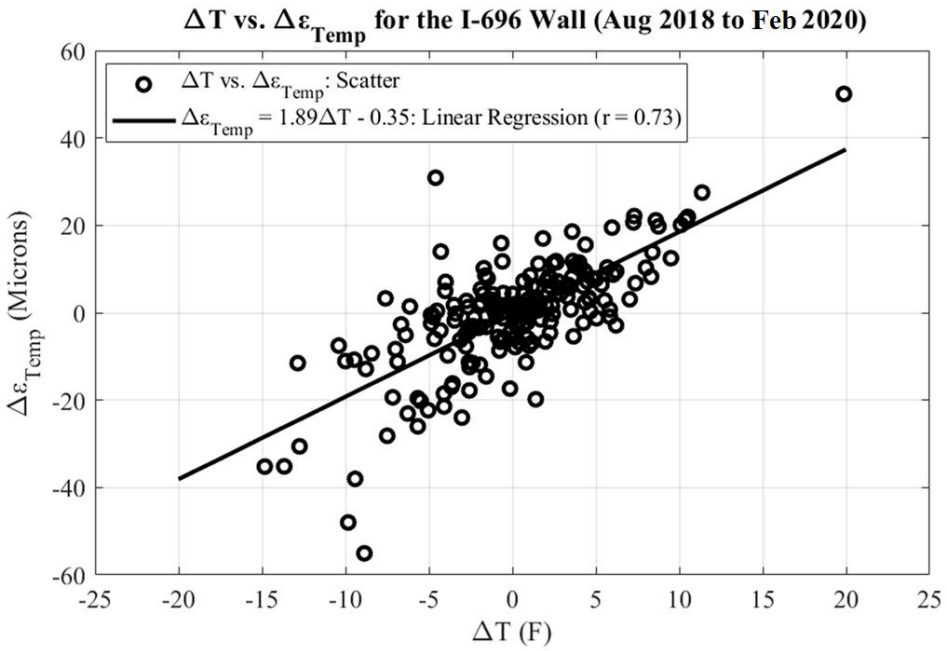

Figure 2-14. Scatter plot showing wall strain response to thermal load versus change in temperature is linear.

2.4.3. Reliability and Risk Analysis

The reliability analysis summarized in **Figure 2-7b** is applied to the mean response, $\bar{M}$, calculated for each day of the measurement campaign using the limit state function of **Equation 2-17** applied at the tensile steel reinforcement at the base of the wall. Continuous drainage at the base of the I-696 retaining wall base suggests the lower portions of the wall backfill are saturated with water. With the cantilever wall experiencing tension on the wall backside, flexural cracks on the wall backside may expose the steel rebar to water. The steel rebar on the wall backside is standard steel (*i.e.*, not epoxy coated) and has a 3" cover (**Figure 2-2**). For the cantilever retaining wall monitored in this study, the steel rebar is suspected of having some form of corrosion and possible section loss, thereby reducing the flexural capacity of the wall. Failures of retaining walls of similar age and design due to the corrosion of steel components have been observed in the past in the region in which

this wall is located. For example, panels of the M-10 retaining wall system in Detroit failed due to corrosion of tieback rods linking a section of the wall system to their caisson elements **[102]**. The challenge with retaining walls is that it is near impossible to assess if corrosion is occurring in buried steel on the backside of the wall without excavating the backfill. Should the backfill be excavated, a number of approaches are available for measuring the degree of corrosion in buried reinforcement including half-cell potential measurements and electro-impedance spectroscopy **[117]**. These methods were not practical for the operational cantilever retaining wall studied in this work.

The work of **[118]** is used to estimate the possible level of corrosion one would expect for a 33-year-old retaining wall with a moderate corrosion rate. If it is conservatively assumed that carbonation and chloride ingress occurred on the first day of construction and a moderate corrosion rate (*e.g.*, 0.5 μA/cm^2) exists, a section loss of 3% in the buried steel rebar is estimated. In this study, three states of buried vertical steel reinforcement on the tensile side of the wall are assumed given the uncertainty associated with the degree of corrosivity of the operational environment: 0, 10 and 20 % section loss of the vertical steel rebar. The reliability, $\beta_{\bar{M}}$, of the retaining wall panel is calculated for these three corrosion states. In the execution of the reliability analysis, the section loss is incorporated into the Euler-Bernoulli beam model of the retaining wall.

To perform a reliability analysis for each day of measurement, the Monte Carlo strategy samples the random variables of the model for a given level of assumed steel reinforcement corrosion (e.g., 0, 10, or 20%). The beam model is formed including the calculation of the neutral axis location, $\bar{y}(x)$, and the moment of inertia of the cracked section, I_{cr}, before being used to extract q and h_{sat} from the tilt measurements. Using the

estimated loads, the beam model is used to estimate the flexural moment at the base of the wall denoted as $M_{max.}$ The limit state function is rewritten as:

$$G(\mathbf{X}) = F_y - \left(\frac{E_s * M_{max} * (d - \bar{y})}{E_c I_{cr}} + \alpha_{eff} * E_s * (T - 68) \right) \qquad (2\text{-}19)$$

The first term within the parentheses corresponds to the flexural strain in the lower tensile steel reinforcement bars. The second term estimates the flexural strain based on the effective coefficient of thermal expansion, α_{eff}, estimated from **Figure 2-14**. The thermal strain is assumed relative to a temperature of 68 °F (20 °C). For each day, the Monte Carlo analysis is run 10 million times before convergence is achieved in the estimation of the probability of failure, P_f. The reliability index, $\beta_{\bar{M}}$, is plotted for each day in **Figure 2-15** for the case of 0, 10 and 20% section loss in the tensile reinforcement bars at the base of the wall. If no samples of the random variables result in a failed case, the reliability index is not calculated as the probability of failure is effectively zero. The calculated reliability

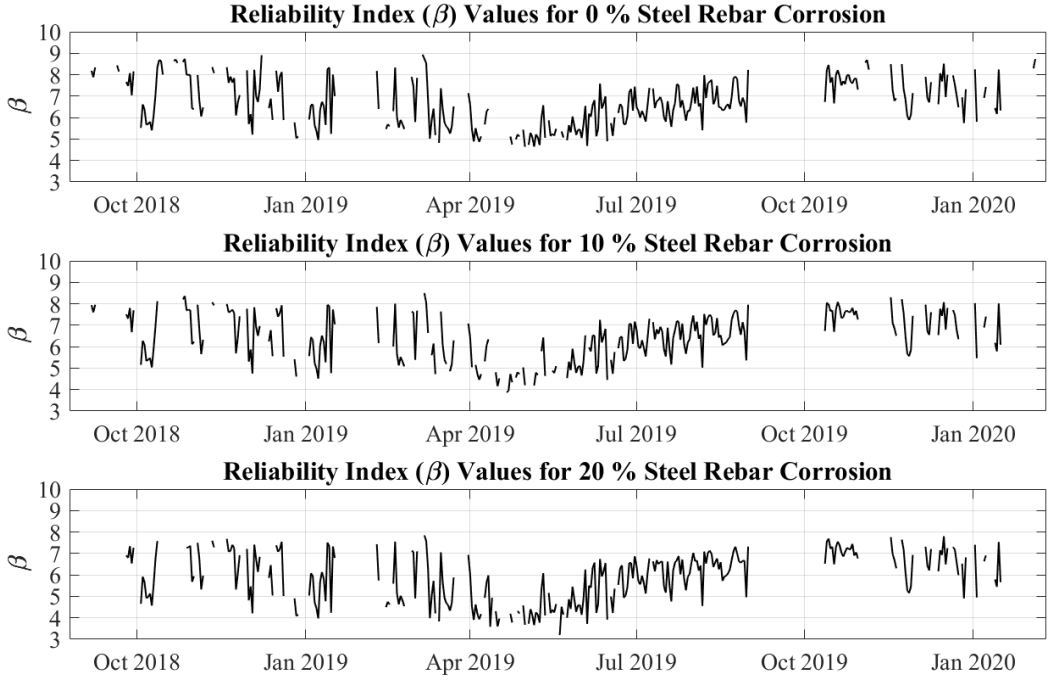

Figure 2-15. Daily variation of the reliability index (β) values of the I-696 retaining wall system for 0, 10 and 20% corrosion states of the steel rebar on the wall tension side.

indices for all three assumed steel reinforcement states are above 3 which is where load resistance and factor design (LRFD) codes today would aim to achieve. For the 10 and 20 % rebar section loss cases, the reliability index is still above 3 but varies between 3 to 9.

Risk assessment considers the reliability index (providing the probability of exceeding a defined limit state) and the consequences associated with exceeding the limit state with risk is simply the probability times the consequence of exceeding the limit state. Clearly, the probability of failure estimated for each day of monitoring can be used to assess the wall risk. However, the estimation of the consequences of failure remains difficult for the wall owner to do. More practical is for the owner to define if the consequences are low, medium, or high as opposed to defining precisely in the form of failure cost. Similarly, the likelihood of failure can be binned into three categories based on two levels of reliability index: β_{low} and β_{high}. In this study, the upper threshold, β_{high}, is set to 3 which corresponds to the level of safety sought in retaining wall designs by LRFD. In consultation with the retaining wall owner (i.e., MDOT), the lower threshold, β_{low}, is set to 2. This established three categories of failure likelihood: low ($\beta_{\bar{M}}$>3), medium (3>$\beta_{\bar{M}}$>2), high (2>$\beta_{\bar{M}}$).

Based on the low-medium-high bins for both failure likelihood and consequence of failure, a table defining the perceived risk of the asset is formulated as shown in **Table 2-2**. The colors green, yellow, and red correspond to low, medium, and high levels of risk. In the case of the I-696 wall monitored in this study, its structural function is to support a

Table 2-2. Red-yellow-green (R-Y-G) risk categories mapping reliability index (β) values with consequence of failure event.

Reliability Index	Consequences		
	Low	Medium	High
β > 3	Low Risk	Low Risk	Medium Risk
2 < β < 3	Medium Risk	Medium Risk	High Risk
β < 2	Medium Risk	High Risk	High Risk

two-lane service road (Eleven Mile) above an eight-lane freeway (I-696) in a high-volume traffic region (i.e., metropolitan Detroit). This means the wall failure would have a level of high consequence if it failed including closure of Eleven Mile, closure of the I-696 ramp, and potential partial or full closure of eastbound I-696. Given the high reliability but high consequences, **Table 2-2** would classify this asset as "yellow" indicating more vigilant observation by visual inspection.

2.5. Conclusions

In this study, a quantitative approach that informs Risk-based Asset Management (RBAM) decisions for retaining wall systems is presented. The approach uses structural monitoring data for the reliability analysis and risk assessment of retaining wall assets. It was motivated by the Transportation Asset Management (TAM) program that is integral to the Moving Ahead for Progress in the 21st Century Act (MAP-21) which requires the adoption of risk management strategies for all highway structures inclusive of retaining walls. As a result, an illustrative example of analysis was conducted using monitoring data of a 30+ years old classical reinforced concrete (RC) retaining wall system along the I-696 freeway corridor in Southfield, Michigan. The monitoring data was combined with visual inspection information to calculate load demands on the wall to be quantitatively assessed and rapid installation of a monitoring system was practiced providing data on wall behavior. The installation adopted tiltmeters to measure wall tilt, long-gage strain gages to measure thermal and flexural strains, and thermistors to measure wall temperatures. Specifically, should tilt be measured on irregular basis (for example, manually) or regularly over a short period (say a few weeks or months), the maximum wall response may not be observed. The

short-term variations of the wall tilt can be significant (such as the top of the I-696 wall); a more accurate view of wall behavior require at least one year of monitoring to see the full range of seasonal variations. The proposed method does not fully replace the current retaining wall visual inspection methods, but it rather uses visual inspections to narrow down on list of alternative retaining wall systems to do structural monitoring on. In addition, current research on the reliability of retaining wall structures primarily focused on the design stage considerations particularly, by defining probabilistic curves on the serviceability side. The strategy was to treat lumped factor of safety useful for the design of foundations and retaining walls. However, this study intends to also contribute on demonstrating after-construction reliability study for retaining wall systems.

Based on the collected wall response data, the I-696 retaining wall system exhibited strong dependence on environmental parameters, most notably temperature. The wall showed higher drifts on its top section as compared to the mid-height. Moreover, for inferring reliability index values from probabilities of failure, Monte Carlo simulation was conducted. The simulation was run on randomly generated 1 million datapoints by computing inverse cumulative distribution function (icdf) values for different modeled probability distributions: E_s (Gaussian), E_c (Gaussian), γ_{b_1} (Uniform), γ_{b_2}(Uniform), γ'_1 (Uniform), γ'_2 (Uniform), ϕ_1 (Uniform), ϕ_2 (Uniform) and F_y (Beta or Gaussian). The analysis of the wall was simplified by discretizing the wall into 1" sections (δh) with equilibrium applied. While the wall could be discretized more finely, the 1-inch discretization size was found to be sufficiently precise. Two specific loads were considered in the analysis: lateral earth pressures (resulting from a surface surcharge and saturation of the soil) and thermal loads associated with the temperature of the wall. Tilt measurements

are not influenced by axial expansion of the wall due to thermal loads; this allows tilt measurements to be used to isolate the flexural behavior of the wall including the flexural strain in the steel rebar, $\varepsilon_{steel,flex}$, in the critical zone at the base of the wall. Provided the visually observed drainage from the lower portions of the wall, it was hypothesized that the uncoated vertical steel reinforcement bars may have experienced corrosion. Without a direct measure of corrosion state, three corrosion states were considered for the wall: 0, 10, and 20 % section loss of the steel reinforcement for calculating the corresponding reliability index, β values. Tilt measurements provided a direct means of estimating the strain in the wall due to flexural bending. The strain measured on the front face of the wall was then used to isolate the thermal strain in the wall associated with the measured wall temperature. Moreover, the thermal axial loading and flexural moment from the backfill were then used to estimate the load effect in the vertical steel reinforcement on the wall backside.

Moving forward, incremental applied research can be extended beyond what is presented in this study. That is, different designs of retaining wall systems could be considered such as, but not limited to: tie-back (caisson) supported retaining walls, mechanically stabilized earth (MSE) walls, gravity walls, sheet piles, etc. Moreover, earth retaining structure (ERS) inspection manuals would need to be rigorously developed and become adopted by state transportation departments by incorporating strategic ways to prioritize existing ERS systems in their inventory requiring due attention because of ageing or any developed damage during operation. This way, critical infrastructure units would be nondestructively monitored for structural responses using sensor installations as a very low-cost solution alternative. Besides, the structural responses could be tied to a reliability framework helpful for quantitative decision-making of asset managers.

Chapter 3: Rapid-to-Deploy Water Pressure Sensors for the Assessment of Water Distribution Systems

3.1. Introduction

Municipal water distribution systems are designed to provide safe drinking water to communities while also providing high-pressure water for firefighting purposes. Ensuring the system meets intended performance objectives including maintaining adequate pressure in the system is the system operator's responsibility **[119]**. A well-performing drinking water distribution system must be well maintained to ensure it can respond to customer demands, especially as the community demand may change over time **[120]**. Proper management of the system entails the use of sensors to monitor system performance and hydraulic models that simulate system behavior under various user demand scenarios **[121]**.

Pressure and flow sensors are used commonly in water transmission and distribution systems. Such sensors are connected to supervisory control and data acquisition (SCADA) systems to centrally aggregate the operational data collected. SCADA-based sensors are expensive and must be properly maintained resulting in operators deploying them to only the most critical locations (e.g., in the treatment plant and vicinity of system pump stations). Concurrent with data collection, system operators also rely on hydraulic models to simulate the behavior of their systems and to forecast system behavior to changing community demand **[121]**. Models are created using information from the system design including pipe

locations and properties (e.g., material type, diameter, head loss per unit length) along with the location of the system water intakes, reservoirs, and pumps. The models are useful for estimating steady-state pressure and flow responses allowing operators to determine pressure thresholds that ensure the delivery of safe water to consumers **[122]**. More sophisticated hydraulic models are also capable of measuring transient behaviors associated with the operation of system pumps. Such models are being used to better understand the spatiotemporal patterns of transient pressures that may be adversely impacting pipes over long operational periods.

There are four major reasons to monitor water pressure in distribution systems: preserving water quality, reducing operational costs, reducing the frequency of pressure variants, and preventing pipe failure **[123]**. High pressure is needed to ensure groundwater does not seep into the distribution system pipes, thereby preventing contamination of the treated water. Pressure with flow information is essential for monitoring the time it takes for treated water to transit through the system. This information is used to estimate the concentrations of treatment chemicals (e.g., chlorine) present at consumer taps. Pressure also provides sufficient head for the reliable operation of hydrants during firefighting operations. Major leaks in the system due to pipe deterioration over time are costly because the lost treated water is not paid for by customers. Steady-state hydraulic models like EPANET are often used to explore variations in pressure to estimate leak locations **[124]**. Once areas of leaks are suspected, pressure measurements can be used as input to management strategies that aim to assess leak severity and estimate long-term service degradation **[125]**. To improve the modeling capacity of simulation tools, researchers have altered the source code of EPANET to exhibit greater modeling sensitivity in pressure-

deficient systems **[126]**. The role of sensor data in modeling of water systems also have rich traditions **[127]**, **[128]**, **[129]**. In particular, pressure transients are serious concerns for long-term structural integrity of water systems. Large and frequent pressure transients can fatigue system components and may trigger structural failures that result in major leaks **[130]**.

Pressure-deficient water distribution systems have been an area of active research over the past two decades with hydraulic models explored to inform sensing strategies aiming to detect undesired system behaviors **[131]**. For example, researchers have explored pressure- and demand-dependent hydraulic models to estimate steady-state pressure and flow in a system in order to optimally place sensors in the system **[132]**. Water pressure sensors have been proposed to identify leaks in the municipal water distribution system of Barcelona, Spain; the deployment of a finite number of sensors to detect leaks was proposed based on solving discrete optimization problems using genetic algorithms **[133]**. Other studies have also focused on sensor placement strategies for their respective monitoring and system evaluation objectives **[134]**, **[135]**, **[136]**, **[137]**. Most of them assume a monitoring paradigm of permanent pressure and flow sensors in the water distribution system. With the emergence of low-cost urban sensors, new monitoring paradigms for distribution systems are now possible. This study builds upon these advances to demonstrate a modular, user-friendly wireless water pressure sensor capable of rapid deployment across a system to collect pressures for short observation periods (e.g., a few days).

The key intellectual merit of this study was to develop a simple and cost-efficient data-driven approach to model system pressures in aging water distribution systems administered by cities with limited resources and whose use of the water distribution system has changed over time due to disconnects and changing populations. Thus, the goal was

twofold. First, it was to report on the design of a standalone and low-cost water pressure sensor that can be rapidly deployed on-demand across a city to measure steady-state water pressures. The wireless pressure sensor was designed to move freely from consumer to consumer to allow for dense pressure mapping in a water distribution system with sensor locations tracked by a GPS receiver included in the sensor design. The pressure data collected was locally analyzed by the wireless sensor with average pressures communicated by cellular modem to a cloud database where data was stored for long-term management. The second goal of the work was to use the proposed pressure measurement solution to monitor water pressures in the City of Benton Harbor, Michigan. The water distribution system operator sought a means of identifying low, medium, and high-pressure zones in their pipe network. To enhance the value of the data collected, hydraulic models were used to explore collected measurement data and to model performance of the distribution system.

3.2. Wireless Monitoring System

To provide a rapid-to-deploy wireless sensing solution to measure pressures in water distribution systems, a pressure sensor requiring minimal training was proposed. The sensor must be accurate in measuring pressures without requiring entry to a consumer's home or place of business. The system design assumed the installation of the sensor on outdoor hose spigots. Also, the sensors must be free from dependence on a hard-wired electrical power supply; hence, they needed to be battery operated capable of two deployment days. To minimize the need to keep accurate logs of sensor locations and times of deployment, the sensor had to include a GPS receiver to track installation location and data collection times. If these objectives were met, they ensure a technician can go to a location, attach the sensor to a hose spigot, turn on the sensor, and leave before returning few days later to retrieve it.

3.2.1. Urbano Wireless Sensing Node

To collect water pressure, a wireless sensing node termed *Urbano* **[94]** was adopted in this study. *Urbano* had been previously used for retaining wall monitoring **[138]**, structural asset management **[68]**, methane emission monitoring in landfills **[139]**, and to track pedestrians in urban settings **[94]**. *Urbano* (**Table 3-1** and **Figure 3-1a**) was a low power node that utilizes cellular communications to directly transmit its data to the Internet. This was a very attractive feature because it eliminated the need for on-site access points to communicate measurement data. Use of a 4G cellular modem (Nimbelink Skywire) had other advantages including high data rates (5 Mbps) and the ability to time synchronize the sensor. The radio consumed 616 mA (referenced at 3.3V) when transmitting, 48 mA when idle, and 8.6 mA when in low-power mode. To minimize the energy consumption of the radio, it was mostly in sleep mode and turned on only to transmit data to the Internet. For operation, the design of *Urbano* relied on an 8-bit microcontroller (Atmel Atmega2561V) that was powered with a 3.3V source and clocked at 8 MHz; when active, the microcontroller consumed only 7.3 mA (and 4.55 μA in power-save mode). The microcontroller had 256 kB of flash memory for program storage and 8 kB of SRAM for data storage. The limited SRAM required additional off-chip memory; 512 kB of SRAM (Cypress CY62148EV30) was included in the node design. The microcontroller included a multi-channel, 10-bit analog-to-digital converter (ADC) capable of a sample rate of 200 kHz. In this study, the on-chip ADC was used to measure water pressure from a pressure transducer interfaced.

3.2.2. Sensing Transducers

For the measurement of water pressure, a resolution of about 1 pound per square inch (psi) (6.895 kPa) was sought; the Seeed Studio (Product No 114991178) pressure sensor (**Figure**

3-1b) was selected. The pressure transducer was powered by a 5V source and had a working current of 10 mA. Depending on the amount of water pressure to sense, the sensor outputted a voltage (V_{out}) ranging from 0.5 to 4.5V corresponding to 0 psi (0 Mpa) to 174 psi (1.2 Mpa), respectively. With water distribution systems having steady-state pressures well below 174 psi, the pressure sensor was considered ideal for the application. In theory, the pressure sensor could withstand a surge pressure of 348 psi (2.4 Mpa). The response time of the pressure sensor was less than 2 ms. Moreover, the working temperature of the sensor was -20 to +105 ℃ ensuring it would operate properly in most outdoor applications **[140]**. The pressure sensor was interfaced to the *Urbano* 10-bit ADC for data sampling. Even though the pressure sensor could output voltages up to 4.5V, the *Urbano* could only measure

Table 3-1. Specifications of the *Urbano* wireless sensor for data collection.

Characteristic	Specification
Computational Core	8-bit RISC at 8 MHz
Memory	256 kB Flash; 512 kB SRAM
Sensor Interface	10-bit ADC (8 differential or 16 single-ended channels)
Base Power without Cell	75 mW (Active); 21 uW (Sleep)
Cellular Communications	Verizon 4G Cellular Modem (2W power)

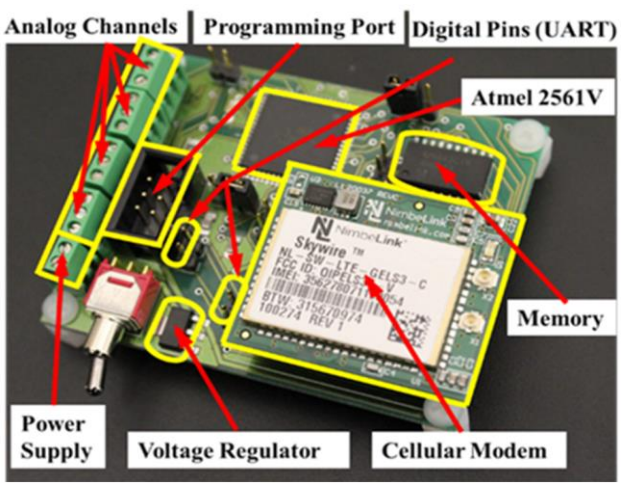

(a)

(b)

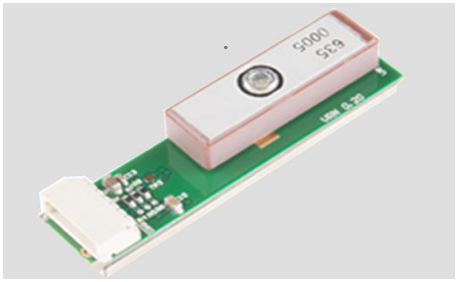

(c)

Figure 3-1. (a) Hardware components of the *Urbano* wireless sensor; (b) Seeed Studio (Product No 114991178) pressure sensor; (c) ADH GP-735 GPS receiver.

voltages up to 3.3V (corresponding to 121.8 psi (0.84 Mpa)). Given the ADC resolution of 0.98 mV, *Urbano* could measure pressure down to 0.04 psi (0.276 kPa).

To measure the spatial coordinates of the unit and to track time, a GPS receiver (**Figure 3-1c**) was integrated with the *Urbano* node. The ADH Technology GP-735 GPS receiver with a horizontal position accuracy 8.2 feet (2.5 meters) was selected. The GPS receiver had a start time of 29 s when first turned on in order to lock onto the GPS satellite constellation. The receiver was operated at 3.3V while drawing 37 mA of current. The GPS receiver transmitted its data to *Urbano* using the UART serial communication protocol. The output data rate could be varied based on the configuration of the receiver from 1 to 10 Hz **[140]**. The ADH GP-735 receiver data packet could output seven NMEA sentences that contain positioning data: GPGGA, GPGLL, GPGSA, GPGSV, GPRMC, GPVTG, and GPTXT. Of the 7 sentences, the GPRMC sentence (time, date, position, course, and speed) was read by *Urbano* to obtain the latitude, longitude, and UTC time. An additional feature of the GP-735 is that it included temperature compensation between - 40 ºC to 85 ºC **[141]**.

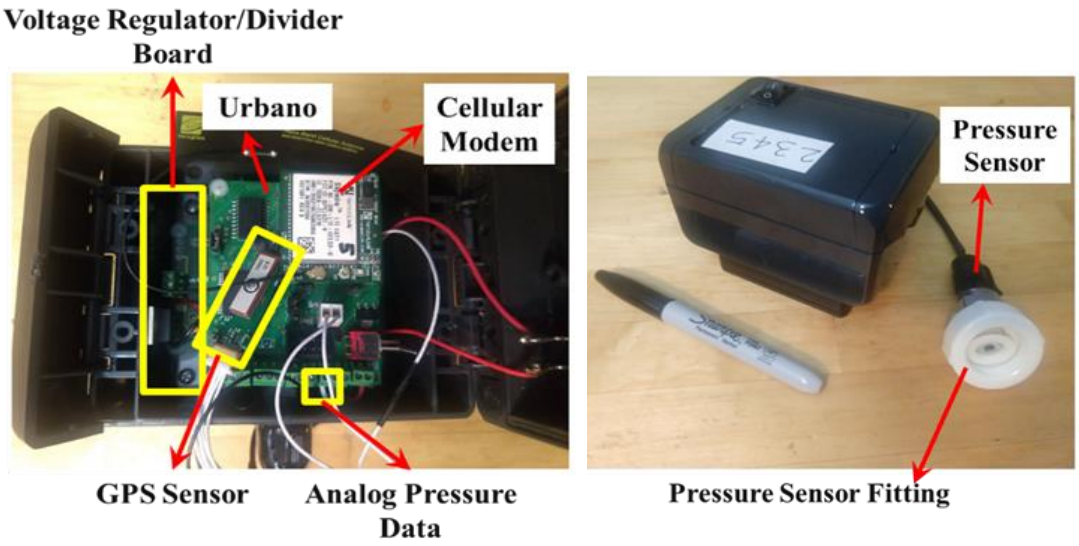

(a) (b)

Figure 3-2. (a) Electronics components inside the pressure sensor unit; (b) Finished wireless pressure sensor unit.

3.2.3. Finishing and Packaging

The *Urbano* wireless sensor node was packaged in a small water-tight enclosure from Bopla (~10 x 10 x 7 cm^3) with an external on/off switch installed (**Figure 3-2**). Inside the enclosure was an *Urbano* node, GPS smart antenna receiver, and signal conditioning circuit for the pressure transducer. The water pressure sensor was kept outside the enclosure but connected to the *Urbano* ADC through a multi-stranded shielded wire that penetrates the enclosure wall. A battery pack with four rechargeable 1.5V AA batteries was attached to the outside of the enclosure with a wire penetrating the enclosure to deliver power to 3.3V and 5V voltage regulators used to power the *Urbano*, GPS receiver, and pressure transducer. The Seeed Studio pressure sensor was connected to a hose spigot during use. This required a custom threaded and watertight fitting to be created. Initially, a 3D printed connection was attempted but lacked robustness over multiple uses. Hence, the final fitting was made from

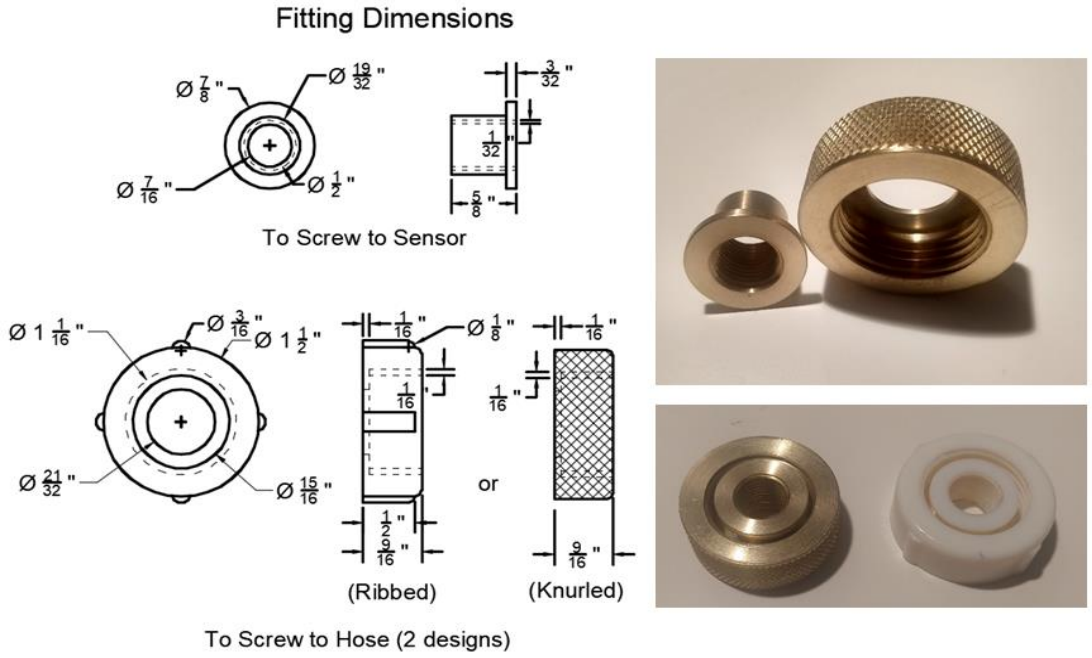

(a) (b)

Figure 3-3. (a) Designed dimensions of brass fittings, (b) Manufactured brass fittings compared to 3D printed plastic fittings.

brass on a lathe with a standard thread machined for typical household hose spigots. The fitting (**Figure 3-3**) proved to be watertight, extremely robust, and easy to use.

3.3. Data Acquisition and Communication Architecture

The wireless water pressure sensor was designed with an external switch that could turn the unit on once the fitting end of the pressure sensor was connected to the hose spigot (and the spigot valve was fully opened). After turning on, the embedded firmware of *Urbano* (whose state diagram is shown in **Figure 3-4**) entered into a start mode where it waited for 5 minutes to connect the 4G LTE modem to the cellular network and GPS receiver to the GPS satellite constellation. Once confirmed, the node recorded the node location (longitude and latitude) and time (UTC) from the GPS receiver. Next, the pressure was measured for 10 s at 1 Hz with the 10-bit voltage of the sensor output stored temporarily in memory. After collecting data for 10 s, the node converted the 10-bit numbers to floating-point pressure measurements with the 10 data points averaged. The node location, time, and average pressure were then communicated before the cellular modem was put to sleep. The node woke the radio up after 1 hour to repeat its data collection process. If the node was deployed in a location where the GPS receiver could not lock onto the satellite constellation after five minutes, the node moved on without logging time or location.

The cloud platform used in this study was Amazon Web Service (AWS) IoT Core that enabled communication between the cellular modem on the *Urbano* node with the AWS IoT Core using the MQ Telemetry Transport (MQTT) protocol. AWS IoT Core had a setting that enabled the definition of a device shadow on the portal to permit for the reception of *Urbano* data. To facilitate this connection via the cellular modem, the appropriate security

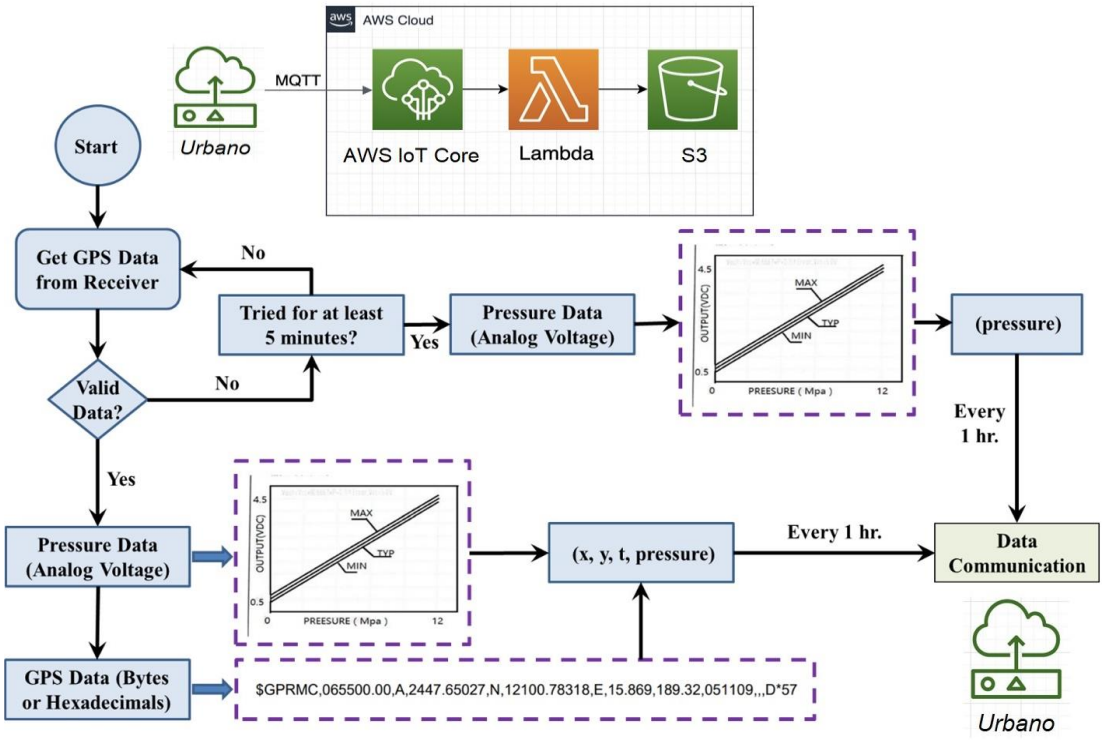

Figure 3-4. State machine diagram of *Urbano* node's data acquisition and communication to AWS.

certificates were installed on the 4G LTE cellular modem. The data posted by the wireless water pressure sensor to the AWS IoT Core device shadow was then stored in a CSV file contained in the AWS storage bucket (s3) using AWS Lambda (see **Figure 3-4**).

3.4. Water Distribution System Modeling

3.4.1. Overview of the System in Benton Harbor, Michigan

The City of Benton Harbor (pop. 10,036) is located in southwest Michigan and is distributed over a 4.7 sq. mile (12.2 sq. km) area near the shore of Lake Michigan **[142]**. The city water distribution system has 1701 water main segments (**Figure 3-5**), 518 hydrants, and several system truncated locations due to adjoining townships having detached from the Benton Harbor system over time to operate their own systems. These disconnections have affected the performance of the Benton Harbor water system with zones of low-pressure raising

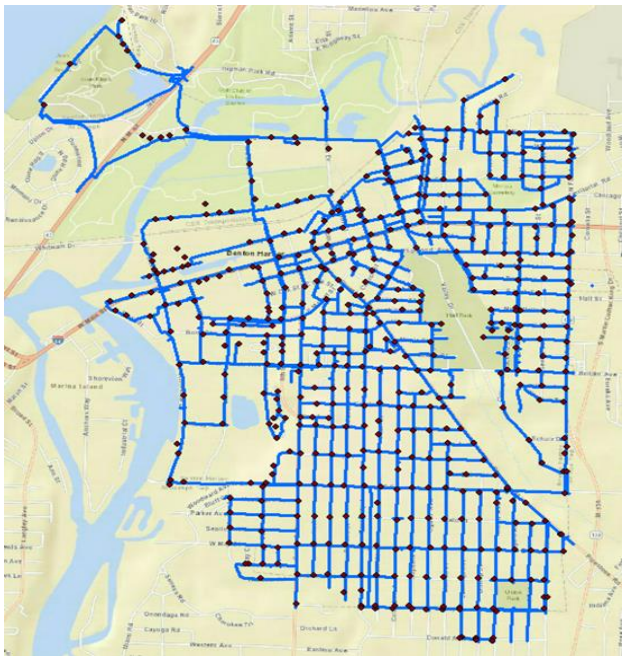

Figure 3-5. Pipe network of the water distribution system in Benton Harbor.

water service quality concerns within the community [143]. With the resource base of the city limited, the community sought simple wireless water pressure sensors that citizens could use to verify zones suspected of low water pressure.

3.4.2. Modeling using InfoWater

Benton Harbor's water distribution system contains a water treatment plant, a reservoir, and a pump station. The majority of the system was installed during periods of city growth (e.g., 1910s, 1930s, 1950's and 1960s). Pipe sizes vary in which diameters vary from 4 inches (10 cm) to 20 inches (50 cm); pipe materials also vary but cast iron is most common. Hydraulic simulation was conducted using InfoWater (by Innovyze) which incorporates GIS mapping of the water system (**Figure 3-5**). InfoWater is an advanced modeling tool for water distribution networks that uses hydraulic simulation in an ArcGIS environment based on continuum equations of mass, momentum, and energy [144], [145]. A hydraulic model (calibrated in April 2022) from the water department of the city government of Benton

Harbor was used for simulation. In addition to the pipe material, year of pipe installation, dimensions, roughness, component type, GIS coordinate, etc. details defined in the model, the hydraulic head from the pumping station was calibrated as in the following equation:

$$H\ (feet) = 340 - 0.035 * Q(gpm)^{1.5} \quad (3\text{-}1)$$

To calculate the pressure levels in Benton Harbor's pipe network, Bernoulli's and continuity equations were used to solve the steady-state flow of incompressible fluid (i.e., water). **Equation 3-2** is listed to consider the hydraulic loss between two points along a pipe:

$$\frac{v_1^2}{2g} + \frac{p_1}{\rho g} + z_1 = \frac{v_2^2}{2g} + \frac{p_2}{\rho g} + z_2 + \Delta h \quad (3\text{-}2)$$

where z is the elevation head, $v^2/2g$ is the velocity head, and $p/\rho g$ is the pressure head. Hydraulic loss (Δh) can be caused by friction or other factors and is expressed by the Darcy-Weisbach equation:

$$\Delta h = f\frac{L}{D}\frac{v^2}{2g} \quad (3\text{-}3)$$

where f is the friction factor, L is the length of the pipe, and D is the diameter of the pipe. Moreover, SCADA data including pump curve, valve status, and flow rates can be used in InfoWater to calculate the pressure in the entire water distribution system.

3.5. Data Collection and Analysis

3.5.1. Field Installation

In Fall 2021, five (5) wireless pressure sensor units were installed at nine (9) selected locations in Benton Harbor as shown in **Figure 3-6**. Specifically, six monitoring days were picked between 09/15/2021 to 09/27/2021 for at least 24 hours of continuous pressure measurement per day per location. The reason for the selection of these specific days was

(a) (b) (c)

Figure 3-6. Photos of 3 sample installations out of the 9 selected locations that were monitored using water pressure sensors.

to get the possible variation of water pressure over the day and during the week (e.g., weekday versus weekend variation). The field installation procedure had two phases: Phase I monitored 5 locations on 2 weekdays and 1 weekend day; Phase II then monitored 4 locations on another 2 weekdays and 1 weekend day. When installing the water pressure sensors at the selected locations (**Figure 3-7c**), a technician with limited expertise in the operational principles of the nodes deployed the nodes for data collection. Once placed, each node was attached to a hose spigot, the spigot was opened, and the node was turned on at which time the technician left the location to install another.

3.5.2. Water Pressure Data and Model Comparisons

The *Urbano* wireless sensor nodes successfully collected data from all nine (9) deployment locations. Overall, the collected pressure measurements were stable while significant pressure drops were observed at three (3) locations (**Figure 3-8a**). The causes for these drops were unknown, but a faulty pressure sensor was ruled out. Nonetheless, for most of the observation period, water pressure measured over a 24-hour period resulted in reliable steady-state measurements. This clearly indicated that water pressure variation was minimal over time with the occurrence of short-lived outliers that may have incidental influence.

Moreover, average water pressure measurements per location and per day (**Table 3-2**) were calculated from the raw pressure data as shown in the time series plots of **Figure 3-7**.

Table 3-2. Daily average water pressure (*p*) per location.

Unit	X	Y	Average Pressure – psi (kPa)	2021 Date	Phase
1022	-86.4456	42.1205	61.94 (427.1)	9/15	I
4004	-86.4429	42.1120	42.97 (296.3)	9/15	I
1022	-86.4457	42.1205	62.42 (430.4)	9/17	I
1234	-86.4551	42.1176	77.00 (530.9)	9/17	I
3003	-86.4463	42.1038	61.29 (422.6)	9/17	I
5005	-86.4541	42.1053	62.84 (433.3)	9/17	I
1022	-86.4456	42.1204	62.70 (432.3)	9/20	I
1234	-86.4551	42.1176	76.61 (528.2)	9/20	I
3003	-86.4463	42.1038	61.59 (424.6)	9/20	I
5005	-86.4541	42.1053	64.71 (446.2)	9/20	I
1022	-86.4374	42.1181	58.88 (406.0)	9/22	II
1234	-86.4597	42.1194	39.03 (269.1)	9/22	II
5005	-86.4535	42.1021	60.81 (419.3)	9/22	II
1234	-86.4597	42.1194	45.49 (313.6)	9/24	II
3003	-86.4432	42.0952	55.81 (384.8)	9/24	II
5005	-86.4536	42.1021	59.40 (409.5)	9/24	II
3003	-86.4432	42.0952	57.15 (394.0)	9/27	II

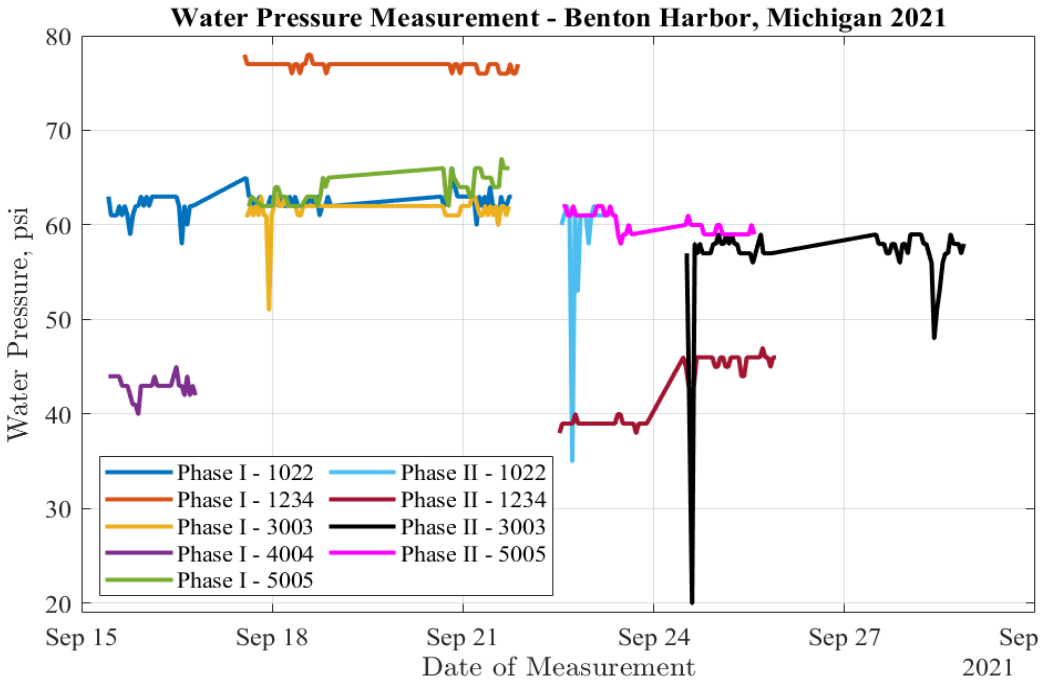

Figure 3-7. Mapping of average water pressure (*p*).

To visually observe the spatial variation in pressure, the average water pressure measurements collected were mapped (**Figure 3-8a**) to identify zones of high, medium and low pressure. For example, location 4004 during Phase I and location 1234 during Phase II reported low water pressure values (42.9 (296) and 39.0 (269) psi (kPa), respectively. The

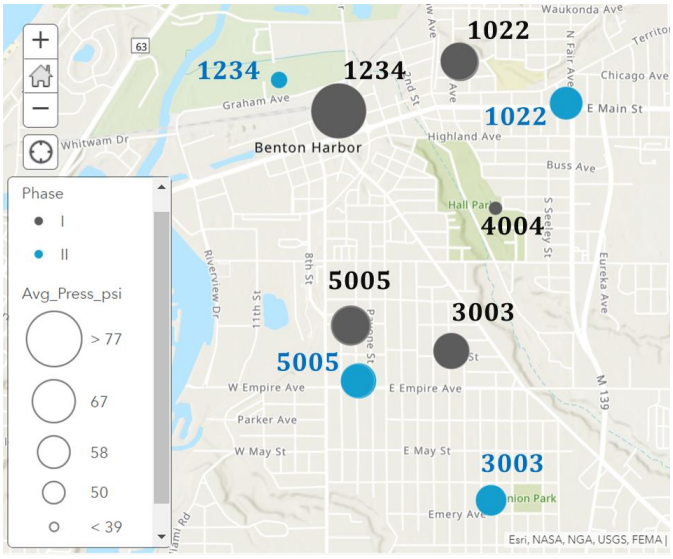

(a)

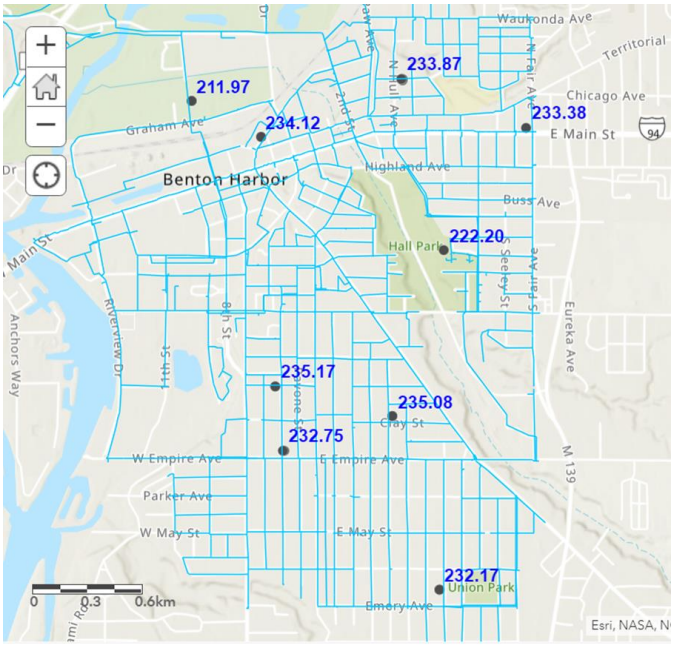

(b)

Figure 3-8. (a) Time series plot of water pressure measurements at 9 locations; (b) mapping of water pressure head ($h = p/\gamma$) + elevation above mean sea level (z) in meters with the pipeline network layer.

first contributing factor considered was the potential effect of ground elevation; therefore, pressure head ($h = p/\gamma$) and elevation head (z) were mapped (**Figure 3-8b**). Based on these results, it was deduced that ground elevation was not a major contributing factor to the lower pressures observed at 4004 (Phase I) and 1234 (Phase II); rather, systemic issues were hypothesized to be the cause. Incidentally, after data was collected, a pipe ruptured close to 1234 (Phase II) in October 2021. This rupture led to the cutting of water pressure for the entire city for more than a day. Water system officials have different views on the causes of the breakage ranging from irregularity in water pressure in the pipe network **[146]**, **[147]** to a water pipe failing from age **[148]**.

3.5.3. Evaluation of InfoWater Model Results

When designing a water distribution system, a water pressure of at least 33 psi is recommended to satisfy system pressure requirements **[149]**. However, minimum of 20 psi (138 kPa) is necessary to ensure groundwater doesn't enter the system and water quality is maintained **[150]**. To ensure adequate hydrant pressure, minimum residual pressure of 25 psi (172.4 kPa) is also recommended **[151]**. The measurements in Benton Harbor met these requirements at all locations with 42 psi (289.60 kPa) being the lowest pressure measured.

In **Figure 3-9a**, a comparison is made between the pressure sensor measurements and InfoWater steady-state hydraulic simulation results. It is important to note that the hydraulic model made a number of assumptions about the distribution system so perfect agreement (0-10%) between the model and the measurements wa not expected. Rather, only general agreement (10-25%) was desired to verify that the model offers a reasonable depiction of system behavior. Once verified, the model was then used to explore possible scenarios of system leaks to help describe what is observed.

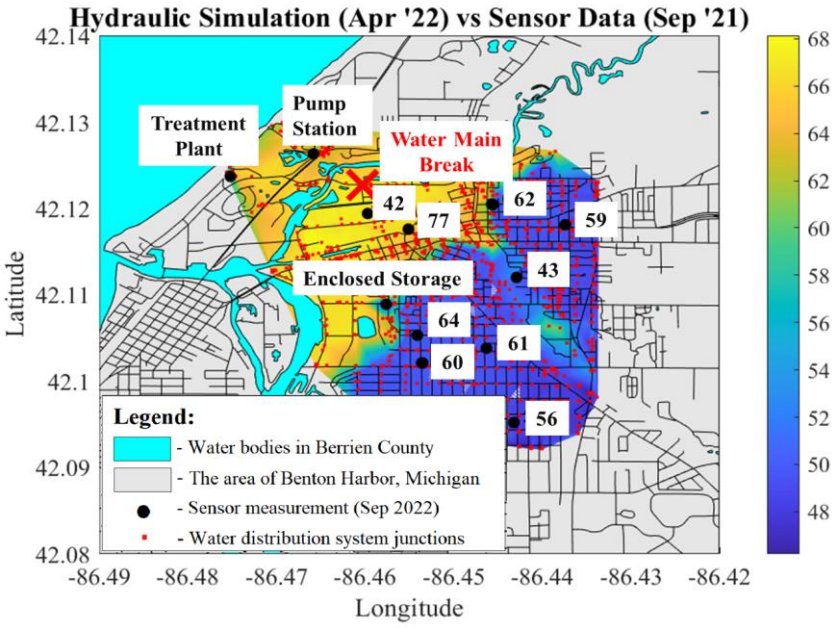

(a)

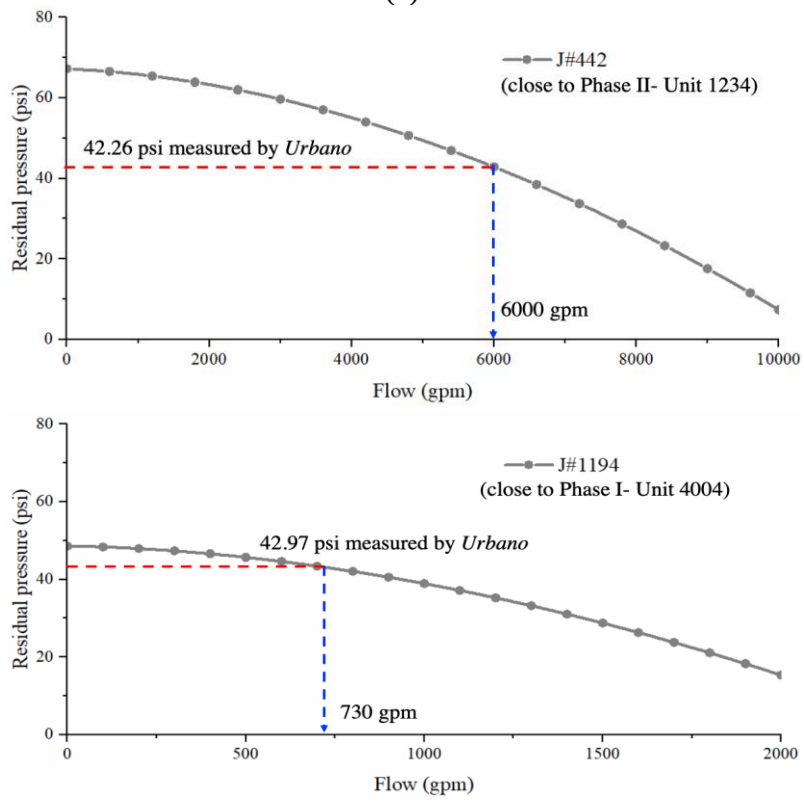

(b)

Figure 3-9. (a) Comparison of the hydraulic simulation result from InfoWater versus water pressure sensor measurement collected in Sep 2021 with the location of the Oct 2021 water main break denoted (measurement units are psi); (b) flow vs residual pressure for the two locations where pressure sensor measurements were low in Sep 2021.

The hydraulic simulation results were plotted as a contour map with the measurements (in psi) overlayed. Aside from location 4004 during Phase I and location 1234 during Phase II, the measurements collected followed the general spatial pattern of pressure predicted by the model. In short, as you move further away from the pump station, the pressure drops. Table 3-3 shows the measured pressures from the sensors deployed and that predicted by InfoWater at the junctions closest to the nine sensor locations. As can be seen from the table, the absolute average values of pressures measured and that predicted by the model differ, but all were within 25% excluding location 1234 in Phase II (37.6% difference). When comparing the numerical results, the measurements at location 4004 in Phase I were in good agreement even though it looked like an outlier as seen in **Figure 3-9a**. The average measured pressure values had greater variation (i.e., 42 – 77 (290 – 531) psi (kPa)) as compared to hydraulic simulation results (i.e., 49 – 67 (338 – 462) psi (kPa)).

The location of greatest interest was 1234 in Phase II. Here, the average pressure was 42 psi (290 kPa) but it fluctuated ranging from 39 psi (270 kPa) on Sep 23, 2021

Table 3-3. Comparison of sensor measurements and simulation results.

Wireless sensor measurements				**Simulation results (Assuming no leaking)**		
Sensor Location (Phase)	**Longitude**	**Latitude**	**Average Pressure (psi)**	**Longitude**	**Latitude**	**Pressure (psi)**
1022 (I)	-86.4456	42.1204	62.35	-86.4457	42.12033	60.05
1234 (I)	-86.4551	42.1176	76.81	-86.4553	42.11715	66.31
3003 (I)	-86.4463	42.1038	61.44	-86.4464	42.10336	50.70
5005 (I)	-86.4541	42.1053	63.78	-86.454	42.10533	51.23
4004 (I)	-86.4429	42.1120	42.97	-86.4441	42.1115	48.59
1022 (II)	-86.4374	42.1181	58.88	-86.4367	42.11845	49.88
1234 (II)	-86.4597	42.1194	42.26	-86.459	42.11903	67.72
5005 (II)	-86.4535	42.1021	60.11	-86.4541	42.10174	50.08
3003 (II)	-86.4432	42.0952	56.48	-86.4425	42.09593	49.05

(Thursday) and 45.49 psi (314 kPa) on Sep 25, 2021 (Saturday). This sensor observed some of the largest sustained changes in pressure. The location of the measurement was very close to the location where a water main broke in October 2021 (marked as 'X' in **Figure 3-9a**). The pressure variations observed in September 2021 might have indicated an issue was occurring in the system near this measurement location.

In order to study the difference in model and measured pressures under a scenario of a failed pipe, a junction close to the water main break was simulated in InfoWater as "partially open". The hypothesis was that a "partially open" pipe represents a significant leakage resulting in lower pressure. The leak was controlled by allowing water to flow out of the system at this junction with the model exploring various flows in 100 gallon per minute (6.3 liters per seconds) increments. As more flow comes out of the system, pressure at this point in the system is reduced (**Figure 3-9b)**. As shown in **Figure 3-9b**, two locations near location 1234 in Phase II and 4004 in Phase I were partially opened. Both units reported low pressures (42 (290) and 43 (297) psi (kPa), respectively) warranting this exploration.

The sensor at location 1234 had reported significantly lower pressure by 25 psi (173 kPa) while that at location 4004 was just slightly lower by 5 psi (35 kPa). The "partially open" analysis is plotted (**Figure 3-9b**) with the leak flow at the junction plotted against the residual pressure at the junction. In order to realize the significant drop in pressure from 67.72 (467) to 42.26 (291) psi (kPa), the leaking flow at junction J#442 (near 1234 in Phase II) would have needed to be about 6000 gpm (378 L/s). In comparison, J#1194 (near 4004 in Phase I), the leaking flow rate would have needed to be 730 gpm (46 L/s) which lowers the residual pressure from 48.59 (335) to 42.97 (296) psi (kPa) to match the measurement.

The leak size needed to reduce the pressure at 1234 (Phase II) as predicted by InfoWater was significant enough that this reinforced the view that this segment was in distress.

3.6. Conclusion

In this study, the implementation of a low-cost, rapid-to-deploy, and unattended monitoring solution for evaluating water pressure was presented. The monitoring solution consisted of pressure sensors with a time synchronized GPS receiver to measure the spatial and temporal variations of water pressure in a distribution system. To detect changes in pressure and to locate target measurement spots, sensors were selected to have high resolutions (1 psi (7 kPa) in water pressure and 2.5 m in GPS location). The wireless sensor system performed reliably and accurately monitored nine locations in the City of Benton Harbor. The results from the field measurement have been compared to pressures predicted by InfoWater, a hydraulic modeling tool widely used in the drinking water field. Both the hydraulic simulation and pressure sensor measurements indicated that the Benton Harbor water distribution system met minimum required pressures. Pressure measurements were within 25% of those predicted by the model except for one location (Location 1234 in Phase II) which was 37.6% in disagreement. Deeper investigation using the model suggested a possible leaking pipe at this location. The hypothesis of a leaking pipe was later confirmed by a water main rupture a month after data collection in this location.

Chapter 4: Bayesian Truck Re-Identification Model for Asset Management of Highway Network Systems

4.1. Introduction

Road transport is the nearest to people among all modes of transportation, thus passengers and freight are at least first transported by roads before transferring to other modes or end points **[152]**. In the United States alone, 11.9 billion tons of freight is carried on highways that comprise approximately 615,000 bridges **[153]** and more than 2.5 million miles of paved roads **[154]**. Thus, since the upkeep, maintenance, and safety of such sheer size highway infrastructure is crucial, freight loading profiles that may have damaging impact on pavements and bridges shall be regulated. As a result, State Departments of Transportation (DOTs) in the United States spend a lot of resources on their existing intelligent transportation systems (ITS) infrastructure to provide data for their motor carrier weight regulations and safety enforcement schemes **[155]**. The ITS infrastructure measures freight weightage using Weigh-In-Motion (WIM) sensor stations embedded in highway pavements. Embedded sensing has been innovatively used for assessing different applications in transportation infrastructure systems such as: retaining wall monitoring **[89]**, structural asset management **[68]**, pipe network monitoring **[99]**, pavement management and traffic control **[156]**, **[157]**, GPS tracking of freight trucks **[158]**, etc. In particular, WIM station sensors have currently been used for the regulation of freight truck

weights, and they report large WIM signature record of trucks in motion. WIM is the measurement of necessary attributes of vehicles in motion with the means of sensors embedded in roadway pavements through the process of measuring the dynamic tire forces of a moving vehicle and estimating the corresponding tire loads of the static vehicle **[159]**. WIM stations detect a change in voltage caused by pressure exerted on the sensor by the tires on an axle and they are also capable of estimating the Gross Vehicle Weight (GVW) of a vehicle that is carried by the tires of each wheel assembly, axle, and axle group on the vehicle **[159]**, **[160]**. Truck attributes from WIM sensor measurement are usually transcribed alphanumerically, and records of a single truck have axle weights, GVW, axle spacing, speed, timestamp, number of axles, vehicle class, travel direction and station ID **[161]**. The recorded WIM data can have several applications including but not limited to: designing road pavements, determining freight traffic flows, checking the share of heavy vehicles in traffic stream, infrastructure asset management, etc.

The notion of WIM was invented in the 1950s **[162]**, and WIM data started being used for the design of highway pavements and for developing the specifications of the AASHTO code **[163]**. In the 1970s, it was adopted by Eurocode and Canadian manuals for bridge design code calibration studies **[164]**. By design, WIM stations were initially bending plates which evolved to piezoelectric sensors (e.g., ceramic, quartz, etc.) and fiber optic technologies **[165]**. In 1993, Eurocode made code revisions in revisiting Finite Element Analysis (FEA) of bridges with more accurate understanding of bridge capacity to carry load. But there was little known about the traffic loading on bridges. Thus, WIM data became increasingly important for research and practice across Europe **[166]**. In the 2000s, estimating the performance in Gross Vehicle Weight (GVW) measurement

adequacy levels of WIM station systems became popular research theme. As a result, calibration studies were conducted, starting with vehicles with known axle weights and corresponding spacing. This was basically done in two methods: (1) by selecting in random of trucks flowing in commute traffic streams, and (2) with the recommended use of multiple sensors **[167]**. For the latter, there exists research for the re-identification of trucks passing WIM station pairs in the objective of improving accuracy of freight truck measurements limited to local extent. Thus, they have not rigorously been yet leveraged to fully address some important freeway asset management questions.

The spatiotemporal distribution of freight truck loading profiles is very essential for determining the service life of freeway assets (e.g., pavements and bridges). Thus, a more accurate way of counting Commercial Annual Average Daily Traffic (C-AADT) along with a robust probabilistic method of predicting freight truck weightage are important for the actual service life a freeway asset to be in a desired congruence to or greater than its design service life. The current estimation of C-AADT in the State of Michigan fuses different datasets from the Michigan Department of Transportation (MDOT), cities, counties, and Metropolitan Planning Organizations (MPOs) **[168]**. Traffic counts are then conducted throughout the year by using continuous and short-term count sites that have limited precision (i.e., from the quality of data acquisition and missing dates of traffic count) in C-AADT estimations. For major truck flows between states on national level, truck flows are mapped by collecting data from different sources such as: commodity flow survey, freight analysis framework (from agriculture, extraction, utility, construction, service, and other sectors), vehicle travel information system (VTRIS), highway statistics and transborder freight data **[169]**. Nonetheless, these counted flow information (i.e., on

either state or national level) might not be rigorous for enabling the conduction of freeway asset management with only just knowing the estimated volume of trucks (i.e., without quantifying the distribution of freight truck loading spatiotemporally). In addition, MDOT guides oversize and overweight vehicle owners to get single day or annual permit to operate on Michigan's network. Thus, it regulates the annual registration of trucks by GVW, and reports annual revenues, safety, and trends **[170]**. On the other hand, there may be unaccounted or non-permitted overweight and oversize freight truck movements that make short and long-haul distances on the highway network damaging pavements and aged bridges that needs to be accounted for better management of highway networks. Qualitatively, the current practice of pavement condition assessment is via the collection of primary data such as: structural adequacy/deflection, surface distress, serviceability/ride-quality, and surface friction **[171]**.

The main motivations of this study are to fill the existing gaps in research and practice with respect to: (1) the current quantification of C-AADT on state highway level contains only freight truck volume counts, nonetheless C-AADT counts with corresponding spatiotemporal distribution of freight truck loading profiles are required for conducting quantitative asset management of freeway assets, and (2) probabilistic truck re-dentification using WIM data have not been explored on a state highway network-level for informing asset managers for their regulations on motor carrier weights and safety enforcement schemes. Therefore, the key contribution of this study is that, with the demonstration of a Bayesian Inference-based truck re-identification algorithm scalable for leaky state highway-level networks, short- and long-haul movements of freight trucks are not only quantified, but the actual spatiotemporal distribution of Equivalent Standard Axle

Loads (ESALs) are also precisely estimated for informing the management of freeway assets such as pavements and bridges. Thus, discrete WIM measurements by WIM station sensors distributed spatially are analyzed for informing the network-level assessment of highway infrastructure systems for reliability-based pavement performance management and to also support the upkeep, maintenance, and safety of highway network system assets.

4.2. Weigh-In-Motion (WIM) Dataset

The Michigan Department of Transportation (MDOT) compiles Weigh-In-Motion (WIM) records for each month of the year from all its 42 pairs of WIM station sensors (i.e., comprised of 4 Piezo sensors, 1 Bending Plate, 1 Dual Loop, and 36 Quartz-based sensors) distributed spatially on the freeway network connecting different locations within the State of Michigan. As shown in **Figure 4-1**, 5 pairs of WIM stations were installed at the upper peninsula on the corridor that connects the State of Wisconsin with the State of Michigan's lower peninsula. The remaining 37 pairs of WIM stations were distributed in the lower peninsula with most sensors concentrated on the lower parts of the state **[172]**. Thus, these 42 WIM stations record WIM data by transcribing measured freight truck attributes into a single comma delimited (i.e., csv) formatted file for further data processing.

Raw WIM record of 10 years duration was saved in the server of the Laboratory of Intelligent Systems Technology (LIST) at the University of Michigan. The data was collected from the aforementioned 42 pairs of WIM stations in the State of Michigan between January 2011 and May 2022. But for every month, MDOT only reports WIM records from 33 to 38 WIM stations by saving raw data into a single large csv file format. The remaining 4 to 9 WIM stations, out of the 42 available pairs of WIM stations, stay

offline for maintenance in rotation from station to station in the objective of reassuring WIM measurement accuracy. WIM station sensor records (or freight truck signatures) contain 43 data attributes for all 650+ million freight trucks that were recorded in the past 10 years of data collection. For all recorded truck signatures in inventory, these 43 data attributes include axle weights (13 columns), axle spacing (12 columns), datetime information (7 columns), Gross Vehicle Weight (1 column), vehicle speed (1 column), number of axles (1 column), vehicle class (1 column), lane (1 column), direction (1 column), station ID (1 column), county code (1 column), state code (1 column), record type (1 column), and vehicle ID (1 column).

In this study, the raw WIM data from October 29, 2020, was used as a training dataset for the Bayesian Inference-based truck re-identification algorithm presented. In addition, testing and validation datasets were extracted from continuous 2+ hours long video recording frames on the same day on 2 pairs of WIM stations located on a heavily

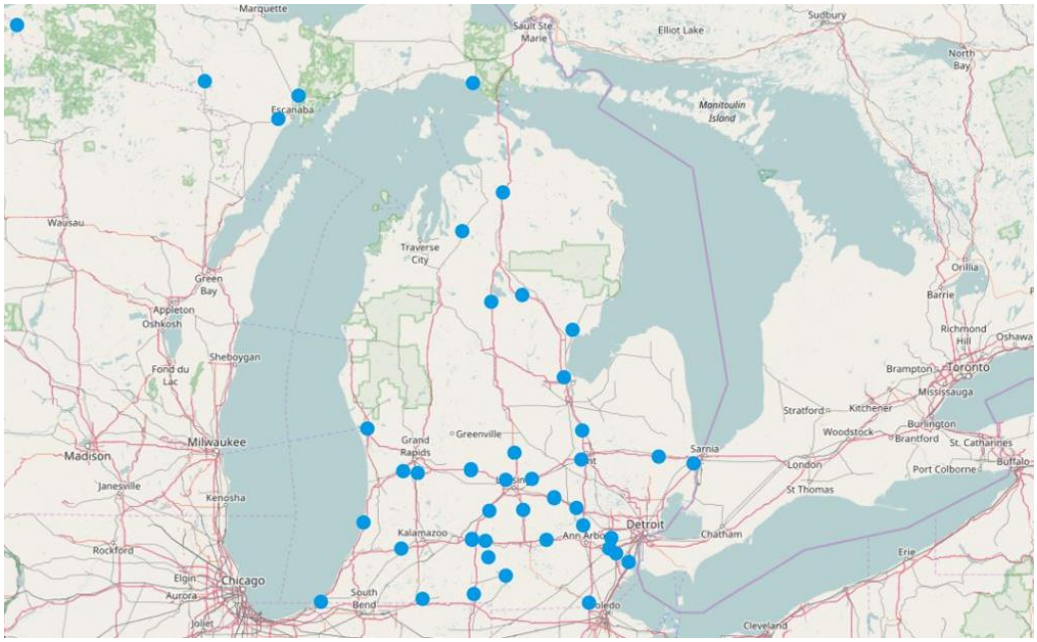

Figure 4-1. Distribution of pairs of Weigh-In-Motion (WIM) stations in the State of Michigan administered by the Michigan Department of Transportation (MDOT).

trafficked corridor along the I-275 highway for both North Bound (NB) and South Bound (SB) directions in the metro region of Michigan close to the Detroit Metropolitan Wayne County Airport (DTW) (**Figure 4-2**). The video recording was conducted by setting up GoPro camera stations with frames of observation as shown in **Figure 4-3** for at least 2 hours. The camera frames of observation were also able to show features of trucks heading on both NB and SB directions. The selected pair of WIM stations have 2 interchanges in between where US-12 and I-94 highways cross. The I-94 highway is also a heavily trafficked corridor with freight truck traffic going to both East Bound (EB) and West Bound (WB) directions. This enabled investigating a heavily trafficked and leaky highway corridor example to conduct a testing and validation study that is very insightful to scale the analysis to a state highway network-level assessment of freight truck loading profiles.

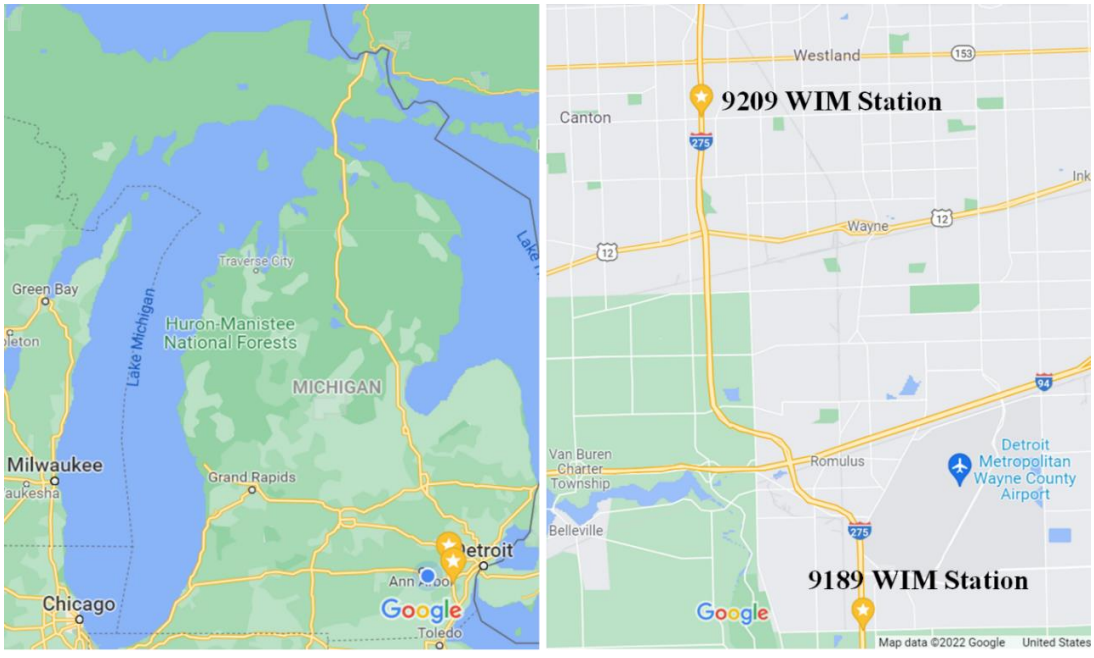

(a) (b)

Figure 4-2. Two (2) pairs of WIM stations located in the metro region of Michigan close to DTW international airport selected for testing and validation study: (a) small scale view; (b) large scale view (*Source:* Google Maps, 2022).

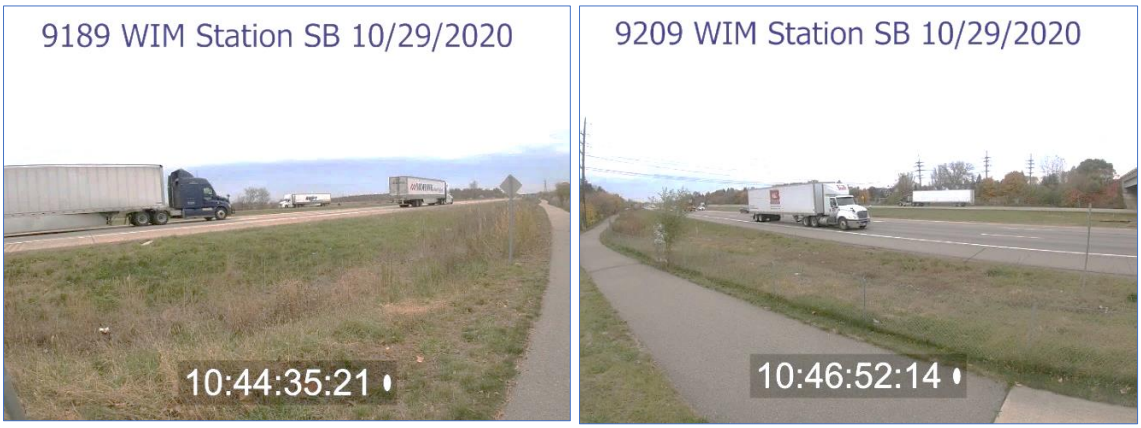

(a) (b)

Figure 4-3. Video recording frame shots from the installed GoPro cameras: (a) 9189 camera station view; (b) 9209 camera station view.

4.3. Methodology

4.3.1. Overview of Existing Truck Re-Identification Methods

Vehicle re-identification (re-ID) aims to spot a vehicle of interest by using multiple camera footages without overlapping instances **[173]**. In urban areas, the main objective of vehicle re-ID has been mostly for surveillance purposes, and beyond manual re-ID, deep learning-based methods have been used popularly in assessing similarity of vehicles in corresponding image datasets **[174]**, **[175]**, **[176]**. On the other hand, a recent study demonstrated the re-identification of freight truck vehicles on an interstate highway corridor using convolutional neural networks (CNNs) to augment the analysis of responses in bridge monitoring studies **[177]**. Since most WIM station locations have no continuously recording camera systems nearby, re-identification of freight trucks using WIM measurement records remain to be still used majorly for WIM station calibration studies. For instance, a study conducted in Irvine, California proposed a remote calibration monitoring system for WIM stations in the objective of quantifying percent accuracy of measurements at stations. The case study picked a pair of WIM stations named SR-57 SB

Orange and I-5 SB Irvine and analyzed WIM records with certain truck re-identification algorithm. The algorithm considered steer axle weights, GVWs and drive tandem axle spacing. In addition, probability level by number of correct and incorrect matches were identified for class 9 trucks (i.e., according to FHWA Classification) and the probability levels were acquired by adjusting matching time windows for GVW comparison **[178]**. Moreover, speed accuracy metric was proposed by **[179]** using WIM data based on tandem axle spacing (i.e., not a fixed standard but inherent in design that manufacturers in the U.S. primarily use 4.25', 4.33', 4.50' and 4.58' spacing) of Class 9 trucks. When the average drive tandem axle spacing was outside of a prescribed threshold, then speed calibration was conducted in that traffic monitoring lane should be checked with a speed gun.

Quantification of measurement uncertainties with respect to GVW and axle spacing attributes has been crucial for WIM calibration studies for more than two decades. The main objective has been to generate valid statistics for various WIM data applications in transportation. As indicated in **Table 4-1**, percentage of GVW uncertainty varied among different types of WIM stations. Accuracy of a system of WIM stations depends on the types of sensors in use and the most popular kind of WIM stations in the United States are Piezoelectric (Piezo) sensors. For successful Piezoelectric sensors installation, it is assumed that the entire system will have a service life of 4 years, after which time the inroad equipment would have to be replaced. Thus, during the 4-year service life of the system, sensor failures are assumed to be: 5% in year one, 15% in year two, 25% in year three, and replacement required in year four. As a result, raw WIM data for all WIM stations in a certain time duration may not be available for a few stations due to replacement

Table 4-1. Accuracy of WIM stations (*Source:* Bushman et al., 1998) **[180]**.

Item	Piezoelectric	Bending Plate	Load Cell
Accuracy (95% confidence interval)	+/- 15%	+/- 10%	+/- 6%
Expected life	4 years	6 years	12 years
Initial installation cost	$ 9,000	$ 21,500	$ 48,700
Annual life cycle cost	$ 4,750	$ 6,400	$ 8,300

and maintenance of the sensors **[180]**. For instance, it is common to see data reports of 33 to 38 stations per a given month out of the 42 stations in the State of Michigan.

Truck re-identification for calibration studies was also proposed by utilizing a Bayesian framework. The method relied on calculating the posterior probability of a match between two vehicles given two sets of data points collected for a vehicle pair (i, j) at the upstream and downstream stations. A vehicle j at the downstream station is matched to the upstream vehicle i that yields the largest probability of a match as formulated in **Equation 4-1** **[181]**. The Bayesian model in **[181]** was formulated as follows:

$$P(\delta_{ij} = 1|x_{ij}) = \frac{f(x_{ij}|\delta_{ij} = 1)P(\delta_{ij} = 1)}{f(x_{ij}|\delta_{ij} = 1)P(\delta_{ij} = 1) + f(x_{ij}|\delta_{ij} = 0)P(\delta_{ij} = 0)} \quad (4\text{-}1)$$

where $P(\delta_{ij} = 1|x_{ij})$ is the a-posteriori probability, $f(x_{ij}|\delta_{ij} = 1)$ is the probability of data given there is a match, $P(\delta_{ij} = 1)$ is the initial (a-priori) probability and $f(x_{ij}|\delta_{ij} = 1)P(\delta_{ij} = 1) + f(x_{ij}|\delta_{ij} = 0)P(\delta_{ij} = 0)$ is probability of measurement.

The curb of this work is associated with its limited scalability from a highway segment connecting a pair of stations with no interchange (or leak) in between to a realistic leaky highway network system with diverse statistics of WIM data from multiple pairs of WIM station sensors. Moreover, the output from such Bayesian framework would be useful to be channeled for informing the management of freeway assets such as bridges and pavements existing in highway networks.

4.3.2. Proposed Truck Re-Identification Method

A Bayesian Inference-based model is presented in this study for the re-identification of trucks on a state highway network-level in the essence for quantifying freight traffic flow characteristics and the corresponding freight loading profiles on pavements and bridges in the State of Michigan. To implement the model, a single fully automated algorithm was written in MATLAB for loading, preprocessing, analyzing, and visualizing raw WIM records. The algorithm's main body is a two-stage truck re-identification procedure (i.e., Heuristic, and Bayesian Inference models), followed by mapping and visualization of results. Data preprocessing included extracting WIM data attributes from the raw WIM data structure by converting truck information to appropriate unit values and saving the corresponding parsed data to a table of freight truck records. A lookup table is then defined to pair adjacent WIM stations by identifying potential movement of trucks from one WIM

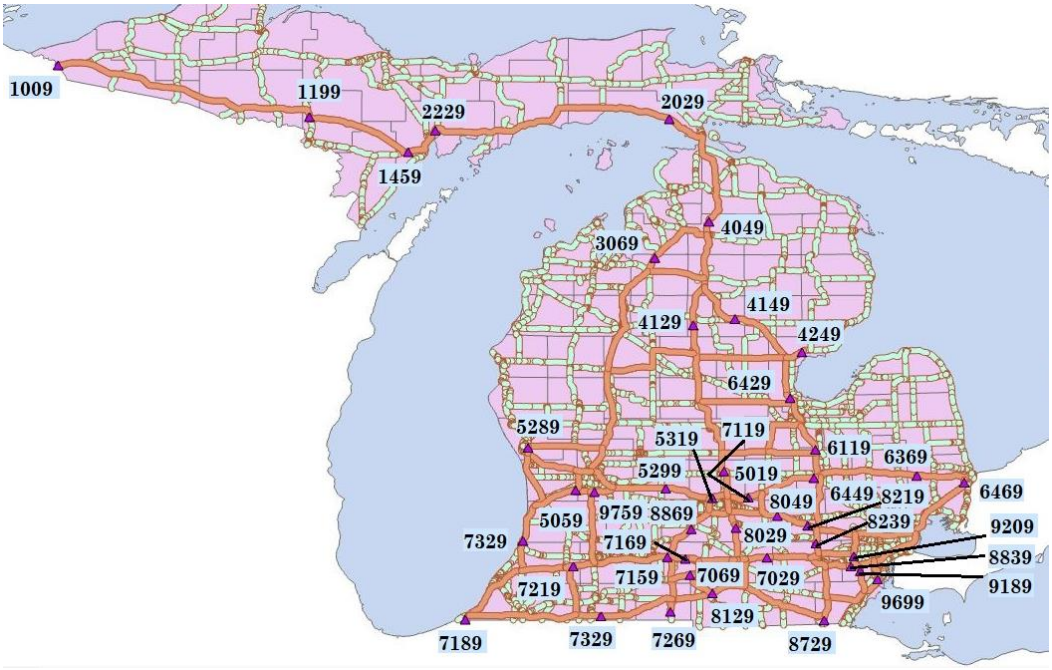

Figure 4-4. Distribution and labels of pairs of WIM Stations with the shortest path trajectories that freight trucks can use to go between adjacent pairs of WIM stations in the State of Michigan.

station to the other, considering path and direction intuitions. Thus, a highway network considered for analysis is a collection of truck flow trajectories shown in **Figure 4-4**.

In addition, the corresponding ground drive distance and an uncongested traffic based estimated time of arrival (ETA) was obtained for specified direction of truck movement for potential WIM station Origin-Destination (O-D) pairs from Google Maps. Thus, a lookup table is attributed by WIM station O-D pair IDs, pair of potential truck movement directions, ground drive distance between WIM station O-D pairs and normal day traffic (i.e., uncongested traffic state) ETA per direction. Therefore, the presented two-stage truck re-identification algorithm is designed to analyze raw WIM data on a daily basis using the defined lookup table scalable to a number of days of interest (i.e., severe stormy weather or other days) with no algorithm improvement requirement.

For better probability of truck re-identification, the presented two-stage algorithm uses all WIM data attributes to do matching between potential pairs of truck signatures for a selected pair of WIM stations. The first-stage truck re-identification procedure applies heuristics for informing parameter error distributions and truck flow retention percentages for the second-stage Bayesian probability-based truck re-identification framework. The heuristic procedure comprises of setting equality and inequality constraints for matching truck signatures (**Figure 4-5**). The equality constraints comprise of setting direction of truck movement, number of axles, vehicle class and pair of WIM station IDs to be the same for selected truck pairs, while the inequality constraints set travel time bounds, error in GVW, error in axle weights and error in axle spacing.

Algorithm 1 Heuristic Procedure

Load: **Raw WIM Data** and **Lookup Table**
HeuristicResults = [ ]
for $ErrorBoundScenario = 1, 2, \ldots, 20$ **do**
  Set bound for ratio of error in GVW to be β while γ is set for ratio of error in Axle Weight
  for $AdjacentWIMStationPair = 1, 2, \ldots, length(LookupTable)$ **do**
    for $i = 1, 2, \ldots, N_A$ **do**
      for $j = 1, 2, \ldots, N_B$ **do**
        Compute travel time windows: LB = $\text{Time}_i + \frac{Distance}{min(Speed_A)}$ *and* $UB = Time_i + \frac{Distance}{max(Speed_A)}$
        if $LB <= Time_j <= UB$ **and** $NumAxles_i == NumAxles_j$ **and** $VehType_i == VehType_j$ **then**
          Calculate errors: $\varepsilon_{GVW} = GVW_j - GVW_i; \varepsilon_{AW} = AW_j - AW_i$ *and* $\varepsilon_{AS} = AS_j - AS_i$
          if $|\frac{\varepsilon_{GVW}}{GVW_i}| <= \beta$ **and** $|\frac{\varepsilon_{AW}[k]}{AW_i[k]}| <= \gamma$ **and** $|\varepsilon_{AS}[k]| <= 1', \ \forall\, k = 1, 2, \ldots, 13$ **then**
            $\text{TT}_{Actual} = Time_j - Time_i; TT_{Estimated} = \frac{Distance}{ETA}$ **and** $\varepsilon_{TT} = TT_{Actual} - TT_{Estimate}$
            When duplicate cases exist, take the pair with min ε_{TT}
            HeuristicResults = [HeuristicResults; All Attributes of $Truck_i$ and $Truck_j$]
          end if
        end if
      end for
    end for
  end for
end for

Figure 4-5. Stage 1 of Truck Re-identification Algorithm: Heuristic Procedure.

Table 4-2. Selected description of variables shown in the Heuristic Procedure.

Variable	Description	Variable	Description
N_A	Number of data records at origin	AS	Axle spacing
N_B	Number of data records at destination	AW	Axle weight
LB	Earliest time for truck to arrive at B	TT	Travel time
TB	Latest time for truck to arrive at B	k	Label of axle on truck

The utility of the presented heuristic procedure is to provide error distribution information and a probability of retention (P(Ret)) estimate between pair of WIM stations useful for the second-stage Bayesian Inference-based truck re-identification algorithm. The probability of retention (P(Ret)) incorporates the cases where there is an interchange or ramp in between a pair of WIM stations in which either some trucks sensed at the upstream WIM station left the network without traversing through the downstream WIM station or some trucks might have merged to the highway to be sensed at the downstream WIM station. Thus, probability of retention (P(Ret)) is calculated to count the number of trucks that have passed through both upstream and downstream WIM stations, divided by the total

number of trucks sensed at the upstream WIM station. The probability of retention P(Ret) is then unique to every potential pair of WIM stations and time of analysis.

The second-stage truck re-identification algorithm is a Bayesian framework for the probabilistic matching of truck signatures. It has analogous flow with the heuristic algorithm presented in **Figure 4-5** but the criteria to select the probability of match between a number of potential truck pairs is using the probability that trucks i and j are a match given attributes of the pair of trucks, x_{ij} under model assumptions, M (i.e., defined in **Equation 4-2** as $P(\delta_{ij} = 1|x_{ij}, M)$). The Bayesian Inference described below is motivated by the model in **[181]** and presented in **Equation 4-1**. Nonetheless, the presented model in **Equation 4-2** has key framework contributions attributed to:

- Scaling up truck re-identification study to a leaky freeway network-level,
- Utilizing prior (or initial) probability density function (pdf) using speed measures at WIM stations, actual (or shortest path) drive distances, normal uncongested traffic ETAs and retention of freight trucks in a corridor between WIM station pairs,
- A multi-variate likelihood function with axle weight error distributions, and
- Coupling with Receiver Operating Characteristic (ROC) curves to set probability threshold for precisely matching trucks between pair of WIM stations.

$$P(\delta_{ij} = 1|x_{ij}, M) = \frac{f(x_{ij}|\delta_{ij} = 1, M)P(\delta_{ij} = 1, M)}{f(x_{ij}|\delta_{ij} = 1, M)P(\delta_{ij} = 1, M) + f(x_{ij}|\delta_{ij} = 0, M)P(\delta_{ij} = 0, M)} \quad (4\text{-}2)$$

$$P(\delta_{ij} = 1|x_{ij}, M) = c_1 f(x_{ij}|\delta_{ij} = 1, M)P(\delta_{ij} = 1, M) \quad (4\text{-}3)$$

where $P(\delta_{ij} = 1|x_{ij}, M)$ is the posterior probability (i.e., the probability of trucks i and j are a match given attributes of the pair of trucks, x_{ij} under model assumptions, M),

$f(x_{ij}|\delta_{ij}=1,M)$ is the likelihood probability (i.e., the probability of attributes of a truck pair, x_{ij} given a match, $\delta_{ij}=1$ under model assumptions, M), $P(\delta_{ij}=1,M)$ is the prior probability (i.e., the probability that trucks i and j are a match, $\delta_{ij}=1$ under model assumptions, M) and $c_1 = \frac{1}{f(x_{ij}|\delta_{ij}=1,M)P(\delta_{ij}=1,M) + f(x_{ij}|\delta_{ij}=0,M)P(\delta_{ij}=0,M)}$ is the scaling factor that is the reciprocal of the marginal likelihood, which is constant.

The prior probability in **Equations 4-2 and 4-4** is based on calculating an initial probability density function (pdf). The initial pdf was formulated using available prior information before truck re-identification conception. That is, when thinking of matching between a pair of WIM stations, we have the drive distance between the WIM station O-D pair, the speed of the truck at upstream (origin) station and the normal day ETA from Google Maps. These were used to formulate the error in travel time estimate presented in **Equation 4-5**. In addition, considering the leakiness of the highway network, the probability of retention, $f(Ret,M)$ from the heuristic procedure was treated independently in **Equation 4-4**. **Equations 4-4 to 4-6** discuss the prior pdf formulation in detail:

$$P(\delta_{ij}=1,M) = c_2 f(\epsilon_{t_i},M) f(Ret,M) \tag{4-4}$$

where ϵ_{t_i} is the error on the estimated travel time, t of truck i to go from WIM station A to WIM station B, $f(\epsilon_{t_i},M)$ is the probability of truck i to travel with a certain error in travel time t under model assumptions, M, $f(Ret,M)$ is the probability of retention of truck, i in the link between WIM stations A and B, c_2 *is a* scaling factor.

$$\epsilon_{t_i} = \frac{D_{AB}}{s_i} - ETA_{AB} \tag{4-5}$$

where D_{AB} is the driving distance between WIM stations A and B, s_i is the speed of truck i at WIM station A, ETA_{AB} is the estimated time of arrival between WIM stations A and B under normal uncongested traffic condition.

$$f(\epsilon_{t_i}, M) = \frac{\Gamma\left(\frac{\nu+1}{2}\right)}{\sigma_{\epsilon_{t_i}}\sqrt{\nu\pi} * \Gamma\left(\frac{\nu}{2}\right)} \left(\frac{\nu + \left(\frac{\frac{D_{AB}}{s_i} - ETA_{AB}}{\sigma_{\epsilon_{t_i}}} \right)^2}{\nu} \right)^{-\left(\frac{\nu+1}{2}\right)} \tag{4-6}$$

where $\sigma_{\epsilon_{t_i}}$ is a scaling parameter of the error on estimated travel time, ϵ_{t_i}, $\Gamma(.)$ is the gamma function and ν is the shape parameter that adjust to the distribution of speed data measurements at the WIM station.

The main WIM data variables that can be used to model the likelihood function in the presented Bayesian truck re-identification framework are axle weights, GVW and axle spacing. Since axle spacing doesn't vary much with in the same vehicle class and number of axles, and since GVW is the sum of all axle weights of a truck, the likelihood function in **Equations 4-2 and 4-3** can be modeled using multi-variate error in axle weight (**Equations 4-7 and 4-8**).

$$f\left(x_{ij} \middle| \delta_{ij} = 1, M\right) = c_3 f\left(\epsilon_{AW_{ij}} \middle| \delta_{ij} = 1, M\right) \tag{4-7}$$

$$f\left(\epsilon_{AW_{ij}} \middle| \delta_{ij} = 1, M\right) \sim \frac{1}{(2\pi)^{\frac{d}{2}}} |\Sigma|^{-\frac{1}{2}} exp\left\{-\frac{1}{2}\left(\epsilon_{AW_{ij}} - \mu_{\epsilon_{AW}}\right)\Sigma^{-1}\left(\epsilon_{AW_{ij}} - \mu_{\epsilon_{AW}}\right)^T\right\} \tag{4-8}$$

where $\epsilon_{AW_{ij}}$ is a $d\ x\ 1$ vector for the error in axle weight between respective axles of trucks, i and j, $\mu_{\epsilon_{AW}}$ is a $d\ x\ 1$ vector for the mean error in axle weight between respective axles of all possible truck pairs and Σ is a $d\ x\ d$ the covariance matrix.

4.3.3. Model Assumptions of Proposed Method

A set of model assumptions, M are stated below for the training, testing and validation of the Bayesian Inference-based truck re-identification model presented in this study.

- Measurement error scale of vehicle attributes is analogous for all WIM stations,
- The better consideration of the error in Gross Vehicle Weight (GVW) measurement at the WIM stations is within +/- 15 % of the actual GVW of the truck **[180]**,

$$|GVW_{actual} - GVW_{measured}| \leq 0.15$$

- The error in GVW between adjacent WIM stations is distributed Gaussian,

$$\varepsilon_{GVW} = GVW_{measured_j} - GVW_{measured_i}\ and\ \varepsilon_{GVW} \sim N(0, \sigma^2_{GVW})$$

- Axle spacing does not vary much since most trucks are manufactured standard,
- Constant speed of freeway traffic in the corridor between pair of WIM stations,
- The error in axle weight measurement is distributed Gaussian (multi-variate),
- The prior pdf is the probability of match under model assumptions ($P(\delta_{ij} = 1, M)$). It is the product of the probability of error in travel time given model assumptions ($f(\epsilon_{t_i}, M)$) and the probability of retention ($f(Ret, M)$), and
- A truck from a company with specific physical features, color and text is unique for at least a window of time the truck is expected to arrive at the next adjacent or destination WIM station.

4.4. Results and Discussions

4.4.1. Pre-Training Stage: WIM Data Insights

The two-stage truck re-identification algorithm presented in this study demonstrates a scalable (i.e., to multiple days) leaky highway network-level analysis using truck signature records measured by WIM station sensors dispersed spatially in the State of Michigan. To investigate the weightage of trucks coming to and leaving the State of Michigan, an interesting way would be to first show the comparison of which borderline WIM stations are reporting the highest number of freight truck traffic records. This analysis is useful to quantify Commercial Annual Average Daily Traffic (C-AADT) and freight truck load profiles informative for the management of freeway and bridge infrastructure by MDOT. As a result, the raw WIM record from a partly cloudy day with no precipitation or snow (i.e., Thursday, October 29, 2020) is analyzed as an example. As presented in **Figure 4-6a**, 7189 WIM station in the borderline with the State of Indiana has the highest reported raw WIM data as compared with the other three WIM stations. The 7189 WIM station is located in close proximity to the suburb of Chicago, Illinois. Even though all the four WIM stations in **Figure 4-6** have 5 axle trucks to be the most popular, the 7189 WIM station 5 axle truck records had a considerable share percentagewise from other freight truck classes as well.

Moreover, another observation would be the raw truck records at the WIM station located in close proximity to the borderline with the State of Wisconsin is the lowest, thus C-AADT in that corridor is not many. As shown in **Figure 4-6a**, two, three and six axle trucks are also significant in the WIM record along with five axle trucks. Thus, a small number of freight trucks come to the State of Michigan on the upper peninsula side. Therefore, a preliminary insight would be, most freight trucks to the State of Michigan

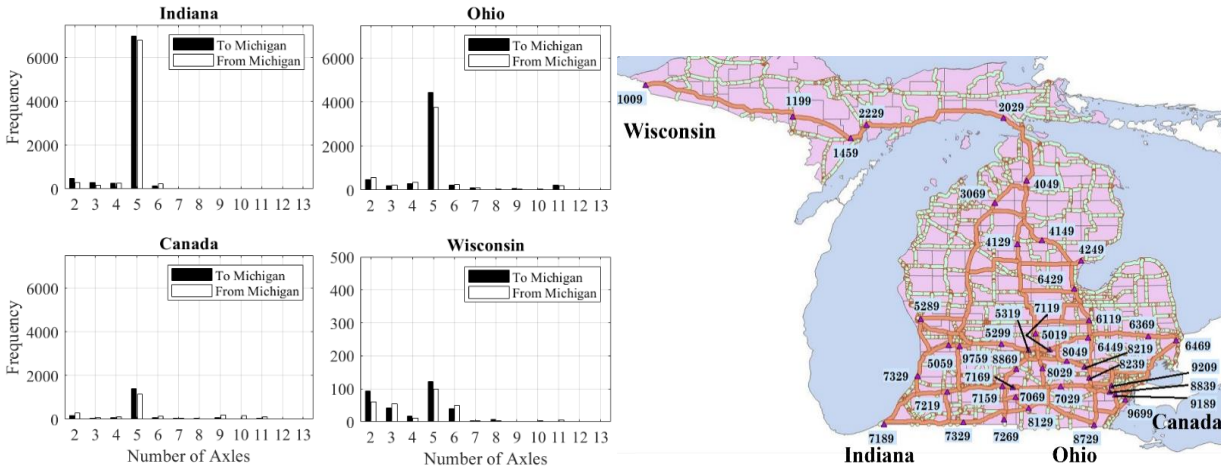

(a) (b)

Figure 4-6. (a) Total inflow or outflow truck volume per direction on 10/29/2020; (b) Station ID (State): 1009 (Wisconsin), 7189 (Indiana), 8729 (Ohio) and 6469 (Canada).

come from Chicago, Illinois side after passing through the State of Indiana (that is, 52 miles stretch) and from the State of Ohio side. This incoming freight truck volume is not exiting the country with the border with Canada but destining to most locations in the State of Michigan probably the majority going to the metro region of Michigan which has been proven by the peak truck volume shown in **Figure 4-13**.

In addition, C-AADT would not only be enough to show at the borderline stations but in overall, knowing the amount of oversize and overweight trucks in the system over a selected duration of analysis period is essential for MDOT. As a result, the presence of overweight and/or oversize (i.e., in length) trucks was investigated using the raw WIM station records from all WIM stations. To investigate oversize trucks in length, all axle spacing measurements were added to get Vehicle Length in ft. by adding 5 to 7 ft. to represent the truck parts that go beyond the front and rearmost axle. As shown in **Figure 4-7a**, a histogram of Vehicle Lengths is presented. By referring to **[182]**, the extended permit is valid for trucks which have overall length of truck less than 85 ft. Thus, from **Figure 4-7a**, it is evident that a very small number of trucks exist that pass the maximum

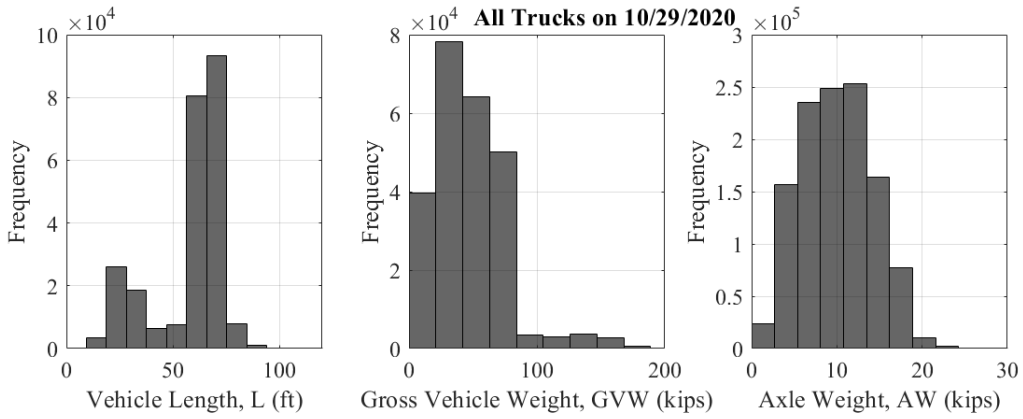

Figure 4-7. Investigation of overweight and oversize trucks from raw WIM data collected on 10/29/2020: (a) vehicle length histogram; (b) GVW histogram; (c) axle weight histogram.

85 ft. mentioned in **[182]**. In the same manual, extended permits are also standardized for potential overweight trucks by suggesting maximum allowable values for GVW and axle weight. According to **[182]**, the maximum allowable GVW of a truck is 150 kips and the maximum allowable axle weight is 24 kips. For 10/29/2020, it is apparent that all trucks have axle weight measurements to be less than 24 kips, but small number of trucks have GVW exceeding 150 kips. The key utility of such analysis would be to inform MDOT about the existence of oversize and overweight trucks operating in the highway pavement and bridge infrastructure inventory.

4.4.2. Training Stage: Heuristic Procedure

The main purpose of the heuristic procedure (i.e., first-stage algorithm) of the two-stage truck re-identification algorithm is to inform the second-stage Bayesian procedure with respect to error distributions for the likelihood function presented in **Equation 4-8** and probability of retention values for the prior probability presented in **Equation 4-4**. A pair of WIM stations mapped in **Figure 4-2** were considered for the training, testing, and validation analysis. For the training stage, the results of the heuristic procedure were

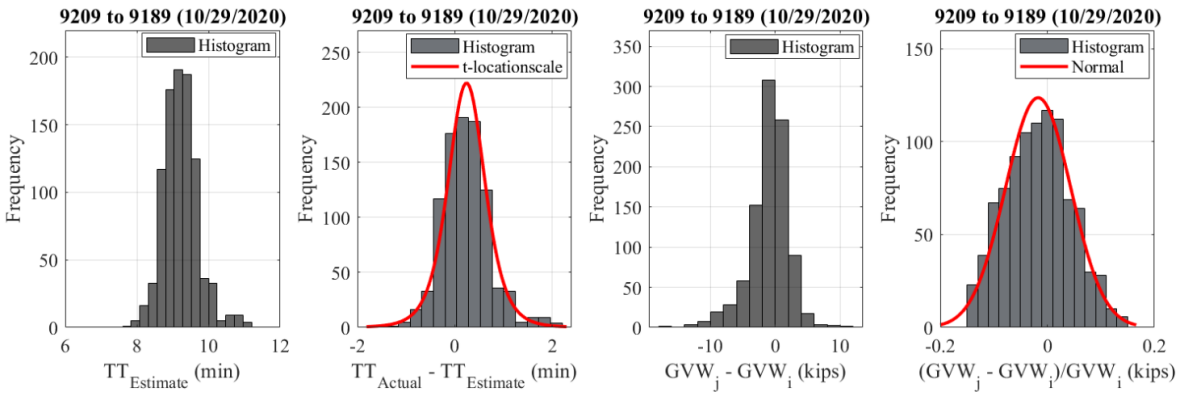

(a) (b) (c) (d)

Figure 4-8. Stage 1 truck re-identification (i.e., heuristic procedure) selected results for October 29, 2020: (a) travel time histogram; (b) error in travel time histogram; (c) error in GVW histogram; (d) error in GVW ratio histogram.

inspected to verify some of the assumptions listed in **Section 4.3.3** and the t-location scale distribution defined in **Equation 4-6**. The error in travel time shown in **Figure 4-8b** is best fit by t-location scale distribution while the percentage error in Gross Vehicle Weight (GVW) shown in **Figure 4-8d** is best fit by gaussian distribution.

4.4.3. Testing and Validation Stage: Video Recording Data Analysis

The 2 hours video recording data from October 29, 2020, was processed to extract testing and validation datasets from the South Bound (SB) and North Bound (NB) directional truck flows, respectively. From the presented video frames (an example shown in **Figure 4-3**), a snapshot of every truck was saved in a table with the corresponding timestamp and number of axles. This information was used to manually match trucks between the pair of WIM stations. In the 2 hours duration, the 9209 WIM station had 1793 trucks (1008 NB and 785 SB) while the 9189 WIM station had 1481 trucks (691 SB and 790 NB) observed in the video recording frames (**Table 4-3**).

With the assumption presented in **Section 4.3.3**, a truck from a company with specific physical features, color and text is assumed to be unique for at least a window of

Table 4-3. Freight truck volumes at and between WIM stations (observed from videos).

Attribute	Direction	Origin	Destination	Matched from Video
SB/NB Details		10/29/2020; NB (9189 to 9209); SB (9209 to 9189)		
Duration	SB	10:00 to 12:11	10:03 to 12:16	10:00 to 12:07
	NB	10:03 to 12:16	10:00 to 12:11	10:03 to 12:11
Truck Volume (V)	SB	785	691	220
	NB	790	1008	287
10am to 11am	SB	365	293	112
	NB	345	455	138
11am to 12pm	SB	362	315	107
	NB	355	465	148
12pm to End	SB	58	83	11
	NB	90	88	1

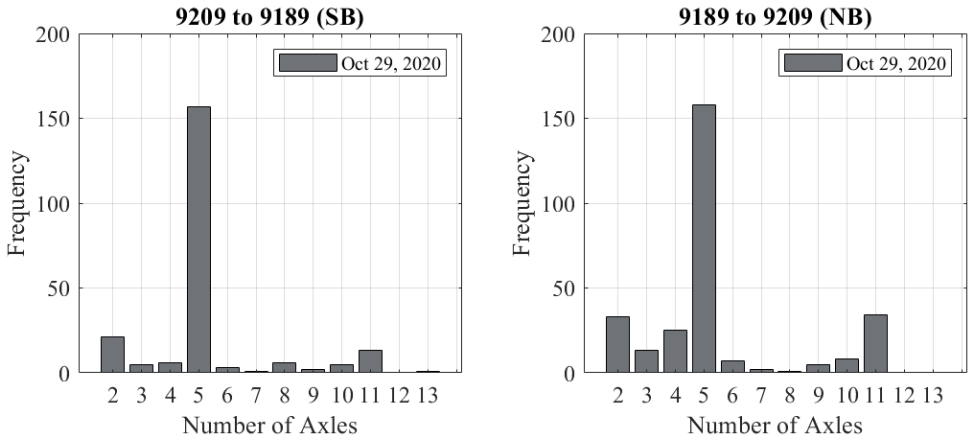

(a) (b)

Figure 4-9. Truck histograms by number of axles (from videos) (a) SB; (b) NB.

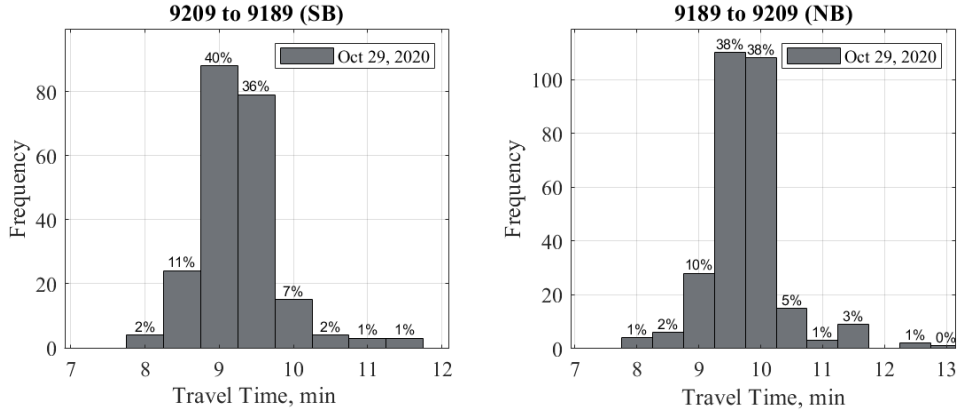

(a) (b)

Figure 4-10. Histograms of trucks by travel time (from videos) (a) NB; (b) SB.

time the truck is expected to arrive at the next adjacent destination WIM station. A window of travel time was calculated by first measuring the ground driving distance between the two WIM stations to be 10.2 miles and by defining the corresponding minimum (50 mph) and maximum (80 mph) speed of trucks knowing the posted 65 mph truck speed limit. Therefore, freight truck signatures were matched with this strategy for both NB and SB flows keeping timestamp and number of axles information along with their snapshots. As a result, histograms for the number of axles on vehicle and travel time were plotted in **Figures 4-9 and 4-10**, respectively.

4.4.4. Partial Receiver Operating Characteristic (ROC) Curves

Truck re-identification is inspecting if a truck vehicle recorded at upstream (origin) WIM station is correctly matching to a truck vehicle at downstream (destination) WIM station. Thus, matching trucks i and j is modeled in the defined Bayesian framework as $\delta_{ij} = 1$ while nonmatching trucks are defined as $\delta_{ij} = 0$. Given that the Bayesian framework presented in this study is a binary classifier system, receiver operating curves (ROCs) are thought to be best tools that helps identify which windows and probability thresholds are yielding close values to an ideal test **[183]**, **[184]**, **[185]**. Two inequality constraints (i.e., percentage error in GVW and axle weights) in the pseudo algorithm presented in **Figure 4-5** were varied from 0 to 100% and the corresponding $P(\delta_{ij} = 1 | x_{ij}, M)$ was calculated according to **Equation 4-3**. In addition, the video matching results were coupled with the truck re-identification results to calculate False Positive (FP), False Negative (FN), True Negative (TN) and True Positive (TP) characteristic values.

After obtaining the above characteristic values, we can calculate False Positive Rate (FPR) and True Positive Rate (TPR) using **Equation 4-9**.

$$(FPR, TPR) = \left(\frac{FP}{FP + TN}, \frac{TP}{TP + FN}\right) \tag{4-9}$$

$$FP = N_{Algorithm} - TP \tag{4-10}$$

$$FN = M - TP \tag{4-11}$$

$$TN = N_{WIM} - N_{Algorithm} - FN \tag{4-12}$$

$$P\left(\delta_{ij} = 1 \middle| x_{ij}, M\right) \geq \alpha \tag{4-13}$$

where FPR is the false positive rate, TPR is the true positive rate, FP is the number of false positive examples, TN is the number of true negative examples, TP is the number of true positive examples, FN is the number of false negative examples, $N_{Algorithm}$ is the number of trucks re-identified using the two-stage truck re-identification algorithm, M is the number of manually matched trucks from video records, N_{WIM} is the number of records at the WIM station and α is the probability threshold.

Partial ROCs are shown in **Figures 4-11 and 4-12** for the test (SB) and validation (NB) datasets, respectively. The curves are partial because the nature of the WIM station

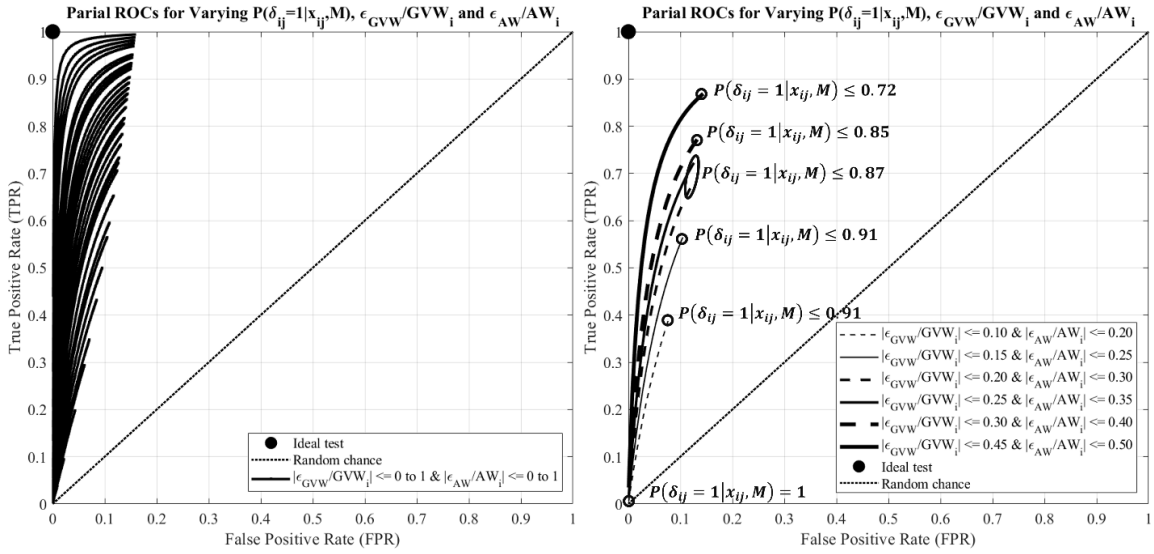

(a) (b)

Figure 4-11. Partial ROC curves using test dataset (SB) (a) all curves; (b) selected curves.

pairs is situated where there is a large interchange in between the link which freight traffic leak from the corridor. Partial ROCs have been used in scenarios where ROC analysis is considered to span only for a subset of the full spectrum of areal predictions **[186]**, **[187]**, **[188]**. Both WIM stations are on the Interstate-275 freeway but there is an interchange in between 9209 and 9189 WIM stations which large number of trucks exit to Interstate-94 freeway (**Figure 4-2b**) heading to Chicago, Illinois which makes the probability of retention between 9209 and 9189 to be lower (**Table 4-3**). Therefore, for leaky highway network scenarios presented in this study, only partial ROCs (i.e., (FPR, TPR) not hitting $(1,1)$ since TN and FN values couldn't be 0) are plotted by defining curves for varying inequality constraints and probability thresholds.

For both test (SB) and validation (NB) partial ROCs shown respectively in **Figures 4-11 and 4-12**, percentage error values for GVW and axle weight are presented. The accuracy of the Bayesian re-identification model is above 91 % for any desired 95 % confidence interval bound on GVW and axle weights at the point on the ROC curves close to the ideal test. In **Figures 4-11a and 4-12a**, all possible inequality constraint values are plotted while selected percentage error values are shown in **Figures 4-11b and 4-12b**. A threshold α for deciding what value of $P(\delta_{ij} = 1 | x_{ij}, M)$ is appropriate for a Bayesian truck re-identification framework is related to defining (FPR, TPR) closer to the ideal test $(FPR, TPR) = (0,1)$. Thus, the best utility of the drawn partial ROCs is to guide the definition of appropriate α values for best binary classification. Partial ROC coordinate of $(FPR, TPR) = (0,0)$ corresponds to $P(\delta_{ij} = 1 | x_{ij}, M) = 1$ and this probability gets lower with the curve rising up. For both test and validation cases, the partial ROCs are similar which justified the validity of the truck re-identification algorithm presented in this

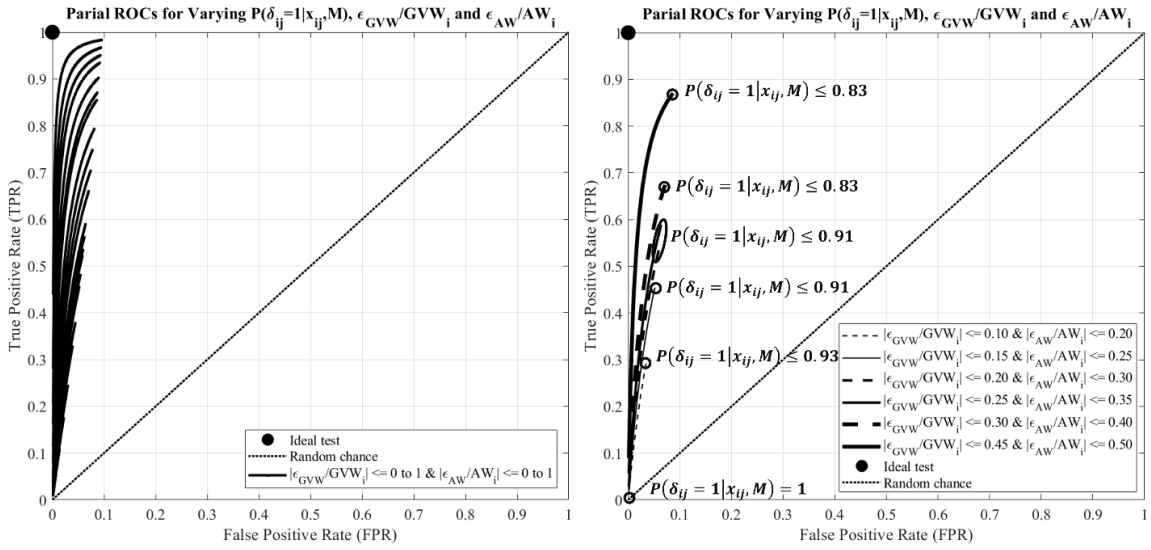

(a) (b)

Figure 4-12. Partial ROC curves using validation dataset (NB) (a) all; (b) selected curves.

study. This implies, we can scale up to highway network-level truck re-identification analysis to provide insights to some of the objectives we have set in introduction section.

4.4.5. Highway Network-level Truck Re-identification

With the 42 WIM stations reporting raw WIM record, 212 potential pairs of WIM station pairs were saved in a lookup table. Since a few WIM stations were down for maintenance, after running the two-stage truck re-identification algorithm, 141 adjacent WIM station pairs resulted in freight truck flow information. This matched data was saved making sure a single truck at origin (upstream) WIM station is re-identified uniquely to a single truck at destination (downstream) WIM station. The matched truck information was then assigned to actual highway routes by collecting overlapping WIM station pair flows and a truck flow animation video was created for the day of October 29, 2020. During the selected day, the peak flow was observed to be in the 15 minutes between 2:30 PM and 2:45 PM as shown in **Figure 4-13**.

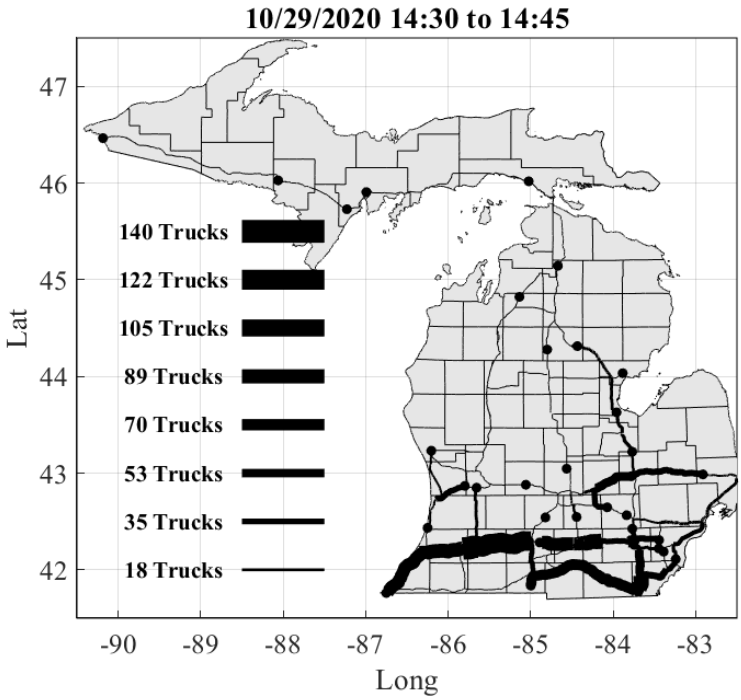

Figure 4-13. Peak freight traffic in the State of Michigan on October 29, 2020.

Furthermore, a maximum total GVW coming to the State of Michigan from Chicago, Illinois direction was found to be of magnitude 185,270 kips per direction. Nonetheless, this wouldn't be of better use for asset management of bridges and pavements, but rather converting the axle weights on each truck into an Equivalent Axle Load Factor (EALF) and summing all EALFs for each truck (**Equation 4-14**) results Truck Factor (TF) to convert to ESAL. **Equation 4-14** is termed the Generalized 4th Power Rule for converting axle loads in to an ESAL **[189]**. The TFs of each truck would be summed (**Equation 4-15**) for any duration of analysis (e.g., 10/29/2020 is only demonstrated in this study and shown in **Figures 4-15 and 4-16**) to result in the total ESAL loading the bridge and pavement infrastructures in place over some time.

$$TF_i = \sum_{j=1}^{NA} EALF_i = \sum_{j=1}^{NA} \left(\frac{AW_j}{18\ kip}\right)^4 \tag{4-14}$$

$$TF_{Total} = \sum_{i=1}^{N} TF_i = \sum_{i=1}^{N}\sum_{j=1}^{NA} EALF_i = \sum_{i=1}^{N}\sum_{j=1}^{NA} \left(\frac{AW_j}{18\ kip}\right)^4 \quad (4\text{-}15)$$

where TF – is the truck factor used to convert a truck to an Equivalent Standard Axle Load (ESAL), $EALF$ – is the Equivalent Axle Load Factor required to convert an axle weight to a ratio of ESAL, i – is the i^{th} truck in the analysis period, NA – is the total number of axles on the truck, AW_j – is the axle weight measurement of the j^{th} axle on the truck, and $18\ kip$ – is a 80 KN Equivalent Standard Axle Load used in manuals and design practices.

An interesting analysis was tracing trucks in Michigan's highway network and the number of trucks that traversed 2, 3, 4, 5, 6, 7, 8, 9, 10 and 11 WIM stations is also presented in **Figure 4-14**. Since all truck information is available, quantifying the total daily Equivalent Standard Axle Loads (ESALs) that is loading the freeway and bridge infrastructure in the State of Michigan for trucks traversing 2, 3, 4, 5, 6, 7, 8 and 9 WIM stations are presented in **Figure 4-15**.

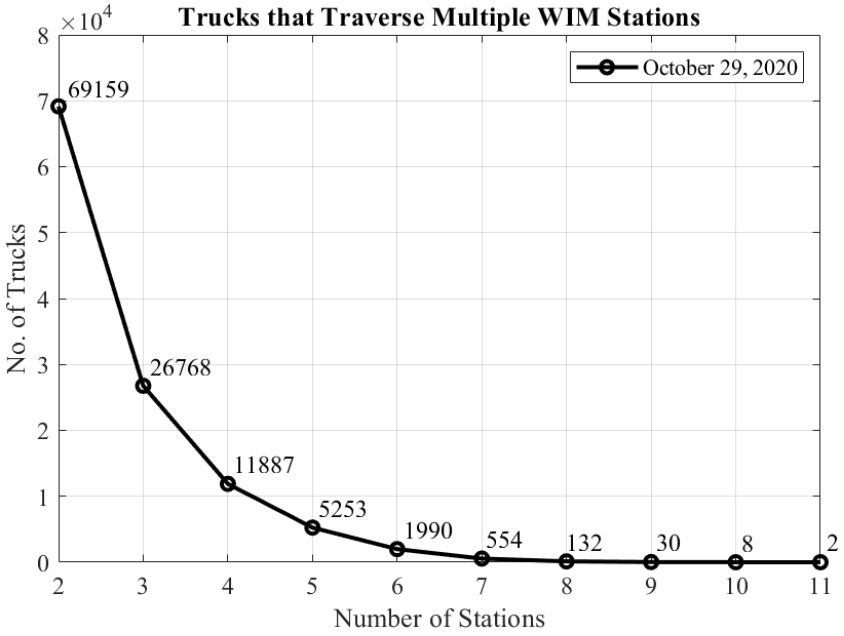

Figure 4-14. Volume of freight trucks that traverse multiple WIM stations in the State of Michigan on October 29, 2020.

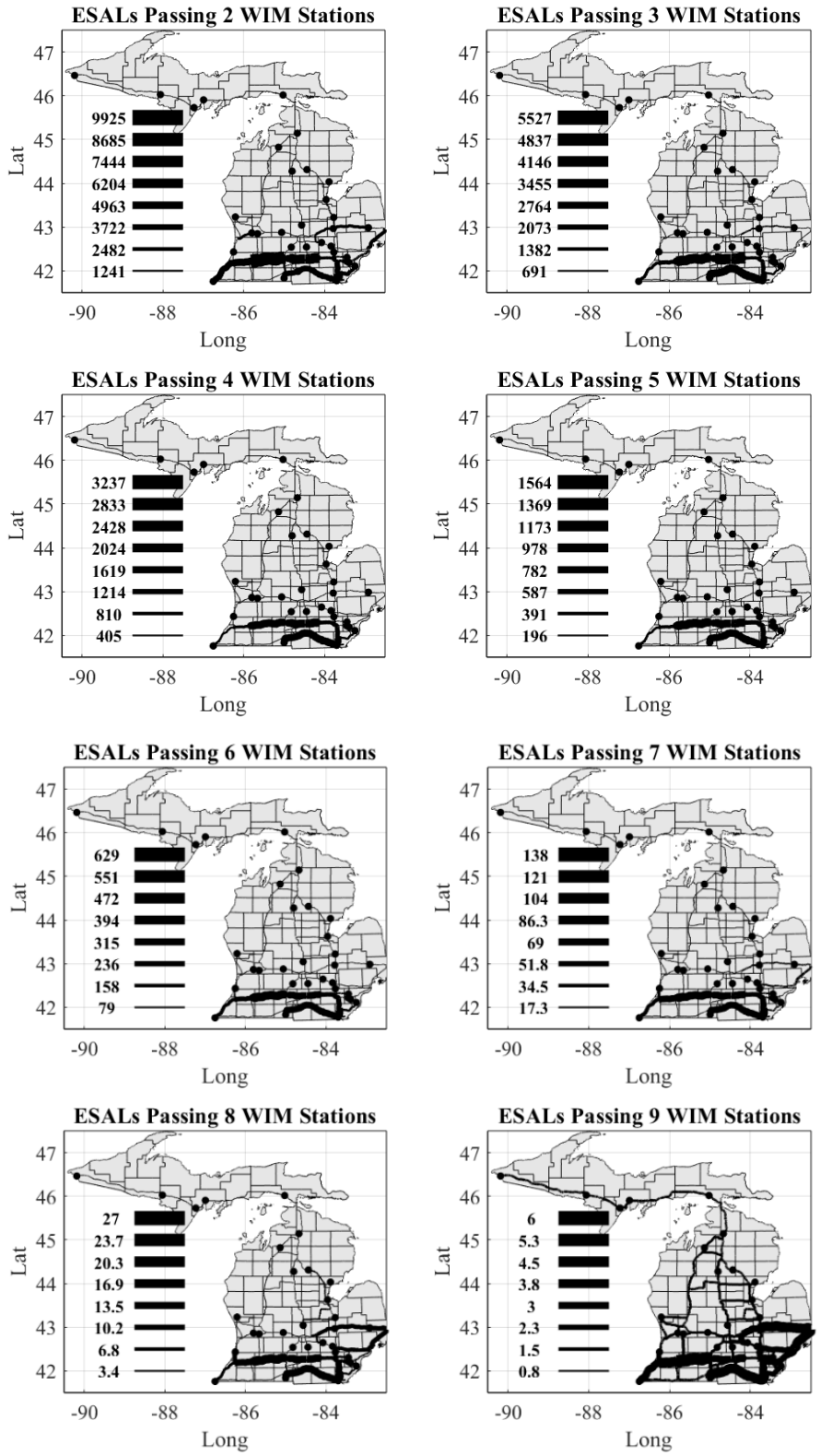

Figure 4-15. Total number of Equivalent Standard Axle Loads (ESALs) that traversed 2, 3, 4, 5, 6, 7, 8 and 9 WIM stations, respectively in the State of Michigan on October 29, 2020.

4.4.6. Proposed Freeway Asset Management Frameworks

The end goal of the Bayesian Inference-based truck re-identification analysis presented in this study is to quantitatively inform freeway and bridge asset managers on how many freight trucks are making a long haul in the State of Michigan with the corresponding freight truck loading on the in-place pavement and bridge assets. This study have shown quantitative risk-based asset management approaches for aged retaining wall assets **[89]**, **[68]** and for water distribution systems serving under resourced municipalities **[99]**. A preliminary framework is proposed in this study for highway and bridge assets with the notion of alternatively informing the quantitative asset management practices of highway managers. In **Figure 4-16**, truck traffic information is highlighted in the proposed framework to show the relevance on the analysis demonstrated in the previous sections. Truck axle loads of each vehicle can be converted to an Equivalent Axle Load Factor

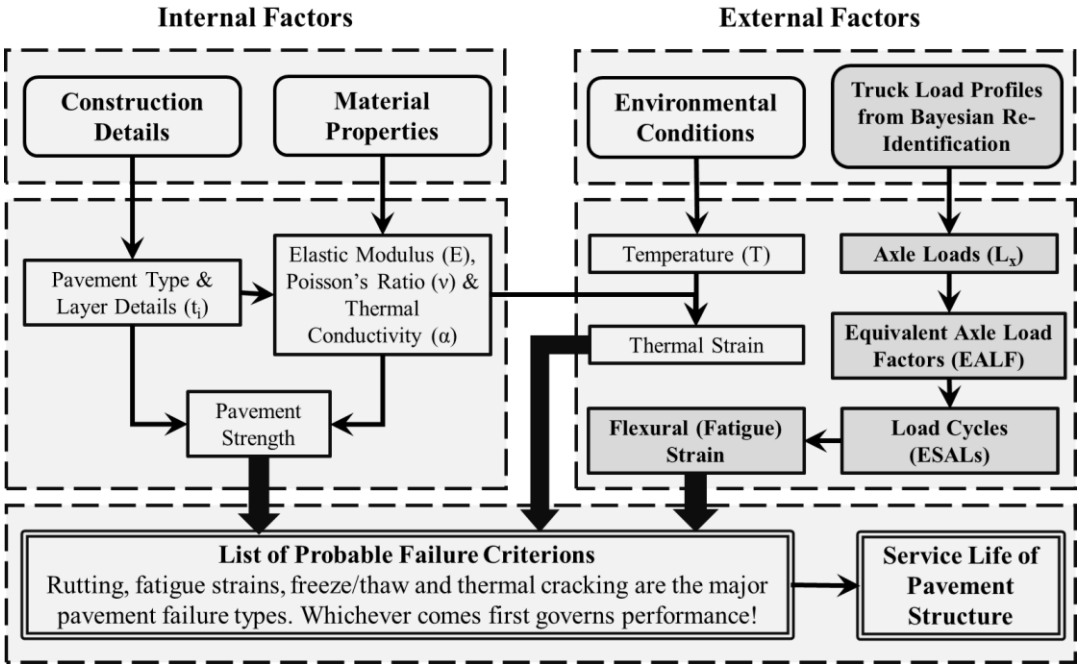

Figure 4-16. Proposed freeway pavement asset management framework and an outline of how the truck traffic information result from this research can be used.

(EALF) that sums to give a quantified number of Equivalent Standard Axle Loads (ESAL) essential for framing the number of cycles of load associated with flexural strains in a pavement. Thermal conductivity of pavement on the other hand is essential for quantifying thermal strain. Failure criterions entertain pavement strength with fatigue and thermal strain values to see which one threatens the performance of a pavement structure. Therefore, whichever of the many distress types that potentially deteriorate the strength condition of the pavement structure, the service life of the pavement comes to an end.

Moreover, even though fatigue analysis framework for bridge assets is an independent research area, the objective of the proposed bridge asset management framework in **Figure 4-17** contains few notes that inform the elements required to conduct a rigorous study. Unlike pavement asset management that looks for which failure strain kind governed pavement deterioration as an indication to its end of service life, super position of strains is a possible procedure, and the end analysis result is attributed to obtaining Probability of Failure (P_f).

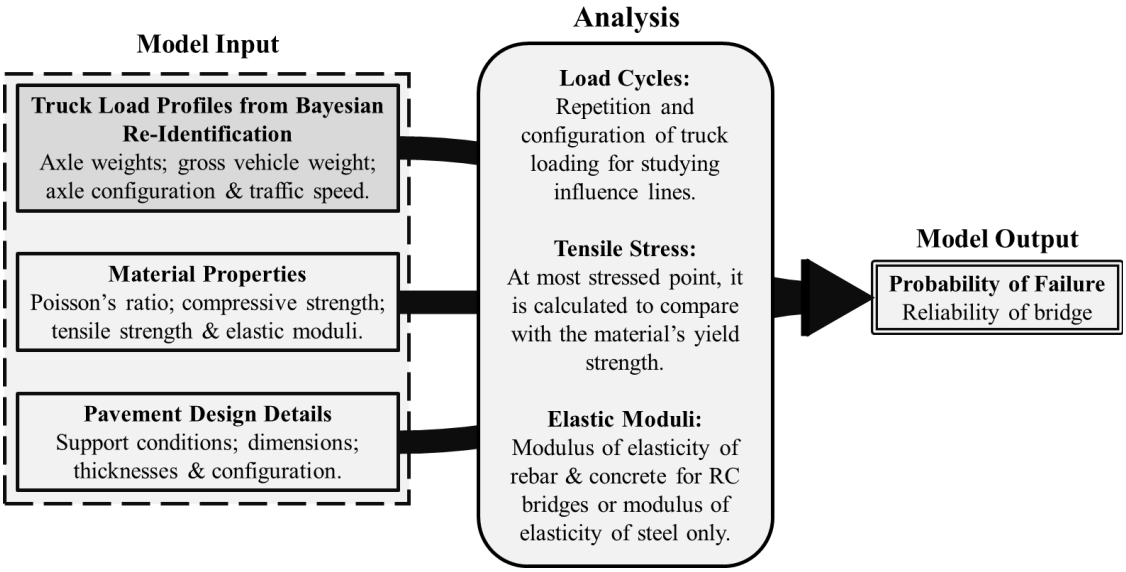

Figure 4-17. A proposed bridge asset management framework and notes of how the truck traffic information result from this research can be used.

4.5. Conclusion

In this study, a Bayesian Inference-based truck re-identification model is presented for matching freight truck signatures between adjacent pairs of WIM stations using raw WIM measurement data. The raw data was recorded by sensors embedded in freeway pavement locations dispersed spatially in the State of Michigan. The developed Bayesian Inference framework uses discrete WIM measurements for assessing the network level distribution of freight truck loading profiles (i.e., normal, and oversize vehicles) on freeway pavements and bridges inside (i.e., highway network-level), entering to, and exiting from the State of Michigan. The analysis of the discrete WIM measurements was conducted using a two-stage truck re-identification algorithm which a first-stage heuristic procedure informs the second-stage Bayesian framework with error distribution and probability of retention estimates. The heuristic procedure utilizes all attributes of measured truck signatures for better matching of trucks between pairs of adjacent WIM stations by setting equality and inequality constraints. The Bayesian framework on the other hand probabilistically matches truck signatures with a likelihood function defined by multi-variate gaussian model based on error distribution of axle weights, while the prior (initial) pdf is defined by the independent product of the probability of error in travel time and the probability of retention estimates. To decide on the threshold of probability that sets a cutoff value for considering a pair of trucks as a best match, partial Receiver Operating Characteristics (ROC) curves were plotted to identify threshold values that can take (False Positive Rate (FPR), True Positive Rate (TPR)) coordinates close to the ideal test (0,1). For this analysis, False Negative (FN) and True Negative (TN) values were extracted from ground truth via

video recording at a pair of WIM stations for generating test and validation datasets, as presented in earlier sections of this study.

The main contribution of this study is two-fold. The first one is with respect to demonstrating Bayesian Inference-based truck re-identification between pairs of WIM stations that is scalable to a bigger and realistic highway network-level analysis. The potential leakiness between a pair of WIM stations is then treated by calculating probability of retention values using a heuristic procedure that provides an essential input for a Bayesian framework. The second contribution is by quantifying the volume and loading of freight trucks making short-haul and long-haul movements in Michigan's highway network. Moreover, the total volumes of Equivalent Standard Axle Loads (ESALs) are delineated on map to demonstrate the movement of freight truck loading profiles that is valuable for quantitatively informing the reliability-based pavement performance management of highway asset managers. As a result, pavement, and bridge assets of interest in the network can be further investigated to study fatigue caused deteriorations by the operating freight traffic loading and volume. Thus, asset managers would be able to do quantitative asset management decisions for their deteriorated infrastructure.

Future works from this study can potentially be extended in different directions. The first work could be by observing the pair of WIM stations that were assessed for extracting test and validation datasets from continuous video recording over 2+ hours duration. That is, pavement material and construction details along with bridge design information could be collected and a full condition-based reliability analysis for risk assessment can be made. The second work could be investigating more on alternative probabilistic or mathematical models for matching truck signatures.

Chapter 5: Real-time Transit Performance Dashboard for the Management of Public Bus Transit Systems

5.1. Introduction

Public transportation plays a very important role in serving the mobility needs of communities across the United States. For transit-dependent communities (i.e., under resourced communities with low rates of car ownership), transit systems are critical to help them meet their essential needs including gaining access to food, jobs, education, and healthcare. These transit dependent communities are usually socially disadvantaged groups with poor access to workforce opportunities, thus they are assessed for their degree of social vulnerability **[190]**, their offered transit equity **[191]**, etc. To ensure essential needs of these communities are met including opportunities for social mobility, public transit systems must perform to high standards and offer riders both convenience and reliability. A recent study of 88 small and medium-sized local transit agencies in the United States provides evidence that the effectiveness of the public transit system increases whenever extensive use of performance management practices is in place **[192]**. For instance, transit agencies can assess the performance of their systems by looking at metrics such as **[193]**, **[194]**: per capita accessibility to public bus transit service, carrying capacity-km per person, travel time performance, and minutes per mile of buses.

In order to make novel research that demonstrate potential extensive use of an innovative performance management practice, this study has picked the public transit system serving the transit dependent communities of the city of Benton Harbor, Michigan. The city is located in Berrien County, Michigan which is in the southwest corner of the state in close proximity to Chicago, Illinois. Benton Harbor is a post-industrial mid-western city that has experienced a 45 % population decline since 1960 due to manufacturing jobs relocating over time **[195]**. The residents of the city have a low per capita income and low average household car ownership making the community transit dependent. Thus, there is huge responsibility on the shoulders of the local transit agency (i.e., the Twin Cities Area Transportation Authority (TCATA)) in supplying reliable and low fare transit service to the community under its available limited operating budget. Therefore, this study has two major contributions to make to the public transit field. The first one is with regard to using GPS trackers to assess the on-time performance of all buses in a transit provider's fleet, while the second is the development of a real-time performance dashboard based on the data available and by engaging TCATA, key stakeholders, and the community.

To have the transit provider TCATA become impactful, qualitative and quantitative assessments were conducted for the main goal to provide TCATA and the communities of Benton Harbor with a trust-worthy, transparent, adaptive, and quantitatively assessed view of their public transit system that can empower community stakeholders in system governance, to encourage community members to use the system, and to help the transit agency assess their system performance to allow for iterative improvements. Therefore, the study has two (2) research hypotheses with respect to the employing quantitative and qualitative methods: (1) for quantitative assessment, designing a low-cost solution for GPS

tracking of bus fleet and running a real-time performance dashboard for a small public transit agency can develop trust and transparency between transit riders and the transit agency. This could enable increased ridership if the community can observe that system performance exceeds community expectations. The report by **[196]** presents the adoption of transparency by transit providers in creating opportunities for transit riders to access transit information and to eventually improve qualities of transit service. It also highlights the insights it offers into performance elements that enable necessary disclosure and delivery of digital information to the public so that potential users would be able to act upon. (2) for qualitative assessment, the use of questionnaire and interview survey instruments for collecting perspectives of the transit agency, key stakeholders, and selected community members would enable the development of an adaptive and useful transit information tool that elevates the level of community trust. This is because community engagement and formation of a true equitable partnership is essential in improving the lack

Table 5-1. Key objectives and sub objectives of the study.

Objectives	Sub objectives
To quantitatively assess the performance of the existing public transit system as it currently operates	Define performance elements
	Offer real-time information to drivers, dispatch staff, and management to drive the operational efficiency
To encourage community input for the design of transit performance website	Collect deeper perspectives essential for developing an adaptive web dashboard
To make TCATA be able to make iterative improvements on service by looking at the reported performance elements	Provide TCATA's administration staff the ability to make real-time decisions on bus fleet operations
To administer the best management of bus and human resources	Assess active, idle, and stopped buses on the hours of transit operation
To improve community confidence (trust) in TCATA's service	Access to data and information on the performance elements (i.e., transparency)
To encourage community members to use the system	Inform the community about the on-time performance of the transit system

of trust in services supplied to underserved communities **[197]**. Moreover, with the appropriate design of a transit system performance dashboard website, we can have a powerful influence on users' trust perceptions **[198]**. The key objectives and sub objectives of this study are as highlighted in **Table 5-1**.

5.2. Literature Review

5.2.1. Resident Mobilities and Transit Performance

The underlying focus in perceiving service quality improvement of an existing transit system should be directed towards studying the system itself. Numerous studies exist that characterize resident mobilities and transit system performance. Activity-based approaches were used to characterize the mobility patterns of transit users for understanding the mobility needs of transit dependent communities. For example, the study by **[199]** used mobile phone call detail record (CDR) data to extract individual mobility networks and used the data to assess the use of various mobility solutions. Another study used CDR data to validate regularity of community movement by studying the spatiotemporal distribution of a half million bank notes distributed in the community **[200]**. In addition, smart mobile phones with embedded apps have also been used to track individual trips of selected study groups including identification of trip destinations **[201]**. In the mobility field, GPS trackers with cellular modems designed to track mobile assets including delivery trucks, long haul trucks, and buses have also been explored. When applied to buses, GPS data can be invaluable for better understanding of trip modes and system performance including resilience to extreme events **[202]**, **[203]**, **[204]**, **[205]**.

With regard to studies on transit system performance, the default approach is manual observation of the system (including the use of driver ridership logs and service managers tracking on-time arrival at stops). However, such methods are laborious leading to spatially sparse and infrequent observation of the system. Continuous monitoring based on wireless telemetry is now emerging in many fields of study including monitoring infrastructure assets **[206]**, **[207]**, **[208]**. Quantitative evidence of transit system performance is vital to assess system compliance to Federal Transit Administration (FTA) requirements imposed on public transit agencies **[209]**. Real-time GPS data is also critical for populating public-facing user interfaces including apps that map bus locations in real-time and performance dashboards that showcase the level system performance over time.

5.2.2. Quantitative Techniques and Qualitative Methods

Quantitative and qualitative assessment methods of public transit systems supplied by transit agencies have many utilities depending on the target audience. Particularly with performance measurements in place either with the use of dashboards or other report systems, the synthesized information would be useful for creating awareness about a transit system for managers, decision-makers, and planners. In such cases, the target audience would be primarily transit agencies, state transportation departments and other similar entities **[210]**. Thus, awareness about the supplied operational system is vital for iterative actions that transit agencies take, which a specific purpose can be to just identify real-time outliers. For cases where feedback data comes from end users and transit providers, the data may be processed using analytical models in a decision support system (DSS) that provide knowledge **[211]**. The feedback from end users not only influences the operation and configuration of a transit system in place but also the strategic planning of the details

of a new transit service as a semi-flexible system that maximizes better utility **[212]**. For existing transit systems, rider satisfaction is of utmost importance for transit providers to identify unmet transportation needs using customer satisfaction surveys (CSS) that guide them prioritize transit service concerns for respective decision actions **[213]**.

Qualitative assessment methods are generally employed whenever the measured attribute cannot be numerically presented. It is the best way of directly connecting to the community in study best utilizing the human factor. It also enables deeper understanding of service qualities and perspectives. Some of the methods include individual interviews, group interviews, observation, community or other large meetings, and interpretation of records, transcripts, etc. **[214]**. Several qualitative assessment techniques have been employed to monitor the condition of a public transit system in place. Service quality of public facilities that are used for public transit services can be assessed using Level of Service (LOS) rating scheme. These measures are the average of different responses of transit users for LOS A to LOS E **[215]**. In addition to service quality, transit user perspectives can be obtained by using qualitative methods such as interviews and surveys. In such cases, the categories of concerns and perspectives would be reported with the respective frequency of responses as opposed to categorizing into rating scales **[216]**.

The employment of quantitative techniques encompasses the measurement of numerical variables and statistical values of the assessment in question. Some of the standard methods include but are not limited to benchmarking, cost benefit analysis, existing data analysis, mixed methods, and tracking. Benchmarking involves comparing specifics to aspects of best practices while Cost Benefit Analysis involves assessing the cost effectiveness of implementing or maintaining programs or services. Existing data

analysis uses data from large databases to understand a phenomenon and how it affects a population while Mixed-Methods employ the use of two or more methods, with at least one being quantitative and one being qualitative. Moreover, tracking encompasses the recording of service utilization rate of individuals **[217]**. For dashboard information tools, Web Assessment Index (WAI) has been utilized since merely counting "hits" on a page is not an accurate measurement of quality or success. Thus, website quality can be assessed using four broad categories of accessibility, speed, navigability, and content **[218]**.

5.2.3. Transit Information Tools

Transit information tools play an important role for transit providers and riders for presenting quantitative measurements of a service in place. On the transit rider side, real-time arrival information significantly increases public transit system usability **[219]** while on the transit provider side, performance measurements guide their awareness about the system they run **[220]**. For both scenarios, a real-time GIS in a dynamic environment can be presented in a Dashboard Information Systems (DIS) **[220]**. DIS are commonly used by metropolitan transit agencies/authorities to report transit performance measurements **[221]**. In addition, transportation authorities utilized DIS for the performance measurement of freeways **[222]**, railway transit **[223]**, construction performance **[224]**, transit accessibility, and transit equity **[225]**. These DIS have limitations with respect to real-time attributes for varying computational and technical reasons. But for example, the real-time DIS of COVID-19 daily new cases with public moving average trend models has been an advancement in the domain of DIS to supply updated information to a wider range of audiences **[226]**, **[227]**. The key utility of transit information tools is to provide a transparent service. Reporting performance measures on a selected information tool are

necessitated to comply with statutory and funding requirements and to promote transparency of transit operations, establish service standards to evaluate goals, and identify underperforming routes or service matters lagging and needing improvement. For this purpose, a quarterly report that presents a high-level analysis and communicates if the Metro system's performance is improving, worsening, or steady **[197]**.

5.2.4. Development of Transit Performance Web Dashboards

Performance dashboards are often designed to track specific performance metrics. According to **[228]**, four points of view exist with regard to performance metrics that should be considered for the development of a public performance dashboard: customer, community, agency, and vehicle/driver. Customer-specific metrics often consist of service availability (e.g., service coverage, frequency, hours of service) and convenience (e.g., service delivery, travel time, safety, maintenance). Community-specific metrics often include the financial costs of the system and net community usage of the system. Agency-specific data is often focused on highly detailed on-time data and the spatiotemporal mapping of user demand. To ensure these metrics can be provided, high-quality real-time data from the system is needed. Also, concerned advocates often ask agencies to make their data public to ensure accountability **[229]**. A recent study **[230]** has identified major qualities of a transit dashboard that meet customer and community needs: 1) measures the right things, 2) is easy to use, 3) presents historical context, 4) provides open and accessible data, and 5) links metrics to goals.

Transit agencies operating in major metropolitan areas in the United States have existing public bus transit system performance dashboards online for the public. This study reviewed seven (7) of these transit agencies for assessing the current practice of transit

performance dashboards. For instance, Capitol Metro (CapMetro) of Austin, Texas has ridership, safety, reliability, finance, route performance, and COVID response **[231]** on their dashboard, while Metropolitan Transit Authority (MTA) of New York City has service delivered, bus speeds, additional bus stop time, additional travel time, customer journey time performance, mean distance between failures, passenger environment survey, wait assessment, additional bus stop time, additional travel time, and performance of an access-a-ride **[232]**. Tri-County Metropolitan Transportation (TriMet) of Portland, Oregon on the other hand has ridership, efficiency, budget, safety, and open-source data **[233]**, Washington Metropolitan Area Transit Authority (WMATA) of Washington, District of Columbia has average ridership/bus boardings, year-over-year change in ridership, and ridership data by time, route, and station **[234]**, and Transit Chicago of Chicago, Illinois has historical bus crowding, availability of seats, and crowding graph **[235]**. Moreover, Massachusetts Bay Transportation Authority (MBTA) of Boston, Massachusetts has reliability, ridership, financials, and customer satisfaction **[236]** on their dashboard, while Detroit Department of Transportation (DDOT) of Detroit, Michigan has monthly ridership, on-time performance weekday, and average weekday pull out **[237]**. Nonetheless, main contributions could be added to the current practice of transit performance dashboards with respect to: (1) enabling existing dashboards with real-time performance analytics (i.e., dashboards presented in **[231]**, **[232]**, **[233]**, **[234]**, **[235]**, **[236]**, **[237]** are updated monthly), (2) informing the management of transit systems owned by small transit agencies, (3) real-time performance dashboards informed by data coming off GPS modules tracking the whole bus fleet, and (4) engaging the transit agency, key stakeholders, and selected community members of a city using designated survey programs is applied to a

limited extent. In this study, real-time performance metric assessment in an AWS platform using a data feed from GPS trackers is presented as key end result of this work.

5.2.5. Community Engagement

Community engagement and the collection of their perspectives are keyways of collecting qualitative information from the target audience in study. Particularly when there exist quantitatively informed transit information tools, user participation is essential to make it an even more effective tool **[238]**. With information tools, participatory design processes play an important role in building a tool with accessible interfaces with the potential of delivering service to a range of users. Not only do the designers and developers know very little about how the target audience interacts with their tool, but they also have little exposure to adaptive tools **[239]**. Thus, the engagement of a community in a participatory design process requires the design and implementation of workshops **[240]**, **[241]**. Such workshops have relevance in the design of information tools in a participatory design process employing perspectives on tools using surveys and interview programs. The workshops have utility in informing outcomes that impact tool design entertaining diverse perspectives and open engagements **[242]**.

5.3. Public Transit System in Benton Harbor, Michigan

5.3.1. Benton Harbor, Michigan

The City of Benton Harbor (pop. 10,036 **[195]**) is located in southwest Michigan and is distributed over a 4.7 square mile area on the shore of Lake Michigan (**Figure 5-1**). It is located in Berrien County and is known as the "twin city" of St. Joseph, Michigan (pop. 8,365). Benton Harbor is an under resourced community with a median per capita income of $10,309 (with 50.3% of the population living below the poverty line); this is in stark

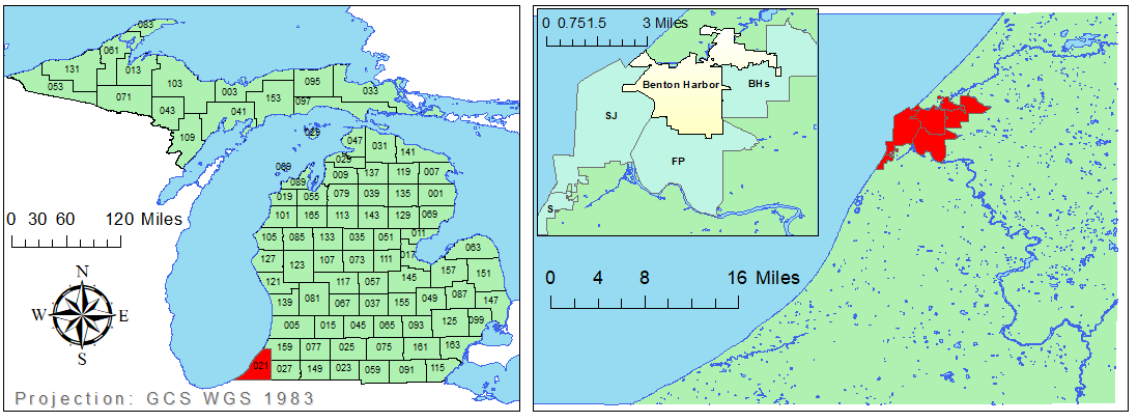

(a) (b)

Figure 5-1. (a) Location of Berrien County in the State of Michigan; (b) location of Benton Harbor, MI in Berrien County alongside Saint Joseph (SJ), Flair Plain (FP) and Benton Heights (BH's).

contrast to its "twin" city St. Joseph which has a per capita income of $28,930 **[195][243]**. At one time, Benton Harbor was an affluent city with manufacturing jobs available for city residents. However, the migration of these jobs over the years to locations outside of the region has eroded the city's workforce pipeline resulting in high levels of unemployment (15.8%), steady population loss (45% since 1960), and a severe decline in city resources.

5.3.2. Twin Cities Area Transportation Authority (TCATA)

While many jobs and job training resources exist outside of Benton Harbor, they can be difficult for segments of the population to access because of the high number of households (i.e., up to 51% **[244]**) with zero vehicle ownership. This requires much of the community to be reliant on the public transit system that is managed by the Twin Cities Area Transportation Authority (TCATA). TCATA runs three schedule-based bus routes (**Figure 5-2**) and an on-demand shuttle service which services the greater Benton Harbor area; service run Monday through Saturday from approximately 6am to 10pm. The system consists of 27 buses (used for fixed route and on-demand service) supporting more than 200,000 rides per year. Limited studies exist for surveying public concerns regarding

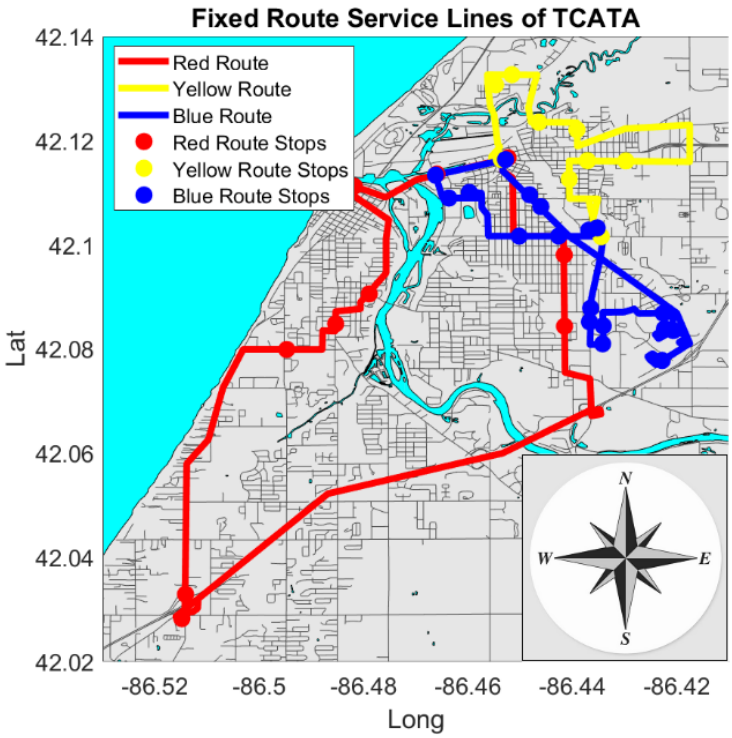

Figure 5-2. TCATA's fixed route service lines: "Red", "Blue", and "Yellow" routes.

transit system performance in Berrien County. The studies by **[244]** and **[245]** investigated the assessment of transportation needs and issues, transportation resources analysis, unmet transportation needs and issues, and strategies for exploring transit projects in the twin city area and Berrien County. The need assessment identified three potential transit dependent populations: seniors (i.e., above 65 years of age), people with disabilities, and people with lower incomes. The studies also highlighted some of the causes of unmet transportation needs including limited services on Saturdays, Sundays and evenings, and the lack of fixed routes in areas with high population densities.

5.4. Methodology: Qualitative Assessment Methods

As part of this study, the qualitative methods used for conducting small-scale research consist of two approaches in assessing TCATA's public transit system. The first one aimed to collect general opinions via questionnaire surveys distributed to key stakeholders, and

community members that were participating in a scenario planning workshop **[240]**, while the second one aimed to record open ended responses and deeper perspectives via semi-structured one-to-one interview conducted with TCATA's drivers, dispatchers, directors (former and current), board members, and affiliates. Therefore, a questionnaire survey is designed to collect qualitative data essential for the development of a real-time web DIS. The book by **[246]** identifies important stages in questionnaire design that answers different research questions related to qualitative information essential for an impactful quantitative real-time web DIS. The Questionnaire Survey Research Design Documents presented in **Appendix A** and **Appendix B** were prepared using the important stages (from **[246]**):

I. Identify questionnaire objectives and research hypotheses
II. Define the target population, sampling frame and sampling
III. Generate the topics to be addressed and data required
IV. Decide the kinds of responses required and write the questionnaire items
V. Address the sequence, length, design and format of the questionnaire
VI. Check that each issue has been addressed, with several items for each issue
VII. Pilot, refine, and administer the questionnaire
VIII. Send reminders

The scenario planning workshop in **[240]** presented the collaboration with 10 stakeholder and community participants on May 13, 2022, to discuss opinions as well as collect feedback on alternative new route options sought for optimizing the in-place fixed-route transit system of TCATA. The stakeholder participants came from Benton Harbor Downtown Development Authority (DDA), Benton Harbor City Commission, Benton Charter Township, TCATA Board, McKenna (i.e., Master Plan Consultant), Intercare (i.e.,

Community Health Network), and TCATA. Among the 10 participants, 8 of them returned complete questionnaire survey responses. The questionnaire aimed to survey deeper perspectives on community trust, transit system performance, and web dashboard. Moreover, from July 21, 2022, to September 2, 2022, an extensive one-to-one semi-structured interview was conducted with 9 individuals comprised of 6 members of TCATA's current staff (i.e., 1 dispatcher, 1 maintenance director, and 4 drivers), 1 board member, 1 former director, and 1 affiliated senior transportation planner. The interviews provided wide and deep inputs in response to the asked 34 questions regarding: their regular roles at TCATA, TCATA's primary objectives, works of TCATA with the community, use of transit data for agency decisions, real-time bus maps, transit data shared with community, delay threshold for on-timeness of fixed-route buses, high-performance transit service metrics, building community confidence on transit provider, real-time transit performance on a web dashboard information system, etc.

5.5. Methodology: Quantitative Assessment Techniques

It is proposed herein that the service quality of the transit system supplied to the Benton Harbor community needs to be first observed continuously over a long observation period to capture the performance of the transit system. Data from GPS receivers installed in the system buses are used to calculate the performance of the existing transit system design including on-time performance of the fixed route service. In addition, a database of dispatch logs associated with on-demand service is integrated to observe the performance of that important transit solution for disabled and elderly community members. Dispatch data offers information about trip purposes, age of riders, disability status, number of companions and the origin-destination pair of individual trips. Long-term observation of

the transit system in Benton Harbor can suggest areas for improving system efficiency by identifying the root causes of performance challenges.

5.5.1. Data Sources

TCATA has provided access to a large amount of data and information available for this study. Traditional data sources associated with baselining existing mobility services include dispatch logs associated with on-demand shuttle service (also called "dial-a-ride" service by residents of Benton Harbor). The dispatch logs have recorded for more than 220,000 scheduled trips (successful or not) from March 2017, to present (with the author still collecting dispatch logs quarterly). The recorded data contains comprehensive information on individual trips with respect to pick-up origin-destination pairs, date of trip, scheduled time of pick up (but not confirmed pickup or drop-off times), trip purpose, disability status, age group, and number of companions.

As mentioned, the system has already been instrumented with GPS trackers that provide high resolution GPS coordinates of all TCATA buses with data streaming to a Verizon Connect portal. The GPS trackers were installed on 27 buses and have been reporting spatiotemporal information of each bus since January 2019 (with data continuing to communicate to the present day). The data is reported every 1 minute and contains information on: latitude, longitude, timestamp, date, mean speed, maximum speed, instantaneous speed, and bus ID. Coupled with dispatch logs, the GPS trackers provided a valuable data source to identify service quality (e.g., on-time rate of the fixed route service, wait and delivery times of on-demand users) and overall utilization of TCATA's fleet.

5.5.2. Cloud Computing Framework

This study focuses on a scalable cloud-based data management solution built in Amazon Web Service (AWS) to collect and process TCATA's GPS fleet data as illustrated in **Figure 5-3**. The GPS trackers on TCATA's 27 buses (that address fixed-route and on-

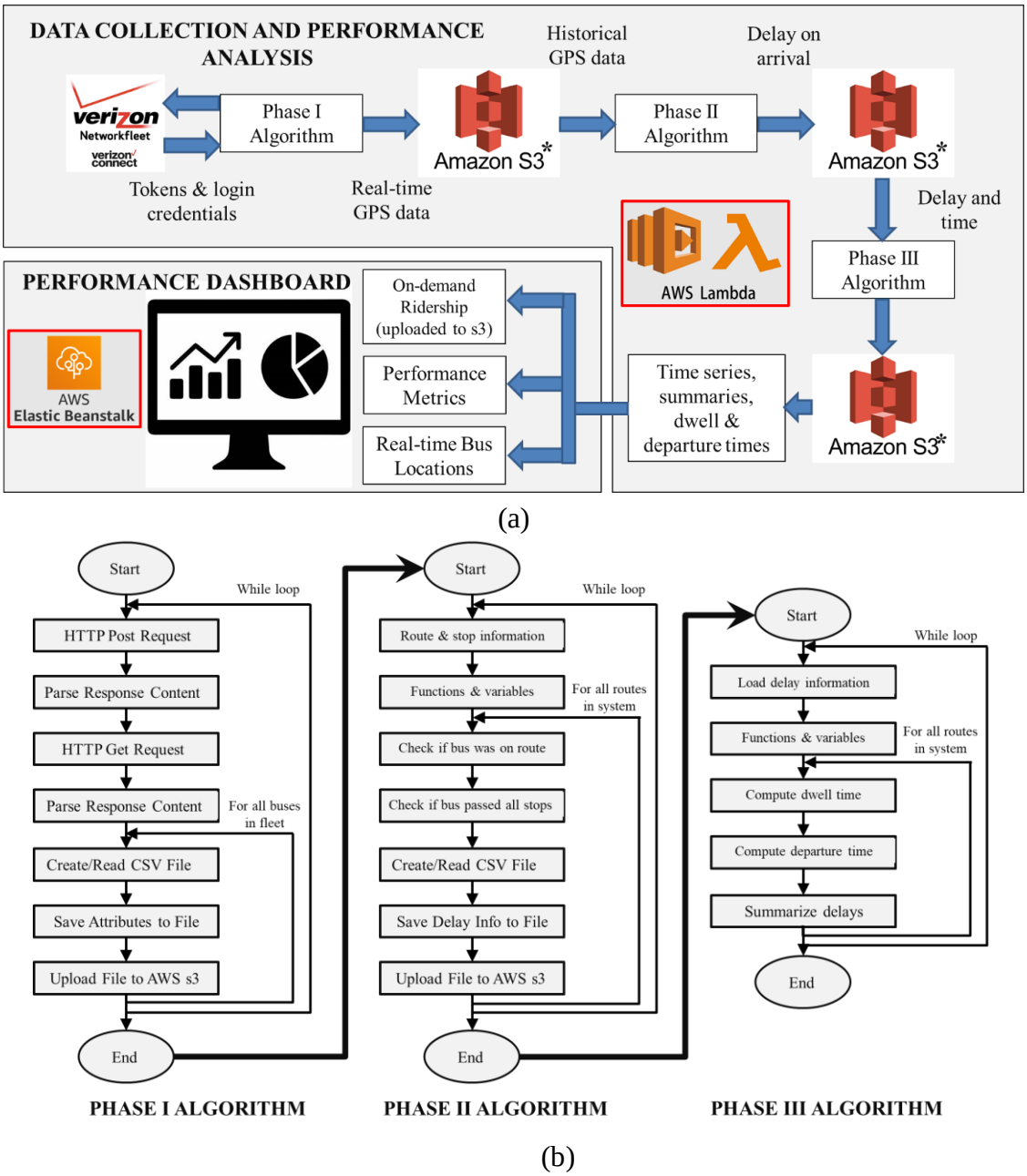

Figure 5-3. (a) Framework for the development of website Graphical User Interface for the public bus transit system in Benton Harbor, Michigan; (b) Algorithms for data collection and performance analysis.

demand services) report data to the data portal called Verizon Connect which this data service is independent of the AWS cloud platform. In AWS, the event-driven Lambda service is adopted to automate the execution of code in response to events such as data availability and timers. AWS Lamda executes Phase I by the querying of data from Verizon Connect by HTTP request with GPS data received written to a CSV file that is stored in an S3 (Simple Storage Service) file repository. Phase II then reads the CSV file from S3 to analyze the GPS data to identify which buses are serving fixed route buses. Finally, Phase III uses the GPS data of those buses assigned to fixed routes to ascertain their on-time performance. The data processing scripts of Phase I through III are all written in Python and executed by AWS Lambda with processed results stored in files contained in S3, as delineated in **Figure 5-3**. The performance dashboard for TCATA is also developed using AWS Elastic Beanstalk and uses system performance metrics from the S3 repository in addition to real-time GPS data to visualize the real-time location of buses. Real-time GPS data is taken and analyzed generating performance metrics and a raw on-demand dispatch log uploaded to the AWS S3 bucket.

5.5.3. Performance Assessment Framework

In this section, the analytical steps used to process data in Phase II and III algorithms are described in detail. Since the GPS trackers were installed on both fixed-route and on-demand buses, the collected GPS data from fleet tracking needed to be divided into two kinds of trajectories – fixed-route service trajectories (loops of service) and on-demand service trajectories (dial-a-ride trips). This is due to the fact that TCATA could not fully commit buses by route for the entire analysis period. Buses are often reassigned randomly from fixed route service to on-demand service. The Phase II algorithm cleanly divide the

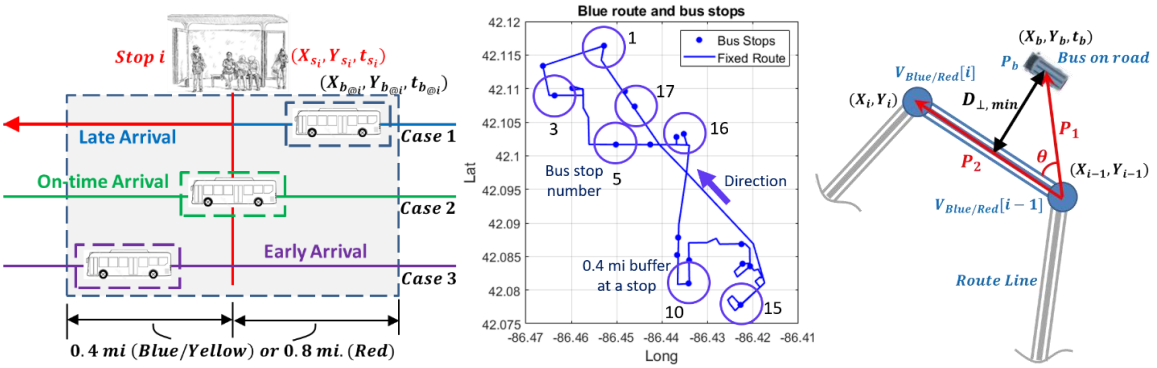

(a) (b) (c)

Figure 5-4. (a) Illustration of late, on-time and early arrivals; (b) assigning spatial buffers around stops (e.g., "Blue" route), and (c) vectors to calculate offset of bus from route.

GPS data of each bus into one of the two trajectory types. The algorithm has five major functions to execute the performance analysis. These include parsing raw GPS data, assessing if a bus stayed on route (using the known routes of the "Blue", "Red", and "Yellow" service lines), calculating late or early arrival rates of buses and checking trajectories for validity of fixed-route loop of service (or not). Moreover, no manual work is needed to precisely calculate early and late arrival rates (Phase II), dwell time at stops, and late and early departure from stops (Phase III). Therefore, this is very scalable for the continuous analysis of real-time GPS data continuously streaming in. In the source code, spatial flexibility is allowed in the assignment algorithm to ensure flexing operations used by TCATA drivers of the fixed routes does not lead to misassignment of a fixed route bus to that of an on-demand bus.

The first step in disentangling the downloaded GPS data was to look for fixed route loops of service that can be evidently traced. A 0.4-mile buffer radius (**Figure 5-4b**) (to account for the sampling rate of the GPS receivers in use) was considered for "Blue", "Yellow", and "Red" routes, respectively. Since the I-94 highway corridor is a sizable part of the "Red" route and by looking at the average speed histogram of buses on the "Red"

route compared to "Blue" and "Yellow", it was inferred that the buses on the "Red" route are approximately twice as fast. Therefore, a larger buffer radius was used for their stops (0.8 mile). A bus is considered to be on a fixed route service if it is seen in the buffer circle of all the stops and has been within 0.05 miles of the route at all times ($D_{\perp,min}$= 0.05 miles which is the perpendicular offset distance from the route as shown in **Figure 5-4c**). The offset calculation is presented as:

$$P_1 = P_b - V_{Blue}[i-1] \tag{5-1}$$

$$P_2 = V_{Blue}[i] - V_{Blue}[i-1] \tag{5-2}$$

$$\theta = cos^{-1}\left(\frac{P_1 . P_2}{||P_1||||P_2||}\right) \tag{5-3}$$

$$D_\perp = \begin{cases} [D_\perp, ||P_1|| * sin(\theta)] & if\ ||P_1|| * cos(\theta) \le ||P_2||\ and\ |\theta| \le 90^o \\ N/A & otherwise \end{cases} \tag{5-4}$$

$$D_{\perp,min} = min(D_\perp) \tag{5-5}$$

where, V_{Blue} is a vector which contain vertices (X_i, Y_i) of all edges composing the route; i is an index within the length of V_{Blue}, P_1 is a vector from vertex $i-1$ to the bus at a given time, P_b is the coordinate of bus (X_b, Y_b), P_2 is a vector from vertex $i-1$ to vertex i, θ is the angle between P_1 and P_2, $D_\perp$ is perpendicular offset distance of the bus from a route line segment, and $D_{\perp,min}$ is min perpendicular offset distance of the bus from route.

The second step is to calculate the early and late arrival (**Figure 5-4a**) rate of a bus at every stop. There are two approaches for this analysis. The first is to match a timestamp from the GPS data with the bus schedule at a particular stop and then calculate drive distance to get the estimated time of arrival (ETA) of each bus. The second is to identify first when the bus entered the buffer circle and deduct the scheduled time from the timestamp of the GPS receiver in a particular bus. The second method is more precise since

it does not necessarily need to address the discrepancy between drive distance and geometric distance since the distance part is calculated when the bus has passed a stop as sampled in the next recording of the bus location (within 20 to 60 seconds) (**Equation 5-7**) **[247]**. Finally, it is checked if the bus is arriving at all stops within 15 minutes of before (early) or after (late) scheduled arrival. It is then concluded that the bus was making a fixed route loop of service. The offset and ETA calculations are as formulated below as:

$$Distance = \sqrt{\left(X_{s_i} - X_{b_{@i}}\right)^2 + \left(Y_{s_i} - Y_{b_{@i}}\right)^2} \quad (5\text{-}6)$$

$$t_{delay} = t_{b_{@i}} - t_{s_i} + \frac{Distance_{in\ buffer\ radius} * 60}{V_{avg}} \quad (5\text{-}7)$$

where, $Distance_{in\ buffer\ radius}$ is the geometric distance between the bus and stop i in the buffer radius; (X_{s_i}, Y_{s_i}) is the geometric coordinate of fixed route stop i; $(X_{b_{@i}}, Y_{b_{@i}})$ is the GPS coordinate of the bus at t_{s_i}, t_{delay} is the estimated time of arrival of the bus at stop i, t_{s_i} is the scheduled time of bus arrival from TCATA's timetable, $t_{b_{@i}}$ is the time of the bus while in the buffer radius, and V_{avg} is the average speed of the bus in the previous 20 to 60 seconds of drive in the buffer radius.

The Phase III algorithm focuses on the delay upon arrival results and computes dwell and departure times at individual bus stops. **Figure 5-5** presents the breakdown of the time a bus takes between two successive stops (i.e., arrival, dwell, and departure timestamps presented in **Equations 5-8 to 5-12**).

$$t_{b_{@n+1}} = t_{b_{@n}} + t_{dwell_n} + TT_{n\ to\ n+1} \quad (5\text{-}8)$$

$$TT_{n\ to\ n+1} = \sum_{i=1}^{n-1} \frac{d_i}{v_i} \quad (5\text{-}9)$$

$$t_{delay_{n+1}} + t_{s_{n+1}} = t_{delay_n} + t_{s_n} + t_{dwell_n} + TT_{n\ to\ n+1} \quad (5\text{-}10)$$

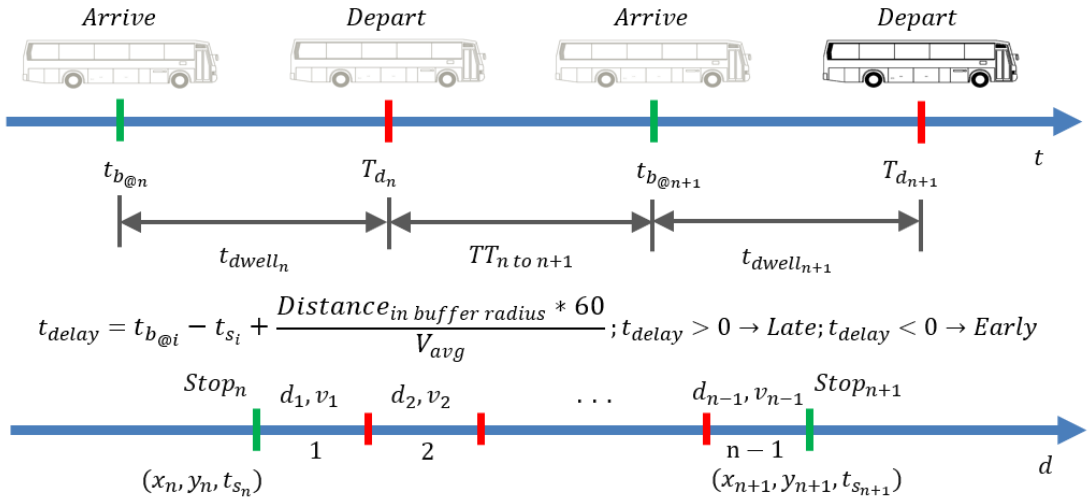

Figure 5-5. Illustration of arrival, dwell, and departure of buses on fixed route between two successive stops.

$$t_{dwell_n} = \left(t_{delay_{n+1}} - t_{delay_n}\right) + \left(t_{s_{n+1}} - t_{s_n}\right) - TT_{n\ to\ n+1} \qquad (5\text{-}11)$$

$$t_{departure_n} = t_{delay_{n+1}} + t_{s_{n+1}} + t_{dwell_n} \qquad (5\text{-}12)$$

where, t_{dwell_n} is the dwell time at stop n, $TT_{n\ to\ n+1}$ is the travel time it takes a bus to depart stop n and arrive at stop $n+1$, $t_{departure_n}$ is departure time at stop n, t_{delay_n} is the estimated time of arrival of the bus at stop n, t_{s_n} is the scheduled time of bus arrival at stop n from TCATA's timetable, d_i is the distance traveled in the i^{th} min, v_i is the speed of bus in the i^{th} min, and $t_{b_{@n}}$ is timestamp of the bus while in the buffer radius close to stop n.

5.6. Results and Discussions

5.6.1. Analysis of Survey and Interview Responses

As presented in **Appendices A and B**, the questionnaire survey and 1-to-1 interview responses comprised of open-ended statements, rating scale preferences, and 'Yes' or 'No' answers. The questionnaire surveys were distributed in paper printouts to workshop participants while the 1-to-1 semi-structured interviews were recorded conversations. Both

group of responses were later electronically saved into Microsoft Word (.docx) documents through typing and transcribing, respectively. The analysis of the rating scale preferences and 'Yes' or 'No' question answers are straight forward in which rating responses were averaged, while the total number of respondents saying 'Yes' or 'No' are counted. For the open-ended responses, all sentences of respondents were collected manually, and duplicate

Figure 5-6. Word cloud (by frequency of words in expressions) of questionnaire survey and semi-structured interview responses.

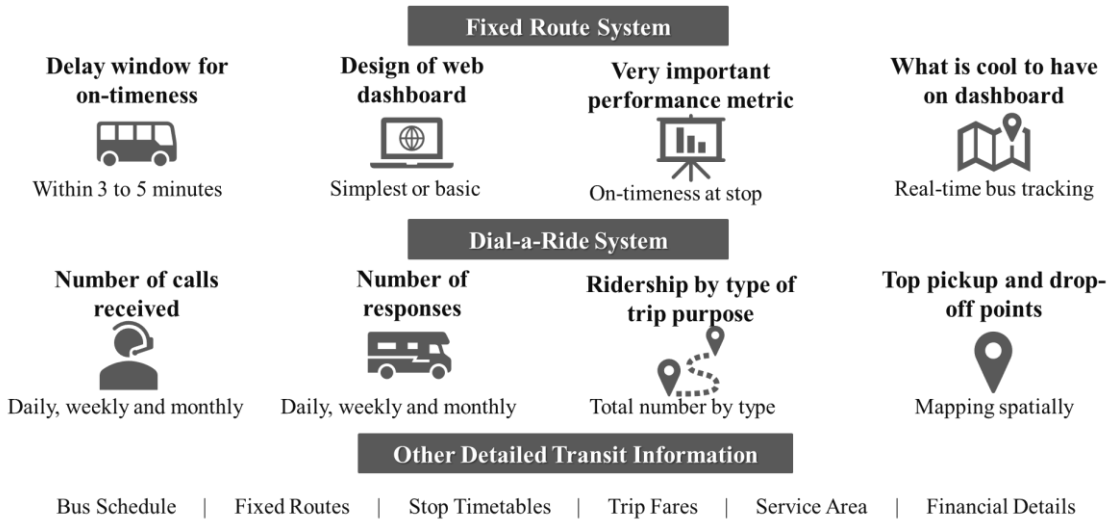

Figure 5-7. Inputs that were found helpful for finishing performance dashboard design.

ideas, space-filler words, and non-insightful out of topic responses were removed to make results more concise, and relevant. Moreover, long sentences were shortened to result in list of responses that are easy-to-read and open-ended (presented in **Appendices C and D)**.

The respondents of both the questionnaire surveys and semi-structured interviews provided diverse perspectives for the asked open-ended questions. Thus, even though the original intention of the qualitative study was to adequately inform the design of a real-time transit performance web dashboard, the respondents also provided organizational inputs (**Table 5-2**) for TCATA that would be helpful to run an efficient and high-performing public transit system. Most frequent words were highlighted by setting higher font sizes in the word cloud shown in **Figure 5-6** to visualize the word contents of responses. As a result, beyond answering community trust, transit performance, and web dashboard specific questions, respondents also emphasized on the importance of focusing on drivers that are end operators of the system determining transit performance, and daily challenges of the transit dependent community being served. Moreover, in **Figure 5-7**, responses collected from dashboard specific questions were processed to summarize what

Table 5-2. Organizational inputs for TCATA from surveys and interviews.

Performance is affected by	TCATA should focus on	Key suggestions
• Timeliness of bus drivers in running the transit service operations • How TCATA admin treat their employees • Adequately training for the current staff • Putting new policies, procedures, and along with their enforcement	• Paying bus drivers right • Community members riding their system • Having real-time map for showing the locations of active buses on duty • Increasing staff size for supplying fixed-route and dial-a-ride service needs	• Existing financial resources could be better utilized to run an optimal system • Can improve better to become the best transit agency in Berrien County • Business knowledge is very essential for administration staffs and the board • Drivers are end personnel to assure on-time bus delivery

would is important to have on a public facing dashboard with respect to the fixed-route system, the dial-a-ride (on-demand) system, and general transit information tabs.

5.6.2. Performance of TCATA's Public Transit System

For the fixed route portion of the system, TCATA previously utilized two routes (namely, "Blue", and "Red" routes). The "Blue" route (**Figure 5-2a**) provides a one-way (running counterclockwise (CCW) in **Figure 5-4b**) fixed route loop of service starting at TCATA's transit center, traversing through the city of Benton Harbor, to the regional mall (i.e., Meijer, Walmart) and then back to the transit center. It has larger ridership as compared to the "Red" route and operates every 30 minutes starting from 6:00 am to 10:00 PM, Monday to Friday (8:00 am on Saturdays). The third route (the "Yellow" route) was introduced as a new route in mid-January of 2020 to encompass neighborhoods in Benton Harbor with historically low household car ownership that are not currently served by the "Red" or "Blue" routes. In **Figure 5-8**, the performance of the system from January 2, 2019, to September 25, 2022, is presented. Histograms of delay in early/late arrival of the buses at the corresponding stops of the four fixed route schedules (i.e., two 30-minute schedules on the "Blue" route (denoted as Blue :00 and Blue 0:30), one hourly schedule on the "Red" route, and one hourly schedule on the "Yellow" route) are presented. The first row of histograms in **Figure 5-8** presents *average* delays on arrival at the stops in a single loop of fixed route service while the second row of histograms present the data of all delays at the stops of the corresponding fixed routes over the 31 months of GPS sensor monitoring.

For the "Blue" route, two delay histograms were drawn for the :00 minutes after the hour and :30 minutes after the hour services on the route (i.e., four histograms). The first row in **Figure 5-8** shows the average of delays at all the 18 stops, for every completed

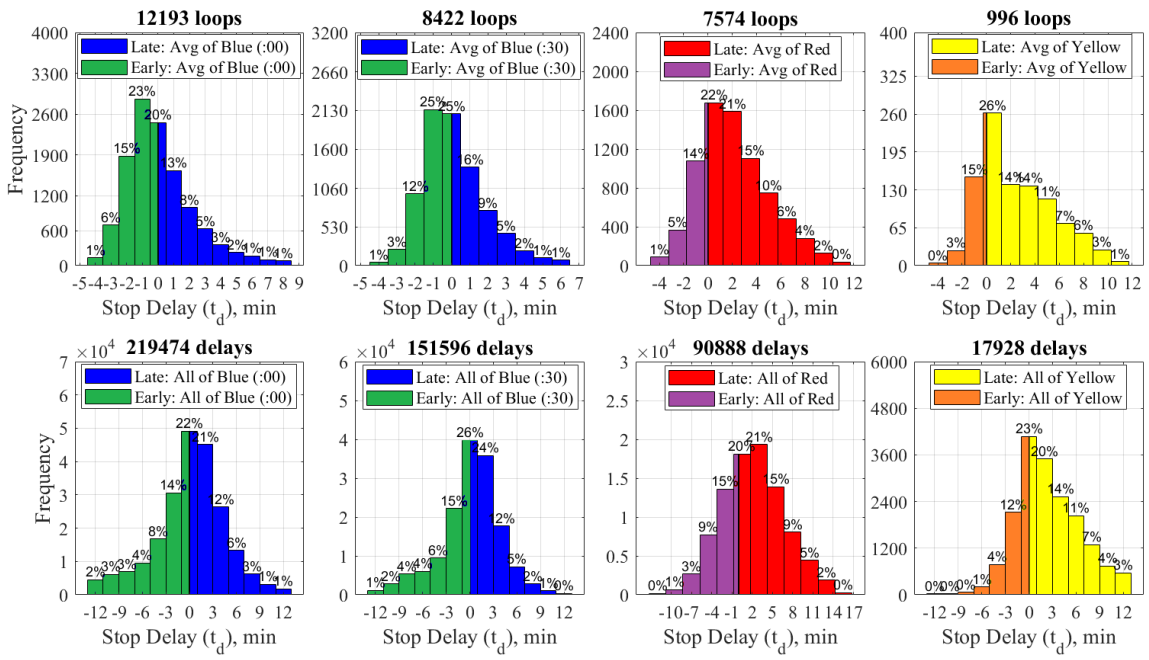

Figure 5-8. Histograms for arrival delay of TCATA's fixed route system (1/2/2019 to 9/25/2022): (top row) histogram of average stop arrival delay per loop; (bottom row) histogram of delay of all stops.

loop of service while the second row contains every delay at the stops. If we consider all stop delays on arrival, the percentages of time the buses came within 3 minutes of the posted arrival time were 56% (:00 after the hour) and 66% (:30 after the hour) while the ones that arrived within 5 minutes of the posted arrival time were 74% (:00 after the hour) and 83% (:30 after the hour). The "Red" route supplies one-way fixed route service connecting Benton Harbor and St. Joseph, thus covering a much larger geographic area. The fixed-route system tends to show slightly more delays as compared to the "Blue" route where buses arrive at stops within 5 minutes of scheduled arrivals 67% of the time. The "Yellow" route supplies two-way hourly fixed route service starting at TCATA's transit center, reaching a health care facility, a Boys and Girls Club community center, and then turns back to the transit center along the same line. It runs Monday to Friday from 7:00 am

to 5:00 pm every 30 minutes with on-time arrival within 3 minutes for 58% of the time and within 5 minutes for 75% of the time.

An interesting observation of the delay performance of the system can be seen by looking at delay accumulation and variation along the routes. In **Figure 5-9**, delay variations for the whole analysis period are plotted as shown. As seen in the plots, buses tend to consistently follow a repetitive arrival trend at individual stops. This presents an interesting observation on system operations. Buses on the "Blue" route arrives at the stops near the malls very early and dwell there for extended periods of time to pick up passengers. By arriving there early, these buses then maintain the route schedule before returning to the TCATA's transit center. But for the "Red" route, the bus rather reaches at the stops near the mall on time but traverses through the stops until TCATA's center very late. A number of analyses were done to characterize the causes of delay on arrival of the buses at the stops, particularly the environmental (i.e., weather) and operating conditions (EOC)

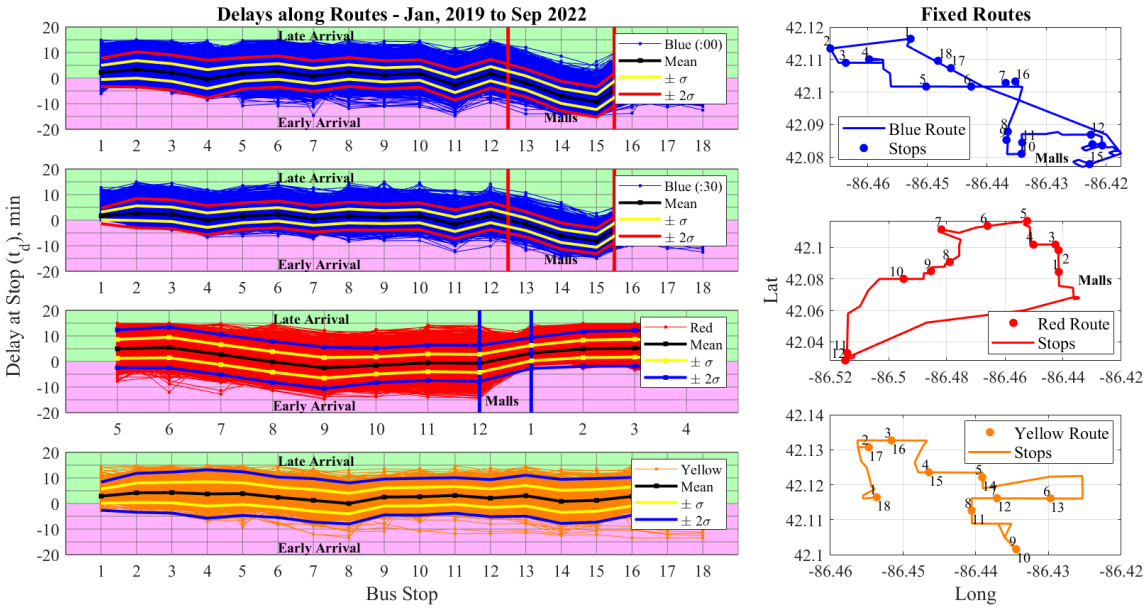

Figure 5-9. Delay (late/early) variations along fixed-route bus stops of TCATA's fixed route system (January 2, 2019, to September 22, 2022).

that may contribute were assessed but the operational conditions were more dominant in governing system performance.

With regard to assessing fixed route system performance, the delay on arrival at stops may not be the primary element necessary to assess if a bus is late or not. This is because a bus may come early to a stop and then dwell for some time waiting for passengers before departure. Therefore, delay in departure of buses at a stop clearly tells lateness or earliness of a bus. The "Blue" route was assessed with this regard after looking at the delay variation along the route shown in **Figure 5-9**. As seen in **Figure 5-9**, it may appear that early arrival of the buses at the mall stops along the "Blue" route would mean these buses depart the malls earlier than their scheduled times creating a situation of passengers missing the bus even if they arrived at the stop on time.

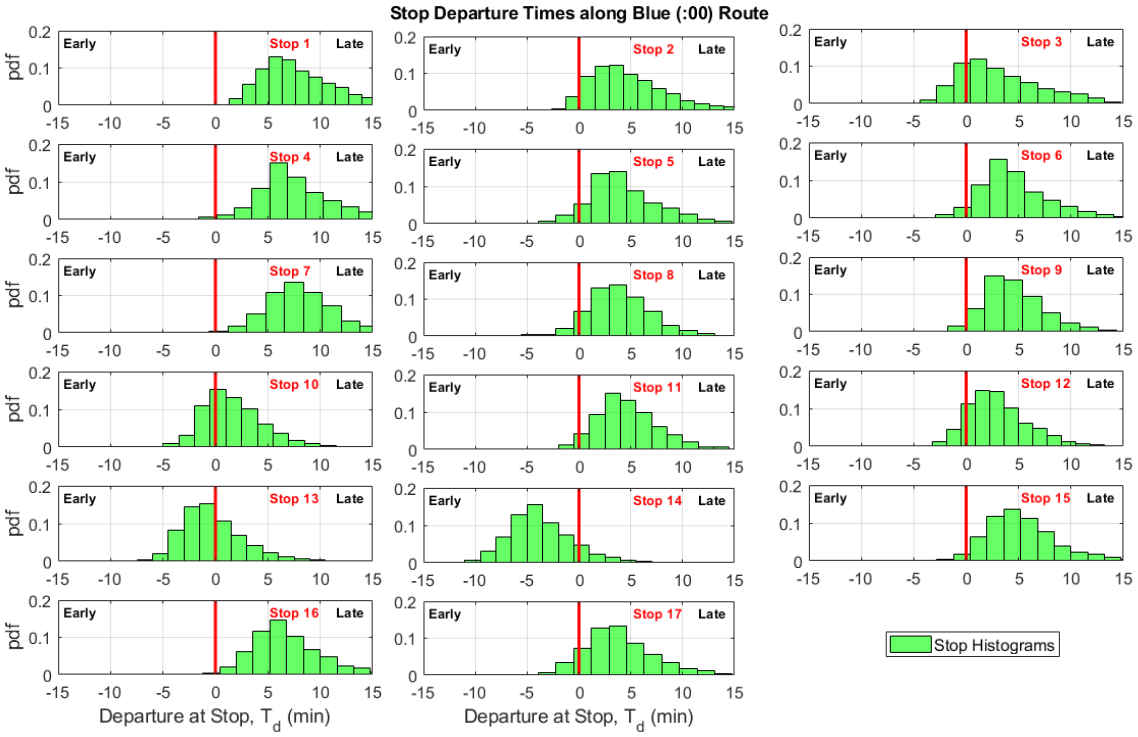

Figure 5-10. Delay in departure of buses along the "Blue" route for :00 after the hour schedule.

Using **Equations 5-8 to 5-12**, dwell and departure time analysis were made. An example for departure analysis is presented in **Figure 5-10** for the "Blue" route :00 minutes after the hour schedule. From the figure we can see that the buses arriving on the 17 stops out of the 18 depart the stops on time. For stop 14, it is pertinent that the bus departs the stop earlier than scheduled. The reason of early departure at this particular stop can be because the stop is located where the malls are and the other stops at the mall location may be utilized more by passengers that may make the bus drivers skip stopping at this stop since there may not be passengers waiting. Such reason and the presented delay variation in **Figure 5-7** entail operational conditions are more governing than environmental conditions for the performance of the public transit system in Benton Harbor. For environmental conditions, it could be expected that a bus may arrive at a stop later on a snowy/cold day but a bus driver may also be aware of the weather so the bus may get at the stop on-time to not make passengers wait at a bus stop on such harsh weather.

5.6.3. Transit Performance Dashboard of TCATA's System

A web-based performance dashboard is created for the TCATA system in Benton Harbor; the website was developed using the framework presented in **Figure 5-3**. The inputs from the questionnaire surveys and semi-structured interviews along with a number of visualization elements learned from in-place metropolitan area transit performance dashboards were used for the development of the dashboard. Real-time mapping of bus locations and real-time performance metric assessment in an AWS platform using a data feed from GPS trackers are key contributions of this work. The AWS Elastic Beanstalk was used to integrate the various AWS elements to drive the website developed (using the Dash web app development platform). The developed performance dashboard is a tab-

based application environment that has 5 main components as presented in **Figures 5-11 to 5-15**. The first tab is presented in **Figure 5-11** where fixed-route options and duration settings are shown. A user may start a selection by choosing from the two "Blue" route schedules (:00 or :30 routes), "Red" route schedule, and "Yellow" route schedule. Correspondingly, the list of stops change based on the selection of a particular route. In addition, a time duration is shown in the tab with a range-slider bar to display performance metrics for a specific time period between January 2, 2019, and a current date. Moreover, average values of delay in arrival, delay in departure and dwell time are shown in tabs for the selected start date, end date, route and stop.

In the second tab, histograms of arrival and departure are shown for the user selected route, stop and duration settings. Alongside the histograms, a real-time map is shown for bus locations in the area of St. Joseph and Benton Harbor. The real-time map is updated every 1 minute or, whenever new GPS data is reported from the sensors installed

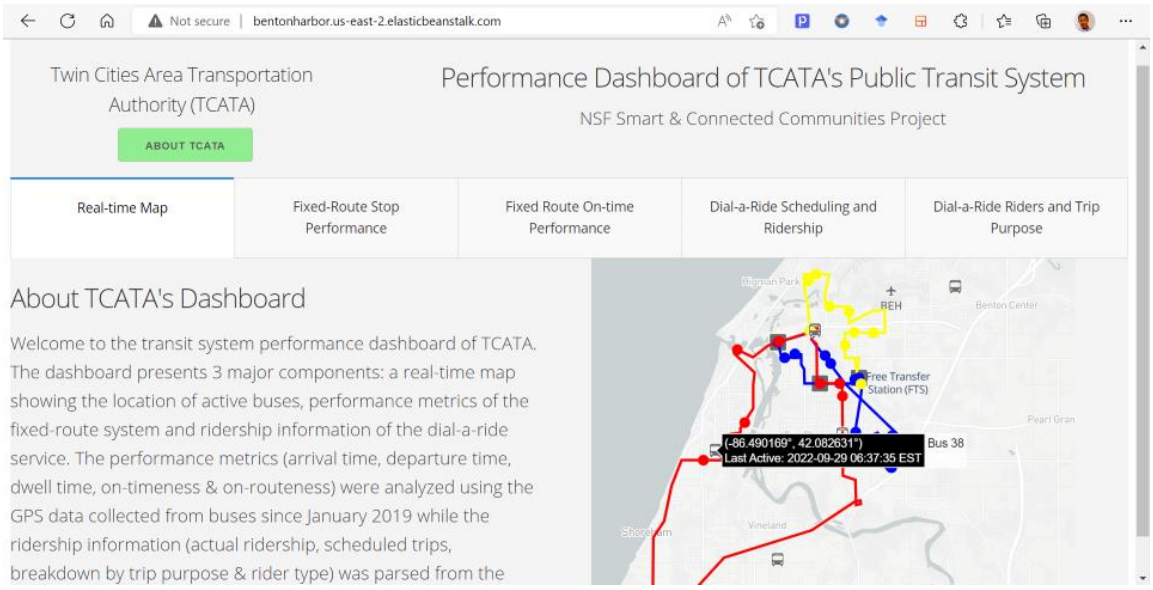

Figure 5-11. Developed performance dashboard for TCATA's public bus transit system: Tab 1 screenshot.

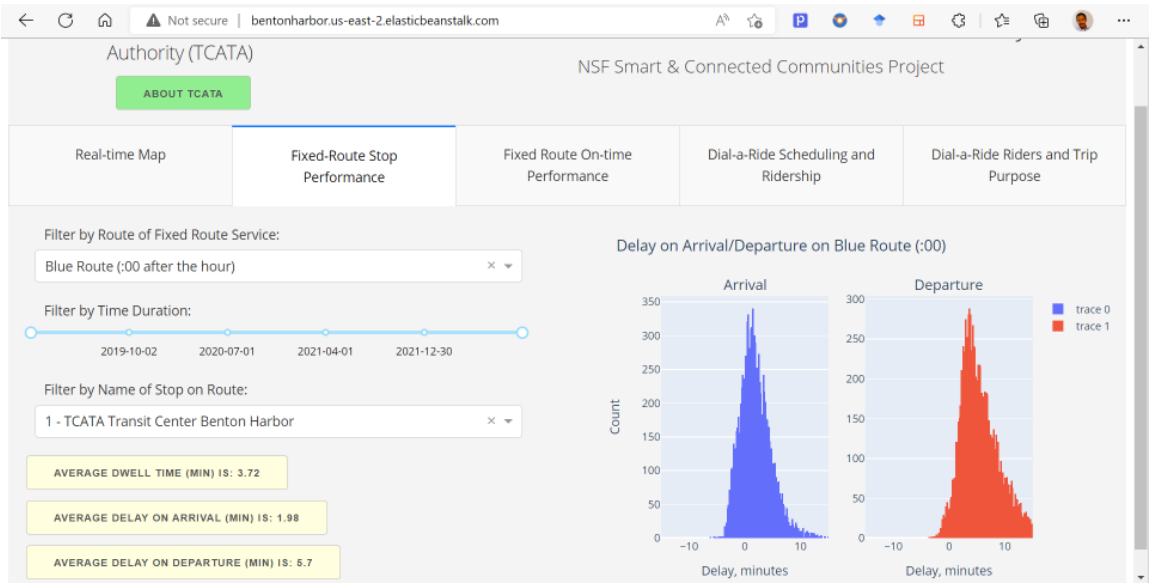

Figure 5-12. Developed performance dashboard for TCATA's public bus transit system: Tab 2 screenshot.

on the buses. The real-time map is interactive in that a user may zoom to a local location to see details. Hovering on one of the 3 routes displays detailed route information, direction, fares, and hours of operation while hovering on a stop informs the user on schedules and free transfer availability to another fixed route. In addition, hovering on a

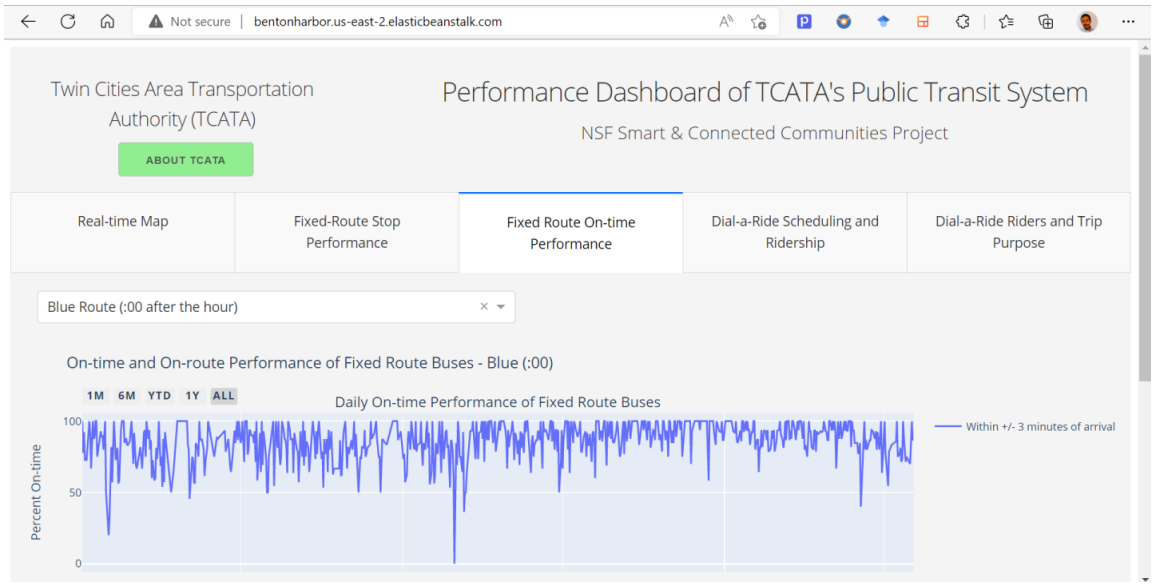

Figure 5-13. Developed performance dashboard for TCATA's public bus transit system: Tab 3 screenshot.

Figure 5-14. Developed performance dashboard for TCATA's public bus transit system: Tab 4 screenshot.

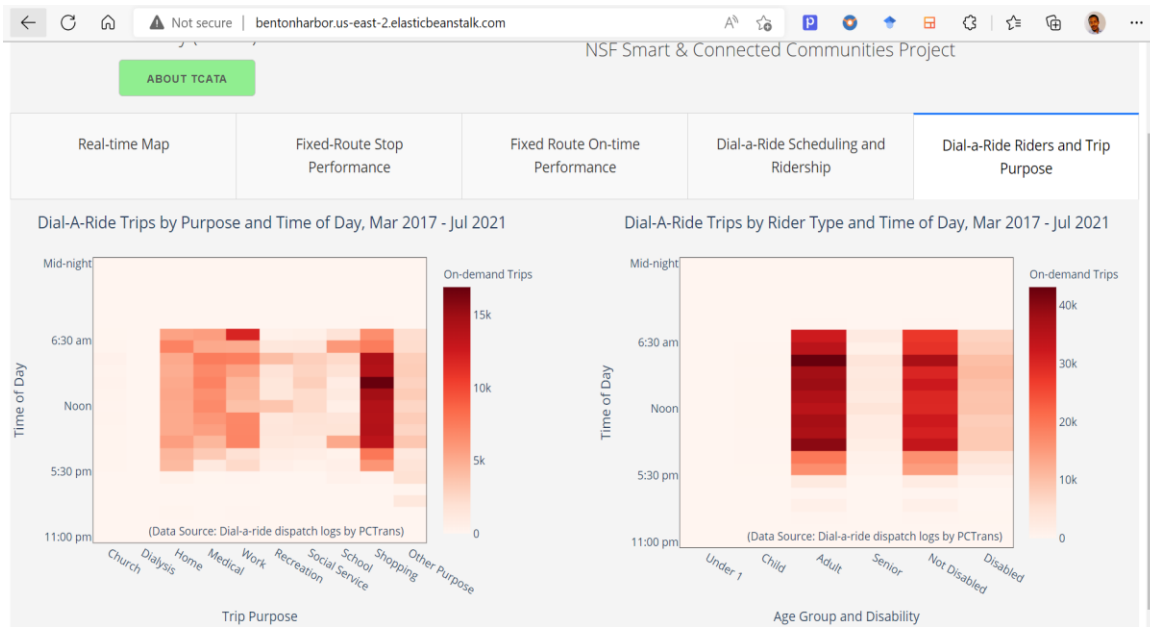

Figure 5-15. Developed performance dashboard for TCATA's public bus transit system: Tab 5 screenshot.

coordinates and the last time the bus was active.

On-time performance of the system was assessed by looking at the number of times the bus was arriving at a specific stop within 3 minutes of time window and the number of times the bus was operating on the designated route for more than 80 % of the time, respectively (**Figure 5-13**). The on-demand portion of the transit system was assessed as presented in tabs 4 and 5 of **Figures 5-14 and 5-15**, respectively. The daily ridership of the on-demand system was presented in time series for more than 4 years of data. In reviewing time history data, it is evident that the ridership of the on-demand buses has lower rider counts on Saturdays. In addition, impacts of the global COVID-19 pandemic can be seen in lower ridership in the supply of on-demand (dial-a-ride) trips following March of 2020. Additional analysis has been made to divide the total count of ridership of the on-demand buses into hours of the day, trip purposes, age group and disability status. **Figure 5-15** presents the frequency of the on-demand trips in a heatmap.

5.7. Conclusions

The community of Benton Harbor, Michigan has a significantly low vehicle ownership rate making it reliant on the public transit system managed by TCATA (including three schedule-based and on-demand shuttle service). Thus, this study on service quality was directed towards assessing the TCATA's system and the Benton Harbor community. In this study, continuous long-term observation of the TCATA's system was demonstrated to assess the performance of the public transit system. Data from installed GPS receiver sensor units informed about the performance of the bus fleet running in the system. In addition, a performance dashboard was developed to inform both current and future riders

and the transit agency by utilizing the GPS data feed from the monitored bus fleet. The customers (current and prospective) may be interested to look at the on-time performance of the overall system, and delay in arrival/departure at a specific stop in addition to locating the buses they are interested to ride in real-time. In review of the data collected, it is evident that close to the location where the Benton Harbor malls are, buses on the blue route tend to arrive 7+ minutes early and dwell there to depart back to the transit center for another loop of service until end of operation for the day. In addition, the performance of the fixed route system is very good with the vast majority of buses on the fixed route arriving within 3-5 minutes of their posted time. Thus, the ridership (i.e., on both fixed route and on-demand portions) may increase after having a sense of the coverage and performance of the system. The transit agency may be interested to look at the dashboard to make iterative changes to the administered system for better service supply and performance which again can be manifested in the real-time performance dashboard developed. In summary, this study demonstrated a low-cost monitoring and data visualization scheme for local transit agencies using GPS trackers. In addition, the real-time data feed was used to populate real-time bus locations on map and to develop real-time performance dashboard. Future research will focus on assessing if such transparency of system performance to the public builds trust, and if it efficiently helps TCATA make iterative changes on system for improved system performance and ridership.

Chapter 6: Conclusions and Future Research Directions

6.1. Conclusions

6.1.1. Summary of Research Works

In this dissertation, research has been presented that motivates, develops, and demonstrates quantitative decision-making tools that can help asset managers administering large-scale transportation systems. Decision making related to system performance can be challenging based on the size of the system (e.g., large inventories, spatial range) and the resources available to ensure performance attainment. The latter consideration is especially relevant for financially strained municipalities that have limited resources available to help meet adequate levels of system performance. Two partners are recruited for the work to consider decision making. The first partner was the Michigan Department of Transportation (MDOT). MDOT is challenges by the demands of having to manage large inventories of structural assets including retaining walls, pavements, and bridges, all of which are distributed spatially across all areas of the state. The second partner was the Twin Cities Area Transportation Authority (TCATA) in the City of Benton Harbor. TCATA manages the public transit system which is operated using a fleet of 27 buses used to provide fixed-route and on-demand (also termed "dial-a-ride") transit services for the transit dependent communities of Benton Harbor. The TCATA public transit system is a vital community resource that addresses the mobility needs of community members for essential trips such

as shopping, work, school and healthcare. The third partner was the Water Department of City of Benton Harbor. The Water Department administrates the water supply system (i.e., water source intake, treatment (clarification), disinfection, to distribution) that supplies safe drinking water for the residents of Benton Harbor. These three partners provided a diverse set of transportation systems used herein.

In Chapter 2, a quantitative risk-based asset management (RBAM) framework for a 35+ years old cantilever reinforced concrete (RC) retaining wall system was presented. While there has been the advancement of quantitative asset management of highway bridges over the past decades, little advancement has been made in employing structural health monitoring (SHM) for the health and safety of aged retaining wall assets. As a result, an illustrative example of an RC retaining wall system constructed in mid-1980s was considered and a wall panel with visible defects such as cracks, tilt, and leakage of water through weep holes and expansion joints was selected for wireless sensor monitoring over a long period (well over 12 months). The monitoring system demanded high resolution measurements on tilt (within 0.01 degrees), strain (within 1 microstrain), and temperature (within 1 F) which were actualized by the field deployed system. Moreover, the monitoring system was designed to be wireless and installed on the façade of the wall but yet capable of providing insight to the structural response of the wall to acting lateral earth pressures and environmental loads. A beam model was developed to infer lateral earth pressures using tilt measurements and to predict the flexural strain response of the wall. A reliability framework was then adopted to analyze the probability of failure of the wall based on the estimated loads and random variation of the material properites of the system. To aid asset managers, the reliability analysis resulted in a daily measure of the reliability index for a

defined limit state function. This scalar index was further integrated into a risk assessment framework where the consequences of failure are qualitatively defined and combined with the reliability index to define low, medium and high risk of the monitored asset.

In Chapter 3, an extension of the wireless sensor system that was demonstrated for the retaining wall assets in Chapter 2 was considered for monitoring the water distribution system in the City of Benton Harbor. The monitoring system used water pressure sensors synchronized with GPS smart antenna receivers for tagging pressure measurements with location and timestamp. The water distribution system of the city was constructed in various phases in the 1920s, 1930s, 1940s and 1960s, when the City of Benton Harbor was prosperous with a wealth of manufacturing jobs for residents. As an aging water distribution system that has been modified from several disconnections over the past thirty years, the system has performance issues including variations of water pressure. The rapid-to-deploy wireless water pressure sensors were deployed in September 2021 to measure pressure at various locations across the city. The pressures were used to update a hydraulic model that could provide a more complete picture of system performance. The model revelaed low levels of service in a location in the system where a major pipe failure occurred in October 2021. Thus, the wireless monitoring program proved to be useful in helping the asset manager understand the origins of the failure.

In Chapter 4, data from 42 weigh-in-motion (WIM) stations distributed spatially across the state of Michigan and managed by MDOT was utilized to conduct Bayesian Inference-based truck re-identification to spatiotemporally map the flow of freight trucks throughout the state. This work aimed to spatially map loads on critical transportation system assets including bridges and pavements so that asset management methods could

account for the loads experienced over the assets' service life. The truck re-identification algorithm is two staged where a heuristic approach informs the Bayesian framework with the probability of truck retention within a corridor segment with exits to inform the Bayesian prior probability density function, and the error distribution of axle weights essential for informing the Bayesian likelihood function. To validate the framework for truck re-identification, a data set of video capturing trucks on a specific corridor between two WIM stations from which data was simultaneously collected was formed to serve as a ground truth dataset. Receiver operating characteristics (ROC) curves were drawn to establish a threshold for the posterior probability that assigns two trucks from separate WIM stations as a re-identified pair; the role of the ROC was to minimize false positives. Thus, the end utility of such analysis is to informing asset managers in MDOT of the truck loading assets are seeing in order to help with estimation of long-term fatigue-like deterioration on assets in their highway systems.

In Chapter 5, the public bus system supplying transit services in the form of both on-demand (dial-a-ride) and fixed-route options, was explored in the transit dependent community of Benton Harbor. The buses of the TCATA system were instrumented with cellular-enabled GPS tags to report bus locations continuously to a cloud database system developed for the application. The hypothesis of the work was that location data from buses could be used to extract performance metrics of the system which could be shared with community stakeholders to build awareness and confidence in the system performance. The assessment method initially used to inform use of the data collected considered qualitative assessment methods using questionnaire surveys and semi-structured interviews with the TCATA staff (current and former) in addition to key

stakeholders and selected community members. The main goal of the qualitative assessment was to deeply understand stakeholder perspectives on transit performance and community confidence in existing solutions. An additional goal was to inform the design of a transit system performance dashboard for stakeholder future use. A cloud computing architecture was built on Amazon Web Service's (AWS's) platform for storing real-time data coming from the GPS modules installed on the buses (AWS s3), for analyzing performance parameters real-time automatically (AWS Lamda), and to power an online dashboard visualizing: 1) the mapping of active bus locations, 2) on-time performance of the TCATA fixed route service, and 3) characteristics of TCATA on-demand service (AWS Elastic Beanstalk). The study advanced understanding of the needs and challenges (such as, the adequate management of human and budget resources, running a high-performance public transit service that is trust-worthy, compliance with state and federal mandates with respect to reporting transit performance transparently on a public facing web dashboard, and the ability to be quantitatively informed for making iterative changes) of the transit provider TCATA. This resulted in providing TCATA with an adaptive, quantitatively assessed, innovatively devised, and transparent view of their transit system.

6.1.2. Key Dissertation Contributions and Potential Impacts

This dissertation focuses on contributing advanced methods and technologies for the management of civil infrastructure systems; thus, it presents novel set of knowledges essential for improving the current limited practices. These limited practices are with respect to low advancements in quantifying the risk of structural failure of retaining wall systems, the statistical estimation of freight truck loading profiles on spatially distributed highway surface assets (i.e., bridges and pavements), and community engaged real-time

transit performance dashboard development for the management of small transit agencies operating under limited budget resources. The advanced methods and technologies are attributed to wireless sensor nodes and cloud platforms, and they are integrated in this dissertation to address the above set of limitations, and to automatically collect and analyze data to provide data-driven approaches for the management and decision-making within broad categories of transportation infrastructure systems. In addition, the presented data-driven approaches have benefits attributed to providing tools that foster the improvement of infrastructure asset management in resource constrained environments; under the notion of frugal innovation that derives values by utilizing existing data and infrastructure. Moreover, the involvement of communities through engagements in decision-making tool development programs make the end results become more impactful.

The potential scalable deployment of the wireless sensor products integrated with cloud-based data architectures presented in this dissertation are very essential. For instance, the wireless sensor nodes that were used for the monitoring of aged retaining wall systems presented in this dissertation can be used at scale by asset managers like MDOT as a low-cost and easy-to-deploy solutions for augmenting the current qualitative observation or visual inspection practices. The key end impact of the wider usage of these nodes is to clear the dilemma of whether replacing a retaining wall system with slight defects is a good decision or not. Such decision has a huge capital investment consequence and public safety concern if we think of 10s of thousands of retaining walls in the U.S. therefore, as compared to opting for always replacing such walls with visible defect, knowing on how to narrow down to wall systems that their defect is clearly tied to their deteriorated structural integrity is very crucial. Moreover, the mobile wireless water pressure sensor units can be products

that non-technical personnel use to do short-term to long-term measurement of municipal water pressures. Thus, technical assistance barriers couldn't hinder their wider use for impacting the current management of aged water distribution systems. Moreover, the synchronization of water pressure measurements with GPS smart antenna receivers makes it a lot easier for engineers in municipal water departments to tag cloud reported water pressure data points with timestamp and geographical coordinates for easy addition to their GIS layers to compare and validate their hydraulic simulation results.

6.2. Future Research Directions

The different methods and approaches used in this Ph.D. research can be further developed and improved in several ways, breadths, and widths. That is, a number of technological innovations and scientific methods can either augment different embedded wireless sensing and cloud computing methods composing the presented end-to-end quantitative transportation cyber-physical system (CPS) data pipelines useful for decision-making or a new architecture of data pipeline framework for quantitative asset management can be devised. As far as informing the decision-making of asset managers in administering vast inventory of transportation infrastructure systems or city municipalities serving under-resourced communities with limited operating budget in concerned, incremental additions to this interesting area of research is recommended. Therefore, the following could be done.

In Chapter 2, an RC retaining wall system was demonstrated for quantitative risk-based asset management study. But the current construction of retaining wall structures comprises of mechanically stabilized earth (MSE), caisson (tie-back) supported, etc. wall types depending on whichever type allows the economical construction of new wall assets.

Moreover, a different approach than a discrete element model (DEM) framework could also be devised by fusing different sensor data from, for instance, ground penetration radar (GPR), LiDAR imaging, etc. In addition, the proposed method in this dissertation still uses visual inspection for narrowing which walls warrant to be instrumented, thus thinking innovative ways of identifying walls for instrumentation would be a great study.

In Chapter 3, rapid-to-deploy water pressure sensors have been used to measure at 9 locations for a few days. But designing a low-cost monitoring system that continuously assess pressure levels, and that flag when pressures are exceeding certain minimum and maximum pressure levels would be very smart to have particularly in mitigating water main failures (i.e., highest pressure scenario) and water quality or fire hydrant issues (i.e., lowest pressure scenario). Moreover, trying to measure as many pressure measurements as possible would provide better insights than discrete measurements.

In Chapter 4, the presented Bayesian framework could be improved. Only a single pair of WIM stations were used to validate the presented truck re-identification algorithm, but multiple pairs of WIM stations would be great to consider since the different truck flow characteristics would signal better formulation of a Bayesian binary classifier framework for matching truck signatures on the highway network level. Moreover, non-Bayesian methods also could be considered to compare accuracy measures.

For Chapter 5, an interesting extension of the work could be explored. The dispatch logs that have been recorded since March 2017 by TCATA have detailed information such as destination trip purpose, pick up coordinates, drop off coordinates, age group, and disability status; this big data set can be divided into training, test, and validation datasets for a deep learning architecture (most probably Graph Neural Network (GNN)) that takes

latitude, longitude, end trip purpose, age group, and disability as graphical inputs and output predictions for forecasted scenarios where there is a new mass employment location in the area, etc. Since TCATA operates on a limited operating budget, knowing ahead of the number of drivers they may require at a certain peak time is a question they want to answer. For example, LSTM approach based Recurrent Neural Networks have been developed by Uber for predicting or engineering extreme event forecasting **[248]** on a dataset with analogous trend as presented in **Figure 5.14**.

Appendix A: Questionnaire Survey Design for Benton Harbor Mobility Workshop

Thank you for participating in today's workshop. Please complete this survey to help the team improve our collaborative process, as well as contribute to research about the effectiveness of the workshop to foster effective planning. Your participation in this survey is voluntary, and you may choose to end your participation at any time or skip any questions you wish. Your answers will be kept anonymous, and no one will be identified as a participant in the resulting research.

1. What is your honest opinion about how well TCATA's transit system is performing?
2. How do you think TCATA could build greater trust with the community?
3. What are three types of information that a transit provider should have on their website?
4. Have you ever seen a transit agency performance dashboard before?
   - No
   - Yes, if so, name city: _____
5. People have different views about how high-performance transit service should be defined. How important are the following metrics to your personal definition of high-performance transit?

	Not Important				**Very Important**
Whether the bus arrives at each stop around the scheduled time	1	2	3	4	5
Frequent service	1	2	3	4	5
Customer satisfaction ratings	1	2	3	4	5

6. Rate the importance of the following ways a transit system can build community trust?

	Not Important				**Very Important**
Ensuring the buses are on-time and reliable	1	2	3	4	5
Making system operation metrics transparent on web	1	2	3	4	5
Providing real-time system information on a website	1	2	3	4	5
Solicit rider feedback via surveys	1	2	3	4	5
Other: _____	1	2	3	4	5

7. Transit agencies differ in how they define when a bus is on time, to allow for minor deviations from the schedule. How late should a TCATA bus arrive and still be considered on-time?
   - 1 to 3 minutes
   - 3 to 5 minutes
   - 5 to 7 minutes
   - 7 to 9 minutes
   - 9 to 11 minutes

Thank you for your participation and feedback!

Appendix B: Semi-Structured Interview Design for TCATA's Staff and Affiliates

B.1. Research Design

We are conducting a research project within the Benton Harbor community funded by the National Science Foundation (NSF) focused on assessing the impact of Twin Cities Area Transportation Authority's (TCATA's) public transit service on the community. One of the primary objectives of the project is to provide TCATA's staff with access to the data being collected from the system via an online data dashboard. Our plan is to develop a Dashboard Information System (DIS) that may have the potential to assist you in your role at TCATA. To ensure the DIS is well suited to the needs you may have as a TCATA stakeholder, we would like to invite you to serve as a participant in our study given the importance of your perspectives in shaping the final design of the DIS. Specifically, your input would help guide the DIS design by illuminating which data and performance metrics you might like to see in the final DIS design.

B.1.1. What is Involved in this Study?

If you decide to participate, we will interview you in person at the TCATA facility in downtown Benton Harbor. We estimate the interview will take 30-45 minutes to conduct. During the interview, we will take notes, but we will not record the conversation.

B.1.2. Data Security and Storage Risks

For this study, we will be recording your views about the existing performance of the TCATA system, how the agency makes operational decisions, and your opinion about how system performance can be improved. After the study period, we will store our notes of the interview on our data servers housed at the University of Michigan. While the university uses the latest technology in data security, there is a chance that the servers can be broken into by cyber attackers. In order to mitigate this security risk, we will be sure to remove all identifying information from our interview summaries and notes.

B.1.3. Benefits of Participating in our Study

As a result of this study, we expect to produce a transit performance dashboard information system for use by both TCATA staff and by other stakeholders. The information provided by the dashboard may offer you insights into the performance of the TCATA system that may assist you in your role at the agency. Other community stakeholders may also benefit in the future from the information we find in this study.

B.1.4. Confidentiality

We are interested in collecting your information for current and future research purposes only. In order to protect your information from misuse and unauthorized disclosure, we will separate your personal information from the logs taken of the interview. The logs will be stored on a secured server, where only the University faculty and research staff will have direct access.

B.1.5. Incentives

All participants who participate in the interview will receive a $25 gift certificate. These are distributed at the end of the interview. Note that this incentive can only be provided to participants who complete the interview and will not be provided to those who withdraw from the interview before its conclusion.

B.1.6. Your Rights as a Research Participant?

Participation in this study is entirely voluntary. You have the right not to participate at all or to leave the study at any time. In the event that you decide to withdraw from our study, we will be sure to remove your information from our records.

B.1.7. Contacts for Questions or Problems?

Please feel free to contact at (###) ###-#### or email at ########@umich.edu if you have questions about the study or any problems. If you have questions about your rights as a research participant, or wish to obtain information, ask questions, or discuss any concerns about this study with someone other than the researcher(s), please contact the University of Michigan Health Sciences and Behavioral Sciences Institutional Review Board, 2800 Plymouth Rd. Building 520, Room 1169, Ann Arbor, MI 48109-2800, (734) 936-0933, or toll free, (866) 936- 0933, irbhsbs@umich.edu.

B.2. Interview Questions

B.2.1. Establishing Subject Background

1. What is your official title and position in the TCATA organization?
2. How long have you been a member of TCATA?
3. Can you describe like, in detail, like what you do on a regular basis at TCATA?
4. Have you worked at other transit providers before? If yes, which one(s) and what were your roles in those organizations?

B.2.2. Subject's Perceptions of TCATA and Community

5. Can you describe what TCATA's primary objectives are?
6. How does TCATA's transit system meet those objectives?
7. How would you describe the ways TCATA works with the community to meet them?
8. Do you see ways TCATA can better meet the needs of the community, especially offering community members with more convenient access to essential services (healthcare, jobs, schooling)

B.2.3. Subject's Views on Transit Data for their Role

9. What types of information and/or data do you use in your role at TCATA to help you make decisions?
10. If you do use data or information regularly in your role, can you describe the data used, who produces it, and any gaps you see in the quality and type of data available?
11. How do you use real-time maps of buses provided by the project (DoubleMap or Verizon Connect/Network Fleet)?
12. If you look at the real-time bus maps regularly, what shortcomings do you see, if any?
13. What data related to the performance of the transit system would you like to see that you currently do not have access to? Why do you feel that data would be helpful?

B.2.4. Subject's Views on Transit Data Shared with Community

14. What data do you think would be helpful to share with the community and why?
15. How would you feel about on-time performance data being shared with the community?
16. How likely is it for ridership on TCATA's buses to increase if current riders had access to data of TCATA's transit system performance?

17. How likely is it that Benton Harbor residents currently not choosing to ride TCATA would choose to do so if they had access to transit performance data?

B.2.5. Dashboard Specific Questions

18. Have you ever seen a transit agency performance dashboard before?
    - No
    - Yes, if so, name the city: _____
19. People have different views about how high-performance transit should be defined. How important are the following metrics to your definition of "high-performance"?
    - Whether the bus arrives at each stop at the scheduled time
        - Rating: _____; Why: _____
    - Frequency of fixed route service
        - Rating: _____; Why: _____
    - Customer satisfaction ratings
        - Rating: _____; Why: _____
20. Rate the importance of the following statements in building community confidence in their public transit system?
    - Buses are on-time and reliable
        - Rating: _____; Why: _____
    - System performance data is available on a website
        - Rating: _____; Why: _____
    - Providing real-time bus location on a cell phone app
        - Rating: _____; Why: _____
    - Soliciting rider feedback via surveys
        - Rating: _____; Why: _____
21. What are other ways public transit agencies like TCATA can work toward building community confidence in their systems?
22. Transit agencies differ in how they define when a bus is on time, to allow for minor deviations from posted arrival schedules. How late should a TCATA bus arrive and still be considered on-time?
    - 1 to 3 minutes / 3 to 5 minutes / 5 to 7 minutes / 7 to 9 minutes / 9 to 11 minutes

Marked will be a single 'x' in response to the statements presented below on the left

Qn. Num.	Trust in transit dependent communities	Strongly Disagree (1)	Disagree (2)	Neutral (3)	Agree (4)	Strongly Agree (5)
23	Benton Harbor's community has full trust in the TCATA to provide the mobility services their needs					
24	Ridership of the community on TCATA's transit system is dependent on the level of trust that the transit dependent communities have					
	Real-time transit performance web dashboard	**SD (1)**	**D (2)**	**N (3)**	**A (4)**	**SA (5)**
25	A real-time map showing bus locations is important for TCATA to administer bus operations					
26	A website showing transit performance helps TCATA meet its requirements of becoming a transparent service provider					
27	Displaying on-time performance on a website can help current non-users to start riding the buses					
	Performance of the public transit system in place	**SD (1)**	**D (2)**	**N (3)**	**A (4)**	**SA (5)**
28	The existing public transit system supplied by TCATA is performing well given the financial resources that the transit provider has					
29	TCATA's public transit system performance would improve if we can introduce a real-time performance dashboard for use					
30	TCATA traces the on-timeness of active buses					
31	Transit service utilization or customer ridership is highly dependent on how on-time the buses are arriving at stops					
32	Overall, TCATA's system is performing as equal to or better than other transit systems supplied by other small transit agencies in Berrien County					

33. Do you have any comments or ideas related to questions 23-32?

34. Any Other Comments?

Thank you for your participation and feedback!

Appendix C: Questionnaire Survey Results

On May 13, 2022, 8 survey responses of stakeholders and others was recorded.

1. What is your honest opinion about how well TCATA's transit system is performing?
    - We need to create new plans and goals since change is coming
    - Underperforming, needs to expand, TCATA has room for improvement
    - It has underperformed in recent years mostly due to staff turnover, lack of stability, and inexperience
    - Terrible operation, do not trust the Board and City to work with others
2. How do you think TCATA could build greater trust with the community?
    - Talking to the drivers and the people having more meeting with them
    - Marketing plan, listen to others, and be willing to work with others
    - By welcoming people of the Twin Cities Area, greater trust can be built
    - Provide more consistent and reliable service. Offer more regular communication with the riding public
3. What are three types of information that a transit provider should have on their website?
    - How the app works, service area, financial details, and contact info
    - Routes, times of service, fare rates, and locations of service
    - Direct access, payment options, and resources
    - Schedule, stops, and all maps of the attractions on the route
4. Have you ever seen a transit agency performance dashboard before
    - All responded No
5. People have different views about how high-performance transit service should be defined. How important are the following metrics to your personal definition of high-performance transit?

Average score on scale: Not Important (1) - Very Important (5)	
Whether the bus arrives at each stop around the scheduled time	4.90/5.00
Frequent service	4.50/5.00
Customer satisfaction ratings	4.60/5.00

6. Rate the importance of the following ways a transit system can build community trust?

Average score on scale: Not Important (1) - Very Important (5)	
Ensuring the buses are on-time and reliable	4.90/5.00
Making system operations metrics transparent on a website	4.40/5.00
Providing real-time system information on a website	4.60/5.00
Solicit rider feedback via surveys	4.60/5.00
Other: Community Needs; Hold town hall meetings in the neighborhood and with businesses	5.00/5.00

7. Transit agencies differ in how they define when a bus is on time, to allow for minor deviations from the schedule. How late should a TCATA bus arrive and still be considered on-time?
    - 3 to 5 minutes - Mean and Mode

Appendix D: Semi-Structured Interview Results

From July 21, 2022, to September 2, 2022, 9 interviews with TCATA's staff and affiliates were conducted. Summary of responses is as reported below:

D.1. Establishing Subject Background

1. What is your official title and position in the TCATA organization?
    - 1 Dispatcher, 1 Maintenance Director, 1 Former Director, 1 Member of Board of Directors, 1 Senior Transportation Planner, and 4 Drivers - 8 Interviewees.
2. How long have you been a member of TCATA?
    - ½, 6, 2, 1¾, 16, 13, ½, 7, and 5 years, respectively - 5¾ Years Average.
3. Can you describe in detail what you do on a regular basis in your role at TCATA?
    - Dispatcher:
        - Keep up with the role assignments and
        - Send the rounds to the different drivers available
    - Maintenance Director:
        - Keep up preventive maintenance records (oil changes, tires, etc.)
    - Former Executive Director:
        - Led an effort that corrected 21/27 violations of TCATA
    - Member of Board of Directors:
        - Look at bus, driver, and ride performances to see how they do
    - Senior Transportation Planner:
        - Mobility management program funded by FTA that serves people with disability, seniors, and people with low income
    - Drivers:
        - Safely pick up and drop off customers or passengers daily
        - Transport passengers to & from work, doctor's appt., grocery, etc.

- Punch in, get my sheets, pre-trip inspection on the bus, pick up people, ask them where they're going and then take them safely

4. Have you worked at other transit providers before? If yes, which one(s) and what were your roles in those organizations?
   - 4 No and 5 Yes (Fort Lauderdale, FL; Chicago, IL; 3 for BH Area).

D.2. Subject's Perceptions of TCATA and Community

5. Can you describe what TCATA's primary objectives are?
   - Public transportation serving majorly the disabled and the seniors
   - Take people where they need to go (work, doctor's appt., grocery, etc.)
   - Provide reasonable & low-cost transport to the poor, disabled & elderly
   - Transport residents from A to B timely with a professional attitude
   - Making sure people are happy, satisfied, and safe with what's going on
   - Expanding to bigger and better for serving the community
   - No formal objective or strategy but a transit provider serving at-risk population with a higher disability level, poverty, lower education, very low household income and no vehicles
6. How does TCATA's transit system meet those objectives?
   - TCATA gives them timely fashioned, low fare rides for different trips.
   - They work with disabled passengers and give them reduced fares.
   - I think it has met them very well and there was always room for improvement which included automated dispatch.
   - They don't, they are fairly short. The reason is because TCATA is understaffed (i.e., in administration, dispatch office, drivers, etc.).
   - They send drivers to get people timely in cases of scheduled appt.
   - Not at all, from a service standpoint
7. How would you describe the ways that TCATA works with the community to meet those objectives?
   - We would like to have a shorter wait time for the community
   - Dial-a-ride and fixed routes, more so than larger door to door
   - Current routes are a waste of time and money, we need better system

- Be honest with the community. First time you tell them something that's not right, they lose trust in you, all the good stuff goes away
- We need a better updated dispatch system to show where the bus is at
- I don't think there is a lot of working with the community
- There is a lot of outreaches including the mobility program

8. Do you see ways TCATA can better meet the needs of the community, especially offering community members with more convenient access to essential services (healthcare, jobs, schooling)
    - Once TCATA gets fully staffed, the wait won't be as long for customers
    - Try to interact with them to get people to where they need to be
    - 1 or 2 more fixed routes and to help them understand the system better
    - Teach TCATA's staff with a reluctance to change what they had for long
    - Improve the routes that go in a circle one way. It takes an hour to go from point A to B where it should take only a few minutes with a car
    - One of the things that all transit agencies struggle with is funding
    - A lot more training, policy procedures, and enforcement

D.3. Subject's Views on Transit Data for their Role

9. What types of information and/or data do you use in your role at TCATA to help you make decisions?
    - Location, destination, wait time, time of the call, and trip purpose
    - Easily track a bus with issues with respect to seeing the location of it
    - Number of people served by age group, trip category and disability
    - DoubleMap/GPS for pickup and also take a look at drivers and riders
    - Considered handwritten driver logs of a month in 2014, mapped it, saw top origins/destinations, and looked at 5 min walk to a transit station
10. If you do use data or information regularly in your role, can you describe the data used, who produces it, and any gaps you see in the quality and type of data available?
    - Tablets for collecting automated, more accurate and verifiable data
    - The DoubleMap app has technical issues so no more useful
    - GPS is not utilized at dispatch properly, it's not always bus sitting there

- The computers go out, we need better data system or up to date tablet
- We have our log sheets, and we just log whoever gets on the bus
- Cameras all over the inside of the bus and one on the outside
- Handwritten driver logs, very hard to interpret and time-consuming. It would depend on the driver, thus it wasn't consistent

11. How do you use real-time maps of buses provided by the project (DoubleMap or Verizon Connect/Network Fleet)?
    - We use the network fleet. It gives you different information in regard to the bus, speed, landmarks and how long it was at each place
    - I don't use a map because I know my way around this town
    - I looked at the DoubleMap the other night when I wondered where the bus was and what we were waiting for
12. If you look at the real-time bus maps regularly, what shortcomings do you see, if any?
    - Sometimes it seems like it's a little delayed, it has technical issues
    - The tablets need updating and they don't stay charged long
    - It is important to have accessibility features for blind users for instance
13. What data related to the performance of the transit system would you like to see that you currently do not have access to? Why do you feel that data would be helpful?
    - Track ridership for it to go up, to see where high and low points are
    - Ascertain the response time on calls by the operators of the buses
    - Before data and other things, we need to have a better system. That is 3 things: better pay to drivers (e.g., currently $14/hr for drivers with 15 years of experience, where students get $15/hr), well experienced admin staff, and every rider with a phone.
    - Updated tablet and dispatch to help people be able to get around faster
    - A tracking system since some streets are not known by some people
    - Better maintenance, right pay, and safety come first than all fancy stuff
    - Reporting revenue expenses, ridership by type, number of riders, cost per hour per passenger, and performance measures

D.4. Subject's Views on Transit Data Shared with Community

14. What data do you think would be helpful to share with the community and why?
    - For the fixed routes: software to track the actual bus real time
    - For on-demand daily pickups: exact time when the bus is coming
    - The number of (calls received, responses)/month, average call response time, pick up points, and the ridership by the various routes
    - The kind of data that we the staff could actually understand
    - We need to share the holidays, and other days we have off
    - Benton Harbor is different, they don't care about fancy stuff
    - Real-time data for users, trips entering and leaving an area
15. How would you feel about on-time performance data being shared with the community?
    - If they don't know what's going on and a bus is late, after they get on the bus, they're grouchy, they're cursing, etc. so it's good thing to share
    - I sometimes wait 30+ minutes for the bus. Do you want to show that?
    - Generally, the blue route arrives at a stop on-time 80% of the time within two or three minutes. Send information like that.
    - When you do come on time, some people complain. "Why do you call for a bus when you're not ready?"
    - If they can understand it, I think that's great. From the operations side, looking to see where it is, where things are good, where things are bad
16. How likely is it for ridership on TCATA's buses to increase if current riders had access to data of TCATA's transit system performance?
    - It probably could increase, and the system may become more efficient
    - Many people are still stuck in ancient times, they call and just wait
    - On-time performance data is good => a positive impact on the ridership
    - If people are picked up/dropped off on-time, ridership would increase
    - It might not do just about anything, but you can give it a try
    - The goal is moving on up so, I think it makes it better
    - A lot of people have been buying cars lately, I don't think it matters

- Data is not necessarily going to change someone's mind

17. How likely is it that Benton Harbor residents currently not choosing to ride TCATA would choose to do so if they had access to transit performance data?
    - It can potentially help us in the areas that we provide service for, but if it's out of our service area, it wouldn't be of any use
    - Provided data showed positive performance, it would have an impact
    - If there is a large event or traffic is worse. Nonetheless, no ridership
    - It may work for a lot of people with a chance of 60, 70% maybe
    - No, because a lot of people don't have access to the internet
    - If I don't ride transit, looking at the data and seeing it's on time won't change my mind to not drive my car and take the bus

D.5. Dashboard Specific Questions

18. Have you ever seen a transit agency performance dashboard before?
    - 7 Nos and 2 Yes by Former Director and Senior Transportation Planner.
19. People have different views about how high-performance transit services should be defined. How important are the following metrics to your personal definition of "high-performance"?
    - Whether the bus arrives at each stop at the scheduled time **(4.78/5.00)**
        - A few minutes late is okay, but people are waiting to get to work, etc. Thus, certain people have to be at a certain spot at a certain time.
        - You can see it's on time and reliable, that is really good!
    - Frequency of fixed route service **(4.23/5.00)**
        - It doesn't matter if it's every 1 or ½ hour, it matters more if it's on time
        - Can go to the website and see when buses are supposed to come
        - Route frequency allows more flexibility in a travel
    - Customer satisfaction ratings **(3.67/5.00)**
        - They're going to complain anyway, since they are not driving themselves
        - Always good to hear public comments, you get constructive criticism
        - You want to make sure your customers are happy
        - Sometimes we don't care, we try to do what we have to do

    - Some people that don't like you because they take it personally

20. Rate the importance of the following statements in building community confidence in their public transit system?

- Buses are on-time and reliable **(4.78/5.00)**
    - The more accurate it is, the more chances you'll take to try and use it
    - Building confidence is more than just being on time. The riders would expect reliability, cleanliness, and a friendly driver.
    - If they run on-time, ridership would increase since people read existing performance and they make decisions
    - Everyone has different personalities. Data would speak to analytical people, while customer comments would speak to another.
- System performance data is available on a website **(3.78/5.00)**
    - That gives you time to get yourself ready so, it saves time for you
    - Most riders are 45+ and disabled, so might consider it unnecessary
    - Seeing is believing so if they see that, they're going to trust the system
    - They'll be able to keep up with what's going on
    - If a person wants to go through it but I don't think it's necessary
- Providing real-time bus location on a cell phone app **(4.56/5.00)**
    - You don’t need to go so far when you can see and take care of things
    - You know where to go so you don't have to call about directions
    - For new people who don't know the area, they could benefit a lot because if they can view it, they can use it to start riding the buses
    - Okay, if the data is correct. Otherwise, it could do the opposite.
- Soliciting rider feedback via surveys **(2.89/5.00)**
    - People are tired of surveys, opinions, etc., so they don’t matter
    - If you're rating somebody and getting numbers, that looks good
    - People don't like feedback so that'd be waste of time and money
    - Everyone wants to survey four people and it doesn't change a thing

21. What are other ways public transit agencies like TCATA can work toward building community confidence in their systems?
    - Having policy making people that have business knowledge and sense
    - Pay the drivers good => good service to riders => confidence will be built
    - Short on drivers and some people are upset of longer wait times
    - How they answer the phone, their on-time performance, how they treat their staff, training, putting to other policies and procedures and the enforcement of those
22. Transit agencies differ in how they define when a bus is on time, to allow for minor deviations from posted arrival schedules. How late should a TCATA bus arrive and still be considered on time?
    - 3 to 5 minutes - Mean and Mode

All marked single 'x' responses were collected and an average rating was computed for each of the statements presented below on the left

Qn #	Trust in transit dependent communities	Strongly Disagree (1)	Disagree (2)	Neutral (3)	Agree (4)	Strongly Agree (5)
23	Benton Harbor's community has full trust in the TCATA team to provide the mobility services they need **(3.44/5.00)**	**xx**	**x**	**x**	**x**	**xxxx**
24	Ridership on TCATA's system is dependent on the level of trust that the transit dependent communities have **(4.56/5.00)**				**xxxx**	**xxxxx**
	Real-time transit performance web dashboard information system	**SD (1)**	**D (2)**	**N (3)**	**A (4)**	**SA (5)**
25	A real-time map showing the locations of active buses is important for the transit provider TCATA to administer bus operations **(4.89/5.00)**				**x**	**xxxxxxxx**
26	A website showing transit performance helps TCATA meet its requirements of becoming more transparent **(4.22/5.00)**			**xx**	**xxx**	**xxxx**
27	Displaying on-time performance measure on a website can help the current non-users to start riding the buses **(3.67/5.00)**		**x**	**xxx**	**xxx**	**xx**

	Performance of the public transit system in place	SD (1)	D (2)	N (3)	A (4)	SA (5)
28	The existing public transit system supplied by TCATA is performing well given the financial resources that the transit provider has **(2.89/5.00)**	**xx**	**x**	**xxxx**		**xx**
29	TCATA's system performance would improve if we can introduce real-time performance dashboard for use **(3.89/5.00)**		**x**	**xxx**	**x**	**xxxx**
30	TCATA trace ontimeness of active buses **(3.78/5.00)**	**x**	**x**	**x**	**xx**	**xxxx**
31	Transit service utilization or customer ridership is highly dependent on how on-time buses are arriving at stops (fixed route or on demand) **(4.00/5.00)**	**xx**			**x**	**xxxxxx**
32	Overall, TCATA's system is performing as equal to or better than transit systems supplied by other small agencies in Berrien County **(3.33/5.00)**		**xxx**	**xxx**		**xxx**

33. Do you have any comments or ideas related to questions 23-32?

- People need to be transported from point A to B in a timely manner, with good attitude and professional service
- I disagree about TCATA's overall service being better than other transit agencies in Berrien County because of a combination of on-demand and fixed route data.

34. Any Other Comments?

- A bus shouldn't sit for long. It's the drivers that make it efficient. If they do so much for themselves, they may forget passengers are waiting.
- Boards in cities like Benton Harbor should be represented with experienced, educated, and trained businesspeople.
- At some point in time, I strongly hope TCATA gives its energy to drivers and riders. We have enough money and administrative staff.
- We pushed many people out. There used to be 30 drivers but now it is down to 10. We need more people to do good (i.e., ridership would go up).
- The data you collected is so important in understanding opportunities to educate the board and going back to your transit dashboard.

Bibliography

[1] A. Bolar, S. Tesfamariam, and R. Sadiq, "Management of civil infrastructure systems: QFD-based approach", Journal of Infrastructure Systems, American Society of Civil Engineers (ASCE), 20(1), Reston, VA, USA, 2013.

[2] University of Delaware, "Transportation engineering and civil infrastructure systems", Research Overview, Newark, DE, USA. [Retrieved March 19, 2022, from <https://ce.udel.edu/research/research-overview/transportation-engineering-and-civil-infrastructure-systems/>].

[3] O. Skorobogatova, and I. Kuzmina-Merlino, "Transport infrastructure development performance", 16th Conference on Reliability and Statistics in Transportation and Communication, Riga, Latvia, 2016.

[4] Federal Highway Administration (FHWA), "Policy and governmental affairs", Office of Highway Policy Information, Washington, DC, USA, 2008. [Retrieved March 19, 2022, from <https://www.fhwa.dot.gov/policyinformation/statistics/2008/>].

[5] T. C. Pharris, and R. L. Kolpa, "Overview of the design, construction, and operation of interstate liquid petroleum pipelines", Argonne National Laboratory, Environmental Science Division, Argonne, IL, USA, 2007.

[6] E. Yilma, K. Woldeyohannes, K. Ayalneh, and Y. Bekele, "The design of a roadway section from Adama to Awash using rigid pavement and its implication in Ethiopian road construction", Addis Ababa University, Addis Ababa, Ethiopia, 2014.

[7] K. A. Admasu, "Development of models of interrupted traffic flow conditions of Addis Ababa from a study of an urban multi-lane highway", Master of Science Thesis, Addis Ababa University Digital Library, Addis Ababa, Ethiopia, 2016.

[8] American Society of Civil Engineers (ASCE), "ASCE's infrastructure report card gives U.S. 'C-' grade, says investment gap trillion, bold action needed", Washington, DC, USA, 2021. [Retrieved May 30, 2022, from: <https://www.asce.org/publications-and-news/civil-engineering-source/society-news/article/2021/03/03/asces-infrastructure-report-card-gives-us-c>].

[9] The White House, "President Biden's bipartisan infrastructure law", Legislation Overview, Washington, DC, USA, 2021. [Retrieved on July 14, 2022, from: <https://www.whitehouse.gov/bipartisan-infrastructure-law/>].

[10] American Society of Civil Engineers (ASCE), "Deteriorating infrastructure and growing investment gap will reduce U.S. GDP by $10 trillion in 20 years: Economic study", Washington, DC, USA, 2021. [Retrieved on July 14, 2022, from: <https://www.asce.org/publications-and-news/civil-engineering-source/society-news/article/2021/01/12/deteriorating-infrastructure-and-growing-investment-gap-will-reduce-us-gdp/>].

[11] J. Short, and A. Kopp, "Transport infrastructure: Investment and planning. Policy and research aspects", European Conference of Ministers of Transport (ECMT), Transport policy, 12(4), pp. 360 – 367, Paris, France, 2005.

[12] L. Rowan, "Bipartisan Infrastructure Bill signed: Here's what's in Biden's $1 Trillion Bill", Forbes. [Retrieved on July 15, 2022, from: <https://www.forbes.com/advisor/personal-finance/biden-signs-bipartisan-infrastructure-bill/>].

[13] C. Juma, and L. Yee-Cheong, "Innovation: applying knowledge in development", Volume 14, Earthscan, Sterling, VA, USA, 2005.

[14] B. J. Pauli, "The Flint water crisis", Wiley Interdisciplinary Reviews (WIREs): Water, 7(3), e1420, 2020.

[15] E. Kgomo, "DFI funding and infrastructure development: A case of the under-resourced municipalities in South Africa", Master's Thesis, University of Cape Town, Cape Town, South Africa, 2020.

[16] Bipartisan Policy Center, "America's aging water infrastructure", September 2016, Washington, DC, USA, 2016.

[17] D. Agdas, J. A. Rice, J. R. Martinez, and I. R. Lasa, "Comparison of visual inspection and structural-health monitoring as bridge condition assessment methods", American Society of Civil Engineers (ASCE), 30(3), pp. 1 – 10, Reston, VA, USA, 2015.

[18] T. Omar, and M. L. Nehdi, "Condition assessment of reinforced concrete bridges: Current practice and research challenges", Infrastructures, 3(3), 36, Basel, Switzerland, 2018.

[19] L. Meyerhoff, "Assessment and planning", Cornell University, Ithaca, NY, USA. [Retrieved on February 20, 2022, from <https://scl.cornell.edu/staff/assessment-and-planning>].

[20] E. J. Cha, and B. R. Ellingwood, "Risk-Averse Decision-Making for Civil Infrastructure Exposed to Low-Probability, High-Consequence Events", Reliability Engineering and System Safety, Elsevier Science Ltd, UK, 2012.

[21] R. Madhavan, E. Tunstel, and E. Messina, "Performance evaluation and benchmarking of intelligent systems", Springer publisher, pp. 139 – 168, Boston, MA, USA, 2009.

[22] A. E. Aktan, I. Bartoli, and S. G. Karaman, "Technology leveraging for infrastructure asset management: Challenges and opportunities", Frontiers in Built Environment, 5, 61, Zurich, Switzerland, 2019.

[23] University of Michigan, "Intelligent systems", Civil Infrastructure Systems Program Overview, Ann Arbor, MI, USA. [Retrieved March 19, 2022, from <https://cee.engin.umich.edu/research/infrastructure/intelligent-systems/>].

[24] C. S. Raghavendra, K. M. Sivalingam, and T. Znati, "Wireless sensor networks", Book, Springer, New York, NY, USA, 2004.

[25] K. Sohraby, D. Minoli, and T. Znati, "Wireless sensor networks: technology, protocols, and applications", John Wiley and Sons, Hoboken, NJ, USA, 2007.

[26] Z. Dai, S. Wang, and Z. Yan., "BSHM-WSN: A wireless sensor network for bridge structure health monitoring", Proceedings of the 2012 Proceedings of International Conference on Modelling, Identification and Control, IEEE, pp. 708 - 712, Wuhan, China, 2012.

[27] S. E. Chen, W. Liu, K. Dai, H. Bian, and E. Hauser, "Remote sensing for bridge monitoring", Geotechnical Special Publication No. 214, American Society of Civil Engineers (ASCE), Reston, VA, USA, 2011.

[28] S. Kalenjuk, W. Lienhart, and M. J. Rebhan, "Processing of mobile laser scanning data for large-scale deformation monitoring of anchored retaining structures along highways", Computer-Aided Civil and Infrastructure Engineering, 36(6), pp. 678 – 694, Denver, CO, USA, 2019.

[29] R. Bushman, and A. J. Pratt, "Weigh-in-motion technology: economics and performance", presented at NATMEC '98 Charlotte, NC, USA, 1998.

[30] W. W. Greenwood, J. P. Lynch, and D. Zekkos, "Applications of UAVs in civil infrastructure", Journal of Infrastructure Systems, American Society of Civil Engineers (ASCE), 25(2), p.04019002, Reston, VA, USA, 2019.

[31] L. Gonga, T. Morikawab, T. Yamamotoc, and H. Satob, "Deriving personal trip data from GPS data: A literature review on the existing methodologies", The 9th International Conference on Traffic & Transportation Studies (ICTTS '2014), Elsevier, 2014.

[32] S. E. Chen, "Laser scanning technology for bridge monitoring", Laser scanner technology, pp. 71 – 92, Charlotte, NC, USA, 2012.

[33] R. Pérez, V. Puig, J. Pascual, A. Peralta, E. Landeros and Ll. Jordanas, "Pressure sensor distribution for leak detection in Barcelona water distribution network", Water Science and Technology: Water Supply – WSTWS, IWA, Elsevier Science, Ltd., U.K., 2009.

[34] G. P. Hancke, B. C. Silva, and G. P. Hancke, "The role of advanced sensing in smart cities", Sensors, 13(1), pp. 393 – 425, Basel, Switzerland, 2012.

[35] F. S. Campos-Sánchez, R. Reinoso-Bellido, and F. J. Abarca-Álvarez, "Sustainable environmental strategies for shrinking cities based on processing successful case studies facing decline using a decision-support system", International Journal of Environmental Research and Public Health, 16(19), pp. 3727, 2019.

[36] F. K. Shaikh, A. Khelil, B. Ayari, P. Szczytowski, and N. Suri, "Generic information transport for wireless sensor networks", In 2010 IEEE international conference on sensor networks, ubiquitous, and trustworthy computing, IEEE, pp. 27 – 34, Newport Beach, CA, USA, 2010.

[37] S. K. Dash, S. Mohapatra, and P. K. Pattnaik, "A survey on applications of wireless sensor network using cloud computing", International Journal of Computer Science & Emerging Technologies, Volume 1 – Issue 4, pp. 50 – 55, 2010.

[38] X. Hu, L. Yang, and W. Xiong, "A novel wireless sensor network frame for urban transportation", IEEE Internet of Things Journal, 2(6), pp. 586 – 595, 2015.

[39] J. Kim, H. Kim, K. Lakshmanan, and R. Rajkumar, "Parallel scheduling for cyber-physical systems: Analysis and case study on a self-driving car", In Proceedings of the ACM/IEEE 4th international conference on cyber-physical systems, pp. 31-40, Philadelphia, PA, USA, 2013.

[40] Z. Liu, T. Tsuda, H. Watanabe, S. Ryuo, and N. Iwasawa, "Data driven cyber-physical system for landslide detection", Mobile Networks and Applications, 24(3), pp. 991 – 1002, 2019.

[41] H. Schlune, M. Plos, and K. Gylltoft, "Improved bridge evaluation through finite element model updating using static and dynamic measurements", Engineering structures, 31(7), Elsevier Science Ltd, pp. 1477 – 1485, U.K., 2009.

[42] S. Jianjun, W. Xu, G. Jizhen, and C. Yangzhou, "The analysis of traffic control cyber-physical systems", Procedia - Social and Behavioral Sciences, 13th COTA International Conference of Transportation Professionals, Elsevier Science Ltd, U.K., 2013.

[43] J. Zhou, H. N. Dai, and H. Wang, "Lightweight convolution neural networks for mobile edge computing in transportation cyber physical systems", ACM Transactions on Intelligent Systems and Technology (TIST), 2019.

[44] H. Song, Q. Du, P. Ren, W. Li, A. Mehmood, and L. M. Patnaik, "Cloud computing for transportation cyber-physical systems", In Cyber-Physical Systems: A Computational Perspective, Vol. 15, Chapman & Hall, 2015.

[45] Y. Zhang, C. Wu, and J. Wan, "Mathematical modeling of the effects of speech warning characteristics on human performance and its application in transportation cyber-physical systems", IEEE Transactions on Intelligent Transportation Systems, 2016.

[46] J. K. S. Lau, C. Tham, and T. Luo, "Participatory cyber physical system in public transport application", 2011 Fourth IEEE International Conference on Utility and Cloud Computing, 2011.

[47] D. M. Siringoringo, and Y. Fujino, "Seismic response of a suspension bridge: Insights from long-term full-scale seismic monitoring system", Structural Control and Health Monitoring, 25(11), e2252, John Wiley & Sons, Ltd., 2018.

[48] C. Jin, S. Jang, X. Sun, J. Li, and R. Christenson, "Damage detection of a highway bridge under severe temperature changes using extended Kalman filter trained neural network", Journal of Civil Structural Health Monitoring, Springer, 6(3), pp. 545 – 560, 2016.

[49] C. Wu, P. Wu, J. Wang, R. Jiang, M. Chen, and X. Wang, "Critical review of data-driven decision-making in bridge operation and maintenance", Structure and Infrastructure Engineering, 18(1), pp. 47 – 70, 2022.

[50] D. B. Rawat, C. Bajracharya, and G. Yan, "Towards intelligent transportation cyber-physical systems: Real-time computing and communications perspectives", In SoutheastCon 2015, pp. 1 – 6, IEEE, 2015.

[51] A. Shalaby, and A. Farhan, "Bus travel time prediction model for dynamic operations control and passenger information systems", Transportation Research Board, Washington, DC, USA, 2003.

[52] S. Rani, R. Maheswar, G. R. Kanagachidambaresan, and R. Jayarajan, "Integration of WSN and IoT for smart cities", Book, Springer Publisher, 2020.

[53] M. Batty, "Smart cities, big data", Environment and Planning B: Planning and Design, Volume 39 – Issue 2, pp. 191 – 193, 2012.

[54] M. Angelidou, "The role of smart city characteristics in the plans of fifteen cities", Journal of Urban Technology, 24(4), Taylor & Francis Group, pp. 3 – 28, 2017.

[55] M. Angelidou, "Smart city policies: A spatial approach", Cities, 41, S3-S11, Elsevier Science Ltd, U.K., 2014.

[56] J. H. Lee, M. G. Hancock, and M. C. Hu, "Towards an effective framework for building smart cities: Lessons from Seoul and San Francisco", Technological Forecasting and Social Change, 89, pp. 80 – 99, Elsevier Science Ltd, U.K., 2014.

[57] J. V. Winters, "Why are smart cities growing? Who moves and who stays?", Journal of regional science, Volume 51 – Issue 2, Wiley Online Library, pp. 253 – 270, 2011.

[58] J. B. Hollander, K. Pallagst, T. Schwarz, and F. J. Popper, "Planning shrinking cities", Progress in planning, Volume 72 – Issue 4, pp. 223 – 232, 2009.

[59] Federal Highway Administration (FHWA), "Strengthening our world-class highway system", U.S. Department of Transportation, Washington, DC, USA, 2022. [Retrieved on June 30, 2022, from: <https://highways.dot.gov/>].

[60] Central Intelligence Agency (CIA), "The world factbook: roadways", 2022. [Retrieved on June 30, 2022, from: <https://www.cia.gov/the-world-factbook/field/roadways/>].

[61] Federal Highway Administration (FHWA), "Earth retaining structures and asset management", Publication No. FHWA-IF-08-014, U.S. Department of Transportation, Washington, DC, USA, 2008.

[62] D. Cebon, "Vehicle generated road damage: a review", Vehicle system dynamics, 18(1-3), Taylor & Francis Group, pp. 107 – 150, 1989.

[63] W. Uddin, W. R. Hudson, and R. Haas, "Public infrastructure asset management", 2nd edition, McGraw Hill, New York, NY, USA, 2013.

[64] B. Yanev, "Bridge management", John Wiley and Sons, Hoboken, NJ, USA, 2007.

[65] Federal Highway Administration (FHWA), "2014 transportation asset management peer exchange – preparing for MAP-21 implementation", Publication No. FHWA–HIF–14–013, U.S. Department of Transportation, Washington, DC, USA, 2014.

[66] Federal Highway Administration (FHWA), "Incorporating risk management into transportation asset management plans", Office of Asset Management, U.S. Department of Transportation, Washington, DC, USA, 2017.

[67] M. Vessely, W. Robert, S. Richrath, V. R. Schaefer, O. Smadi, E. Loehr, and A. Boeckmann, "Geotechnical asset management for transportation agencies", Volume 2: Implementation Manual, NCHRP Research Report 903, National Academies, Washington, DC, USA, 2019.

[68] A. Athanasopoulos-Zekkos, J. Lynch, D. Zekkos, A. Grizi, K. Admassu, B. Benhamida, R. J. Spino, and M. Mikolajczyk, "Asset management for retaining walls", Final Report Submitted to the Michigan Department of Transportation (MDOT) – ORBP Number OR15-114, Ann Arbor, MI, USA, 2020.

[69] M. DeMarco, D. Keough, and S. Lewis, "Retaining wall inventory and assessment program (WIP) national park service procedures manual", Publication No. FHWA-CFL/TD-10-003, Federal Highway Administration (FHWA), U.S. Department of Transportation, pp. 188, Washington, DC, USA, 2010.

[70] W. Jensen, "Inspector's manual for mechanically stabilized earth walls", Publication No. SPR- P1(09) P320, Nebraska Department of Roads (NDOR), pp. 36, Ord, NE, USA, 2009.

[71] B. X. Walters, M. P. Collins, N. E. Funk, M. J. Vessely, B. L. Widman, J. W. Koonce, M. J. Garlich, and P. D. Thompson, "Colorado retaining and noise walls inspection and asset management manual", Colorado Department of Transportation (CDOT), pp. 300, Denver, CO, USA, 2016.

[72] Oregon Department of Transportation (ODOT), "ODOT Specifications – 2007", Specifications, Section 00596.11, Salem, OR, USA, 2007.

[73] VicRoads Technical Services, "Road structures inspection manual", State Government of Victoria, Victoria, Australia, 2014.

[74] Y. Fujino, and D. M. Siringoringo, "Bridge monitoring in Japan: the needs and strategies", Journal of Structure and Infrastructure Engineering, Taylor & Francis, pp. 597 – 611, 2011.

[75] D. Zonta, B. Glisic, and S. Adriaenssens, "Value of information: impact of monitoring on decision-making", Structural Control and Health Monitoring, 21: pp. 1043 – 1056, 2014.

[76] K. A. Flanigan, J. P. Lynch, and M. Ettouney, "Quantitatively linking long-term monitoring data to condition ratings through a reliability-based framework", Structural Health Monitoring, Sage Publishing, Thousand Oaks, CA, USA, 2020.

[77] K. Yen, B. Ravani, and T. Lasky, "LiDAR for data efficiency", Washington State Department of Transportation (WSDOT), Office of Research and Library Services, Report No. WA-RD 778.1, pp. 101, Olympia, WA, USA, 2011.

[78] S. Kalenjuk, W. Lienhart, M. J. Rebhan, and R. Marte, "Largescale monitoring of retaining structures: new approaches on the safety assessment of retaining structures using mobile mapping", Proc. SPIE 10970, Sensors and Smart Structures Technologies for Civil, Mechanical, and Aerospace Systems 2019, 109700T, Denver, CO, USA, 2019.

[79] P. Oskouie, B. Becerik-Gerber, and L. Soibelman, "Automated measurement of highway retaining wall displacements using terrestrial laser scanners", Automation in Construction 65 (2016), Elsevier Science Ltd, pp. 86 – 101, U.K., 2016.

[80] Y. R. Kim, J. E. Hummer, M. Gabr, D. Johnston, B. S. Underwood, D. J. Findley, and C. M. Cunningham, "Asset management inventory and data collection", Publication No. FHWA/NC/2008-15, North Carolina Department of Transportation (NCDOT), pp. 286, Raleigh, NC, USA, 2009.

[81] R. M. Koerner, and G. R. Koerner, "Recommended layout of instrumentation to monitor potential movement of MSE walls, berms, and slopes", Geosynthetic Institute, Folsom, PA, USA, 2011.

[82] Washington State Department of Transportation (WSDOT), "Geotechnical design manual", Publication No. M 46-03.04, Environmental and Engineering Programs, Olympia, WA, USA, 2011.

[83] P. Wu, D. Tan, S. Lin, W. Chen, J. Yin, N. Malik, and A. Li, "Development of a monitoring and warning system based on optical fiber sensing technology for masonry retaining walls and trees", Journal of Rock Mechanics and Geotechnical Engineering, Elsevier, U.K., 2021.

[84] Bridge Diagnostics Inc (BDI), "5.2 BDI strain transducer – ST350", STS - WiFi Operations Manual, Boulder, CO, USA, 2006.

[85] D. Zonta, R. Zandonini, and F. Bortot, "A Reliability-based bridge management concept", Journal of Structure and Infrastructure Engineering, Taylor & Francis, 3(3): pp. 215 – 235, 2007.

[86] D. M. Frangopol, A. Strauss, and S. Kim, "Bridge reliability assessment based on monitoring", Journal of Bridge Engineering, ASCE; 13(3): pp. 258 – 270, 2008.

[87] P. Jansson, "Rotation/movement of retaining wall, I-696 at Evergreen Road, Southfield, MI, Technical Investigation TI-2103", Office Memorandum, Michigan Department of Transportation, Lansing, MI, 2007.

[88] Michigan Department of Transportation (MDOT), "63102 – I-696 retaining wall details (plan and profile)", Working Drawings, Lansing, MI, USA, 1986.

[89] K. A. Admassu, J. P. Lynch, A. Athanasopoulos-Zekkos, and D. Zekkos, "Long-term wireless monitoring solution for the risk management of highway retaining walls", Proc. SPIE 10971, Nondestructive Characterization and Monitoring of Advanced Materials, Aerospace, Civil Infrastructure, and Transportation XIII, 1097103, Denver, CO, USA, 2019.

[90] E. G. Straser, A. S. Kiremidjian, T. H. Meng, and L. Redlefsen, "Modular, wireless network platform for monitoring structures", Proceedings of the 16th International Modal Analysis Conference (IMAC), Vol. 1, pp. 450 – 456, 1998.

[91] S. N. Pakzad, G. L. Fenves, S. Kim, and D. E. Culler, "Design and implementation of scalable wireless sensor network for structural monitoring", Journal of Infrastructure Systems, 14(1): pp. 89 – 101, 2008.

[92] N. Kurata, B. F. Spencer, and M. Ruiz-Sandoval, "Risk monitoring of buildings with wireless sensor networks", Structural Control and Health Monitoring, Vol. 12, No. 3, pp. 315 – 327, 2005.

[93] R. A. Swartz, J. P. Lynch, S. Zerbst, B. Sweetman, and R. Rolfes, "Structural monitoring of wind turbines using wireless sensor networks", Smart Structures and Systems, Techno Press, 6(3), 2010.

[94] K. Flanigan, and J. P. Lynch, "Community engagement using urban sensing: technology development and deployment studies", 25th International Workshop on Intelligent Computing in Engineering, Lausanne, Switzerland, 2018.

[95] R. A. Swartz, D. Jung, J. P. Lynch, Y. Wang, D. Shi, and M. P. Flynn, "Design of a wireless sensor for scalable distributed in-network computation in a structural health monitoring system", Proceedings of the 5th International Workshop on Structural Health Monitoring, pp. 1570–1577, 2005.

[96] R. Hou, J. P. Lynch, M. Ettouney, and P. O. Jansson, "Partial composite action and durability assessment of slab-on-girder highway bridge decks in negative bending using long-term structural monitoring data", Journal of Engineering Mechanics, ASCE, 146(4): 04020010, 2020.

[97] Y. Zhang, M. Kurata, and J. P. Lynch, "Long-term modal analysis of wireless structural monitoring data from a suspension bridge under varying environmental and operational conditions: system design and automated modal analysis", Journal of Engineering Mechanics, ASCE, 143(4): 04016124, 2017.

[98] M. Kurata, J. Kim, J. P. Lynch, G. Van Der Linden, H. Seddat, E. Thometz, P. Hipley, and L. H. Sheng, "Internet-enabled wireless structural monitoring systems: development and permanent deployment at the new Carquinez suspension bridge", Journal of Structural Engineering, ASCE, 139(10): pp. 1688 – 1702, 2013.

[99] K. A. Admassu, K. Flanigan, W. Wang, C. Wolf, and J. P. Lynch, "Rapid-to-deploy wireless water pressure sensors for the assessment of water distribution systems", In IEEE ISC2 Conference, Paphos, Cyprus, 2022.

[100] Bosch Sensortec, "BNO055: intelligent 9-axis absolute orientation sensor", Sensor Datasheet - BST-BNO055- DS000-14, Bosch Sensortec GmbH, Reutlingen, Germany, 2016.

[101] Exosite Website, "We were doing this before "IoT" was even a thing". [Retrieved on August 20, 2022, from: <https://www.exosite.com/about>].

[102] Michigan Department of Transportation (MDOT), "Preliminary findings of retaining wall investigations", Office Memorandum, Lansing, MI, USA, 2013.

[103] American Concrete Institute (ACI), "Prediction of creep, shrinkage, and temperature effects in concrete structures", Committee 209, Farmington Hills, MI, USA, 1997.

[104] C. P. Coduto, "Foundation design: principles and practices". 2nd edition, Pearson Education, Inc., 2001.

[105] Naval Facilities Engineering Command (NAVFAC), "Soil mechanics – design manual 7.01", Alexandria, VA, USA, 1986.

[106] J. W. Koloski, S. D. Schwarz, and D. W. Tubbs, "Geotechnical properties of geologic materials, engineering geology in Washington – Volume I", Washington Division of Geology and Earth Resources, Bulletin 78, Olympia, WA, USA, 1989.

[107] B. K. Low, "Reliability-based design applied to retaining walls", Geotechnique 55, No. 1, Institution of Civil Engineers, pp. 63 – 75, London, U.K., 2015.

[108] I. A. Basheer, and Y. M. Najjar, "Reliability-based design of reinforced earth retaining walls", Transportation Research Record, Washington, DC, USA, 1996.

[109] A. T. C. Goh, and F. H. Kulhawy, "Reliability assessment of serviceability performance of braced retaining walls using a neural network approach", Int. J. Numer. Anal. Meth. Geomech., 2005; 29: pp. 627 – 642, John Wiley & Sons, Hoboken, NJ, USA, 2005.

[110] A. Mokhtar, R. Belarbi, F. Benboudjema, N. Burlion, B. Capra, M. Carcassès, J. Colliat, F. Cussigh, F. Deby, F. Jacquemot, T. Larrard, J. Lataste, P. Bescop, M. Pierre, S. Poyet, P. Rougeau, T. Rougelot, A. Sellier, J. Séménadisse, J. Torrenti, A.

Trabelsi, P. Turcry, and H. Yanez-Godoy, "Experimental investigation of the variability of concrete durability properties", Cement and Concrete Research, Volume 45, pp. 21 – 36, Elsevier Science Ltd, U.K., 2013.

[111] I. Arrayago, K. J. R. Rasmussen, and E. Real, "Statistical analysis of the material, geometrical and imperfection characteristics of structural stainless steels and members", Journal of Constructional Steel Research, 175 (2020), Elsevier Science Ltd, U.K., 2020.

[112] S. A. Mirza, and J. G. MacGregor, "Variability of mechanical properties of reinforcing bars", American Society of Civil Engineers (ASCE), Journal of the Structural Division, 105(5), pp. 921 – 937, 1979.

[113] M. Bournonville, J. Dahnke, and D. Darwin, "Statistical analysis of the mechanical properties and weight of reinforcing bars", Structural Engineering and Materials Laboratory, Report 04-1, University of Kansas, Lawrence, KS, USA, 2004.

[114] Weather Underground, "Detroit, Michigan", The Weather Company (TWC). [Retrieved on August 20, 2022, from: <https://www.wunderground.com/weather/us/mi/detroit>].

[115] Federal Highway Administration (FHWA), "Design and construction of mechanically stabilized earth walls and reinforced soil slopes: Volume II", Publication No. FHWA NHI-10-025, Federal Highway Administration, Washington, DC, USA, 2009.

[116] C. Berwanger, and F. Sarkar, "Thermal expansion of concrete and reinforced concrete", ACI Journal, American Concrete Institute, 73(11): pp. 618 – 621, 1976.

[117] B. Elsener, C. Andrade, J. Gulikers, R. Polder, and M. Raupach, "Half-cell potential measurements – potential mapping on reinforced concrete structures", Materials and Structures, RILEM, 36(4): pp. 461 – 471, 2003.

[118] C. Andrade, and C. Alonso, "Corrosion rate monitoring in the laboratory and on-site", Construction and Building Materials, 10(5), Elsevier Science Ltd, U.K., 1996.

[119] United States Environmental Protection Agency, "Systems measures of water distribution system resilience", Report, EPA 600/R-14/383, Cincinnati, OH, USA, pp. 1-3, 2014.

[120] E. Alperovits, and U. Shamir, "Design of optimal water distribution systems", Water Resources Research, 13(6), 885-900, Wiley, New York, NY, USA, 1977.

[121] U. Zessler, and U. Shamir, "Optimal operation of water distribution systems", Journal of Water Resources Planning and Management, American Society of Civil Engineers (ASCE), 115(6), 735-752, Reston, VA, USA, 1989.

[122] Y. Bao, and L. W. Mays, "Model for water distribution system reliability", Journal of Hydraulic Engineering, American Society of Civil Engineers (ASCE), 116(9), 1119-1137, Reston, VA, USA, 1990.

[123] T. Campbell, "4 reasons to monitor pressure in water distribution systems", C. C. Lynch and Associates. [Retrieved on April 23, 2022, from: <https://cclynch.com/4-reasons-to-monitor-pressure-in-water-distribution-systems/>].

[124] J. Van Zyl, and C. R. I. Clayton, "The effect of pressure on leakage in water distribution systems", In Proceedings of the Institution of Civil Engineers-Water Management, 160(2), 109-114, London, U.K., 2007.

[125] R. Gomes, A. S. Marques, and J. Sousa, "Estimation of the benefits yielded by pressure management in water distribution systems", Urban Water Journal, 8:2, 65-77, Taylor and Francis, London, U.K., 2011.

[126] M. A. Sayyed, R. Gupta, and T. T. Tanyimboh, "Modeling pressure deficient water distribution networks in EPANET", Procedia Engineering, 89, 626-631, Elsevier Science Ltd, U.K., 2014.

[127] J. J. Quevedo Casín, M. A. Cugueró Escofet, R. Pérez Magrané, F. Nejjari Akhi-Elarab, V. Puig Cayuela, and J. M. Mirats Tur, "Leakage location in water distribution networks based on correlation measurement of pressure sensors", 2011.

[128] T. Lambrou, C. Anastasiou, C. Panayiotou, and M. Polycarpou, "A low-cost sensor network for real-time monitoring and contamination detection in drinking water distribution systems", IEEE Sensors Journal, 14(8), 2765-2772, 2014.

[129] J. Quevedo, V. Puig, G. Cembrano, J. Blanch, J. Aguilar, D. Saporta, G. Benito, M. Hedo, and A. Molina, "Validation and reconstruction of flow meter data in the Barcelona water distribution network", Control Engineering Practice, 18(6), 640-651, 2010.

[130] R. K. Mazumder, A. M. Salman, Y. Li, and X. Yu, X., "Performance evaluation of water distribution systems and asset management", Journal of Infrastructure Systems, American Society of Civil Engineers (ASCE), 24(3), 03118001, Reston, VA, USA, 2018.

[131] W. K. Ang, and P. W. Jowitt, (2006), "Solution for water distribution systems under pressure-deficient conditions", Journal of Water Resources Planning and Management, ASCE, 132(3), 175-182, 2006.

[132] O. Piller, S. Elhay, J. Deuerlein, and A. R. Simpson, "Local sensitivity of pressure-driven modeling and demand-driven modeling steady-state solutions to variations in parameters", Journal of Water Resources Planning and Management, American Society of Civil Engineers (ASCE), 143(2), 04016074, Reston, VA, USA, 2017.

[133] R. Pérez, V. Puig, J. Pascual, A. Peralta, E. Landeros and Ll. Jordanas, "Pressure sensor distribution for leak detection in Barcelona water distribution network", Water Science & Technology: Water Supply—WSTWS, IWA, Elsevier, U.K., 2009.

[134] E. Raei, M. E. Shafiee, M. R. Nikoo, and E. Berglund, "Placing an ensemble of pressure sensors for leak detection in water distribution networks under measurement uncertainty", Journal of Hydroinformatics, 21(2), 223-239, 2019.

[135] F. Soroush, and M. J. Abedini, "Optimal selection of number and location of pressure sensors in water distribution systems using geostatistical tools coupled with genetic algorithm", Journal of Hydroinformatics, 21(6), 1030-1047, 2019.

[136] Y. Shao, X. Li, T. Zhang, S. Chu, and X. Liu, "Time-series-based leakage detection using multiple pressure sensors in water distribution systems", Sensors, 19(14), 3070, 2019.

[137] A. Soldevila, J. Blesa, R. M. Fernández-Canti, S. Tornil-Sin, and V. Puig, "Data-driven approach for leak localization in water distribution networks using pressure sensors and spatial interpolation", Water, 11(7), 1500, 2019.

[138] K. A. Admassu, J. P. Lynch, A. Athanasopoulos-Zekkos, D. Zekkos, and B. Benhamida, "Data-driven risk assessment method for asset management of highway retaining wall systems using long-term structural monitoring", Submitted, 2022.

[139] G. Draughon, J. Lynch, D. Zekkos, and S. O'Laughlin, "Development of an autonomous flux chamber for continuous methane measurements at MSW landfills", 17th International Waste Management & Landfill Symposium, Sardinia 2019, Italy, 2019.

[140] Seeed Studio Technology, "Water pressure sensor G1/4 1.2 MPa", SKU 114991178 Product Details, [Retrieved on April 16, 2022, from: <https://www.seeedstudio.com/Water-Pressure-Sensor-G1-4-1-2MPa-p-2887.html>].

[141] ADH Technology, "Easy to use, slim, ultra-high performance, GPS smart antenna module", 2014. [Retrieved on April 16, 2022, from: <https://cdn.sparkfun.com/datasheets/GPS/GP-735T-150203.pdf>].

[142] U. S. Census Bureau (USCB), "U.S. Census Bureau QuickFacts: Benton Harbor City, Michigan". [Retrieved on April 16, 2022, from:

<https://www.census.gov/quickfacts/fact/table/bentonharborcitymichigan/PST045219>].

[143] C. L. Moe, and R. D. Rheingans, "Global challenges in water, sanitation and health", Journal of water and health, 4(S1), 41-57, 2006.

[144] H. Oertel, "Introduction to fluid mechanics, fundamentals and applications", University of Karlsruhe, pp. 43 – 48, 2001.

[145] R. V. Giles, J. B. Evett, and C. Liu, "Schaum's outline of fluid mechanics and hydraulics", McGraw-Hill Education, 2014.

[146] MLive News, "Benton Harbor water service restored following major main break". [Retrieved on April 25, 2022 from: <https://www.mlive.com/public-interest/2021/10/benton-harbor-water-service-restored-following-major-main-break.html>].

[147] 94.5 WSJM News, "State working to ensure Benton Harbor residents have water following main break". [Retrieved on April 25, 2022 from: <https://www.wsjm.com/2021/10/21/state-working-to-ensure-benton-harbor-residents-have-water-following-main-break/>].

[148] WNDU News Update, "UPDATE: Benton Harbor water main Break repaired, use of bottled water to continue". [Retrieved on April 25, 2022, from: <https://www.wndu.com/2021/10/21/water-main-break-leaves-much-benton-harbor-without-water/>].

[149] M. A. Al-Zahrani, and J. L. Syed, "Evaluation of municipal water distribution system reliability using minimum cut-set method", Journal of King Saud University-Engineering Sciences, 2005.

[150] Berkeley County Water and Sanitation Notices, "Water distribution system design guidelines", Berkeley, CA, USA, 2021.

[151] Hydrotech, "Chlorination systems", Carmel, IN, USA, 2019.

[152] S. K. Khanna, and C. E. G. Justo, "Highway Engineering", Published Book, Nem Chand, and Bros., Roorkee, India, 2011.

[153] Federal Highway Administration (FHWA), "Strengthening our world-class highway system", U.S. Department of Transportation, Washington, DC, USA, 2022. [Retrieved on June 30, 2022, from: <https://highways.dot.gov/>].

[154] Central Intelligence Agency (CIA), "The world factbook: roadways", 2022. [Retrieved on June 30, 2022, from: <https://www.cia.gov/the-world-factbook/field/roadways/>].

[155] R. N. Fries, M. R. Gahrooei, M. Chowdhury, and A. J. Conway, "Meeting privacy challenges while advancing intelligent transportation systems", Transportation Research Part C: Emerging Technologies, pp. 34-45, Washington, DC, USA, 2012.

[156] W. Xue, L. Wang, and D. Wang, "A prototype integrated monitoring system for pavement and traffic based on an embedded sensing network", IEEE Transactions on Intelligent Transportation Systems, Blacksburg, VA, USA, 2015.

[157] M. Tubaishat, P. Zhuang, Q. Qi, and Y. Shang, "Wireless sensor networks in intelligent transportation systems". Wireless Communications and Mobile Computing, Wiley & Sons, New York, NY, USA, 2009.

[158] L. Gonga, T. Morikawab, T. Yamamotoc, and H. Satob, "Deriving personal trip data from GPS data: A literature review on the existing methodologies", The 9th International Conference on Traffic & Transportation Studies (ICTTS '2014), Elsevier Science, 2014.

[159] American Society for Testing and Materials (ASTM), "Standard specification for highway weigh-in-motion (WIM) systems with user requirements and test methods", ASTM E1318-09, West Conshohocken, PA, USA, 2009.

[160] Federal Highway Administration (FHWA), "Weigh-in-motion pocket guide: Part 1 – WIM technology, data acquisition, and procurement guide", Publication No. FHWA-PL-08-015, Washington, DC, USA, 2018.

[161] C. D. Eamon, and S. Siavashi, "Developing representative Michigan truck configurations for bridge load rating", Wayne State University, Final Report Submitted to Michigan Department of Transportation (MDOT), MDOT ORBP Reference Number: OR14-023, Detroit, MI, USA, 2018.

[162] B. Jacob, and V. F. Beaumelle, "Improving truck safety: Potential of weigh-in-motion technology," IATSS Research, Elsevier Science, pp. 9 -15, 2010.

[163] M. Gindy, and H. H. Nassif, "Multiple presence statistics for bridge live load based on weigh-in-motion data", Transportation research record, pp. 125-135, Washington, DC, USA, 2007.

[164] E. M. Hernandez, "Statistical analysis of weigh-in-motion data for bridge design in Vermont", TRC Report 14-014, Agency of Transportation. Research and Development Section, University of Vermont, Burlington, VT, USA, 2014.

[165] J. Labarrere, "What is WIM and its history", International Society for Weigh-In-Motion (IS-WIM), France, 2017. Retrieved on June 30, 2022, from: <http://www.is-wim.org/index.php%3Fnm%3D2%26nsm%3D1%26lg%3Den>.

[166] E. O'Brien, "History of weigh-in-motion and technologies", Presented on 1st International Seminar of Weigh-In-Motion, Santa Catarina, Brazil, 2011.

[167] J. L. Carson, "Weigh-in-motion system calibration", Transportation Research Board (TRB), Washington, DC, USA, 2008.

[168] Michigan Department of Transportation (MDOT), "Annual Average Daily Traffic (AADT) map", 2013 Traffic Volumes, Lansing, MI, USA, 2013. [Retrieved on January 01, 2022, from: <https://www.michigan.gov/mdot/0,4616,7-151-11151_11033-22141--,00.html>].

[169] Federal Highway Administration (FHWA), "Major flows by truck to, from, and within Michigan: 2012 and 2045", United States Department of Transportation (USDOT), Washington, DC, USA, 2012. [Retrieved on January 01, 2022, from: <https://ops.fhwa.dot.gov/freight/freight_analysis/state_info/michigan/truckflow.htm>].

[170] Michigan Department of Transportation (MDOT), "Michigan's truck-weight law and truck-user fees", MDOT Intermodal Policy Division, Lansing, MI, USA, 2017. [Retrieved on January 01, 2022, from: <https://www.michigan.gov/documents/mdot/MDOT_013-4-16TruckWeightsMichigan_418609_7.pdf>].

[171] Michigan Department of Transportation (MDOT), "Performance-based planning and programming for pavement management", Center for Automotive Research (CAR), Ann Arbor, MI, USA, 2016. [Retrieved on January 01, 2022, from: <https://www.michigan.gov/documents/mdot/Performance-based_Planning_and_Programming_for_Pavement_Management_533869_7.pdf>].

[172] Michigan Department of Transportation (MDOT), "Statewide PTRs 2011 – Map", Data Collection Section, Lansing, MI, USA, 2011.

[173] Y. Zhou, and L. Shao, "Aware attentive multi-view inference for vehicle re-identification", In Proceedings of the IEEE conference on computer vision and pattern recognition, pp. 6489 – 6498, Salt Lake City, UT, USA, 2018.

[174] X. Liu, W. Liu, T. Mei, and H. Ma, "A deep learning-based approach to progressive vehicle re-identification for urban surveillance", In European conference on computer vision, 14th European Conference, Springer, pp. 869 – 884, Amsterdam, The Netherlands, 2016.

[175] D. Zapletal, and A. Herout, "Vehicle re-identification for automatic video traffic surveillance", In 2016 IEEE Conference on Computer Vision and Pattern Recognition Workshops (CVPRW), pp. 1568 – 1574, Las Vegas, NV, USA, 2016.

[176] P. Khorramshahi, A. Kumar, N. Peri, S. S. Rambhatla, J. C. Chen, and R. Chellappa, "A dual-path model with adaptive attention for vehicle re-identification", In Proceedings of the IEEE/CVF international conference on computer vision, pp. 6132 – 6141, Seoul, South Korea, 2019.

[177] R. Hou, S. Jeong, K. H. Law, and J. P. Lynch, "Reidentification of trucks in highway corridors using convolutional neural networks to link truck weights to bridge responses", In Sensors and Smart Structures Technologies for Civil, Mechanical, and Aerospace Systems, SPIE Vol. 10970, pp. 180 – 193, Denver, CO, USA, 2019.

[178] L. Chu, M. Cetin, and S. T. Jeng, "Weigh-in-motion station monitoring and calibration using inductive loop signature technology", Presented on the 94th Annual Meeting of the Transportation Research Board (TRB), Washington, DC, USA, 2015.

[179] A. P. Nichols, and D. M. Bullock, "Quality control procedures for weigh-in-motion data", Final Report FHWA/IN/JTRP-2004/12, Purdue University, West Lafayette, IN, USA, 2004.

[180] R. Bushman, and A. J. Pratt, "Weigh-in-motion technology: economics and performance", presented at NATMEC '98 Charlotte, NC, USA, 1998.

[181] M. Cetin, C. M. Monsere, and A. P. Nichols, "Bayesian models for re-identification of trucks over long distances based on axle measurement data", Journal of Intelligent Transportation Systems - Volume 15, Issue 1, UK, 2011.

[182] Michigan Department of Transportation (MDOT), "Information on the movement of oversize or overweight vehicles and load", Information Report 2, Transport Permits Unit, Lansing, MI, USA, 2004. [Retrieved on July 04, 2022, from: <https://www.michigan.gov/documents/MDOT_MoveOS_OW_T2_92127_7.pdf>].

[183] J. V. Carter, J. Pan, S. N. Rai, and S. Galandiuk, "ROC-ing along: Evaluation and interpretation of receiver operating characteristic curves", Surgery, 159(6), Elsevier Science, pp. 1638 – 1645, 2016.

[184] S. G. Baker, and B. S. Kramer, "Peirce, Youden, and receiver operating characteristic curves", The American Statistician, 61(4), Taylor & Francis Group, pp. 343 – 346, London, U.K., 2007.

[185] A. P. Sinha, and J. H. May, "Evaluating and tuning predictive data mining models using receiver operating characteristic curves", Journal of Management Information Systems, 21(3), Taylor & Francis Group, pp. 249 – 280, London, U.K., 2004.

[186] Y. Jiang, C. E. Metz, and R. M. Nishikawa, "A receiver operating characteristic partial area index for highly sensitive diagnostic tests", Radiology 201, pp. 745 – 750, 1996.

[187] L. E. Dodd, and M. S. Pepe, "Partial AUC estimation and regression", Biometrics 59, pp. 614 – 623, 2003.

[188] A. T. Peterson, M. Papeş, and J. Soberón, "Rethinking receiver operating characteristic analysis applications in ecological niche modeling", Ecological modelling, 213(1), pp. 63 – 72, 2008.

[189] American Association of State Highway and Transportation Officials (AASHTO), AASHTO Guide for Design of Pavement Structures, Washington, DC, USA, 1993.

[190] A. El-Geneidy, D. Levinson, D. Ehab, G. Boisjoly, D. Verbich, and C. Loong, "The cost of equity: Assessing transit accessibility and social disparity using total travel cost", Transportation Research Part A: Policy and Practice – Volume 91, 2016.

[191] N. Foth, K. Manaugh, and A. El-Geneidy, "Towards equitable transit: Examining transit accessibility and social need in Toronto, Canada, 1996–2006", Journal of Transport Geography - Volume 29, Elsevier, 2013.

[192] T. H. Poister, O. Q. Pasha, and L. H. Edwards. "Does performance management lead to better outcomes? Evidence from the U.S. public transit industry", Public Administration Review, The American Society for Public Administration, Vol. 73, Iss. 4, pp. 625 – 636, 2013.

[193] M. G. Badami, and M. Haider, "An analysis of public bus transit performance in Indian cities", Transportation Research Part A, Elsevier, 2007.

[194] H. S. Levinson, "Analyzing transit travel time performance", Transportation Research Record, Washington, DC, USA, 1983.

[195] USCB, "U.S. Census Bureau QuickFacts: Benton Harbor City, Michigan", [Retrieved on July 24, 2020, from: <https://www.census.gov/quickfacts/fact/table/bentonharborcitymichigan/PST045219>].

[196] F. M. Rojas, A. Fung, D. Luberoff, D. Weil, and M. Graham, "Transit transparency: Effective disclosure through open data", Transparency Policy Project, Harvard Kennedy School, Cambridge, MA, USA, 2012.

[197] Florida Department of Transportation (FDOT), "Best practices in evaluating transit performance", Final Report, Freight Logistics and Passenger Operations, Transit Office, Tallahassee, FL, U.S.A., 2014.

[198] K. Fimberg, and S. Sousa, "The impact of website design on users' trust perceptions", 11th International Conference on Applied Human Factors and Ergonomics (AHFE 2020), Springer, Tallinn, Estonia, 2020.

[199] S. Jiang, J. Ferreira, and M. C. González, "Activity-based human mobility patterns inferred from mobile phone data: A case study of Singapore", IEEE Transactions on Big Data – Volume 3, 2017.

[200] M. C. Gonzalez, C. A. Hidalgo, and A. L. Baraba, "Understanding individual human mobility patterns", Nature Volume 453|5, London, U.K., 2008.

[201] C. Zhou, H. Jia, Z. Juan, X. Fu, and G. Xiao, "A data-driven method for trip ends identification using large-scale smartphone-based GPS tracking data", in IEEE Transactions on Intelligent Transportation Systems, Vol. 18, No. 8, pp. 2096 – 2110, Aug. 2017, doi: 10.1109/TITS.2016.2630733.

[202] Y. Zheng, L. Liu, L. Wang, and X. Xie, "Learning transportation mode from raw GPS data for geographic applications on the web", International World Wide Web Conference Committee (IW3C2), April 21-25, 2008, Beijing, China, 2008.

[203] B. Donovan, and D. B. Work, "Using coarse GPS data to quantify city-scale transportation system resilience to extreme events", arXiv preprint, arXiv: 1507.06011, 2015.

[204] L. Gonga, T. Morikawab, T. Yamamotoc, and H. Satob, "Deriving personal trip data from GPS data: A literature review on the existing methodologies", The 9th International Conference on Traffic & Transportation Studies (ICTTS'2014), Elsevier, 2014.

[205] X. Ma, and Y. Wang, "Development of a data-driven platform for transit performance measures using smart card and GPS data", Journal of Transportation Engineering, ASCE, 2014.

[206] S. M. O'Connor, Y. Zhang, J. P. Lynch, M. M. Ettouney, and P. O. Jansson, "Long-term performance assessment of the Telegraph Road Bridge using a permanent wireless monitoring system and automated statistical process control analytics", Journal of Structure and Infrastructure Engineering, 13(5), pp. 604 – 624, Taylor & Francis, 2017.

[207] J. P. Lynch, "An overview of wireless structural health monitoring for civil structures", Philosophical Transactions of the Royal Society A: Mathematical, Physical and Engineering Sciences, 365(1851), pp. 345 – 372, 2007.

[208] H. R. Idris, and R. J. Hansman, "Observation and analysis of departure operations at Boston Logan International Airport", MiT International Center for Air Transportation. Report No. ICAT-2000-7, Cambridge, MA, USA, 2000.

[209] Federal Transit Administration (FTA), "Improving public transportation for America's communities", Washington, DC, USA. [Retrieved July 3, 2021, from <https://www.transit.dot.gov/about-fta>].

[210] A. Antrim, "Real-time transit information: benefits, technologies, components, experiences and recommendations", Trillium Solutions, White Paper for Oregon Department of Transportation, Portland, OR, USA, 2016.

[211] F. Sun, A. Dubey, J. White, and A. Gokhale, "Transit-hub: a smart public transportation decision support system with multi-timescale analytical services", Journal of Cloud Computing, Springer Nature, London, UK, 2018.

[212] F. Errico, T. G. Crainic, F. Malucelli, and M. Nonato, "A Survey on planning semi-flexible transit systems: Methodological issues and a unifying framework", Transportation Research Part C, Transportation Research Board (TRB), Washington, DC, USA, 2013.

[213] C. Zhang, X. Caoa, A. Nagpurea, and S. Agarwal, "Exploring rider satisfaction with transit service in Indore, India: An application of the three-factor theory", Transportation Letters, Taylor and Francis Group, London, UK, 2017.

[214] The University of Kansas, "Community toolbox", Lawrence, KS, USA. Retrieved February 20, 2022, from <https://ctb.ku.edu/en/table-of-contents>.

[215] S. Das, and D. Pandit, "Qualitative assessment of public facilities: the public bus", Emerald Insight, The TQM Journal, 2016.

[216] M. Xylia, "Towards Electrified Public Bus Transport: The case of Stockholm", Doctoral Thesis, KTH Royal Institute of Technology, Stockholm, Sweden, 2018.

[217] L. Meyerhoff, "Assessment and planning", Cornell University, Ithaca, NY, USA. [Retrieved on February 20, 2022, from: <https://scl.cornell.edu/staff/assessment-and-planning>].

[218] F. J. Miranda, R. Sanguino, and T. M. Bañegil, "Quantitative assessment of European municipal web sites", Internet Research, Volume 19 Issue 4, pp. 425 – 441, 2009.

[219] B. Ferris, K. Watkins, and A. Borning, "Location-aware tools for improving public transit usability", IEEE Computer Society, Washington, DC, USA, 2010.

[220] W. Li, M. Batty, and M. F. Goodchild, "Real-time GIS for smart cities", International Journal of Geographical Information Science, Taylor and Francis Group, London, U.K., 2020.

[221] Metropolitan Transportation Authority (MTA), "Bus performance dashboard", New York, NY, USA. [Retrieved February 20, 2022, from <http://busdashboard.mta.info/>].

[222] G. Xie, and B. Hoeft, "Freeway and arterial system of transportation dashboard: Web-based freeway and arterial performance measurement system", Transportation Research Record: Journal of the Transportation Research Board, Washington, DC, USA, 2012.

[223] B. M. Felipe, M. P. Javier, and R. D. Estember, "Computerized maintenance management system for the Philippine's railway transit", Proceedings of the International Conference on Industrial Engineering and Operations Management Bandung, Indonesia, 2018.

[224] J. L. Gifford, and W. H. Carlisle, "Virginia Department of Transportation's dashboard performance measurement and reporting system", Transportation Research Record: Journal of the Transportation Research Board, National Research Council, Washington, DC, U.S.A., 2004.

[225] W. Klumpenhouwer, J. Allen, L. Li, R. Liu, and M. Robinson, "A comprehensive transit accessibility and equity dashboard", The University of Vermont: Transportation Research Center, Burlington, VT, USA, 2021.

[226] Worldometer, "COVID-19: Coronavirus Pandemic". [Retrieved on February 20, 2022, from: <https://www.worldometers.info/coronavirus/>].

[227] John Hopkins University of Medicine, "Coronavirus Resource Center: United States", [Retrieved on February 20, 2022, from: <https://coronavirus.jhu.edu/region/united-states>].

[228] Transit Cooperative Research Program (TCRP), "A guidebook for developing a transit performance-measurement system", TCRP Report 88, Transportation Research Board, Washington, DC, USA, 2003.

[229] Transit Center, "The data transit riders want", A Shared Agenda for Public Agencies and Transit Application Developers, New York, NY, USA, 2018.

[230] Transit Center, "Hey MTA: Here are five qualities of a useful transit dashboard", August 31, 2017, New York, NY, USA. [Retrieved July 3, 2021, from <https://transitcenter.org/mta-five-qualities-of-a-useful-public-dashboard/>].

[231] Capital Metropolitan Transportation Authority, "Performance Dashboard", Austin, TX, USA. [Retrieved on July 3, 2021, from <https://www.capmetro.org/dashboard/>].

[232] Metropolitan Transportation Authority (MTA), "Bus Performance Dashboard", New York, NY, USA. [Retrieved July 3, 2021, from <http://busdashboard.mta.info/>].

[233] Tri-County Metropolitan Transportation (TriMet), "Performance Dashboard", Portland, OR, USA. [Retrieved on July 3, 2022, from: <https://trimet.org/about/dashboard/index.htm#ridership/>].

[234] Washington Metropolitan Area Transit Authority (MATA), "Ridership Data Portal", Washington, DC, USA. [Retrieved on July 3, 2022, from: <https://www.wmata.com/initiatives/ridership-portal/>].

[235] Chicago Transit Authority (CTA), "Coronavirus: Ridership Dashboards", Chicago, IL, USA. [Retrieved July on 3, 2022, from: <https://www.transitchicago.com/coronavirus/dashboard/>].

[236] Massachusetts Bay Transportation Authority (MBTA), "Performance Dashboard", Boston, MA, USA. [Retrieved July on 3, 2022, from: <https://www.mbtabackontrack.com/performance/#/home/>].

[237] Detroit Department of Transportation (DDOT), "DDOT Performance Dashboard", Detroit, MI, USA. [Retrieved July on 3, 2022, from: <https://detroitmi.gov/departments/detroit-department-transportation/ddot-performance-dashboard/>].

[238] M. U. Shalowitz, A. Isacco, N. Barquin, E. Clark-Kauffman, P. Delger, D. Nelson, A. Quinn, and K. A. Wagenaar, "Community-based participatory research: A review of the literature with strategies for community engagement", Journal of Developmental & Behavioral Pediatrics, Philadelphia, PA, USA, 2009.

[239] S. K. Oswal, "Participatory design: Barriers and possibilities", University of Washington, Tacoma, Tacoma, WA, USA, 2014.

[240] R. Goodspeed, K. Admassu, V. Bahrami, T. Bills, J. Egelhaaf, K. Gallagher, J. Lynch, N. Masoud, T. Shurn, P. Sun, Y. Wang, and C. Wolf, "Improving transit in small cities through collaborative and data-driven scenario planning", Submitted and in review, 2022.

[241] S. Kwon, M. Lindquist, S. Sylte, G. Gell, A. Awadhiya, and K. A. Admassu, "Land. Info: Interactive 3D visualization for public space design ideation in neighborhood planning", In Extended Abstracts of the 2019 CHI Conference on Human Factors in Computing Systems, pp. 1 – 6, Glasgow, Scotland, U.K., 2019.

[242] R. Goodspeed, C. Riseng, K. Wehrly, W. Yin, L. Mason, B. Schoenfeldt, "Applying design thinking methods to ecosystem management tools: Creating the great lakes aquatic habitat explorer", Marine Policy - Volume 69, Elsevier, 2016.

[243] USCB, "U.S. Census Bureau QuickFacts: St. Joseph City, Michigan", [Retrieved on July 25, 2020, from: <https://www.census.gov/quickfacts/fact/table/stjosephcitymichigan/PST045219>].

[244] Southwest Michigan Planning Commission (SWMPC), "Twin cities area transportation study", Benton Harbor, MI, USA, 2009.

[245] Southwest Michigan Planning Commission (SWMPC), "Berrien County transit study", Benton Harbor, MI, USA, 2009.

[246] L. Cohen, L. Manion, and K. Morrison, "Research methods in education", Routledge, 8th Edition, Taylor & Francis, London, U.K., 2018.

[247] F. P. Boscoe, K. A. Henry, and M. S. Zdeb, "A nationwide comparison of driving distance versus straight-line distance to hospitals", The Professional Geographer, pp. 188 – 196, Taylor and Francis, 2012.

[248] Nikolay Laptev, Santhosh Shanmugam, and Slawek Smyl, "Engineering extreme event forecasting at Uber with Recurrent Neural Networks" Uber's Intelligent Decision Systems Team, 2017. [Retrieved on September 23, 2022, from: <https://www.uber.com/blog/neural-networks/>.]